SISSA
Scuola
Internazionale
Superiore di
Studi Avanzati

Physics Area
Ph.D. course in Astroparticle Physics

Beyond Perturbation Theory in Cosmology

Candidate:
Vicharit Yingcharoenrat

Supervisor:
Paolo Creminelli

Academic Year 2020-21

ACKNOWLEDGEMENTS

Throughout my Ph.D. and the writing of this thesis I have received a great deal of support and assistance.

First and foremost I extremely grateful to my supervisor, Paolo Creminelli, for his invaluable advice, continuous support, and patience during my Ph.D. study over the last three years. His passion, deep physical intuition, and insightful feedback for physics have pushed me to sharpen my thinking and brought my work to a higher level. It was a great honor and a privilege for me to work with him and I will always be indebted to him for all the efforts he put in bringing me to this point.

During all these years, I had a great pleasure to collaborate with Marco Celoria, Filippo Vernizzi, and especially Giovanni Tambalo from whom I have constantly received a great help and leaned many useful lessons in achieving the results of this thesis.

I would also like to extend my gratitude to my Ph.D. fellows, the postdoc researchers and the staff members at SISSA and ICTP for many fruitful scientifc discussions and for making my experience as a student in Trieste more entertaining. Specially, I would like to thank Jan Tristram Acuna, Eyoab Dejene Bahiru, André Benevides, Lorenzo Bordin, Minahil Butt, Giovanni Cabass, Mehmet Asim Gumus, Diptimoy Ghosh, Marco Gorghetto, Diksha Jain, Oliver Janssen, Supattra Jitsangob, Takeshi Kobayashi, Matthew Lewandowski, Alfredo Gonzalez Lezcano, Daniel Manu-Marfo, Mehrdad Mirbabayi, Zainab Nazari, Adu Offei-Danso, Flavio Riccardi, Arnab Rudra and Goran Senjanovic.

Finally, I would like to thank my parents Supakit and Pilanthana, and my siblings Sirikwan, Phasathon, Chonnikarn and Phenmanta for supporting me over all these years. The accomplishment of this thesis would not have been possible without their help and support.

ABSTRACT

Over many years, our current understanding of the Universe has been extremely relied on perturbation theory (PT) both theoretically and experimentally. There are, however, many situations in cosmology in which the analysis beyond PT is required. In this thesis we study three examples: the resonant decay of gravitational waves (GWs), the dark energy (DE) instabilities induced by GWs, and the tail of the primordial field distribution function. The first two cases are within the context of the Effective Field Theory (EFT) of DE, whereas the last one is within inflation.

We first review the construction of the EFT of DE, which is the most general Lagrangian for the scalar and tensor perturbations around the flat FLRW metric. Specifically, this EFT can be mapped to the covariant theories, known as Horndeski and Beyond Horndeski theories. We then study the implications on the dark energy theories coming from the fact that GWs travel with the speed $c_T = 1$ at LIGO/Virgo frequencies. After that, we consider the perturbative decay of GWs into DE fluctuations ($\gamma \to \pi\pi$) due to the $\tilde{m}_4^2$ operator. This process is kinematically allowed by the spontaneous breaking of Lorentz invariance. Therefore, having no perturbative decay of gravitons together with $c_T = 1$ at LIGO/Virgo, rules out all quartic and quintic beyond Horndeski theories.

As the first non-perturbative regime in this thesis, we study the decay of GWs into DE fluctuations π, taking into account the large occupation numbers of gravitons. When the m_3^3 (cubic Horndeski) and $\tilde{m}_4^2$ (beyond Horndeski) operators are present, the GW acts as a classical background for π and modifies its dynamics. In particular, π fluctuations are described by a Mathieu equation and feature instability bands that grow exponentially. In the regime of small GW amplitude which corresponds to narrow resonance, we calculate analytically the produced π, its energy and the change of the GW signal. Eventually, the resonance is affected by π self-interactions in a way that we cannot describe analytically. The fact that π self-couplings coming from the m_3^3 operator become quickly comparable with the resonant term affects the growth of π so that the bound on α_B remains inconclusive. However, in the case of the $\tilde{m}_4^2$ operator self-interactions can be neglected at least in some regimes. Therefore, our resonant analysis improves the perturbative bounds on α_H, ruling out quartic Beyond Horndeski operators.

In the second non-perturbative regime we show that π may become unstable in the presence of a GW background with sufficiently large amplitude. We find that dark-energy fluctuations feature ghost and/or gradient instabilities for GW amplitudes that are produced by typical binary systems. Taking into account the populations of binary systems, we conclude that the instability is triggered in the whole Universe for $|\alpha_B| \gtrsim 10^{-2}$, i.e. when the modification of gravity is sizable. The fate of the instability and the subsequent time-evolution of the system depend on the UV completion, so that the theory may end up in a state very different from the original one. In conclusion, the only dark-energy theories with sizable cosmological effects that avoid these problems are k-essence models, with a possible conformal coupling with matter.

In the second part of the thesis we consider physics of inflation. Inflationary perturbations are approximately Gaussian and deviations from Gaussianity are usually calculated using in-in perturbation theory. This method, however, fails for unlikely events on the tail of the probability distribution: in this regime non-Gaussianities are important and perturbation theory breaks down for $|\zeta| \gtrsim |f_{NL}|^{-1}$. We then show that this regime is amenable to a semiclassical treatment, $\hbar \to 0$. In this limit the wavefunction of the Universe can be calculated in saddle-point, corresponding to a resummation of all the tree-level Witten diagrams. The saddle can be found by solving numerically the classical (Euclidean) non-linear equations of motion, with prescribed boundary conditions. We apply these ideas to a model with an inflaton self-interaction $\propto \lambda\dot{\zeta}^4$. Numerical and analytical methods show that the tail of the probability distribution of ζ goes as $\exp(-\lambda^{1/4}\zeta^{3/2})$, with a clear non-perturbative dependence on the coupling. Our results are relevant for the calculation of the abundance of primordial black holes.

PUBLICATIONS

The main ideas and figures of this thesis have appeared previously in the following publications:

1. M. Celoria, P. Creminelli, G. Tambalo, and V. Yingcharoenrat, "Beyond Perturbation Theory in Inflation", *JCAP* 06 (2021) 051, 2103.09244.

2. P. Creminelli, G. Tambalo, F. Vernizzi, and V. Yingcharoenrat, "Dark Energy Instabilities induced by Gravitational Waves", *JCAP* 05 (2020) 002, 1910.14035.

3. P. Creminelli, G. Tambalo, F. Vernizzi, and V. Yingcharoenrat, "Resonant Decay of Gravitational Waves into Dark Energy", *JCAP* 10 (2019) 072, 1906.07015.

CONTENTS

1 INTRODUCTION

Perturbation Theory (PT) has long played a crucial role in every field of theoretical physics such as Cosmology, Quantum Field Theory and Particle Physics. It incredibly helps one to understand physics in many circumstances where a remarkable accuracy of the results is required. For example, one of the great successes of perturbative Quantum Electrodynamics (QED), pioneered by Feynman, Schwinger and Tomonaga in 1940s, is the prediction of the loop contributions to the so-called anomalous magnetic moment of the electron $(g-2)_e$, which turned out to agree with the experimentally measured value to more than 10 significant figures. Hence, QED is the most precisely tested theory in the history of science.

As the title of the thesis suggests, our main focus here is to explore various regimes in cosmology where the treatment beyond PT is the key player. However, in order to appreciate why and how one needs to go beyond PT, it is thus instructive to start with the unperturbed Universe followed by perturbed Universe within PT.

UNPERTURBED UNIVERSE

The success of the unperturbed Universe begins with the assumptions of spatially homogeneity and isotropy on very large scales, i.e. the cosmological principle; this is empirically justified on scales larger than ~ 100 Mpc. (Of course, on small scales nothing appears to be homogeneous and isotropic, e.g. the distribution of galaxy clusters.) The metric compatible with those two symmetries is known as Friedmann–Lemaître–Robertson–Walker (FLRW) metric, whose dynamics is governed by the Friedman equation,

$$H^2(t) = \frac{\rho(t)}{3M_{\rm Pl}^2} - \frac{k}{a^2}\,, \tag{1.0.1}$$

where the Hubble rate $H(t) \equiv \dot{a}(t)/a$, $\rho(t)$ denotes the energy density in the Universe and k is the spatial curvature. In general, it is not so trivial to solve the equation above since $\rho(t)$ involves several different species, each of which scales differently in time. For simplicity, assuming that the Universe consists of a single component the energy densities of radiation, non-relativistic matter, and a cosmological constant then go respectively as a^{-4}, a^{-3} and a constant, depicted in Figure 1. With this background evolution, we see that our Universe has been through different phases dominated by radiation, matter and dark energy respectively. In fact, these are the main components in ΛCDM model - the standard model of Big Bang cosmology. Of course, there are a lot of evidences supporting the standard model; some of which as we will see later on heavily rely on PT such as cosmic microwave background (CMB) experiments and large scale structure (LSS) observations.

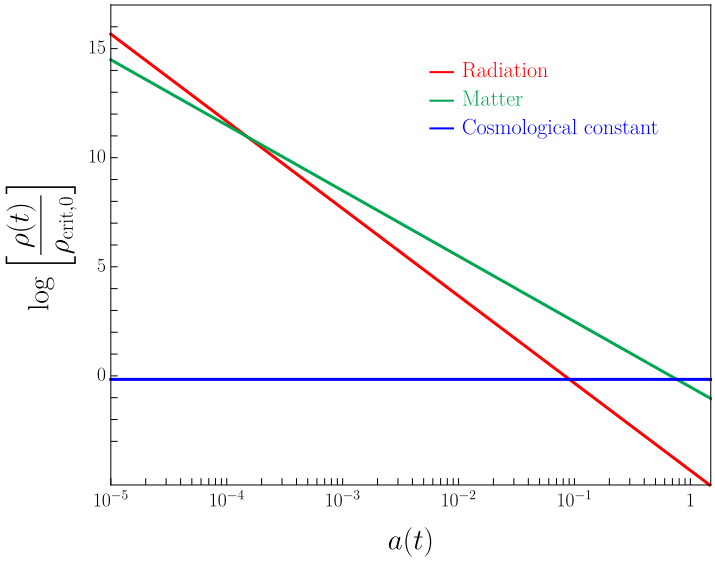

Figure 1: The evolution of energy densities of various species in the flat Universe with respect to the scale factor. $\rho_{\rm crit,0}$ is the critical energy density at the present time.

The existence of dark energy, on the other hand, has been experimentally confirmed requiring only physics at the unperturbed level, i.e. measuring the apparent magnitudes of dozens of Type Ia supernovae [1–3], which are standard candles across cosmological distances - they have almost identical absolute magnitudes. The latest resulting Hubble diagram (see Figure 2), assuming $k = 0$, indicates that the supernovae clearly appear fainter than predicted in a matter-only universe. This tells us that we are currently in the phase of dark energy or accelerated expansion. Note that this discovery of dark energy has been further confirmed by several independent probes, e.g. CMB [4–7] and LSS [8–10], although the use of PT is needed in those measurements.

Notwithstanding a lot of information we have acquired from the background evolution, there are a number of observations for which the unperturbed Universe cannot give an explanation, such as the formation and evolution of large-scale structures and the very tiny anisotropies observed from the CMB experiments.

In addition, ΛCDM model does not provide a complete answer to some of the theoretical questions: nature of dark energy and dark matter at the fundamental level, a solution to the cosmological constant problem, the origin of baryon asymmetry, and the initial conditions for inflation. (See [11] for a detailed discussion.)

All of these questions require one to study the perturbed Universe using PT and sometimes going beyond that. It is actually interesting to point out that the reason we need PT is not only because the system is clearly beyond a homogeneous Universe such as CMB, but also is because a homogeneous quantity such as energy density of dark matter can accurately be inferred by the dynamics of perturbations.

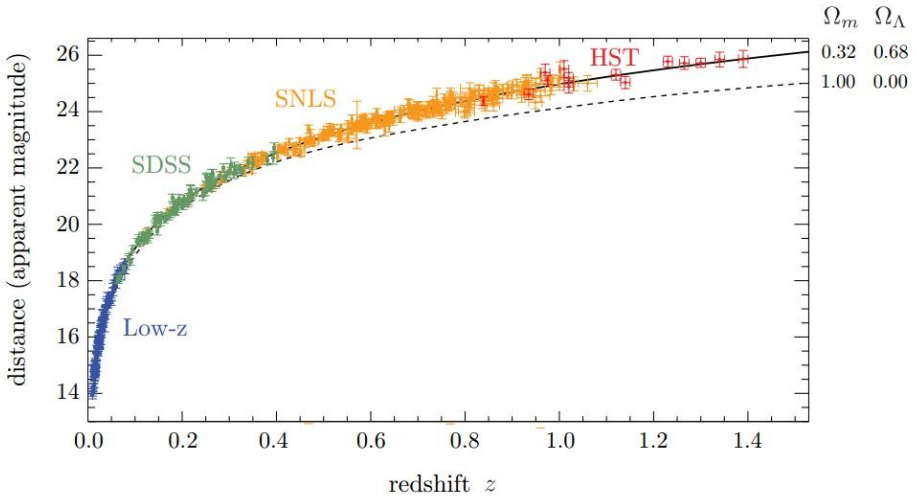

Figure 2: The latest Hubble diagram [12, 13] of the combined sample of Low-z, Sloan Digital Sky Survey (SDSS), SuperNova Legacy Survey (SNLS) and Hubble Space Telescope (HST).

PERTURBED UNIVERSE AND PERTURBATION THEORY

Evidently, we are not living in an unperturbed Universe since there are a lot of structures around us even on super large scales, for example galaxies and clusters of galaxies; those would not have been formed without perturbations. Let us now point out some cases in which PT is used in cosmology.

- The first and the most important example of the use of PT in cosmology is the physics of CMB. At the background level, the CMB appears to be remarkably isotropic and uniform. However, thanks to the incredible accuracy of the measurements (see [14] for the latest Planck data), it has been revealed that the statistics of the temperature fluctuations ΔT on the CMB map is very close to a Gaussain distribution, with small anisotropies $\Delta T \sim 10^{-5}$. With this information, the physics of CMB is well within the validity of PT. One, for example, uses PT to compute the angular power spectrum, $\mathcal{D}_\ell$ - this amounts to solving the linearized Einstein and relevant Boltzmann equations, which can be recast as a system of coupled ordinary differential equations ([15, 16] for early development). As a result, the CMB data points fit very well with the theoretical predictions based on ΛCDM model, see Figure 3. Moreover, the fact that our Universe today consists of dark energy $\sim 71.4\%$, cold dark matter $\sim 24\%$ and ordinary matter $\sim 4.6\%$ has been confirmed by the CMB measurements; this shows that some information on the background level can only be obtained using PT.

- The second example is in the context of LSS. In first approximation, structure formation on large scales can be described by linear cosmological PT as long as the matter perturbation δ is smaller than unity (see [17] and references therein). The very first object one computes in this linear regime is the matter power spectrum, which encodes all the statistics of δ assuming that it is a Gaussian random field. It turns out that the prediction from linear PT matches

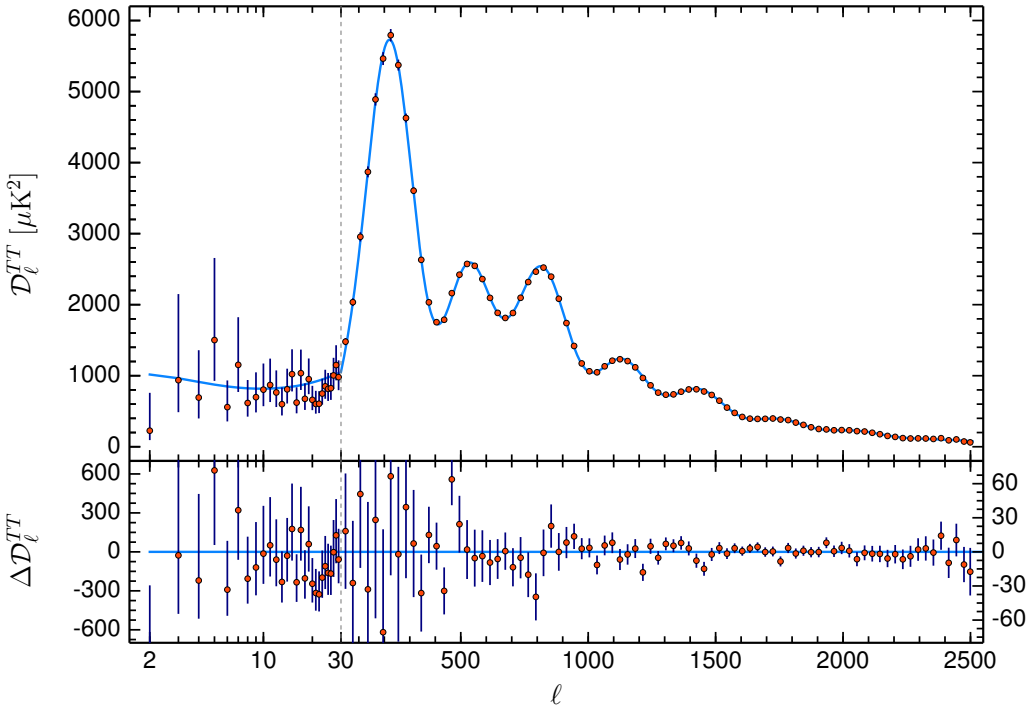

Figure 3: The CMB temperature power spectrum measured by Planck satellite [7]. The blue solid line shows the prediction of best fit ΛCDM model. The lower panel shows the residuals.

incredibly well with observations on large scales, shown in Figure 4. Clearly, at sufficiently high momenta, $k \gtrsim 0.1$ Mpc^{-1}, non-linearities become important; the standard PT is no longer applicable. Actually, using the EFT of LSS [18] one obtains the correction to the power spectrum at order $\delta(k)^4$, which is in agreement at percent level with the non-linear theory up to $k \simeq 0.24h$ Mpc^{-1}. This is indeed the current state-of-the-art calculations within PT (see [19, 20] for recent developments). Nevertheless, the fact that the perturbative technique requires $\delta < 1$ implies that the collapse of matter perturbation which begins at $\delta \sim 1$ is clearly outside the validity of PT. Besides, in this non-linear regime the Gaussian assumption does not apply anymore. We will come back to this point in the next Section.

- Regarding the early Universe, PT plays a central role in the computations of inflationary correlators. Within the framework of perturbative quantum field theory on the cosmological background one typically uses the so-called in-in formalism [22] to compute a correlation function of a primordial field such as the inflaton field ζ and the primordial GW field. For instance, considering the single field inflation one obtains the two-point and the three-point functions of ζ. Using the fact that ζ freezes outside the horizon, it thus allows us to make a connection between CMB correlations and inflationary correlations. Therefore, the fact that the distribution function of δT is nearly Gaussian and its amplitude is $\sim 10^{-5}$ on CMB scales implies that the statistics of ζ is well-described by a small deviation from Gaussianity. There are of course caveats on the use of PT, but we will come back to this point later on.

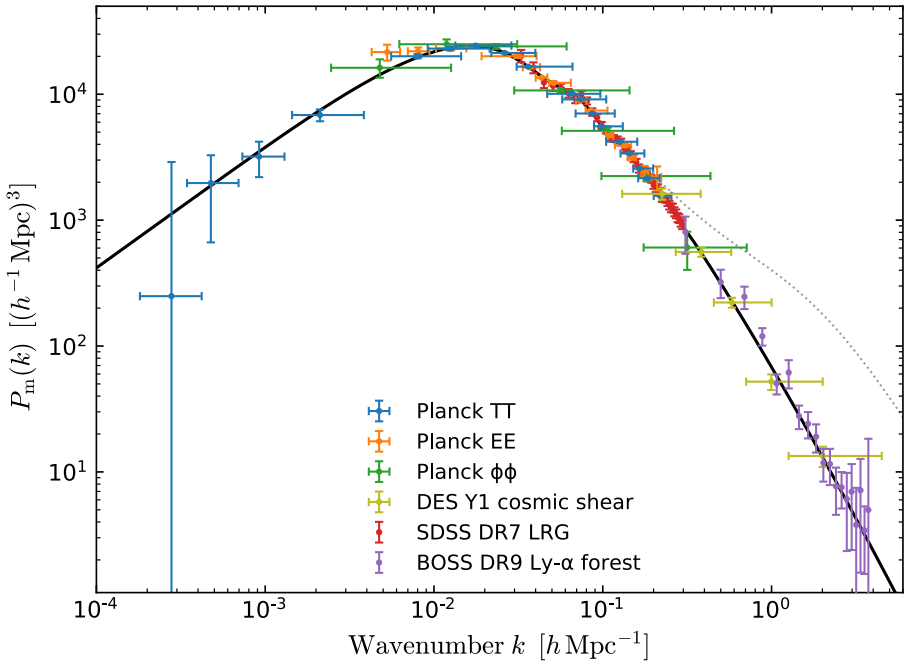

Figure 4: Observational data on the present linear power spectrum (black solid line) of matter perturbations [21].

- The last example is a coalescence of a compact binary such as black holes or neutron stars, providing a natural playground for PT. In particular, in the phase where the two objects are inspiraling each other with small orbital velocities or large separations one typically uses the so-called post-Newtonian (PN) approximation to general relativity to predict the gravitational-wave (GW) signals produced by such astrophysical sources, see [23–25] for reviews. Many results have been obtained in this direction. For instance, the 4PN corrections to the equations of motion of two spinless black holes using an effective field theory approach are obtained in [26]. For non-spinning binaries moving along quasi-circular orbits the gravitational-wave phase evolution has been computed up to 3.5PN [27], whereas amplitude corrections are known up to 3PN order [28]. (See [29] for comparison of numerical relativity simulations with post-Newtonian expansions.) In addition to PN approximation, the so-called black hole perturbation (BHP) theory ([30] and references therein) is a good tool to model compact binaries with mass ratios $m_1/m_2 \ll 1$, even for strong-field orbits with $r \gtrsim M \equiv m_1 + m_2$. The two methods mentioned above are complementary to each other covering different regimes of the mass ratios; this shows the power of PT in black hole physics.

Having seen that, PT is very pivotal for both early-times and late-times Universe. However, in many circumstances as we will study in this thesis PT is no longer a sufficient tool to describe the physics we are interested in. In the following we will point out some examples in cosmology where the analysis beyond PT is required.

LIMITATIONS OF PERTURBATION THEORY AND GOING BEYOND

There are several regimes in cosmology where the perturbative treatment fails to capture the relevant physics, which might be due to the presence of large non-linearities (a dimensionless expansion parameter becomes of order unity). A couple of examples are given below.

- As we have mentioned before, linear PT is not sufficient to describe the structure formation at small scales ($k_{NL} \simeq 0.01$ Mpc^{-1}) due to large non-linearities; therefore, it is necessary to find a new treatment where there is no $\delta \ll 1$ expansion. The concrete example is the gravitational collapse of a spherical top-hat overdensity to form dark matter halo, which occurs when δ exceeds a critical density. Typically, one employs an analytical approach such as the Press–Schechter (PS) formalism [31] and the excursion set formalism (extended Press-Schechter) [32] to determine a halo mass function for a given mass range. Note that the PS approach shows explicitly the relation of the abundance of nonlinear haloes and fundamental quantities from linear physics—the growth factor and the spectrum of fluctuations. On the numerical-simulation side, many works on dark matter haloes have been carried out, for example, the non-linear dynamical evolution (see e.g. [33, 34]) and the effects of the spin and shape [35].

- Cosmological phase transition is another example for which the calculation goes beyond PT. For instance, in the context of inflation, originally proposed in [36], the open FLRW Universe can be naturally realized through an effect of a false vacuum (de Sitter) decaying into the true vacuum (open FLRW). In fact, the decay rate Γ was first obtained in [37], making use of the $O(4)$-symmetric bounce solution: a solution of the Euclidean equation of motion that connects the initial and final configurations. The method to compute Γ is now known as the semiclassical approximation - compute the Euclidean action on the non-trivial field profiles, which captures the non-perturbative behavior. There are many effects on the cosmological observables at late times such as CMB power spectrum [38] and the production of GWs by bubble collisions [39]. Furthermore, as we will see in Chapter 5, the semiclassical method is amenable to capture the statistics of the tail of the distribution function, which is relevant for the primordial black hole (PBH) formation.

- Another example in the early Universe is a reheating, which essentially describes how the inflaton transfers its energy and momentum into the standard model particles. Originally, it was treated perturbatively in a way that one computes a perturbative decay of the inflaton into daughter fields. Later on, the treatment was improved taking into account the coherent effect of inflaton field, i.e. one solves the equation of motion for the daughter field on the time-dependent background of inflaton. This is indeed a non-perturbative reheating, called preheating [40]. Actually, we will see in Chapter 3 that the mathematical tools of preheating can be also applied to the case of GW decaying into dark energy fluctuations.

- The last example of the previous Section showed that PT is a good approximation to model the waveforms of GW during the inspiral phase, it is clearly not valid for predicting gravitational radiations emitted during the last orbits, final plunge and merger. There, one needs to consult numerical relativity (NR) to solve the exact Einstein equation in vacuum using supercomputer simulations (see [41] for recent review). NR simulations makes it possible to systematically capture the non-linear and relativistic effects of the binary, so that the waveform during those phases can be predicted and compared with the observations. Moreover, the ongoing works in this area focus on improving the accuracy and precision of numerical waveforms [42, 43] and taking into account the additional effects on the binaries such as spin [44] and precession [45–47].

Having encountered several non-perturbative examples, we are now going to focus on the topics discussed in this thesis.

SCOPE OF THE THESIS

The thesis is divided into two parts: dark energy and inflation. In the following let us summarize the main ideas of each Chapter.

- We first start reviewing the Effective Field Theory of Dark Energy (EFT of DE) in Chapter 2, constructed for the scalar and tensor perturbations on the flat FRLW background. The EFT can be mapped to the so-called (beyond) Horndeski theories - the most general scalar-tensor theories with second order equations of motion. We then discuss the implications on the EFT after putting the constraints on the speed of GWs, c_T, and the quartic beyond Horndeski parameter α_H. All of these bounds are obtained within PT.

- In Chapter 3, as the first non-perturbative case in this thesis, we study the decay of GWs into DE fluctuations, taking into account the effects of large occupation number of gravitons. This phenomenon is reminiscent of the case of preheating pointed out earlier. The bound on α_H becomes stronger compared to the perturbative one in the regime where non-linerities are not important and GW amplitude is small, whereas the bound on α_B (cubic Horndeski) remains inconclusive.

- The analysis of DE fields evolving in the presence of GW background whose amplitude is large will be studied in Chapter 4. There, we show that around the non-linear solution of DE the scalar fluctuations may not be always stable, i.e. they feature the so-called ghost or gradient instability. The absence of the instabilities amounts to putting a condition on the kinetic metric of the fluctuations which results in constraining the parameter α_B.

- In Chapter 5 we first point out the fact that the usual perturbative calculations in inflation breaks down in the large field limit, i.e. on the tail of the distribution. This is the last non-perturbative case in this thesis. We then propose that in this regime the wavefunction of the

Universe can be computed using a semiclassical approximation, $\hbar \to 0$. The results are relevant for the calculation of the abundance of PBHs.

The examples presented in this thesis are a recent development in understanding the physics beyond PT in cosmology. There are, of course, many theoretically and phenomenologically interesting questions; some of them will be pointed out at the end of each Chapter.

Part I

DARK ENERGY THEORIES

2

DARK ENERGY THEORIES AND THEIR CONSTRAINTS: A REVIEW

As a setup of our framework, this Chapter is devoted to give a quick review on the Effective Field Theory of Dark Energy (EFT of DE) and its constraints. In the first Section we will be dealing with the construction of the EFT of DE, following [48, 49]. Note that the main idea behind the EFT of DE is closely related to the EFT of Inflation, which will be used in Chapter 5. Exploiting the propagation and the perturbative decay of gravitational waves (GWs) places a very strong bound on the EFT parameters. These two topics will be discussed in the last two Sections.

2.1 RECAP ON EFT OF DE

The Effective Field Theory (EFT) approach is a very powerful tool to study physics at different scales, i.e. given the underlying symmetries one writes down the action compatible with such symmetries starting from the lowest dimensional operators. The important ingredient of the EFT is the presence of the cut-off, at which the EFT description breaks down and the UV completion is needed to study physics beyond such a scale. The idea of the EFT has been widely used in many areas, for instance, particle physics and condensed matter. The typical example of the EFT is the famous Fermi's theory, which describes the weak interaction of four fermions, such as the decay of neutron, within the mass scale comparable to the mass of W-boson. Of course, above such a mass scale we now know that Fermi's theory should be replaced by Standard Model of particle physics.

Having said that, here we are going to apply the same idea to describe a fluctuation around the cosmological background, namely the FLRW metric.

2.1.1 *EFT Action in Unitary Gauge*

The construction of the EFT is very straightforward, knowing all the field contents and symmetries of the system. In the DE sector we have a homogeneous background $\phi_0(t)$, which is responsible for an accelerating expansion of the Universe. In particular, the background metric is governed by the FLRW metric,

$$ds^2 = -dt^2 + a^2(t)\delta_{ij}dx^i dx^j \,, \tag{2.1.1}$$

where $a(t)$ is the scale factor and the indices $i, j = 1, 2, 3$ (here the convention for the metric is mostly plus). Having the accelerating expansion is equivalent to requiring that $\ddot{a} = a(\dot{H} + H^2) > 0$ in which H is the Hubble parameter $H \equiv \dot{a}/a$ and dot denotes the cosmic time derivative. Note that in the case of pure de Sitter expansion the Hubble parameter is a constant.

Now we are interested in the dynamics of the fluctuations around the background $\phi_0(t)$: $\phi = \phi_0(t) + \delta\phi(x)$. First notice that since the background depends on time, in the language of symmetry breaking we say that the time diffeomorphism is spontaneously broken. Intuitively, this is because of the fact that the scalar field acts as a clock since it gives a preferred-time direction. Indeed, the perturbation $\delta\phi$ is the Numbu-Goldstone field associated to the broken time diffeomorphism. This is to say that $\delta\phi$ transforms non-linearly under time diffeomorphism[1]:

$$t \to t + \xi^0(t, \mathbf{x}) \,, \quad \delta\phi \to \delta\phi + \dot{\phi}_0(t)\xi^0 \,. \tag{2.1.2}$$

Obviously, from the formula above one sees that $\delta\phi$ is a scalar only under spatial diffeomorphism.

Given the transformation of $\delta\phi$ (2.1.2), one can always choose ξ^0 such that $\delta\phi = 0$ and ϕ corresponds to time coordinate. This is the so-called unitary gauge, i.e. all the scalar perturbations are set to zero, while all degrees of freedom are inside the metric. In other words, the fluctuation $\delta\phi$ has been "eaten" by the graviton, which now describes three degrees of freedom: one scalar mode and two tensor helicities. This phenomenon is very similar to the case of spontaneously broken gauge theory, where a would-be Goldstone mode is eaten by a massless spin-1 field, which then becomes a massive spin-1 field. We will come to back to this point when we discuss the Stueckelberg procedure.

Geometrically, in this gauge the spacetime is foliated by a space-like hypersurface of constant ϕ; therefore, it is natural to define a unit time-like vector n_μ perpendicular to such hypersurface,

$$n_\mu \equiv -\frac{\partial_\mu\phi}{\sqrt{-(\partial_\mu\phi)^2}} \to -\frac{\delta^0_\mu}{\sqrt{-g^{00}}} \,, \tag{2.1.3}$$

where g^{00} denotes the time-time component of the inverse metric, and the induced metric on the surface,

$$h_{\mu\nu} \equiv g_{\mu\nu} + n_\mu n_\nu \,. \tag{2.1.4}$$

From the definitions above, it is easy to see that $n^\mu h_{\mu\nu} = 0$. The intrinsic geometry of the hypersurface is determined by the 3d Riemann tensor ${}^{(3)}R_{\nu\mu\rho\sigma}$ made out of the metric $h_{\mu\nu}$, whereas the extrinsic one is described by K^μ_ν:

$$K^\mu_\nu \equiv h^{\mu\rho}\nabla_\rho n_\nu \,. \tag{2.1.5}$$

Notice that from the expression above we have $K^\mu_\nu n_\mu = 0 = K^\mu_\nu n^\nu$.

The question now is what is the most general Lagrangian in this particular gauge? First, since time diffeomorphism has been fixed, one must write down operators that are functions of the metric $g_{\mu\nu}$ and that are invariant under time-dependent 3d diffeomorphism, $x^i \to x^i + \xi^i(t, \mathbf{x})$. Looking at the geometrical objects we have defined above, it is straightforward to realize that they can form an invariant operator under the spatial diffeomorphism. For example, g^{00} transforms trivially under

1 This can be easily seen by the fact that under $x^\mu \to x^\mu + \xi^\mu$ an infinitesimal transformation of a scalar field is given by $\delta_\xi\phi = \xi^\mu\partial_\mu\phi$.

special diffeomorphism, so that it can appear freely in the unitary gauge Lagrangian. In particular, one can have a polynomial in g^{00}, which does not contain derivatives. Also, the 3d scalar objects, for instance, the 3d Ricci scalar or $K^\mu_\nu K^\nu_\mu$ can be included into the Lagrangian. On top of this, the time-dependent functions are allowed to appear in the EFT action in this gauge. Finally, the action can also contain the objects that are invariant under 4d diffeomorphism, such as the 4d Ricci scalar and the various combinations of Riemann tensors.

Overall the EFT action in the unitary gauge, expanded around the flat FRLW metric, $ds^2 = -dt^2 + a^2(t)dx^2$, is given by [48, 50]

$$S_{\rm EFT} = \int d^4x\sqrt{-g}\Big[\frac{M_\star^2}{2}f(t)^{(4)}R - \Lambda(t) - c(t)g^{00} + \frac{1}{2!}m_2^4(t)(\delta g^{00})^2 + \frac{1}{3!}M_3^4(t)(\delta g^{00})^3 - \frac{1}{2}m_3^2(t)\delta K\delta g^{00} - \frac{1}{3!}\bar{M}_2^2(t)\delta K^2 - \frac{1}{3!}\bar{M}_3^2(t)\delta K^\mu_\nu\delta K^\nu_\mu + \dots\Big]\,, \tag{2.1.6}$$

where we have defined $\delta g^{00} \equiv 1 + g^{00}$ and $\delta K^\mu_\nu \equiv K^\mu_\nu - H\delta^\mu_\nu$, and the ellipsis stands for the higher-order operators in perturbations or derivatives. Notice that this action does not correspond to the most general scalar-tensor theories with second-order EoM. We will come back to this point later.

First of all, one sees that all the coefficients are allowed to depend on time since, as explained before, the time diffeomorphism is spontaneously broken.

In (2.1.6) the first three terms contain zeroth-order and first-order in perturbations, while all the other terms are explicitly quadratic or higher. Note that the first term is actually the usual Einstein-Hilbert action with the time-dependent Planck mass. Clearly, one can always perform a conformal transformation (field redefinition) of the metric such that the action looks exactly the same as the one of GR, without time-dependent function. This procedure changes the action from the Jordan frame to the Einstein frame. However, performing such a field redefinition of the metric leads to the fact that matters are no longer minimally coupled to the metric.

It is easy to see that the coefficients $c(t)$ and $\Lambda(t)$ contribute to the background FLRW evolution. In other words, the two coefficients are fixed by requiring that the tadpole terms vanish, so that the background equations remain the same. Assuming that the stress-energy tensor of matter is of a perfect fluid form, $T^\mu_\nu = \mathrm{diag}(-\rho_m, P_m, P_m, P_m)$, then the requirement above gives

$$c(t) = \frac{1}{2}\Big[M_\star^2(-\ddot{f} + \dot{f}H - 2f\dot{H}) - \rho_m - P_m\Big]\,, \tag{2.1.7}$$

$$\Lambda(t) = \frac{1}{2}\Big[M_\star^2(\ddot{f} + 5\dot{f}H + 2f\dot{H} + 6fH^2) - \rho_m + P_m\Big]\,. \tag{2.1.8}$$

where ρ_m and P_m are respectively the energy density and the pressure. Besides, the covariant conservation of $T_{\mu\nu}$ ($\nabla_\mu T^\mu_\nu = 0$) yields the continuity equation, $\dot{\rho}_m + 3H(\rho_m + P_m) = 0$. One thus concludes that the unperturbed FLRW history fixes the parameters $c(t)$ and $\Lambda(t)$, whereas the deviation of different models of DE is encoded into the higher-order operators.

Typically, when the equations of motion contain more than two derivatives per field the theory becomes unhealthy due to the presence of the so-called Ostrogradski ghosts [51]. In particular, in order to avoid such an instability one requires that there are at most two derivatives acting on the

field in the equations of motion. Given this condition, it has been found that the most general EFT of DE, which corresponds to having the second-order equations of motion, is [52, 53]

$$S_{EFT} = \int d^4x\sqrt{-g}\Big[\frac{M_*^2}{2}f(t)\,{}^{(4)}\!R - \Lambda(t) - c(t)g^{00} + \frac{m_2^2(t)}{2}(\delta g^{00})^2 - \frac{m_3^3(t)}{2}\delta K\delta g^{00} - m_4^2(t)\delta\mathcal{K}_2 + \frac{\tilde{m}_4^2(t)}{2}\delta g^{00}\,{}^{(3)}\!R - \frac{m_5^2(t)}{2}\delta g^{00}\delta\mathcal{K}_2 - \frac{m_6(t)}{3}\delta\mathcal{K}_3 - \tilde{m}_6(t)\delta g^{00}\delta\mathcal{G}_2 - \frac{m_7(t)}{3}\delta g^{00}\delta\mathcal{K}_3\Big]\,, \tag{2.1.9}$$

with

$$\delta\mathcal{K}_2 = \delta K^2 - \delta K^\mu_\nu\delta K^\nu_\mu\,, \quad \delta\mathcal{G}_2 = \delta K^\mu_\nu\,{}^{(3)}\!R^\nu_\mu - \delta K\,{}^{(3)}\!R/2\,, \tag{2.1.10}$$

$$\delta\mathcal{K}_3 = \delta K^3 - 3\delta K\delta K^\mu_\nu\delta K^\nu_\mu + 2\delta K^\nu_\mu\delta K^\mu_\rho\delta K^\rho_\nu\,. \tag{2.1.11}$$

In fact, for $m_4^2 = \tilde{m}_4^2$ and $m_6 = \tilde{m}_6$ the action above has been shown to be equivalent to Horndeski theories[2] [55, 56], which are the most general scalar-tensor theories with second-order equations of motion. In addition, the case where $m_4^2 \neq \tilde{m}_4^2$ and $m_6 \neq \tilde{m}_6$ corresponds to the so-called beyond Horndeski theories or Gleyzes-Langlois-Piazza-Vernizzi (GLPV) theories [57][3]. Note that in some gauges, the equations of motion of the metric and the scalar field in these theories appear to contain more than two derivatives per field. Nevertheless, written in terms of the propagating degrees of freedom the equations of motion reduce to the second order. Hence, no Ostrogradski ghosts.

We finish this Subsection by commenting on the scales relevant for the EFT of DE. There are two relevant energy scales: one is the so-called Λ_3 and the other is Λ_2. The scale Λ_3 is the cut-off of the EFT, defined by

$$\Lambda_3 \equiv (M_{Pl}H_0^2)^{1/3}\,, \tag{2.1.12}$$

where H_0 is the Hubble constant at present time, $\sim 10^{-33}$ eV. As usual, if the energy of our interest is above the cut-off scale, the EFT is no longer a good description. Notice that this Λ_3 approximately corresponds to $\sim 10^{-13}$ eV or $\sim (1000\text{ km})^{-1}$ in terms of length scale. The other scale Λ_2 is associated to the background value of DE field (cosmological constant), defined by

$$\Lambda_2 \equiv (M_{Pl}H_0)^{1/2}\,. \tag{2.1.13}$$

In other words, this is the scale at which the Lorentz invariance is spontaneously broken by the background $\phi_0(t)$. Note that $\Lambda_2 \sim 10^{-3}$ eV or $\sim (1\text{ mm})^{-1}$, which is parametrically larger than Λ_3. Indeed, the radiative corrections generated from (2.1.9) at scales $E < \Lambda_3$ are generally suppressed by the ratio $(\Lambda_3/\Lambda_2) \sim 10^{-10}$ (see [59] for more details).

2 Horndeski theories are invariant under $g_{\mu\nu} \to \Omega^2(\phi)g_{\mu\nu} + \Gamma(\phi)\partial_\nu\phi\partial_\nu\phi$, where Ω and Γ are an arbitrary function of ϕ (see [54] for more detail).

3 Actually it has been explicitly shown in [58] that the sub-classes of GLPV theories are related to Horndeski theories via the disformal transformation with an X-dependent function Γ, $X = (\partial\phi)^2$.

2.1.2 *Stueckelberg Procedure*

As we have seen in the last Section, the way we constructed the EFT action was based on the fact that the time diffeomorphism is spontaneously broken in the unitary gauge. General speaking, in order to restore a full gauge invariance without changing the physics, one performs a broken transformation with a gauge parameter being promoted to a field. This procedure is known as the Stueckelberg procedure.

It is actually useful to start with an example of a $U(1)$ massive gauge field A_μ. In this case, the Lagrangian in the unitary gauge reads

$$\mathcal{L} = -\frac{1}{4}F_{\mu\nu}F^{\mu\nu} - \frac{m^2}{2}A_\mu A^\mu - \frac{g^2}{4}(A_\mu A^\mu)^2 \,, \tag{2.1.14}$$

where the field strength $F_{\mu\nu} \equiv \partial_\mu A_\nu - \partial_\nu A_\mu$ and m is the mass of the gauge field. Notice that we have also included the self-interaction term of A_μ with the coupling g. Here it is easy to realize that the mass term and the self-interaction term are not invariant under $A_\mu \to A_\mu + \partial_\mu \Lambda(x)$, where $\Lambda(x)$ is the gauge parameter. Therefore, there are three propagating degrees of freedom of the field A_μ: one longitudinal mode and two transverse modes. Now to restore the gauge symmetry one performs

$$A_\mu \to A_\mu - \partial_\mu \pi \,, \tag{2.1.15}$$

where $\pi(x)$ is a field. Hence we have

$$\mathcal{L} = -\frac{1}{4}F_{\mu\nu}F^{\mu\nu} - \frac{m^2}{2}(D_\mu \pi D^\mu \pi) - \frac{g^2}{4}(D_\mu \pi D^\mu \pi)^2 \,, \tag{2.1.16}$$

where we defined $D_\mu \pi \equiv \partial_\mu \pi - A_\mu \pi$. One can easily verify that the Lagrangian above is now invariant under $A_\mu \to A_\mu + \partial_\mu \Lambda(x)$ and $\pi \to \pi + \Lambda$. Of course, the choice $\Lambda = -\pi$ corresponds to the unitary gauge. It is thus clear that the Lagrangian (2.1.16) describes two transverse vector modes A_μ and one longitudinal scalar mode π (Goldstone boson of broken $U(1)$).

The π field can be canonically normalized as $\pi_c = m\pi$, so that the self-coupling becomes strongly coupled at energy scale m/g, for $g << 1$. On top of this, the mixing between A_μ and π_c goes as $mA^\mu \partial_\mu \pi$. This means that when the energy scales E is much larger than m the longitudinal mode π and the transverse modes A_μ are decoupled. Therefore, in the range $m << E << m/g$ the physics of Goldstone boson π is weakly coupled and it can be studied neglecting the mixing with the transverse modes. (This phenomenon is confirmed by the Goldstone equivalence theorem which states that the scattering amplitude involving the longitudinal gauge bosons at energy scales $E >> m$ is the same as the amplitude replacing the longitudinal modes with the Goldstone bosons plus the corrections of order m/E.)

We are now ready to apply the Stueckelberg procedure to the action (2.1.9). In this case, since the time diffeomorphism is broken, one performs $t \to t + \pi(x)$ and $\mathbf{x} \to \mathbf{x}$, where $\pi(x)$ is the Goldstone boson. Indeed, this $\pi(x)$ field represents a scalar degree of freedom in the DE sector. From the

action (2.1.9) there are two ways which can re-introduce $\pi(x)$ via the Stueckelberg trick. First, any time-dependent coefficient, such as $c(t)$, generates terms which contain π without derivatives:

$$c(t) \to c(t+\pi(x)) = c(t) + \dot{c}(t)\pi + \frac{1}{2}\ddot{c}(t)\pi^2 + \dots \,, \tag{2.1.17}$$

where the arrow means we performed $t \to t+\pi(x)$. Second, operators which are not invariant under 4d diffeomorphism transform under time diffeomorphism and thus generate terms containing derivatives acting on $\pi(x)$. For instance, under $t \to t+\pi(x)$, g^{00} transforms as

$$\begin{aligned} g^{00}(x) &\to \frac{\partial(t+\pi)}{\partial x^\mu}\frac{\partial(t+\pi)}{\partial x^\nu} g^{\mu\nu}(x) \\ &= (1+\dot{\pi})^2 g^{00} + 2(1+\dot{\pi})g^{0i}\partial_i\pi + g^{ij}\partial_i\pi\partial_j\pi \\ &= g^{00} + 2g^{0\mu}\partial_\mu\pi + g^{\mu\nu}\partial_\mu\pi\partial_\nu\pi \,. \end{aligned} \tag{2.1.18}$$

Furthermore, we give a few relevant examples:

$$g^{0i} \to g^{0i} + g^{\mu i}\partial_\mu\pi \,, \tag{2.1.19}$$

$$\delta K^i_j \to \delta K^i_j - \dot{H}\pi\delta^i_j - N h^{ik}\partial_k\partial_j\pi + \mathcal{O}(2) \,, \tag{2.1.20}$$

$$\delta K \to \delta K - 3\dot{H}\pi - N h^{ij}\partial_i\partial_j\pi + \mathcal{O}(2) \,, \tag{2.1.21}$$

$${}^{(3)}R \to {}^{(3)}R - 2\dot{h}^{ij}\partial_i\partial_j\pi + \mathcal{O}(2) \,, \tag{2.1.22}$$

where in the last three lines we have expanded up to linear order in π. The expansions of δK, δK^i_j and ${}^{(3)}R$ up to second order in π can be found in [53]. Note that to obtain the formulas (2.1.20)-(2.1.22) we have used the fact that they can be expressed in terms of the ADM variables (the lapse function N, the shift vector N^i and the spatial metric h_{ij}). For completeness, under $t \to t+\pi(x)$, they transform as

$$N \to N(1-\dot{\pi}) + \mathcal{O}(2) \,, \tag{2.1.23}$$

$$N \to N^i + N^2 h^{ik}\partial_k\pi + \mathcal{O}(2) \,, \tag{2.1.24}$$

$$h_{ij} \to h_{ij} - N_i\partial_j\pi - N_j\partial_i\pi + \mathcal{O}(2) \,. \tag{2.1.25}$$

Finally, let us consider, for example, the first three terms in (2.1.9). After performing the Stueckelberg trick we obtain

$$\begin{aligned} S = \int d^4x\sqrt{-g}\Bigg[&\frac{M_\star^2}{2}{}^{(4)}R - M_\star^2\Big(\dot{H}(t+\pi(x)) + 3H^2(t+\pi(x))\Big) \\ &+ M_\star^2\dot{H}(t+\pi(x))\Big((1+\dot{\pi})^2 g^{00} + 2(1+\dot{\pi})g^{0i}\partial_i\pi + g^{ij}\partial_i\pi\partial_j\pi\Big)\Bigg] \,, \end{aligned} \tag{2.1.26}$$

where we have used (2.1.8) and (2.1.7) to replace $\Lambda(t)$ and $c(t)$ in terms of $H(t)$, setting $\rho_m = P_m = 0$ and $f(t) = 1$. In analogy with the gauge theory case, at sufficiently high energy scales one can focus on the physics of the Goldstone boson, neglecting metric fluctuations. In (2.1.26) one sees that the mixing between $\dot{\pi}$ and δg^{00} is of the form $M_\star^2\dot{H}\dot{\pi}\delta g^{00}$. The fields π and δg^{00} can be canonically

normalized as $\pi_c \sim M_\star \dot{H}^{1/2}\pi$ and $\delta g^{00}_c \sim M_\star \delta g^{00}$. Therefore, the mixing can be neglected for energy scales $E > \dot{H}^{1/2}$. Notice that this conclusion might change when the additional operators in the EFT are present and one needs a more detailed analysis of the mixing.

As we will see later, the Stueckelberg procedure is extremely useful to derive the interactions of gravitons γ_{ij} and DE fields π.

2.1.3 *Connection with the Covariant Formulation*

To complete the Section on EFT of DE, here we would like to give a connection between the EFT action (2.1.9) and the covariant formulation of (beyond) Horndeski theories, also known as GLPV theories [57, 58]. Here we define $X \equiv g^{\mu\nu}\partial_\mu\phi\partial_\nu\phi = (\partial\phi)^2$, $\Box\phi \equiv \phi^{;\mu}_{;\mu}$. Also, a comma denotes a partial derivative and a semicolon the covariant derivative. The GLPV action is given by

$$S = \int d^4x\sqrt{-g}\sum_{I=2}^{5} L_I \,, \tag{2.1.27}$$

where

$$L_2 \equiv G_2(\phi, X) \,, \tag{2.1.28}$$

$$L_3 \equiv G_3(\phi, X)\Box\phi \,, \tag{2.1.29}$$

$$\begin{aligned} L_4 \equiv\ & G_4(\phi, X)R - 2G_{4,X}(\phi, X)[(\Box\phi)^2 - \phi_{;\mu\nu}\phi^{;\mu\nu}] \\ & - F_4(X, \phi)\epsilon^{\mu\nu\rho}_{\ \ \ \sigma}\epsilon^{\mu'\nu'\rho'\sigma}\phi_{;\mu}\phi_{;\mu'}\phi_{;\nu\nu'}\phi_{;\rho\rho'} \,, \end{aligned} \tag{2.1.30}$$

$$L_5 \equiv G_5(\phi, X)G_{\mu\nu}\phi^{;\mu\nu} + \frac{1}{3}G_{5,X}(\phi, X)[(\Box\phi)^3 - 3(\Box\phi)\phi_{;\mu\nu}\phi^{;\mu\nu} + 2\phi_{\mu\nu}\phi^{;\sigma\mu}\phi^{;\nu}_{;\sigma}] \,, \tag{2.1.31}$$

$$- F_5(\phi, X)\epsilon^{\mu\nu\rho\sigma}\epsilon^{\mu'\nu'\rho'\sigma'}\phi_{;\mu}\phi_{;\mu'}\phi_{;\nu\nu'}\phi_{;\rho\rho'}\phi_{;\sigma\sigma'} \,. \tag{2.1.32}$$

This is the most general scalar-tensor theories with second-order EoM. Note that the symbol $\epsilon_{\mu\nu\rho\sigma}$ refers to the totally anti-symmetric Levi-Civita tensor.

On the cosmological background, the EFT parameters in (2.1.6) can be written in terms of the (beyond) Horndeski functions G_2, G_3, G_4, G_5, F_4 and F_5 as

$$M^2 = M_\star^2 f + 2m_4^2 = 2G_4 - 4XG_{4,X} - X(G_{5,\phi} + 2H\dot{\phi}G_{5,X} + 2X^2F_4 - 6H\dot{\phi}X^2F_5 \,, \tag{2.1.33}$$

$$m_4^2 = \tilde{m}_4^2 + X^2F_4 - 3H\dot{\phi}X^2F_5 \,, \tag{2.1.34}$$

$$\tilde{m}_4^2 = -[2XG_{4,X} + XG_{5,\phi} + (H\dot{\phi} - \ddot{\phi})XG_{5,X}] \,, \tag{2.1.35}$$

$$\begin{aligned} m_5^2 = X[&2G_{4,X} + 4XG_{4,XX} + H\dot{\phi}(3G_{5,X} + 2XG_{5,XX}) + G_{5,\phi} + XG_{5,X\phi} - 4XF_4 \\ &- 2X^2F_{4,X} + H\dot{\phi}X(15F_5 + 6XF_{5,X})] \,, \end{aligned} \tag{2.1.36}$$

$$m_6 = \tilde{m}_6 - 3\dot{\phi}X^2F_5 \,, \tag{2.1.37}$$

$$\tilde{m}_6 = -\dot{\phi}XG_{5,X} \,, \tag{2.1.38}$$

$$m_7 = \frac{1}{2}\dot{\phi}X(3G_{5,X} + 2XG_{5,XX} + 15XF_5 + 6X^2F_{5,X}) \,. \tag{2.1.39}$$

The explicit expressions for m_2 and m_3 in terms of the (beyond) Horndeski functions can be found in [52, 53].

We end this Subsection by discussing the relevant dimensionless parameters of the EFT of DE and their physical interpretations. We define the following dimensionless parameters [60, 61]:

$$\alpha_K \equiv \frac{2c + 4m_2^4}{M^2H^2}\,, \quad \alpha_B \equiv \frac{M_\star^2\dot{f} - m_3^3}{2M^2H}\,, \quad \alpha_M \equiv \frac{M_\star^2\dot{f} + 2(m_4^2)^{\cdot}}{M^2H}\,, \tag{2.1.40}$$

$$\alpha_T \equiv -\frac{2m_4^2}{M^2}\,, \qquad \alpha_H \equiv \frac{2(\tilde{m}_4^2 - m_4^2)}{M^2}\,. \tag{2.1.41}$$

The physical implications on DE and GWs of each parameter can be summarized as follows.

- Kineticity α_K: it canonically normalizes the kinetic term of the scalar fluctuation π. Besides, it determines the speed of sound c_s of the scalar mode. In the covariant formulation, all the functions G_i and F_i gives contributions to the parameter α_K, whereas in the EFT only the operator $(\delta g^{00})^2$ contributes to it.

- Braiding α_B: kinetic mixing between the scalar and the metric [62]. Due to this mixing, this parameter α_B also appears in the canonical normalization of the scalar mode through the parameter $\alpha \equiv \alpha_K + 6\alpha_B^2$. In the GLPV theories, all the functions except G_2 contribute to α_B. Moreover, the operator $\delta g^{00}\delta K$ and the time-dependent Planck mass give contributions to the braiding α_B in the EFT Lagrangian.

- Running of the Planck mass α_M: it is the time-dependence of the Planck mass. It parametrizes the non-minimal coupling in the theories, e.g. Brans-Dicke theory. Also, α_M modifies the friction term in the propagation equation of GWs [63], which affects the amplitude of GWs traveling across the cosmological distances. The Horndeski functions G_4 and G_5 give contributions to α_M, while in the EFT only the operator m_4 and the time-dependent function $f(t)$ contribute to it.

- Tensor speed excess α_T: the deviation of the speed of GWs propagation from the speed of light. It gets contributions from G_4, G_5, F_4 and F_5 in the covariant formulation, while the operator $\delta\mathcal{K}_2$ in the EFT modifies the speed of GWs. We will come back to this point in detail in the next Section.

- Beyond Horndeski α_H: it parametrizes the size of beyond Horndeski functions F_4 and F_5 in linear perturbation theory. It is also known as the kinetic matter mixing because it gives rise to the mixing between matter and the scalar mode.

The size of these dimensionless parameters tells us how much the theories are deviated from GR. In the next two Sections we will discuss the bounds on α_T and α_H: roughly speaking the former is obtained by the fact that the speed of GWs differs from the one of light by 10^{-15}, and the latter is obtained by the fact that there is no decay of GWs into two DE fields. Both bounds are applicable at energy scales of LIGO/Virgo.

2.2 DARK ENERGY THEORIES AFTER GW170817 AND GRB170817A

In this Section we give the first constraint on the EFT of DE after the celebrated detection of GW signal (GW170817) [64] and the gamma-ray burst (GRB170817A) [65], both coming from the merging of the two neutron stars. Note that the bounds on specific models of (beyond) Horndeski have been obtained in [50, 66–68].

The association of GW170817 and GRB170817A events allowed to make an extraordinarily precise measurement of the speed of gravitational waves (GWs): it is compatible with the speed of light with deviations smaller than a few 10^{-15} [69]. This measurement incredibly improves our understanding of dark energy/modified gravity. These scenarios are characterized by a cosmological "medium" which interacts gravitationally with the rest of matter. The presence of this medium whose size is determined by a cosmological constant, implies that the Lorentz symmetry is spontaneously broken. Therefore, there is no a priori reason to expect that GWs, which are an excitation of this medium, travel at the same speed of light [70, 71].

The goal here is to extract the quadratic Lagrangian for graviton γ_{ij}. First, we consider the metric fluctuation around the flat FLRW metric, $ds^2 = -dt^2 + a^2(t)(e^{\gamma})_{ij}dx^i dx^j$. We further require that γ_{ij} satisfies the transverse ($\partial_i\gamma_{ij} = 0$) and traceless ($\gamma_{ii} = 0$) conditions, so that it represents the two helicities of GWs. In (2.1.9) there are two operators that contribute to the kinetic term of γ_{ij}: one is the Einstein-Hilbert term and the other is $m_4^2\delta\mathcal{K}_4$ operator. It is easy to see that the former term yields the usual kinetic term for γ_{ij}, in which the speed is unity. On the other hand, the latter term, which contains the extrinsic curvature K_{ij}, only contributes to the time kinetic term for γ_{ij}. Therefore, the quadratic action for γ_{ij} is given by

$$S_\gamma^{(2)} = \frac{M_\star^2 f}{8}\int d^4x\left[\left(1+\frac{2m_4^2}{M_\star^2 f}\right)\dot{\gamma}_{ij}^2 - \frac{(\partial_\ell\gamma_{ij})^2}{a^2}\right] . \tag{2.2.1}$$

Once canonically normalizing γ_{ij} the tensor speed excess α_T reads

$$\alpha_T \equiv c_T^2 - 1 = -\frac{2m_4^2}{M_*^2 f + 2m_4^2} . \tag{2.2.2}$$

Actually, the fact that $c_T^2 \neq 1$ in these theories can be visualized as GWs traveling in a time-dependent dark energy medium. This is indeed in a close analogy with light propagating in a medium such as water.

Before we put the bound on c_T^2, it is useful to discuss the validity of the EFT of DE at LIGO/Virgo scales. First, notice that the GW frequency at LIGO/Virgo is around 10^{-13} eV or 100 Hz, which is close to the scale Λ_3. Of course, above Λ_3 one starts probing new physics and the EFT description is no longer applicable. Despite the fact that the measured GW momentum may be of the same order as the cut-off of the EFT and high-dimensional operators may play some role, we do not expect that high-energy corrections conspire to completely cancel the modification of the GW speed. Moreover, the previous speed limits from gravitational Cherenkov radiation of cosmic rays [72] can only be applied to high energy GWs, which is outside the regime of validity of the EFT.

It is also worth mentioning that if the low-energy EFT breaks down below the cut-off scale Λ_3, the UV completion is required to describe the GW propagation and the bound on c_T^2 at LIGO/Virgo scales does not apply to the low-energy theory. (The concrete example, where the IR theory with $c_T^2 \neq 1$ breaks down below Λ_3 and the new physics enters to recover $c_T^2 = 1$ above Λ_3, is discussed in [73].) However, since the UV completion of the EFT of DE is currently not known, it is very difficult to make a precise statement about the scale at which the theory becomes strongly-decoupled or breaks down. Given the above reasoning, we now assume that the EFT of DE describe the GW propagation at LIGO/Virgo scales.

Now we are ready to put the bounds on the EFT parameters. We use the fact that c_T^2 is constrained to be [69][4]:

$$|c_T^2 - 1| \lesssim 10^{-15} \,, \tag{2.2.3}$$

so that the coefficient m_4^2 must be extremely small. For phenomenological reason one sets $\alpha_T = 0$ or $m_4^2 = 0$.

Yet, this bound on m_4^2 depends on the specific background the EFT is expanded around. In particular, changing a tiny amount of the Hubble expansion or the background energy density of dark matter would result in reshuffling the coefficients of the EFT. Hence, the speed c_T^2 will be different from unity.

Concretely, let us now derive all the changes of the m_4^2-operator due to the variation of the background. Indeed, the variation of the energy density or the pressure of dark matter can be viewed as an independent homogeneous and isotropic variation of the metric, i.e. $g^{00}(t)$ and of the Hubble parameter $H(t)$. From eq. (2.1.9), one sees that the changes in δg^{00} and δK give rise to a shift of the coefficient m_4^2. We denote the independent variations of the background of g^{00} by δg_b^{00} and of $H(t)$ by δH_b. We find that the change of the extrinsic curvature K is

$$\delta K_b = 3\delta H_b - \frac{3}{2} H \delta g_b^{00} \,. \tag{2.2.4}$$

Therefore, only cubic or higher operators in eq. (2.1.9) can contribute to the variation of parameter m_4^2, denoted by δm_4^2.

Let us start with the linear-order changes in m_4^2. First, the $\tilde{m}_4^2$ and m_5^2 operators, once $\delta g^{00} \to \delta g_b^{00}$, change the spatial and the time kinetic terms of γ_{ij} respectively, so that δm_4^2 reads

$$\delta m_4^2 = \frac{1}{2}(\tilde{m}_4^2 - m_5^2)\delta g_b^{00} \,. \tag{2.2.5}$$

For operator $m_6 \delta\mathcal{K}_3$, we can obtain quadratic contributions by evaluating one of its δK_ν^μ on the background. We find that

$$\delta m_4^2 = m_6 \delta H_b - \frac{1}{2} m_6 H \delta g_b^{00} \,, \tag{2.2.6}$$

where we have used eq. (2.2.4) and the fact that $(\delta\mathcal{K}_3)_b = \delta K_b \delta\mathcal{K}_2$.

4 This is due to the arrival time delay which is around 2 seconds between the GW signal and the gamma-ray burst.

The last contribution to δm_4^2 comes from $\tilde{m}_6^2$-operator. This operator turns out to give a change to the spatial kinetic term for γ_{ij}[5], which can be translated to δm_4^2 as

$$\delta m_4^2 = \frac{1}{2}\left[\tilde{m}_6 H \delta g_b^{00} + (\tilde{m}_6 \delta g_b^{00})^{\cdot}\right] . \tag{2.2.7}$$

Therefore, at linear order summing overall contributions to δm_4^2 gives

$$\delta m_4^2 = \frac{1}{2}(m_5^2 - \tilde{m}_4^2)\delta g_{bg}^{00} + m_6 \delta H_{bg} - \frac{1}{2}(m_6 - \tilde{m}_6) H_{bg} \delta g_{bg}^{00} + \frac{1}{2}(\tilde{m}_6 \delta g_{bg}^{00})^{\cdot} . \tag{2.2.8}$$

In order for $c_T^2 = 1$, the change δm_4^2 above should be set to zero at any orders. Since there is only one term containing δH, it is clear that $m_6 = 0$. Also, the term $\delta \dot{g}_b^{00}$ only enters through the coefficient $\tilde{m}_6$ then we set $\tilde{m}_6 = 0$ as well. Lastly, demanding that $\tilde{m}_4^2 = m_5^2$ makes all the remaining contributions vanish, hence $\delta m_4^2 = 0$.

At second order, one considers the operator $m_7 \delta g^{00} \delta \mathcal{K}_3$. In this case we need to evaluate δg^{00} and one δK^{μ}_{ν} on the background. However, since this is the only term in which $\delta g_b^{00} \delta H_b$ appears, we then set $m_7 = 0$.

To sum up, all the constraints on the EFT coefficients compatible with $c_T^2 = 1$ can be summarized as[6]

$$m_4 = 0 , \quad \tilde{m}_4^2 = m_5^2 , \quad m_6 = \tilde{m}_6 = m_7 = 0 . \tag{2.2.9}$$

These constraints are very strong and can be applied to the perturbed FLRW background.

Before closing this Section, it is instructive to express the EFT constraints in terms of the parameters of the covariant theories (see Section 2.1.3). Given the formulas (2.1.34) and (2.1.35), setting $c_T^2 = 1$ implies that

$$G_{5,X} = 0 , \quad F_5 = 0 , \quad 2G_{4,X} - XF_4 + G_{5,\phi} = 0 . \tag{2.2.10}$$

Note that these requirements must be true on any background and thus must hold for any value of $\dot{\phi}$ (or X), $\ddot{\phi}$ and H. Clearly, the beyond Horndeski function F_5 must be absent, whereas the function G_5 can be at most a function of ϕ. The other beyond Horndeski function F_4 remains unconstrained, but it has to satisfy the last condition of eq. (2.2.10), which corresponds to $\tilde{m}_4^2 = m_5^2$ in the EFT formulation. Thus, using eq. (2.2.10) in the Lagrangian (2.1.27) we obtain

$$\mathcal{L}_{c_T^2=1} = G_2(\phi, X) + G_3(\phi, X)\Box\phi + f(\phi, X)\,{}^{(4)}R - \frac{4}{X} f_{,X}(\phi, X)(\phi^{;\mu}\phi^{;\nu}\phi_{;\mu\nu}\Box\phi - \phi^{;\mu}\phi_{;\mu\nu}\phi_{;\lambda}\phi^{;\lambda\nu}) , \tag{2.2.11}$$

where $f(\phi, X) \equiv G_4(\phi, X) + XG_{5,\phi}/2$. Notice that the field redefinition of the metric, $g_{\mu\nu} \to C(\phi, X) g_{\mu\nu}$ which does not change the light-cone, transforms the Lagrangian above to the form of the more general Degenerate Higher-Order Scalar-Tensor (DHOST) [76] or Extended Scalar-Tensor theories [77] (see [50] for the explicit DHOST Lagrangian with $c_T^2 = 1$).

5 One evaluates δg^{00} on the background and uses the formula (8) of [52], disregarding the boundary terms.

6 The discussion of a possible loophole of these constraints can be found in [74, 75].

2.3 PERTURBATIVE GRAVITATIONAL WAVE DECAY INTO DARK ENERGY

In this Section we study another phenomenon which is allowed by the fact that the Lorentz invariance is spontaneously broken[7]: the decay of GWs into two dark energy fluctuations π [78]. Note that in a Lorentz invariant theory, a massless particle can only decay into two or more massless particles with all momenta exactly aligned. Then the IR divergences have to be taken care of by summing over these collinear emissions and the result is finite. Therefore, there is no decay of a massless particle in a Lorentz invariant theory.

We will first derive the interaction $\gamma\pi\pi$ and compute the perturbative decay rate in the framework of the EFT of DE, due to the operator $\tilde{m}_4^2$. At the end, we will put a bound on such an operator and comment on the surviving scalar-tensor theories.

We start with the EFT of DE with $c_T^2 = 1$,

$$S_{EFT} = \int d^4x\sqrt{-g}\left[\frac{M_{Pl}^2}{2}{}^{(4)}R - \Lambda(t) - c(t)g^{00} + \frac{m_2^2(t)}{2}(\delta g^{00})^2 - \frac{m_3^3(t)}{2}\delta K\delta g^{00} + \frac{\tilde{m}_4^2(t)}{2}\delta g^{00\,(3)}R\right], \tag{2.3.1}$$

where the Planck mass squared is $M_{Pl}^2 = M_*^2 f$. Notice that the function $f(t)$ can be set to be constant by performing a conformal transformation of the metric, which does not change the speed of GWs. Generally, the conformal transformation changes the couplings between matter and DE field, but it does not affect the couplings between gravitons and DE. Moreover, we assume for simplicity that the coefficients m_3^3 and $\tilde{m}_4^2$ are time independent; taking into account their slow time dependence is straightforward.

As we have seen before, the functions $c(t)$ and $\Lambda(t)$ are fixed in terms of Hubble expansion and matter quantities (see eqs.(2.1.7) and (2.1.8)). Without loss of generality, we will not work on the particular matter Lagrangian, which is irrelevant for the following discussion. Therefore, we will treat $c(t)$ and $\Lambda(t)$ as independent functions.

2.3.1 *Free Theory*

We first derive the quadratic actions for both graviton and DE field by expanding the action (2.3.1) around the flat FLRW metric. For later use, let us introduce the standard ADM decomposition where the metric can be written as

$$ds^2 = g_{\mu\nu}dx^\mu dx^\nu = -N^2dt^2 + h_{ij}(dx^i + N^i dt)(dx^j + N^j dt)\,, \tag{2.3.2}$$

where N stands for the lapse function and N^i shift vector. It is actually useful to express the components of the metric in terms of N and N^i:

$$g_{00} = -N^2 + N_iN^i\,, \quad g_{0i} = N_i\,, \quad g_{ij} = h_{ij}\,. \tag{2.3.3}$$

7 Since the cosmological background defines a preferred frame and thus spontaneously breaks Lorentz invariance.

Additionally, the components of the inverse metric read

$$g^{00} = -\frac{1}{N^2}\,, \quad g^{0i} = \frac{N^i}{N^2}\,, \quad g^{ij} = h^{ij} - \frac{N^i N^j}{N^2}\,. \tag{2.3.4}$$

The extrinsic curvature K_{ij}, in this decomposition, can be written as

$$K_{ij} = \frac{1}{2N}(\dot{h}_{ij} - D_i N_j - D_j N_i)\,, \tag{2.3.5}$$

where D_i is the covariant derivative with respect to the metric h_{ij}, which is used to raise and lower the spatial indices. At the level of perturbations around the flat FLRW metric, we work in the Newtonian gauge, defined by

$$N^2 = 1 + 2\Phi\,, \quad N_i = 0\,, \quad h_{ij} = a^2(t)(1-2\Psi)(e^{\gamma})_{ij}\,, \tag{2.3.6}$$

where Φ, Ψ denote a scalar perturbation and γ_{ij} is a tensor perturbation satisfying $\partial_i\gamma_{ij} = 0$ and $\gamma_{ii} = 0$.

As explained before, the time diffeomorphism invariance can be restored by Stueckelberg trick. To obtain the quadratic Lagrangians for π and γ_{ij} we need

$$g^{00} \to g^{00} + 2g^{0\mu}\partial_\mu\pi + g^{\mu\nu}\partial_\mu\pi\partial_\nu\pi\,, \tag{2.3.7}$$

$$\delta K^i_j \to \delta K^i_j - \dot{H}\pi\delta^i_j - \frac{1}{a^2}\partial_i\partial_j\pi + \mathcal{O}(2)\,, \tag{2.3.8}$$

$${}^{(3)}R \to {}^{(3)}R + \frac{4}{a^2}H\nabla^2\pi + \mathcal{O}(2)\,. \tag{2.3.9}$$

where $\nabla^2 \equiv \partial_i\partial^i$ and we kept only linear perturbations for δK^i_j and ${}^{(3)}R$.

Varying the action (2.3.1) with respect to Φ gives

$$2M_{\rm Pl}^2\nabla^2\Psi + m_3^3\nabla^2\pi + 4\tilde{m}_4^2\nabla^2(\Psi + H\pi) = 0\,, \tag{2.3.10}$$

where we have focused on the sub-horizon limit, neglecting the higher-order term in spatial derivatives. The eq.(2.3.10) can be solved algebraically for Ψ in terms of π,

$$\Psi = -\frac{m_3^3 + 4\tilde{m}_4^2 H}{2(M_{\rm Pl}^2 + 2\tilde{m}_4^2)}\pi\,. \tag{2.3.11}$$

Similarly, variation with respect to Ψ yields

$$M_{\rm Pl}^2\partial_i(\Phi - \Psi) + 2\tilde{m}_4^2\nabla^2(\Phi - \dot{\pi}) = 0\,. \tag{2.3.12}$$

In the limit where the GW frequencies are much higher than the Hubble expansion, one can only focus on the highest number of time derivatives per field, i.e. we assume $H\pi << \dot{\pi}$. We then obtain

$$\Phi = \frac{2\tilde{m}_4^2}{M_{\rm Pl}^2 + 2\tilde{m}_4^2}\dot{\pi}\,. \tag{2.3.13}$$

Using the solutions (2.3.11) and (2.3.13) the quadratic action for π reads

$$S_\pi^{(2)} = \int d^4x M_{Pl}^2 \frac{3m_3^6 + 4M_{Pl}^2(c + 2m_2^4)}{4(M_{Pl}^2 + 2\tilde{m}_4^2)^2}[\dot{\pi}^2 - c_s^2(\partial_i\pi)^2] \,, \tag{2.3.14}$$

where the sound speed c_s^2 is defined by

$$c_s^2 \equiv \frac{4(M_{Pl}^2 + 2\tilde{m}_4^2)^2 c - M_{Pl}^2(m_3^3 - 2M_{Pl}^2 H)(m_3^3 + 4\tilde{m}_4^2 H) + 8M_{Pl}^2\tilde{m}_4^2(M_{Pl}^2 + 2\tilde{m}_4^2)\dot{H}}{M_{Pl}^2[3m_3^6 + 4M_{Pl}^2(c + 2m_2^4)]} \,. \tag{2.3.15}$$

Notice that in (2.3.14) we considered the frequencies are much higher than H, so that we are approximately in Minkowski space and the scale factor can be set to unity.

We now define the canonically normalized field π_c as

$$\pi_c \equiv \frac{M_{Pl}[3m_3^6 + 4M_{Pl}^2(c + 2m_2^4)]^{1/2}}{\sqrt{2}(M_{Pl}^2 + 2\tilde{m}_4^2)}\pi \,, \tag{2.3.16}$$

therefore we have

$$S_\pi^{(2)} = \int d^4x \frac{1}{2}[\dot{\pi}_c^2 - c_s^2(\partial_i\pi_c)^2] \,. \tag{2.3.17}$$

The quadratic action for the graviton has been obtained in eq.(2.2.1),

$$S_\gamma^{(2)} = \int d^4x \frac{M_{Pl}^2}{8}[\dot{\gamma}_{ij}^2 - (\partial_\ell\gamma_{ij})^2] \,. \tag{2.3.18}$$

Notice that here we have set $m_4^2 = 0$. Defining the Fourier decomposition of γ_{ij} as

$$\gamma_{ij} = \int \frac{d^3k}{(2\pi)^3} \sum_{\sigma=\pm} \epsilon_{ij}^\sigma(\mathbf{k})\gamma_k^\sigma(t)e^{i\mathbf{k}\cdot\mathbf{x}} \,, \tag{2.3.19}$$

where + and - are the two polarizations of the graviton, with

$$\epsilon_{ij}^\sigma(\mathbf{k})\delta^{ij} = k^i\epsilon_{ij}^\sigma(\mathbf{k}) = 0 \,, \quad \epsilon_{ij}^\sigma(\mathbf{k})\epsilon_{ij}^{\star\sigma'}(\mathbf{k}) = 2\delta_{\sigma\sigma'} \,, \tag{2.3.20}$$

the canonical normalized Fourier modes of the graviton are

$$\gamma_{ij}^c \equiv \frac{M_{Pl}}{\sqrt{2}}\gamma_{ij} \,. \tag{2.3.21}$$

Note that the tensor product of two polarizations has to be transverse in each of its indices and traceless in two couples of indices. It is thus given by

$$\sum_{\sigma=\pm} \epsilon_{ij}^\sigma(\mathbf{k})\epsilon_{mn}^{\star\sigma'}(\mathbf{k}) = \lambda_{im}\lambda_{jn} + \lambda_{in}\lambda_{jm} - \lambda_{ij}\lambda_{mn} \,, \quad \lambda_{ij} \equiv \delta_{ij} - \frac{k_i k_j}{\mathbf{k}^2} \,. \tag{2.3.22}$$

2.3.2 *Interaction $\gamma\pi\pi$*

In this Section we derive the interaction vertex $\gamma\pi\pi$ in the gauge specified in (2.3.6). First let us discuss the relevance of the Einstein-Hilbert term[8], which can be decomposed in terms of $3+1$ quantities as

$$S_{EH} = \frac{M_{Pl}^2}{2}\int d^4x\, N\sqrt{h}\,[{}^{(3)}R + K^{ij}K_{ij} - K^2]\,. \tag{2.3.23}$$

The terms $K_{ij}K^{ij}$ and K^2 together with $N\sqrt{h}$ do not give rise to any coupling which is linear γ_{ij}. On the other hand, the term ${}^{(3)}R$ yields a term linear in γ_{ij}, but this will contain fewer derivatives than the one obtained from the $\tilde{m}_4^2$-operator. Hence, we disregard S_{EH}. Also, the terms $\Lambda(t)$ and $c(t)$ do not contribute to the interaction $\gamma\pi\pi$ simply because there is no linear term in γ_{ij}. Actually, the m_3^3-operator contains linear terms in γ_{ij} but with fewer derivatives compared to the one from $\tilde{m}_4^2$-operator. We will discuss the GW decay in the presence of the m_3^3-operator in full detail in Chapters 3 and 4. Here we restrict ourselves to the case of $\tilde{m}_4^2$-operator.

Let us now derive the interaction $\gamma\pi\pi$ due to the $\tilde{m}_4^2$-operator,

$$S_4 = \frac{\tilde{m}_4^2}{2}\int d^4x\, N\sqrt{h}\,\delta g^{00}[{}^{(3)}R + \delta K_{ij}\delta K^{ij} - \delta K^2]\,. \tag{2.3.24}$$

Consider first the term $N\sqrt{h}g^{00}\,{}^{(3)}R$. One realizes that to extract the coupling $\gamma\pi\pi$ the formula (2.3.9) should be expanded up to linear order in both π and γ_{ij}. Notice that N, $\sqrt{h}$ and δg^{00} do not contain linear terms in γ_{ij}. To obtain the Stueckelberg formula for ${}^{(3)}R$ at linear order one starts with the linear expression ${}^{(3)}R = \partial_i\partial_j h_{ij} - \nabla^2 h$. Then we use the following transformations under $t \to t+\pi$,

$$h_{ij} \to h_{ij} - N_i\partial_j\pi - N_j\partial_i\pi + \mathcal{O}(\pi^2)\,, \tag{2.3.25}$$

$$\partial_i \to \partial_i - \partial_i\pi\partial_0 + \mathcal{O}(\pi^2)\,, \tag{2.3.26}$$

to obtain, neglecting the expansion of the Universe,

$${}^{(3)}R \to {}^{(3)}R - \dot{\gamma}_{ij}\partial_i\partial_j\pi\,. \tag{2.3.27}$$

Combining with $N\sqrt{h}\delta g^{00}$ after the Stueckelberg trick (2.3.7) yields

$$S_4 \supset -\int d^4x \frac{\tilde{m}_4^2}{2}(2\Phi - 2\dot{\pi})\dot{\gamma}_{ij}\partial_i\partial_j\pi\,, \tag{2.3.28}$$

where we have kept only terms with the highest number of time derivatives.

For the terms quadratic in the extrinsic curvature in eq. (2.3.24), it is sufficient to use the linear Stueckelberg trick, eq. (2.3.8). It is easy to see that the term δK^2 does not generate terms linear in γ_{ij} unsuppressed by H, while δK_{ij} generates $-\dot{\gamma}_{ij}\partial_i\partial_j\pi$. Multiplying by $N\sqrt{h}\delta g^{00}$, it gives the same

8 One does not need to perform the Stueckelberg trick on S_{EH} since it is invariant under 4d diffeomorphism.

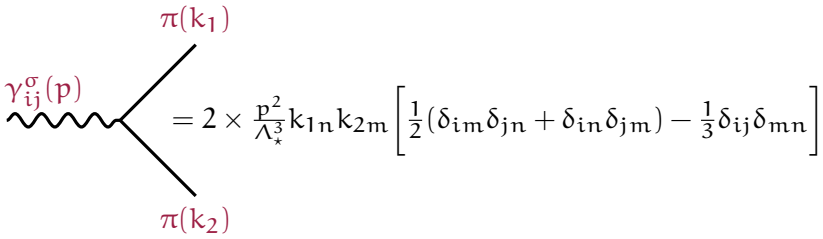

Figure 5: The $\gamma\pi\pi$ vertex.

contribution as eq. (2.3.28). Replacing Φ using eq. (2.3.13) and integrating by parts, we therefore obtain

$$S_{\gamma\pi\pi} = \frac{1}{\Lambda_\star^3} \int d^4x \, \ddot{\gamma}^c_{ij} \partial_i \pi^c \partial_j \pi^c \, , \tag{2.3.29}$$

where we have canonically normalized the fields using eqs. (2.3.16) and (2.3.21), and the suppression scale $\Lambda_\star$ is defined by

$$\Lambda_\star^3 \equiv M_{Pl} \frac{3m_3^6 + 4M_{Pl}^2(c + 2m_2^4)}{2\sqrt{2}\tilde{m}_4^2(M_{Pl}^2 + 2\tilde{m}_4^2)} \, . \tag{2.3.30}$$

The same interaction $\gamma\pi\pi$ can be also obtained in spatially-flat gauge (see Appendix C. of [78]). The $\gamma\pi\pi$ vertex with polarizations σ in Fourier space is shown in Figure 5[9]. We denote the 4-momenta of the decaying graviton and of the two π fields in the final state, respectively by p^μ, k_1^μ and k_2^μ.

2.3.3 *Decay Rate and Constraint on α_H*

In this Section we compute the perturbative decay rate of the process $\gamma \to \pi\pi$ due to the interaction (2.3.29). First let us define the matrix element $i\mathcal{A}$ for a given polarization state σ as

$$\langle \{p, \sigma\}; in | k_1, k_2; out \rangle \equiv (2\pi)^4 \delta(p^\mu - k_1^\mu - k_2^\mu) i\mathcal{A} \, . \tag{2.3.31}$$

The decay is then given by

$$\Gamma = \frac{1}{2} \times \frac{1}{2E_p} \int \frac{d^3k_1}{(2\pi)^3 2E_{k_1}} \frac{d^3k_2}{(2\pi)^3 2E_{k_2}} (2\pi)^4 \delta(p^\mu - k_1^\mu - k_2^\mu) \langle |i\mathcal{A}|^2 \rangle \, , \tag{2.3.32}$$

where the factor of 2 in front comes from the fact that the two final particles are identical, E_q denotes the time component of any 4-vector q^μ and $\langle |i\mathcal{A}|^2 \rangle$ is the square of the matrix element $i\mathcal{A}$ averaged over all possible polarizations for the initial state. The integral above can be further simplified as follows.

First the integral in d^3k_2 can be removed by $\delta(\mathbf{p} - \mathbf{k}_1 - \mathbf{k}_2)$. We define $p \equiv |\mathbf{p}|$, $k_1 \equiv |\mathbf{k}_1|$ and $k_2 \equiv |\mathbf{k}_2|$. Then, the integral in dk_1 can be done by $\delta(E_p - E_{k_1} - E_{k_2})$, imposing the on-shell conditions:

$$E_p = p \, , \quad E_{k_1} = c_s k_1 \, , \quad E_{k_2} = c_s k_2 \, , \tag{2.3.33}$$

9 Note that the factor of 2 comes from the two possibilities of associating k_1 and k_2.

where we have neglected the mass of π which is assumed to be much smaller than the typical frequency of our interest. It is actually useful to define $\Omega \equiv \mathbf{k}_1 \cdot \mathbf{p}/(k_1 p)$ and express k_2 in terms of k_1 as

$$k_2 = \sqrt{k_1^2 + p^2 - 2pk_1\Omega}\,. \tag{2.3.34}$$

Finally assuming $0 < c_s < 1$ and expressing k_1 in terms of p and Ω,

$$k_1 = \frac{p(1-c_s^2)}{2c_s(1-c_s\Omega)}\,, \tag{2.3.35}$$

we obtain

$$\Gamma_{\gamma\to\pi\pi} = \frac{1}{4p}\frac{1}{16\pi c_s^3}\int_{-1}^{1} d\Omega \frac{1-c_s^2}{(1-c_s\Omega)^2}\langle|i\mathcal{A}|^2\rangle\,. \tag{2.3.36}$$

We now compute $\langle|i\mathcal{A}|^2\rangle$. The matrix element of vertex $\gamma\pi\pi$ (Figure 5) is

$$i\mathcal{A} = \frac{2i}{\Lambda_\star^3} p^2 k_{1i} k_{2j} \epsilon_{ij}^{\star\sigma}(\mathbf{p})\,. \tag{2.3.37}$$

Squaring this amplitude and averaging over all possible polarizations in the initial state, we find

$$\langle|i\mathcal{A}|^2\rangle = \frac{1}{2}\sum_{\sigma=\pm}|i\mathcal{A}|^2 = \frac{2p^4}{\Lambda_\star^6}k_1^4(1-\Omega^2)^2\,, \tag{2.3.38}$$

where we have used the conservation of 4-momenta, $p^\mu = k_1^\mu + k_2^\mu$, and the relation (2.3.22). Finally, plugging this $\langle|i\mathcal{A}|^2\rangle$ back into eq. (2.3.36) and integrating over $d\Omega$ using eq. (2.3.35), we therefore obtain

$$\Gamma_{\gamma\to\pi\pi} = \frac{p^7(1-c_s^2)^2}{480\pi c_s^7\Lambda_\star^6}\,. \tag{2.3.39}$$

For LIGO/Virgo observations we have $p \sim \Lambda_3$. Demanding that the gravitons are stable over cosmological distances $\sim H_0^{-1}$ gives

$$\frac{\Gamma_{\gamma\to\pi\pi}}{H_0} = \frac{\Lambda_3}{H_0}\left(\frac{\Lambda_3}{\Lambda_\star}\right)^6\frac{(1-c_s^2)^2}{480\pi c_s^7} \sim 10^{20}\left(\frac{\Lambda_3}{\Lambda_\star}\right)^6\frac{(1-c_s^2)^2}{480\pi c_s^7} \lesssim 1\,, \tag{2.3.40}$$

which implies that $\Lambda_\star >> \Lambda_3$. To compare with large-scale structure constraints, one writes the scale $\Lambda_\star$ in terms of α_H, eq. (2.1.41). One finds that

$$\left(\frac{\Lambda_\star}{\Lambda_3}\right)^3 = \frac{\alpha_H(1+\alpha_H)}{\sqrt{2}\alpha}\,. \tag{2.3.41}$$

Note that $\alpha = \alpha_K + 6\alpha_B^2$. Therefore, from eq. (2.3.40), the parameter α_H-and thus $\tilde{m}_4^2$-must vanish for any practical purpose. In other words, no perturbative decay of GWs at LIGO/Virgo frequencies puts strong bound on α_H: $\alpha_H \lesssim 10^{-10}$. Notice that the conclusion we made above cannot be avoided by taking α very large: this limit corresponds to $c_s << 1$ and further enhances the decay rate (2.3.39).

In addition, one cannot take α_H to be close to -1 since the sound speed squared c_s^2 becomes negative (see eq. (2.3.15)) and then the system is unstable.

Actually, in [78] there are a lot more discussions that we have not mentioned here. For instance, in Appendix D of the paper the authors studied the other decay channel $\gamma \to \gamma\pi$, which turns out to give a smaller decay rate compared to the one we discussed above, so that the associated constraint on α_H is rather weak. Also, the importance of the loop corrections to graviton propagator and its dispersion relation were discussed in great detail in Section 4 of the same reference.

We will summarize the dark energy theories after putting the bounds on both c_T^2 and α_H in the next Section.

2.3.4 *Dark Energies Theories with $c_T^2 = 1$ and No Perturbative Decay*

The GW observation has opened a new way of constraining dark energy and modified gravity theories. The fact that the cut-off of the EFT, describing dark energy, $\Lambda_3 = (M_{Pl}H_0^2)^{1/3}$, is within the LIGO/Virgo band, makes the constraints possible. At these energy scales, interactions involving gravitons and dark energy fluctuations become large. In the presence of spontaneous breaking of Lorentz invariance, this makes gravitons decay at a catastrophically large rate.

As explained in Section 2.2, to be compatible with the GW170817 measurements we have restricted our study to theories where gravitons propagate at the speed of light. The Lagrangian in the covariant language is given by eq.(2.2.11).

In Section 2.3 we have studied the perturbative decay $\gamma \to \pi\pi$, for which the decay rate is roughly given by $\Gamma_{\gamma\to\pi\pi} \sim \alpha_H^2\omega^7/\Lambda_3^6$. The absence of this effect at LIGO/Virgo frequencies $\omega \sim \Lambda_3$ implies that α_H is practically zero. Thus, the surviving theory is

$$\mathcal{L}_{c_T^2=1,\text{nodecay}} = G_2(\phi, X) + G_3(\phi, X)\Box\phi + f(\phi)^{(4)}R\,. \tag{2.3.42}$$

In the context of DHOST, performing $g_{\mu\nu} \to C(\phi, X)g_{\mu\nu}$ brings the theories above to the form,

$$\mathcal{L}_{c_T^2=1,\text{nodecay}} = G_2(\phi, X) + G_3(\phi, X)\Box\phi + C(\phi, X)^{(4)}R + \frac{6C_{,X}(\phi, X)^2}{C(\phi, X)}\phi^{;\mu}\phi_{;\mu\nu}\phi_{;\lambda}\phi^{;\lambda\nu}\,, \tag{2.3.43}$$

where we have redefined the free functions G_2 and G_3 after the transformation and reabsorbed the dependence on $f(\phi)$ in $C(\phi, X)$. This is the most general degenerate theory compatible with $c_T^2 = 1$ and with the absence of perturbative graviton decay.

As already pointed out, the conclusions do not hold if the theories at hand break down at an energy scale parametrically smaller than Λ_3 (for concrete example see [73]). It would be interesting to investigate further whether such an example or any other proposals can be constructed such that it successfully reproduces GR on short scales. Moreover, in this Chapter we have studied the perturbative decay of gravitational waves, neglecting possible coherent effects. Given the very high occupation number of gravitons in the observed waves, we expect that these effects are indeed important and that their absence can be used to rule out another corner of the parameter space of

these DE theories. The investigation of these effects will be discussed in great detail in Chapter 3, which presents the first non-perturbative phenomenon in this thesis.

3

RESONANT DECAY OF GRAVITATIONAL WAVES INTO DARK ENERGY

In Chapter 2 we have seen that in modified-gravity theories gravitational waves (GWs) can decay into dark energy fluctuations, as a consequence of the spontaneous breaking of Lorentz invariance. We focused on dark energy and modified gravity based on a scalar degree of freedom, whose time-dependent background induces a preferred time-foliation of the FRW metric.

In particular, we showed that some of the operators of the EFT of DE display a cubic $\gamma\pi\pi$ interaction, where γ and π respectively denote the graviton and the scalar-field fluctuation, that can mediate the decay. Of course, this can happen only if both energy and momentum can remain conserved during the process, which is when scalar fluctuations propagate subluminally. The same vertex is also responsible for an anomalous GW dispersion, for speeds of scalar propagation different from that of light. Depending on the energy scale suppressing this interaction, these two effects can be important at frequencies observed by LIGO/Virgo and can constrain these theories.

The bound derived in [78] is based on a perturbative calculation, in which individual gravitons are assumed to decay independently of each other. But a classical GW is a collection of many particles with very large occupation number and particle production must be treated as a collective process in which many gravitons decay simultaneously. The classical GW acts as a background for the propagation of scalar fluctuations. This Chapter studies this process in the limit where the GW background acts as a small periodic perturbation (narrow resonance). This is the first non-perturbative phenomenon in this thesis, taking into account a large occupation number of gravitons. We leave the study of large amplitude of GW generating the tachyonic or ghost instabilities to Chapter 4.

Here we work within the framework of the EFT of DE expanded around the flat FLRW metric, as in the previous Chapter. Also, we focus on theories where gravitons travel luminally and, for later convenience, we split the EFT of DE action in the sum of three actions,

$$S = S_0 + S_{m_3} + S_{\tilde{m}_4} \,, \tag{3.0.1}$$

where

$$S_0 = \int d^4x\sqrt{-g}\left[\frac{M_{Pl}^2}{2}\,{}^{(4)}R - \lambda(t) - c(t)g^{00} + \frac{m_2^4(t)}{2}(\delta g^{00})^2\right] , \tag{3.0.2}$$

$$S_{m_3} = -\int d^4x\sqrt{-g}\,\frac{m_3^3(t)}{2}\delta K\delta g^{00} \,, \tag{3.0.3}$$

$$S_{\tilde{m}_4} = \int d^4x\sqrt{-g}\,\frac{\tilde{m}_4^2(t)}{2}\delta g^{00}\left({}^{(3)}R + \delta K^\nu_\mu\delta K^\mu_\nu - \delta K^2\right) \,. \tag{3.0.4}$$

The first action, S_0, contains the Einstein-Hilbert term and the minimal scalar field Lagrangian, which describe the dynamics of the background. Notice that we have removed any time-dependence

in front of the Einstein-Hilbert term by a conformal transformation, which leaves the graviton speed unaffected. We use the notation $\lambda(t)$, and not $\Lambda(t)$ as usual in the literature, to avoid confusion with the energy scale Λ suppressing the cubic vertices studied in this Chapter. The operator m_2^4 does not change the background but affects the speed of propagation of scalar fluctuations, c_s^2. Its typical value is $\mathcal{O}(M_{Pl}^2 H^2)$, see e.g. [48] for details. This action was studied in details in [79] and in the covariant language it describes quintessence [80] or, more generally, a dark energy with scalar field Lagrangian $P(\phi, X)$ [81].

The operator in the second action, S_{m_3}, introduces a kinetic mixing between the scalar field and gravity, mentioned in Section 2.1.3. In the covariant language it corresponds to the cubic Horndeski Lagrangian, of the form $G_3(\phi, X)\Box\phi$. In the regime that leads to sizable modifications of gravity (i.e. for $m_3^3 \sim M_{Pl}^2 H_0$), the operator contained in S_{m_3} displays a $\gamma\pi\pi$ interaction suppressed by an energy scale of order $\Lambda_2 \equiv (M_{Pl}H_0)^{1/2} \sim 10^{-3}$ eV. This energy scale is much greater than the typical LIGO/Virgo frequency. For this reason, in [78] the parameter m_3^3 remains unconstrained by the graviton decay computed in perturbation theory. Finally, the operator in the third action, $S_{\tilde{m}_4}$ was studied in depth in the previous Chapter. This operator displays a $\gamma\pi\pi$ interaction and was constrained with the perturbative decay because the vertex is suppressed by an energy scale close to LIGO/Virgo frequencies.

In Section 3.1, after expanding the action $S_0 + S_{m_3}$ in perturbations in the Newtonian gauge (the same calculation is repeated in the spatially-flat gauge in Appendix C), we study the effect of a classical GW background on the π dynamics, for the operator m_3^3 (Section 3.1.1) and $\tilde{m}_4^2$ (Section 3.1.2). The regime of small GWs can be studied analytically and leads to the so-called *narrow* parametric resonance, which is the subject of Section 3.2. There we compute the energy density of π produced by the parametric instability due to the oscillating GWs (in Section 3.2.2) and we re-interpret the π production in the narrow-resonance regime as an effect of Bose enhancement of the perturbative decay in Appendix A. The back-reaction on the GW signal is computed in Section 3.2.3 for a linearly polarized wave, while the case of elliptical polarization is discussed in Section 3.2.4. In Section 3.2.5 we check that energy is conserved in this process, as expected (the details of the calculations are given in Appendix B).

The treatment in Section 3.2 neglects scalar-field nonlinearities, which are studied in Section 3.3. The operator m_3^3 contains cubic self-interactions suppressed by the scale $\Lambda_3 \equiv (M_{Pl}H_0^2)^{1/3} \sim 10^{-13}$eV, which is much smaller than the one appearing in the vertex $\gamma\pi\pi$. Thus, these become relevant and probably halt the parametric resonance well before the GWs are affected by the back-reaction (Section 3.3.1). This makes the results of Section 3.2 applied to this operator inconclusive. The situation is different for the operator $\tilde{m}_4^2$: in this case the scale that suppresses non-linearities is the same that appears in the coupling $\gamma\pi\pi$. The leading non-linearities are quartic in the regime of interest and are suppressed with respect to a naive estimate due to the particular structure of Galileon interactions. At least in some region of parameters non-linearities do not halt the parametric instability due to the oscillating GWs. In Section 3.4.1 we therefore study in which range of parameters one expects a modification of the GW signal. Moreover, in Section 3.4.2 we discuss

precursors, higher harmonics induced in the GW signal by the produced π, that enter the observational band earlier than the main signal. We conclude discussing the main results of the article and possible future directions in Section 3.5.

3.1 GRAVITON-SCALAR-SCALAR VERTICES

Let us derive the interaction $\gamma\pi\pi$ from the action (3.0.1), using the Newtonian gauge. For the time being, we neglect the self-interactions of the π field; they will be discussed later, in Section 3.3. We initially focus on the operator m_3^3; as a check, in Appendix C we perform the same calculation in spatially-flat gauge.

3.1.1 m_3^3-*operator*

Let us consider the action $S_0 + S_{m_3}$. As already explained in Section 2.1.2, one can restore the π dependence in a generic gauge with the Stuekelberg procedure, $t \to t + \pi(t, \mathbf{x})$. Focusing on the terms relevant for our calculations we have [53]

$$g^{00} \to g^{00} + 2g^{0\mu}\partial_\mu\pi + g^{\mu\nu}\partial_\mu\pi\partial_\nu\pi \,, \tag{3.1.1}$$

$$\delta K \to \delta K - h^{ij}\partial_i\partial_j\pi + \frac{2}{a^2}\partial_i\pi\partial_i\dot{\pi} + \dots \,. \tag{3.1.2}$$

Here, we work in the gauge specified in eq. (2.3.6).

As usual, to find the constraint equations one varies the action $S_0 + S_{m_3}$ with respect to Φ and Ψ and focuses on the sub-Hubble limit by keeping only the leading terms in spatial derivatives,

$$2M_{Pl}^2\nabla^2\Psi + m_3^3\nabla^2\pi = 0 \,, \qquad M_{Pl}^2\nabla^2(\Phi - \Psi) = 0 \,. \tag{3.1.3}$$

From now on we will always consider the Minkowski limit, i.e. that time and spatial derivatives are much larger than Hubble. These equations can be solved in terms of π,

$$\Phi = \Psi = -\frac{m_3^3}{2M_{Pl}^2}\pi \,. \tag{3.1.4}$$

Using these relations, one can find the kinetic term of the π field. As we have seen before, the normalization of π is determined by the dimensionless parameter $\alpha = \alpha_K + 6\alpha_B^2$ which must be positive to avoid ghost instabilities.

The canonically normalized scalar and tensor perturbations are then given by

$$\pi_c \equiv \sqrt{\alpha}M_{Pl}H\pi \,, \qquad \gamma_{ij}^c \equiv \frac{M_{Pl}}{\sqrt{2}}\gamma_{ij} \,. \tag{3.1.5}$$

In terms of these, the interaction term, after integrating by parts, reads

$$-\frac{1}{2}\sqrt{-g}\; m_3^3\delta K\delta g^{00} \supset \frac{1}{\Lambda^2}\dot{\gamma}_{ij}^c\partial_i\pi_c\partial_j\pi_c \,, \tag{3.1.6}$$

where

$$\Lambda^2 \equiv \frac{4M_{Pl}^2(c+2m_2^4)+3m_3^6}{\sqrt{2}m_3^3 M_{Pl}} = -\frac{\alpha}{\sqrt{2}\alpha_B}\frac{H}{H_0}\Lambda_2^2 \ , \tag{3.1.7}$$

and in the right-hand side we have written in terms of α_B, defined in eq. (2.1.40)[1].

We drop the symbol of canonical normalization: γ and π will indicate for the rest of the Chapter the canonically normalized fields. The total Lagrangian is then

$$S_0 + S_{m_3} = \int d^4x \left[\frac{1}{4}(\dot\gamma_{ij})^2 - \frac{1}{4}(\partial_k\gamma_{ij})^2 + \frac{1}{2}\dot\pi^2 - \frac{c_s^2}{2}(\partial_i\pi)^2 + \frac{1}{\Lambda^2}\dot\gamma_{ij}\partial_i\pi\partial_j\pi\right] \ , \tag{3.1.9}$$

and the sound speed squared is given by

$$c_s^2 = \frac{4M_{Pl}^2 c - m_3^3(m_3^3 - 2M_{Pl}^2 H)}{4M_{Pl}^2(c+2m_2^4)+3m_3^6} = \frac{2}{\alpha}\left(\frac{c}{M_{Pl}^2H^2} - \alpha_B - \alpha_B^2\right) \ . \tag{3.1.10}$$

The perturbative decay rate of the graviton can be computed following exactly the same procedure followed for $\tilde m_4^2$ in [78]. It gives

$$\Gamma_{\gamma\to\pi\pi} = \frac{p^5(1-c_s^2)^2}{480\pi c_s^7\Lambda^4} \ , \tag{3.1.11}$$

where p is the momentum of the decaying graviton. One can check that this is negligible for frequencies relevant for GW observations, since by eq. (3.1.7) Λ is of order Λ_2.

The equation of motion of π from the Lagrangian (3.1.9) reads

$$\ddot\pi - c_s^2\nabla^2\pi + \frac{2}{\Lambda^2}\dot\gamma_{ij}\partial_i\partial_j\pi = 0 \ . \tag{3.1.12}$$

Let us use the classical background solution of the GW traveling in the $\hat z$ direction with a linear polarization. Without loss of generality we take the $+$ polarization (the $\times$ one can be obtained by a 45^o rotation of the axes)

$$\gamma_{ij} = M_{Pl}h^+\epsilon_{ij}^+ \ , \qquad h^+(t,z) \equiv h_0^+\sin(\omega(t-z)) \ , \tag{3.1.13}$$

where h^+ is the dimensionless strain of the GW and the polarization tensor is $\epsilon_{ij}^+ = \mathrm{diag}(1,-1,0)$. In this Chapter we will always be away from the source generating the GW, i.e. in the weak field regime $h^+ \ll 1$. Substituting the solution (3.1.13) into eq. (3.1.12), one gets (modulo an irrelevant phase)

$$\ddot\pi - c_s^2\nabla^2\pi + c_s^2\beta\cos[\omega(t-z)](\partial_x^2 - \partial_y^2)\pi = 0 \ , \tag{3.1.14}$$

where the parameter β is defined as

$$\beta \equiv \frac{2\omega M_{Pl}h_0^+}{c_s^2|\Lambda^2|} = \frac{2\sqrt{2}|\alpha_B|}{\alpha c_s^2}\frac{\omega}{H}h_0^+ \ , \qquad \text{for} \quad m_3^3 \neq 0 \ , \ \tilde m_4^2 = 0 \qquad (\alpha_B \neq 0 \ , \ \alpha_H = 0) \ . \tag{3.1.15}$$

1 To write the action (3.0.1), we used a conformal transformation (possibly dependent on $X = (\partial_\mu\phi)^2$) to set to constant the effective Planck mass and to zero higher-order operators of DHOST theories [76, 77]. Using the notation of [82] and the transformation formulas contained therein, one can check that in a general frame the only relevant parameter is

$$\alpha_B - \frac{\alpha_M}{2}(1-\beta_1) + \beta_1 - \dot\beta_1/H \ . \tag{3.1.8}$$

In the following, to evaluate the right-hand side of the above definition we will use $\omega = \Lambda_3$ and $H = H_0$, in which case $\omega/H \sim 10^{20}$. Moreover, note that α and c_s^2 in the second equality appear in the combination αc_s^2. Therefore, thanks to eqs. (3.1.10), β defined above depends only on α_B (or m_3) and we can tune this parameter to make β small.

3.1.2 $\tilde{m}_4^2$-operator

We now consider the operator $\tilde{m}_4^2$. To avoid large π nonlinearities, discussed in Section 3.3, we focus on the case $m_3 = 0$ and consider the action $S_0 + S_{\tilde{m}_4}$. The operator $\tilde{m}_4^2$ has been studied in [78] and details on the calculations can be found there.

In this case, the action for the canonically normalized fields reads

$$S_0 + S_{\tilde{m}_4} = \int d^4x \left[\frac{1}{4}(\dot{\gamma}_{ij})^2 - \frac{1}{4}(\partial_k \gamma_{ij})^2 + \frac{1}{2}\dot{\pi}^2 - \frac{c_s^2}{2}(\partial_i \pi)^2 + \frac{1}{\Lambda_\star^3}\ddot{\gamma}_{ij}\partial_i\pi\partial_j\pi \right] , \tag{3.1.16}$$

where the sound speed of scalar fluctuations is now

$$c_s^2 = \frac{2}{\alpha}\left[(1+\alpha_H)^2 \frac{c}{M_{Pl}^2 H^2} + \alpha_H + \alpha_H(1+\alpha_H)\frac{\dot{H}}{H^2} \right] , \tag{3.1.17}$$

and α_H was defined in eq. (2.1.41) (we assumed $\alpha_H \ll 1$ since this will be the regime of interest). Thus, this operator does not affect the speed of propagation of GWs [50], but, as shown in [78], it contains an interaction $\gamma\pi\pi$ suppressed by the scale

$$\Lambda_\star^3 \equiv \frac{\sqrt{2}M_{Pl}^3(c + 2m_2^4)}{\tilde{m}_4{}^2(M_{Pl}^2 + 2\tilde{m}_4^2)} \simeq \sqrt{2}\frac{\alpha}{\alpha_H}\left(\frac{H}{H_0}\right)^2 \Lambda_3^3 , \tag{3.1.18}$$

where in the last equation we assumed a small α_H. This should be compared with the cubic coupling discussed above, eq. (3.1.9).

The evolution equation for π then reads

$$\ddot{\pi} - c_s^2\nabla^2\pi + \frac{2}{\Lambda_\star^3}\ddot{\gamma}_{ij}\partial_i\partial_j\pi = 0 . \tag{3.1.19}$$

Substituting the solution (3.1.13) into this equation gives

$$\ddot{\pi} - c_s^2\nabla^2\pi - \frac{2\omega^2 M_{Pl} h_0^+}{\Lambda_\star^3}\sin[\omega(t-z)](\partial_x^2 - \partial_y^2)\pi = 0 . \tag{3.1.20}$$

One sees that the evolution equation for π for the $\tilde{m}_4^2$ operator is very similar to the case of the m_3^3 operator, with the replacement $\Lambda^2 \to \Lambda_\star^3\omega^{-1}$. We can thus apply eq. (3.1.14), with β now defined as

$$\beta \equiv \frac{2\omega^2 M_{Pl} h_0^+}{c_s^2|\Lambda_\star^3|} = \frac{\sqrt{2}|\alpha_H|}{\alpha c_s^2}\left(\frac{\omega}{H}\right)^2 h_0^+ , \qquad \text{for} \quad m_3^3 = 0 , \ \tilde{m}_4^2 \neq 0 \qquad (\alpha_B = 0 , \ \alpha_H \neq 0) . \tag{3.1.21}$$

Analogously to the m_3 case, because of eqs. (3.1.17), β defined above depends only on α_H (or $\tilde{m}_4$) and also in this case we can tune this parameter to make β small.

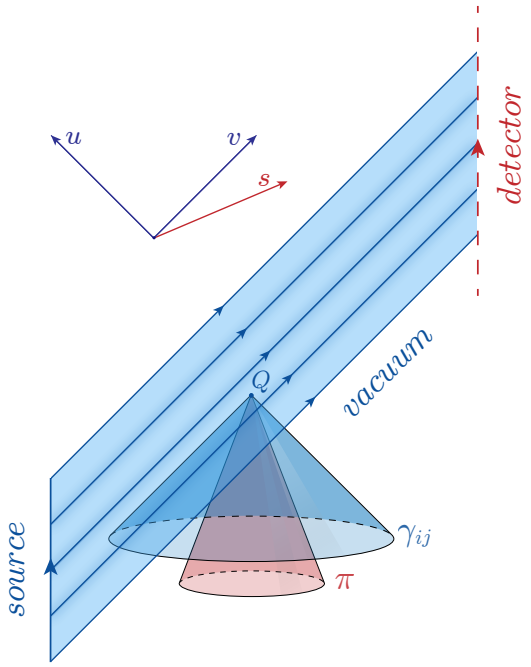

Figure 6: Space-time diagram in (t, z)-coordinates indicating the path taken by the gravitational-wave wave packet (blue region). The π light-cone is narrower than the gravitational wave one.

3.2 NARROW RESONANCE

Equation (3.1.14) describes a harmonic oscillator with periodic time-dependent frequency, which can lead to parametric resonance. As explained in the introduction, in this article we are going to focus on the *narrow-resonance* regime, which corresponds to $\beta \ll 1$. In this case, the solution of the equation of motion of π can be treated analytically and features an exponential growth of scalar fluctuations.

3.2.1 *Parametric resonance*

The GW is emitted at $t = 0$ in the z direction and is detected at some later time, see Figure 6. Using the light-cone coordinates,

$$u \equiv t - z\,, \qquad v \equiv t + z\,, \tag{3.2.1}$$

its solution for $t > 0$ can be written as

$$\gamma_{ij}(u) = M_{Pl} h_0^+ \sin(\omega u)\, \epsilon_{ij}^+\,, \tag{3.2.2}$$

where h_0^+ can be taken as constant, since it varies slowly compared to the GW frequency.

Eq. (3.1.14) takes the form

$$\ddot{\pi} - c_s^2 \nabla^2 \pi + c_s^2 \beta \cos(\omega u)\,(\partial_x^2 - \partial_y^2)\pi = 0\,. \tag{3.2.3}$$

For $c_s < 1$, which we assume in the following, u is a time-like variable for the π metric: hypersurfaces of constant u are space-like to the π-cone. It is then convenient to define the variable s,

$$s \equiv -t + c_s^{-2} z \,, \tag{3.2.4}$$

which is orthogonal to u and is thus space-like with the π metric, see Figure 6, and use the coordinates $\tilde{\mathbf{x}} = (x, y, s)$ to describe the spatial foliations. Since the π-lightcone is narrower than the one of GWs, the solution for the scalar will only be sensitive to a finite region of the GW background. This is the reason why one can approximate the GW as a plane wave with constant amplitude and disregard the process of emission of the GW from the astrophysical source. In particular, for this to be a good approximation we need to require that the past light-cone of π overlaps only with a region of the GW with constant amplitude. From Figure 6 one sees that this is a very weak requirement. It is enough that $1 - c_s$ is larger than the ratio between the duration of the GW signal (of order seconds) and the scale of variation of the amplitude (of order Mpc). Plugging the numbers one gets $1 - c_s \gtrsim 10^{-14}$.

Since for π there is translational invariance in $\tilde{\mathbf{x}}$, it is useful to decompose π in Fourier modes as

$$\pi(u, \tilde{\mathbf{x}}) = \int \frac{d^3\tilde{\mathbf{p}}}{(2\pi)^3} e^{i\tilde{\mathbf{p}}\cdot\tilde{\mathbf{x}}} \pi_{\tilde{\mathbf{p}}}(u) \,, \tag{3.2.5}$$

where $\tilde{\mathbf{p}} = (p_x, p_y, p_s)$ is conjugate to $\tilde{\mathbf{x}}$. In the absence of the interaction with the gravitational wave, one can relate p_s to the momentum written in the original coordinates,

$$p_s = \frac{c_s^2}{1 - c_s^2} (p_z - c_s |\mathbf{p}|) \,. \tag{3.2.6}$$

In the following we are going to use this change of variable also when $\beta \neq 0$, although plane waves in the original coordinates (t, x, y, z) are not solution of eq. (3.2.3).

Then we can quantize π straightforwardly. More specifically, we decompose $\pi_{\tilde{\mathbf{p}}}$ as

$$\pi_{\tilde{\mathbf{p}}}(u) = \frac{1}{c_s \sqrt{2 p_u}} \left[f_{\tilde{p}}(u) \hat{a}_{\tilde{\mathbf{p}}} + f^\star_{\tilde{p}}(u) \hat{a}^\dagger_{-\tilde{\mathbf{p}}} \right] \,, \tag{3.2.7}$$

where

$$p_u \equiv \frac{c_s}{1 - c_s^2} (|\mathbf{p}| - c_s p_z) \,, \tag{3.2.8}$$

and $\hat{a}_{\tilde{\mathbf{p}}}$ and $\hat{a}^\dagger_{-\tilde{\mathbf{p}}}$ are the usual creation and annihilation operators satisfying the commutation relations, $[\hat{a}_{\tilde{\mathbf{p}}}, \hat{a}^\dagger_{\tilde{\mathbf{p}}'}] = (2\pi)^3 \delta^{(3)}(\tilde{\mathbf{p}} - \tilde{\mathbf{p}}')$. The normalization is chosen for convenience. Indeed, for $\beta = 0$ the evolution equation for π satisfies a free wave equation and each Fourier mode can be described as an independent quantum harmonic oscillator. We assume that in this case π is in the standard Minkowski vacuum, given by[2]

$$f_{\tilde{p}}(u) = e^{-i p_u u} \,, \qquad (\beta = 0) \,. \tag{3.2.10}$$

2 It is straightforward to verify that eq. (3.2.10) is equivalent to the standard Minkowski vacuum, i.e.

$$\pi(x) = \int \frac{d^3\mathbf{p}}{(2\pi)^3} \frac{1}{\sqrt{2 c_s |\mathbf{p}|}} \left(e^{-i p\cdot x} \hat{a}_{\mathbf{p}} + e^{i p\cdot x} \hat{a}^\dagger_{-\mathbf{p}} \right) \,, \tag{3.2.9}$$

upon use of $d^3\tilde{\mathbf{p}}/d^3\mathbf{p} = c_s p_u / |\mathbf{p}|$ and, consequently, of $\hat{a}_{\tilde{\mathbf{p}}} = [|\mathbf{p}|/(c_s p_u)]^{1/2} \hat{a}_{\mathbf{p}}$.

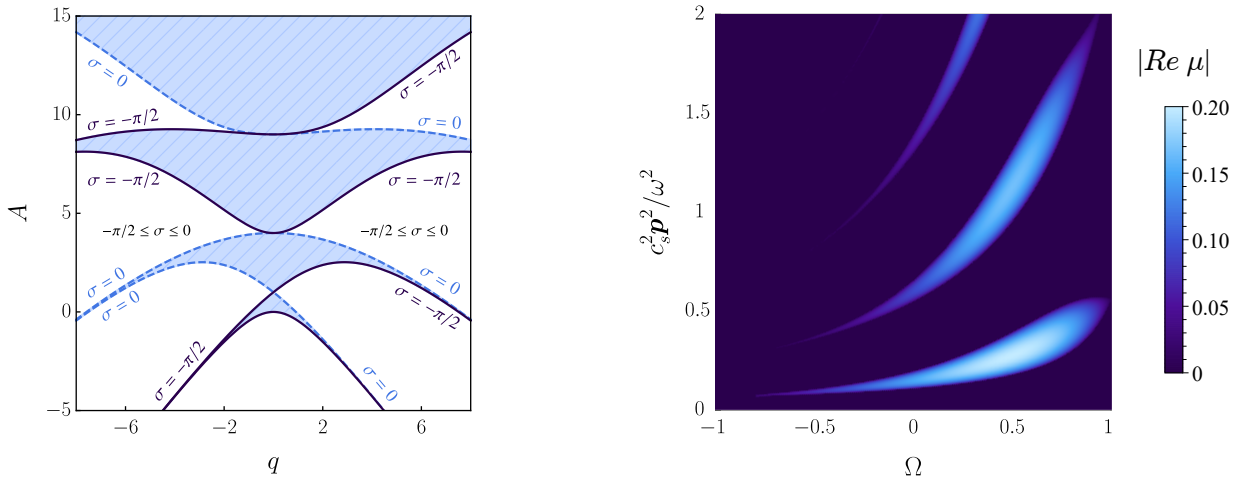

(a) (b)

Figure 7: Left panel (Figure 7a): Instability chart for the Mathieu equation (3.2.13). Colored regions are stable while empty regions are unstable. Each instability band is spanned by $\sigma \in (-\frac{\pi}{2}, 0)$, see eq. (3.2.36) and below for details. Right panel (Figure 7b): Instability bands as functions of Ω and $c_s^2\mathbf{p}^2/\omega^2$ assuming $\varphi = 0$. Light blue regions are unstable: the color grading indicates the coefficient of instability $|\mathrm{Re}\,\mu|$. The plot is obtained using $\beta = 0.8$ and $c_s = 1/2$. (We choose a large value of β for this Figure because the instability bands can be easily located, otherwise the bands would be too narrow to be seen.)

To study the parametric resonance, will now show that eq. (3.2.3) can be written as a Mathieu equation [83]. First, in terms of the new coordinates, eq. (3.2.3) becomes

$$[(1-c_s^2)\partial_u^2 - c_s^{-2}(1-c_s^2)\partial_s^2 - c_s^2(\partial_x^2+\partial_y^2)]\pi + c_s^2\beta\cos(\omega u)(\partial_x^2-\partial_y^2)\pi = 0\,. \tag{3.2.11}$$

For convenience we can also define the dimensionless time variable τ,

$$\tau \equiv \frac{\omega u}{2}\,. \tag{3.2.12}$$

For each Fourier mode, f satisfies

$$\frac{d^2 f}{d\tau^2} + [A - 2q\cos(2\tau)]f = 0\,, \tag{3.2.13}$$

with

$$A = 4\frac{c_s^2\,\mathbf{p}^2}{\omega^2}\frac{(1-c_s\Omega)^2}{(1-c_s^2)^2} = \frac{4p_u^2}{\omega^2}\,, \tag{3.2.14}$$

$$q = 2\beta\frac{c_s^2\,\mathbf{p}^2}{\omega^2}\frac{(1-\Omega^2)\cos(2\varphi)}{1-c_s^2}\,. \tag{3.2.15}$$

To write A and q we have decomposed the vector $\mathbf{p}$ in polar coordinates, $\mathbf{p} = |\mathbf{p}|(\sin\theta\cos\varphi, \sin\theta\sin\varphi, \cos\theta)$, and we have defined $\Omega \equiv p_z/|\mathbf{p}| = \cos\theta$.

The general solution of the Mathieu equation is of the form $e^{\pm\mu\tau}P(\tau)$, where $P(\tau+\pi)=P(\tau)$ [83]. If the characteristic exponent μ has a real part, the solution of the Mathieu equation is unstable for generic initial conditions. Since μ is a function of A and q, the instability region can be represented on the (q,A)-plane, see Figure 7a. The unstable regions are also shown in Figure 7b on the plane $(\Omega, c_s^2\,\mathbf{p}^2/\omega^2)$, for specific values of the other parameters (in the example in the Figure we take $\beta=0.8$ and $c_s=1/2$). Notice that the maximal exponential growth is reached when the ratio q/A has its maximum at $\Omega=c_s$ and $\varphi=0$.

3.2.2 *Energy density of π*

In this Subsection we compute the energy density of π produced by the coupling with the GW. This is given by (see eq. (3.2.52) and explanation below)

$$\rho_\pi=\frac{1}{2}\langle 0|\left[\dot\pi^2+c_s^2(\partial_i\pi)^2\right]|0\rangle\ . \tag{3.2.16}$$

Decomposing in Fourier modes and in the $\hat a$ and $\hat a^\dagger$ coefficients using respectively eqs. (3.2.5) and (3.2.7), the energy density can be rewritten as

$$\begin{aligned}\rho_\pi&=\int\frac{d^3\tilde{\mathbf{p}}}{(2\pi)^3}\frac{1}{4c_s^2p_u}\left[|f'_{\tilde p}-ip_sf_{\tilde p}|^2+c_s^2|f'_{\tilde p}-ic_s^{-2}p_sf_{\tilde p}|^2+2ip_s(f'_{\tilde p}f^\star_{\tilde p}-f'^\star_{\tilde p}f_{\tilde p})+c_s^2(p_x^2+p_y^2)|f_{\tilde p}|^2\right]\\&=\int\frac{d^3\tilde{\mathbf{p}}}{(2\pi)^3}\frac{1}{4c_s^2p_u}\left\{(1+c_s^2)|\partial_uf_{\tilde p}|^2+|f_{\tilde p}|^2\left[p_s^2(1+c_s^{-2})+c_s^2(p_x^2+p_y^2)\right]+4p_sp_u\right\}\ ,\end{aligned} \tag{3.2.17}$$

where we have simplified the expression on the right-hand side using that the Wronskian is time-independent, $\mathscr{W}[f_{\tilde p}(u),f^\star_{\tilde p}(u)]=-2ip_u$.[3] One can verify that in the limit $\beta=0$ the above expression reduces to the energy density of the vacuum, i.e. $\rho_\pi^0=\int\frac{d^3p}{(2\pi)^3}\frac{\omega_p}{2}$.

We can simplify the right-hand side further by making some approximations. Since we are not interested in following the oscillatory behavior of ρ_π, we can perform an average in τ over many periods of oscillation. Since the amplitude of the periodic part of $f_{\tilde p}$ is bounded to be less than unity, it is reasonable to take $\langle|f_{\tilde p}|^2\rangle_T\simeq\langle|\partial_\tau f_{\tilde p}|^2\rangle_T\simeq e^{2\mu\tau}/2$ in eq. (3.2.17). This educated guess will be confirmed in Section 3.2.3. Changing integration variables, from $\tilde{\mathbf{p}}$ to $\xi\equiv c_s^2\mathbf{p}^2/\omega^2$ and the angular variables Ω and φ, we find

$$\rho_\pi\simeq\frac{\omega^4}{(2\pi)^3 16c_s^3}\int d\Omega\,d\varphi\,d\xi\left[\frac{1+c_s^2}{4}+\xi\frac{(c_s-\Omega)^2(1+c_s^2)}{(1-c_s^2)^2}+\xi(1-\Omega^2)\right]e^{2\mu(\xi,\Omega,\varphi)\tau}\ . \tag{3.2.19}$$

3 In general, we can write f as a linear combination of Mathieu-sine and cosine functions, respectively $\mathcal{S}$ and $\mathcal{C}$ [83]. We fix the boundary conditions of the solution such that π is in the vacuum, i.e. the function f satisfies eq. (3.2.10), at $u=0$. This gives

$$f(\tau)=\frac{-i2p_u}{\omega}\,\mathcal{S}(A,q;\tau)+\mathcal{C}(A,q;\tau)\ . \tag{3.2.18}$$

Using this expression and the properties of these functions, we can check that the Wronskian $\mathscr{W}[f_{\tilde p}(u),f^\star_{\tilde p}(u)]$ is constant and with the above normalization is given by $-2ip_u$. As a consequence, the commutation relation in the "interacting" region are satisfied at all times.

We now want to solve the integral on the right-hand side. Since it is dominated by the unstable modes, we restrict the domain of integration to the bands of instability. Actually, we are going to focus on the first instability band for two reasons. The instability rate of the higher bands goes as $\mu_m \sim q^m/(m!)^2 \sim \beta^m$ [83, 84], which implies that for small β the first band is the most unstable. Second, the π produced in this band will modify the GW signal with the original angular frequency ω. (With some contributions at higher frequencies that will be discussed in Section 3.4.2.) We are going to work in the regime $\beta \ll 1$ corresponding to $q \ll 1$, the regime of narrow resonance.

In this situation we can restrict the integral to the first unstable band, which is defined by [83]

$$A_- \leqslant A \leqslant A_+ \,, \qquad A_\pm = 1 \pm |q| \,. \tag{3.2.20}$$

Within this region, the value of the exponent μ is

$$\mu \simeq \frac{1}{2}\sqrt{(A_+ - A)(A - A_-)} \,. \tag{3.2.21}$$

Using the definitions (3.2.14) and (3.2.15) in eq. (3.2.20), the boundary region above can be rewritten in terms of ξ,

$$\xi_- \leqslant \xi \leqslant \xi_+ \,, \qquad \xi_\pm = \frac{(1-c_s^2)^2}{4(1-c_s\Omega)^2}\left[1 \pm \beta|\cos(2\varphi)|\frac{(1-\Omega^2)(1-c_s^2)}{2(1-c_s\Omega)^2}\right] \,, \tag{3.2.22}$$

which fixes the domain of integration in eq. (3.2.19).

The integral in (3.2.19) can be then solved with the saddle-point approximation. In general, an integral of the form

$$I(\tau) = \int d^3\mathbf{X} g(\mathbf{X}) e^{h(\mathbf{X})\tau} \,, \tag{3.2.23}$$

can be approximated for large τ by

$$I(\tau) \approx \frac{1}{\sqrt{\det H_{ij}}}\left(\frac{2\pi}{\tau}\right)^{3/2} g(\mathbf{X}_0) e^{h(\mathbf{X}_0)\tau} \,, \tag{3.2.24}$$

where $\mathbf{X}_0$ is the maximum of the exponent, i.e. the solution of $\partial_i h(\mathbf{X}) = 0$ with the Hessian $H_{ij} \equiv -\partial_i\partial_j h(\mathbf{X}_0)$ positive definite. (If there are more than one maximum one should sum over them.)

In our case we have to maximize μ of eq. (3.2.21), by requiring that $\partial\mu/\partial\xi$, $\partial\mu/\partial\Omega$ and $\partial\mu/\partial\varphi$ vanish. This happens for

$$\xi = \frac{1}{4-\beta^2} \,, \qquad \Omega = c_s \,, \qquad \varphi = n\pi/4 \,, \qquad (n = 0, 1, 2, \ldots) \,, \tag{3.2.25}$$

but we discard the solutions with n odd, because they make q (and the integration region) vanish, see eq. (3.2.15). There are four relevant saddle points ($\varphi = 0, \pi/2, \pi, 3\pi/2$) giving the same value to the integral; without loss of generality we choose $\varphi = 0$. The expression of the Hessian matrix at the saddle point is

$$H_{ij} = 4\begin{pmatrix} \frac{(4-\beta^2)^{3/2}}{\beta} & -\frac{2c_s\sqrt{4-\beta^2}}{\beta(1-c_s^2)} & 0 \\ -\frac{2c_s\sqrt{4-\beta^2}}{\beta(1-c_s^2)} & \frac{4c_s^2(4-\beta^2)+2\beta^2}{(1-c_s^2)^2\beta(4-\beta^2)^{3/2}} & 0 \\ 0 & 0 & \frac{4\beta}{(4-\beta^2)^{3/2}} \end{pmatrix} \,. \tag{3.2.26}$$

Working at leading order in β and using the saddle-point approximation with these values in eq. (3.2.19), the energy density of π as a function of $u = t - z$ reads

$$\rho_\pi(u) \approx \frac{\omega^{5/2}(1-c_s^2)}{c_s(8\pi u)^{3/2}\sqrt{\beta}} \exp\left(\frac{\beta}{4}\omega u\right) . \tag{3.2.27}$$

We can compare ρ_π with the energy density of the gravitational wave, which is roughly constant,

$$\rho_\gamma \simeq (M_{\rm Pl}\omega h_0^+)^2 . \tag{3.2.28}$$

For instance, for $\beta = 0.1$ and $c_s = 1/2$, we get $\rho_\pi \simeq \rho_\gamma$ after $\tau/\pi \simeq 750$ cycles.

The exponential growth studied in this Section can also be seen as a consequence of Bose enhancement, see Appendix A.

3.2.3 *Modification of the gravitational waveform*

The parametric production of π suggests that its back-reaction will modify the background gravitational wave. In this Section we estimate this effect remaining in the narrow-resonance limit, i.e. $|q| \ll 1$ ($\beta \ll 1$). Here we focus again on the case of the operator m_3^3.

To compute the back-reaction on γ_{ij}, we start from the action (3.1.9). The equation of motion for γ_{ij} is

$$\ddot{\gamma}_{ij} - \nabla^2\gamma_{ij} + \frac{2}{\Lambda^2}\Lambda_{ij,kl}\partial_t\left(\partial_k\pi\partial_l\pi\right) = 0 , \tag{3.2.29}$$

where, given a direction of propagation of the wave $\mathbf{n}$, $\Lambda_{ij,kl}(\mathbf{n})$ is the projector into the traceless-transverse gauge, defined by

$$\Lambda_{ij,kl}(\mathbf{n}) \equiv (\delta_{ik} - n_i n_k)(\delta_{jl} - n_j n_l) - \frac{1}{2}(\delta_{ij} - n_i n_j)(\delta_{kl} - n_k n_l) . \tag{3.2.30}$$

We focus again on a wave traveling in the $\hat{\mathbf{z}}$ direction. Using light-cone variables the equation above becomes

$$\partial_u\partial_v\gamma_{ij} + \frac{1}{4\Lambda^2}\partial_u J_{ij}(u) = 0 , \qquad J_{ij}(u) \equiv \Lambda_{ij,kl}\partial_k\pi\partial_l\pi = \Lambda_{ij,kl}\int\frac{d^3\tilde{\mathbf{p}}}{(2\pi)^3}\frac{2p_k p_l}{c_s^2 p_u}|f_{\tilde{p}}(u)|^2 . \tag{3.2.31}$$

We can then split the solution into a homogeneous and a forced one,

$$\gamma_{ij} \equiv \bar{\gamma}_{ij} + \Delta\gamma_{ij} . \tag{3.2.32}$$

The former reads

$$\bar{\gamma}_{ij}(u,v) = \bar{\gamma}_{ij}(u,0) + \bar{\gamma}_{ij}(0,v) - \bar{\gamma}_{ij}(0,0) , \tag{3.2.33}$$

while for the latter, which represents the back-reaction due to π, we find

$$\Delta\gamma_{ij}(u,v) = -\frac{1}{4\Lambda^2}\left[J_{ij}(u) - J_{ij}(0)\right]v . \tag{3.2.34}$$

Because it is transverse and traceless, the source J_{ij} can be projected into a plus and cross polarization. We will focus on the plus polarization. In this case, we can proceed as in the previous Subsection and rewrite the integral in terms of Ω, φ and ξ,

$$J_{ij}(u) = \frac{\omega^4}{4(2\pi)^3 c_s^5} \int d\Omega \, d\varphi \, d\xi \, \xi \, (1-\Omega^2) \cos(2\varphi) |f_{\tilde{p}}(u)|^2 e^+_{ij} \, . \tag{3.2.35}$$

Then, we can evaluate this integral in the narrow-resonance regime with the saddle-point approximation. However, we will now use an approximation for the solution $f_{\tilde{p}}(u)$ that takes into account its oscillatory behavior. In particular, we will split the integral in two regions: $q > 0$ and $q < 0$. Since the sign of q is controlled by the angle φ through $\cos 2\varphi$, this corresponds to splitting the integration over φ.

For $q > 0$, the solution of the Mathieu equation in the first instability band can be approximated by (see pag. 72 of [83])

$$f(\tau) \simeq c_+ \, e^{\mu\tau} \sin(\tau - \sigma) + c_- \, e^{-\mu\tau} \sin(\tau + \sigma) \, , \qquad (q > 0) \, , \tag{3.2.36}$$

where $\mu > 0$ and $\sigma \in (-\frac{\pi}{2}, 0)$ is a parameter, which depends on A and q. It is real inside the instability bands, as shown in the instability chart for the Mathieu equation in Figure 7a. More specifically, in the first instability band one has

$$A = 1 - q\cos(2\sigma) + \mathcal{O}(q^2) \, , \tag{3.2.37}$$

$$\mu = -\frac{1}{2} q \sin(2\sigma) + \mathcal{O}(q^2) \, . \tag{3.2.38}$$

The coefficients c_+ and c_- can be fixed by demanding that at $\tau = 0$ we recover the vacuum solution.

The case $q < 0$ can be obtained by noting that when q changes sign, μ does it as well while A remains the same. The only way to implement this is to consider the simultaneous change $\sigma \to \sigma' = -\sigma - \frac{\pi}{2}$. By performing these two transformations for q and σ on $f(\tau)$ one obtains

$$f(\tau) \simeq c'_- e^{-\mu\tau} \cos(\tau + \sigma) - c'_+ e^{\mu\tau} \cos(\tau - \sigma) \, , \qquad (q < 0) \, . \tag{3.2.39}$$

We can now integrate the right-hand side of (3.2.35) starting from the interval $\varphi \in \left(-\frac{\pi}{4}, \frac{\pi}{4}\right)$. Replacing the growing mode solution of eq. (3.2.36) in the integrand, we obtain

$$\frac{\omega^4}{4(2\pi)^3 c_s^5} \int_{-\pi/4}^{\pi/4} d\varphi \int_{-1}^{1} d\Omega \int d\xi \, \xi \, (1-\Omega^2) \cos(2\varphi) |c_1|^2 \sin^2(\tau - \sigma) e^{2\mu\tau} \, . \tag{3.2.40}$$

The τ dependence in $\sin(\tau - \sigma)$ seems to change the saddle point computed by maximizing μ. However, by rewriting the sine as exponential functions one can check that its effect is simply to add an additional constant to the exponent so that the saddle point remains the same as the one we computed in Section 3.2.2, see eq. (3.2.25). At the saddle point, eqs. (3.2.37) and (3.2.38) give $\tan(2\sigma) \simeq 2/\beta$ while c_+ and c'_+ can be computed by requiring vacuum initial conditions, eq. (3.2.10), at $\tau = 0$. Working for small β, this gives

$$\sigma \simeq -\frac{\pi + \beta}{4} \, , \qquad c_+ \simeq c'_+ \simeq \frac{1 - i}{\sqrt{2}} \, . \tag{3.2.41}$$

Then, applying eq. (3.2.24) to the integral in (3.2.40), the latter can be solved, giving

$$\frac{\omega^4(1-c_s^2)^2}{2c_s^5(16\pi\tau)^{3/2}\sqrt{\beta}}|c_+|^2\sin^2(\tau-\sigma)e^{\beta\tau/2}\,, \tag{3.2.42}$$

where for c_+ and σ we must use the saddle-point values, eq. (3.2.41). We can now repeat this exercise for each part of the integral, using the growing mode of either eqs. (3.2.36) or (3.2.39) depending on the sign of q. Summing them together, we obtain

$$J_{ij} \simeq \frac{\omega^4(1-c_s^2)^2}{c_s^5(16\pi\tau)^{3/2}\sqrt{\beta}}\left[|c_+|^2\sin^2(\tau-\sigma)-|c_+'|^2\cos^2(\tau-\sigma)\right]e^{\beta\tau/2}\epsilon_{ij}^+\,. \tag{3.2.43}$$

Replacing in the solution for $\Delta\gamma_{ij}$, eq. (3.2.34), the expression of $J_{ij}(u)$ of eq. (3.2.43), with σ, c_+ and c_+' fixed by the saddle-point approximation from eq. (3.2.41), the back-reaction on the GWs due to π reads

$$\Delta\gamma_{ij}(u,v) \simeq -\frac{v}{4\Lambda^2}\frac{(1-c_s^2)^2}{c_s^5\sqrt{\beta}}\frac{\omega^{5/2}}{(8u\pi)^{3/2}}\sin\left(\omega u+\frac{\beta}{2}\right)\exp\left(\frac{\beta}{4}\omega u\right)\epsilon_{ij}^+\,, \tag{3.2.44}$$

where we have dropped $J_{ij}(0)$ which is negligible at late time. Thus, the back-reaction grows exponentially in u, as expected from the growth of the energy of π, eq. (3.2.27), and linearly in v. Note that the right-hand side of the above equation diverges for $\beta \to 0$. This is because it has been obtained using the saddle-point approximation, which assumes that $\beta\omega u$ is large. In Appendix A we check that this result reduces to the perturbative calculation when the occupation number is small enough.

Notice that there is no production of cross polarization. Indeed, the integrand of the source term in eq. (3.2.31) now contains $2p_xp_y$ instead of $p_x^2-p_y^2$. Since $p_xp_y \propto \sin(2\varphi) = 0$ and the saddle points are such that $\sin(2\varphi) = 0$, the cross-polarized waves are not generated by the back-reaction of dark energy fluctuations produced by plus-polarized waves and eq. (3.2.44) represents the full result.

3.2.4 *Generic polarization*

So we far we have been discussing linearly polarized waves. Since the resonant effect is non-linear, one cannot simply superimpose the result for linear polarization in order to get a general polarization. In this Subsection we are going to consider a more generic polarization state, that we parametrize as follows

$$\gamma_{ij} = M_{Pl}h_0\left[\cos\alpha\sin(\omega u)\epsilon_{ij}^+ + \sin\alpha\cos(\omega u)\epsilon_{ij}^\times\right]\,, \tag{3.2.45}$$

where $0 \leqslant \alpha < 2\pi$ is an angle characterizing the GW polarization. Note that the state of polarization for generic α is *elliptical*, like the one coming from binary systems [85].

Following the same procedure as in Section 3.2.1, the Mathieu eq. (3.2.13) becomes

$$\frac{d^2f}{d\tau^2} + [A - 2q\cos(2\tau+\hat{\theta})]f = 0\,, \qquad \tan\hat{\theta} \equiv \tan\alpha\tan(2\varphi)\,, \tag{3.2.46}$$

with

$$q = \sqrt{2}\beta \frac{c_s^2\, \mathbf{p}^2}{\omega^2} \frac{(1-\Omega^2)}{1-c_s^2} \sqrt{1+\cos(2\alpha)\cos(4\varphi)}\,, \tag{3.2.47}$$

while A remains the same as before. One needs to shift $\tau \to \tau + \hat{\theta}/2$ in order to use the same form for the Mathieu solution. Given this change in q, one can easily obtain the modified saddle points which are given by

$$\xi = \frac{1}{4 - \frac{\beta^2}{2}[1+(-1)^n \cos(2\alpha)]}\,, \qquad \Omega = c_s\,, \qquad \varphi = n\pi/4\,, \qquad (n = 0, 1, 2, \ldots)\,. \tag{3.2.48}$$

Thus, the saddle points for Ω and φ are unaffected by the angle α. From the saddle point found above one can see that choosing n to be even selects the $+$ polarization, whereas n odd corresponds to $\times$ polarization. The exponent μ of eq. (3.2.21) can be evaluated on these saddle points and, at leading order in β, is given by

$$\mu \simeq \frac{\beta}{4\sqrt{2}} \sqrt{1+(-1)^n \cos(2\alpha)}\,. \tag{3.2.49}$$

Here one can define μ^+ and $\mu^\times$ corresponding to $+$ and $\times$ polarizations respectively as

$$\mu^+ \equiv \frac{\beta}{4\sqrt{2}} \sqrt{1+\cos(2\alpha)}\,, \qquad \mu^\times \equiv \frac{\beta}{4\sqrt{2}} \sqrt{1-\cos(2\alpha)}\,. \tag{3.2.50}$$

Several comments are in order at this stage. First, for $0 < \alpha < \pi/4$ the $+$ contribution in the initial wave is larger. In this case one has $\mu^+ > \mu^\times$ which means that the $+$ polarization dominates also in the back-reaction for $\Delta\gamma_{ij}$. For $\pi/4 < \alpha < \pi/2$ the $\times$ mode dominates. For $\alpha = \pi/4$ both polarization states grow with the same rate, meaning that a circularly polarized wave remains circular. Moreover, by setting $\alpha = 0$ ($\alpha = \pi/2$) we recover the results of the previous Sections for the case of $+$ ($\times$) polarization.

3.2.5 *Conservation of energy*

To check our results and to get a better understanding of the system, it is useful to verify that energy is conserved in the production of the π field and the corresponding modification of the GW, $\Delta\gamma$. From the Lagrangian (3.1.9), one can derive the Noether stress-energy tensor, which is conserved on-shell as a consequence of translational invariance

$$\partial_\mu T^\mu_{\ \nu} = 0\,. \tag{3.2.51}$$

(Notice that this $T^\mu_{\ \nu}$ will be different from the pseudo stress-energy tensor of GR.) Let us consider the region represented in Figure 8. Given the symmetries of the system, it is useful to take the left and right boundaries as null, instead of time-like, surfaces.

At first sight, it is somewhat puzzling that while both the original GW and the induced π are only displaced as time proceeds (see Figures 6 and 8), so that their contribution to the total energy

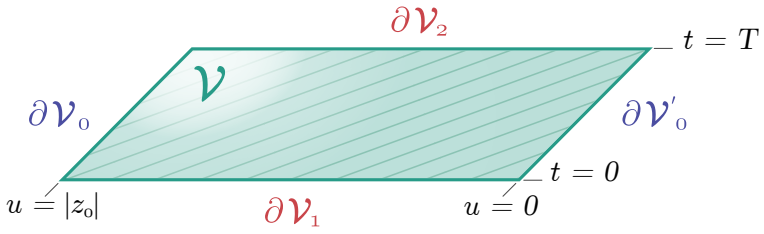

Figure 8: Region $\mathcal{V}$ over which we are checking the conservation of the stress-energy tensor. The boundaries $\partial\mathcal{V}_0$ and $\partial\mathcal{V}'_0$ are null hypersurfaces at $u = \text{const}$.

does not depend on time, $\Delta\gamma$ grows on later time slices since it is proportional to v. What we are going to verify is that the variation of the energy between $\partial\mathcal{V}_1$ and $\partial\mathcal{V}_2$ due to the change in $\Delta\gamma$ is compensated by a flux of energy across the null boundary $\partial\mathcal{V}_0$.[4] (There is no flux across the right null boundary $\partial\mathcal{V}'_0$ since π is in the vacuum for $u = 0$.)

The Noether stress-energy tensor of the action (3.1.9) is given by

$$T^0_{\ 0} = (T^0_{\ 0})_\gamma + (T^0_{\ 0})_\pi\,, \qquad (T^0_{\ 0})_\gamma \equiv -\frac{1}{4}\left[\dot\gamma_{ij}^2 + (\partial_k\gamma_{ij})^2\right]\,, \qquad (T^0_{\ 0})_\pi \equiv -\frac{1}{2}\left[\dot\pi^2 + c_s^2(\partial_i\pi)^2\right]\,, \tag{3.2.52}$$

$$T^0_{\ i} = -\frac{1}{2}\dot\gamma_{kl}\partial_i\gamma_{kl} - \dot\pi\partial_i\pi - \frac{1}{\Lambda^2}\partial_i\gamma_{kl}\partial_k\pi\partial_l\pi\,, \qquad T^i_{\ 0} = \frac{1}{2}\dot\gamma_{kl}\partial_i\gamma_{kl} + c_s^2\dot\pi\partial_i\pi - \frac{2}{\Lambda^2}\dot\gamma_{ij}\dot\pi\partial_j\pi\,, \tag{3.2.53}$$

$$\begin{aligned} T^i_{\ j} = {}& \frac{1}{2}\partial_i\gamma_{kl}\partial_j\gamma_{kl} + c_s^2\partial_i\pi\partial_j\pi - \frac{2}{\Lambda^2}\dot\gamma_{ik}\partial_j\pi\partial_k\pi \\ & + \frac{1}{2}\delta^i_j\left[\frac{1}{2}\dot\gamma_{kl}^2 - \frac{1}{2}(\partial_m\gamma_{kl})^2 + \dot\pi^2 - c_s^2(\partial_l\pi)^2 + \frac{2}{\Lambda^2}\dot\gamma_{kl}\partial_k\pi\partial_l\pi\right]\,. \end{aligned} \tag{3.2.54}$$

Notice that the total energy of the system is simply the sum of the kinetic energy of γ and π without a contribution due to interactions. (This is a consequence of the interaction term being linear in $\dot\gamma$.) This means that the production of π must be compensated by a decrease of the γ kinetic energy. Using the splitting in eq. (3.2.32) and defining $\bar\rho_\gamma \equiv \frac{1}{4}(\dot{\bar\gamma}_{ij})^2 + \frac{1}{4}(\partial_k\bar\gamma_{ij})^2$, $\rho_\pi \equiv \frac{1}{2}\dot\pi^2 + \frac{c_s^2}{2}(\partial_i\pi)^2$, the components (3.2.52) (3.2.54) can be written up to second order in perturbation. For instance

$$T^0_{\ 0} = -(\bar\rho_\gamma + \rho_\pi + \frac{1}{2}\dot{\bar\gamma}_{ij}\Delta\dot\gamma_{ij} + \frac{1}{2}\partial_k\bar\gamma_{ij}\partial_k\Delta\gamma_{ij}) + \mathcal{O}(\Delta\gamma^2) \tag{3.2.55}$$

$$T^i_{\ 0} = \frac{1}{2}\dot{\bar\gamma}_{kl}\partial_i\bar\gamma_{kl} + \frac{1}{2}\Delta\dot\gamma_{kl}\partial_i\bar\gamma_{kl} + \frac{1}{2}\dot{\bar\gamma}_{kl}\partial_i\Delta\gamma_{kl} + c_s^2\dot\pi\partial_i\pi - \frac{2}{\Lambda^2}\dot{\bar\gamma}_{ij}\dot\pi\partial_j\pi + \mathcal{O}(\Delta\gamma^2)\,. \tag{3.2.56}$$

Gauss theorem works also when the region has null boundaries (see for instance [86]):

$$\int_{\mathcal{V}}\partial_\mu T^{\mu 0}d^4x = \oint_{\partial\mathcal{V}} T^{\mu 0}n_\mu\,dS\,. \tag{3.2.57}$$

The only subtlety in the case of null boundaries is that one does not know how to choose the normalization of the null vector n^μ orthogonal to the surface (of course when the boundary is null

4 Notice that, while the original GW is described by a wave packet localised in a certain interval of u, π waves are present at arbitrary large u and thus will always contribute to the flux.

this vector also lies on the surface). A related ambiguity is that there is no natural volume form on the boundary to perform the integration, since the induced metric on a null surface is degenerate. The two ambiguities compensate each other. If one chooses a 3-form $\tilde{\varepsilon}$ as a volume form on the null surface one needs the covector n_μ to satisfy

$$n \wedge \tilde{\varepsilon} = \varepsilon \,, \tag{3.2.58}$$

with ε the volume 4-form, the one used to perform the integration in $\mathcal{V}$ in equation (3.2.57). This equation generalizes the concept of orthonormal vector in the Gauss theorem and one can show that it implies eq. (3.2.57), see [86]. In our case, if one chooses to perform the integral over the null boundary as $dt\,dx\,dy$, which corresponds to a 3-form $\tilde{\varepsilon}_{\alpha\beta\gamma}$ which is completely anti-symmetric in the variables t, x and y, one has to normalize the orthogonal vector n^μ such that

$$\frac{1}{4}\varepsilon_{\alpha\beta\gamma\delta} = n_{[\alpha}\tilde{\varepsilon}_{\beta\gamma\delta]} \,. \tag{3.2.59}$$

This is satisfied by the vector $n^\mu = (1, 0, 0, 1)$ in the Minkowski coordinates (t, x, y, z).

We now apply eq. (3.2.57) to the region depicted in Figure 8 and use eq. (3.2.51). There is no dependence on x and y, so we can factor out the surface $dx\,dy$:

$$\int_{\partial\mathcal{V}_2} T^{00}\,dz - \int_{\partial\mathcal{V}_1} T^{00}\,dz = -\int_{\partial\mathcal{V}_0} \left(T^{00} - T^{z0}\right) dt \,. \tag{3.2.60}$$

We dropped the contribution of the surface $\partial\mathcal{V}_0'$ since all fields vanish on this surface. The LHS is the difference in energy between $t = T$ and $t = 0$, while the RHS gives the flux of energy across $\partial\mathcal{V}_0$. As shown in Appendix B, neither $\bar{\gamma}$ nor $\Delta\gamma$ contribute to the energy flux across $\partial\mathcal{V}_0$ (intuitively GWs move parallel to this surface). Conversely, since π only depends on u, it does not contribute to the difference in energy. Since the flux of energy is only due to π, which is constant on $\partial\mathcal{V}_0$, the flux is proportional to T. We see that the dependence $\Delta\gamma \propto T$ in the LHS is necessary for the cancellation. Notice that the sign of $\Delta\gamma_{ij}$ in (3.2.44) is the correct one: it implies that the amplitude of GW is *decreasing*. Indeed, since the total energy is just the sum of the kinetic energy of γ and π, γ must decrease in amplitude as π grows. In Appendix B we check these statements and verify eq. (3.2.60).

3.3 NONLINEARITIES

We now want to look at the effects of π non-linearities (non-linearities of γ are suppressed by further powers of M_{Pl}). In particular, we are going to study the effect of non-linearities on the exponential amplification of dark energy fluctuations that occurs in the narrow-resonance regime.

3.3.1 m_3^3-*operator*

We start from the operator (3.0.3). In this case, the cubic self-interaction in the Lagrangian is

$$\frac{1}{\Lambda_B^3}\Box\pi\,(\partial_i\pi)^2 \,, \tag{3.3.1}$$

where $\Box \equiv -\partial_t^2 + \nabla^2$ and

$$\Lambda_B^3 \equiv -\frac{[3m_3^6 + 4M_{Pl}^2(c + 2m_2^4)]^{3/2}}{\sqrt{2}m_3^3 M_{Pl}^3} = \frac{\alpha^{3/2}}{\alpha_B}\left(\frac{H}{H_0}\right)^2 \Lambda_3^3 \,. \tag{3.3.2}$$

At early times, when π is in the vacuum state, it is safe to neglect these terms. However, as π grows their importance increases and they become comparable to the resonance term

$$\frac{1}{\Lambda^2}\dot{\gamma}_{ij}\partial_i\pi\partial_j\pi \,. \tag{3.3.3}$$

Since $\Lambda_B \ll \Lambda$, we expect this to happen rather quickly. Comparing the above operators, this takes place when $\Box\pi \sim (\Lambda_B^3/\Lambda^2)\dot{\gamma}_{ij} \sim \sqrt{\alpha}H\dot{\gamma}_{ij}$, which can be written as

$$(\partial_i\pi)^2 \sim \alpha c_s^2 (h_0^+)^2 \Lambda_2^4 \,, \tag{3.3.4}$$

by using $\dot{\gamma}_{ij} \sim \omega M_{Pl} h_0^+$ and $\Box\pi \sim (\omega/c_s)\partial_i\pi$. When this happens, both the energy density of π and the modification of the GW, see eq. (3.2.34), are small. Indeed, using the above equation one finds

$$\frac{\rho_\pi}{\rho_\gamma} \sim \frac{(\partial_i\pi)^2}{(M_{Pl}\omega h_0^+)^2} \sim \alpha\left(\frac{c_s H_0}{\omega}\right)^2 \ll 1 \,, \qquad \frac{\Delta\gamma}{\bar{\gamma}} \sim \frac{\nu(\partial_i\pi)^2}{\Lambda^2 M_{Pl} h_0^+} \sim \nu H_0 h_0^+ \alpha_B c_s^2 \ll 1 \,. \tag{3.3.5}$$

After this point one can no longer trust the Mathieu equation and the solutions for π used earlier, eq. (3.2.36): non-linear terms change the fundamental frequency of the oscillator in eq. (3.2.13), so that originally unstable modes are driven out of their instability bands and a more sophisticated analysis is required. The same conclusion can be obtained from the Boltzmann analysis of Appendix A. When the resonance term is modified by $\sim \mathcal{O}(1)$ corrections, particles are produced also outside the thin-shell of momenta Δk. This dispersion in momentum space implies that the Bose-enhancement factor, and in turn the growth index μ_k, are affected.

The above estimate is also in agreement with numerical results in the preheating literature (see e.g. [87, 88]). These simulations suggest that even small self-interactions of the produced fields are enough to qualitatively change the development of the resonance. In these works it was also shown that attractive potentials for the reheated particles modify, and eventually shut down, the exponential growth found at linear level. This conclusion is not surprising, since in these cases large field expectation values contribute positively to their effective mass, making the decay kinetically disfavored as soon as large field values are reached. This result cannot be applied to our case because the derivative self-interactions in eq. (3.3.1) do not enter with a definite sign in the action. To reach a definitive answer, in the narrow resonance regime, one would need a full numerical analysis.

3.3.2 $\tilde{m}_4^2$-operator

We will now take $m_3^3 = 0$ and focus on the self-interaction of π generated by the operator of eq. (4.5.1). This choice results technically natural since m_3^3 corresponds, in the covariant theory, to cubic Horndeski operators that feature a weakly-broken Galilean invariance (for details, see the discussion in [59, 78, 89]).

Clearly, on sub-Hubble scales the most important nonlinearities are due to operators containing two derivatives per field. Since we are interested in the regime $\alpha_H \ll 1$, in this case the most relevant non-linearities are not cubic but quartic. Indeed cubic non-linearities are suppressed by $\alpha_H/\alpha^{3/2} \cdot \partial^2\pi/\Lambda_3^3$, while the quartic ones by $\alpha_H/\alpha^2 \cdot (\partial^2\pi/\Lambda_3^3)^2$. Thus, for $\alpha_H \ll 1$, quartic non-linearities become relevant for a smaller value of $\partial^2\pi/\Lambda_3^3$ (unless α is huge, we will not be interested in this regime below). Notice that the cut-off of the theory is thus of order $\Lambda_3\alpha^{1/3}\alpha_H^{-1/6}$. This scale is much larger than ω for the values of α_H we are interested in, so that the GW experimental results are well within the regime of validity of the theory. See Figure 9 for a comparison of the scales in the problem.

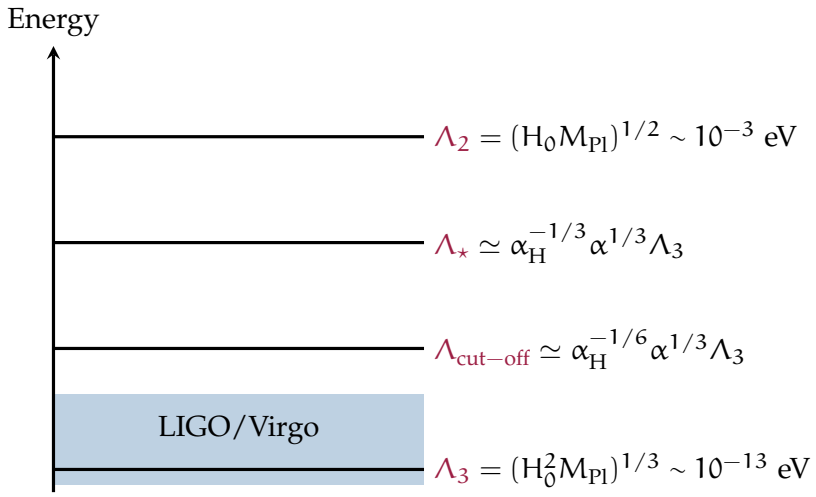

Figure 9: The various energy scales in the limit $\alpha_H \ll 1$. We assume $\alpha \gg \alpha_H^{1/2}$ so that $\Lambda_{cut-off} \gg \Lambda_3$. Notice that in this Chapter we do not consider the regime of parametrically small c_s, which may modify the estimates above.

Let us start with a naive estimate for $c_s \sim 1$. The resonance will be affected by non-linearities when

$$\frac{\alpha_H}{\alpha^2}\left(\frac{\partial^2\pi}{\Lambda_3^3}\right)^2 \sim \beta \,. \tag{3.3.6}$$

Going through the same calculations as in the case of the m_3^3-operator one gets the constraint

$$\frac{\Delta\gamma}{\bar\gamma} \sim \frac{\nu\,\omega(\partial_i\pi)^2}{\Lambda_\star^3 M_{Pl} h_0^+} \lesssim \beta\alpha(\nu H_0)\frac{H_0}{\omega h_0^+} \,. \tag{3.3.7}$$

For typical values of the parameters the RHS of this inequality is at most of order unity. This would mean that non-linearities are important when the GW signal is substantially modified.

Actually, it turns out that the estimate above is not quite correct, as a consequence of the detailed structure of the quartic Galileon interaction. We want to evaluate the importance of the interactions on the modes that grow fastest, i.e. on the saddle point. Using (u, s, x, y) coordinates, one has $p_s = 0$ on the saddle, see eqs. (3.2.6) and (3.2.25). This can be understood from the equation of motion, eq. (3.2.11): for a given frequency of a π wave, i.e. for a given momentum $|\mathbf{p}|$, one maximizes the

forcing term if $p_s = 0$. Therefore in these coordinates the derivative with respect to s vanishes. However, since the coordinate u is null, the inverse metric satisfies $g^{uu} = 0$. This means that also the derivative with respect to u will not appear in the interaction (there are only cross terms $\propto \partial_u \partial_s$). Therefore we are left only with the two coordinates x and y. However, the structure of the quartic Galileon is such that it vanishes if one has less than three dimensions. We conclude that the quartic π self-interaction vanishes on the saddle point. To get a correct estimate one is forced to look at deviations from the saddle, i.e. one has to estimate what is the typical range of p_s around $p_s = 0$ that contributes to the integrals like eq. (3.2.40).

The rms value of the various variables can be read from the inverse of the Hessian matrix eq. (3.2.26). The momentum p_s can be written in terms of the integration variables $\{\xi, \Omega, \varphi\}$ as

$$p_s = \frac{c_s \omega}{1 - c_s^2} \sqrt{\xi} (\Omega - c_s) \, . \tag{3.3.8}$$

One can write

$$(\Delta p_s)^2 = \frac{\partial p_s}{\partial X^i} \frac{\partial p_s}{\partial X^j} \Delta X^i \Delta X^j = \frac{\partial p_s}{\partial X^i} \frac{\partial p_s}{\partial X^j} (H^{-1})^{ij} \, . \tag{3.3.9}$$

Evaluated at the saddle, the matrix of the first derivatives of p_s is zero, except for the entry (Ω, Ω) which is given by

$$\left(\frac{\partial p_s}{\partial \Omega} \right)^2 = \frac{c_s^2 \omega^2}{(1 - c_s^2)^2 (4 - \beta^2)} \, . \tag{3.3.10}$$

The entry (Ω, Ω) of the inverse of the Hessian reads $\left(H^{-1}\right)^{\Omega\Omega} = \frac{(1-c_s^2)^2}{4\beta\tau} (4 - \beta^2)^{3/2}$. Therefore we obtain

$$\Delta p_s = \frac{c_s \omega (4 - \beta^2)^{1/4}}{2\sqrt{\beta\tau}} \simeq \frac{c_s \omega}{\sqrt{2\beta\tau}} \, . \tag{3.3.11}$$

Using this estimate one can revise the bound above as

$$\frac{\Delta\gamma}{\bar{\gamma}} \sim \frac{\nu \, \omega (\partial_i \pi)^2}{\Lambda_\star^3 M_{Pl} h_0^+} \lesssim \beta c_s^3 \alpha (\nu H_0) \frac{H_0}{\omega h_0^+} \sqrt{\beta\tau} \, . \tag{3.3.12}$$

It is important to stress that the coefficient of the quartic self-interaction of π is tied by symmetry with the one of the operator $\ddot{\gamma}_{ij} \partial_i \pi \partial_j \pi$, so that the effect of self-interactions cannot be suppressed. This statement holds even considering models with $c_T \neq 1$: since we are considering a regime of very small α_H, comparable values for $c_T - 1$ are not ruled out experimentally. If one does not impose the constraints on the speed of GWs, instead of the single operator of eq. (4.5.1) one has two independent coefficients. In terms of these parameters, the coefficient of the quartic Galileon was calculated in [90] and it reads

$$\frac{2}{M_{Pl}^2} (\tilde{m}_4^2 + m_5^2) \, . \tag{3.3.13}$$

On the other hand the coefficient of the operator $\ddot{\gamma}_{ij} \partial_i \pi \partial_j \pi$ reads (see Appendix B of [78])

$$\frac{1}{M_{Pl}^2} (\tilde{m}_4^2 + m_5^2 c_T^2) \, . \tag{3.3.14}$$

The two coincide, modulo a factor of 2, up to relative corrections suppressed by $c_T^2 - 1$.

$$\frac{\tilde{m}_4^2}{2} \delta g^{00} \, {}^{(3)}\!R + \frac{m_5^2}{2} \delta g^{00} \left(\delta K^\nu_\mu \delta K^\mu_\nu - \delta K^2 \right) \, . \tag{3.3.15}$$

3.4 OBSERVATIONAL SIGNATURES FOR $\tilde{m}_4^2$

3.4.1 *Fundamental frequency*

In the narrow resonance regime, $\beta \ll 1$, with the replacement $\Lambda^2 \to \Lambda_\star^3 \omega^{-1}$, from eq. (3.2.44) one gets a relative modification of the GW given by

$$\frac{\Delta\gamma(u,v)}{\bar{\gamma}} \simeq -\frac{v}{4\Lambda_\star^3 M_{Pl} h_0^+} \frac{(1-c_s^2)^2}{c_s^5\sqrt{\beta}} \frac{\omega^{7/2}}{(8u\pi)^{3/2}} \exp\left(\frac{\beta}{4}\omega u\right) . \tag{3.4.1}$$

The amplitude of GWs in the plus polarization is given by [85]

$$h_0^+ \sim \frac{4}{r}(GM_c)^{5/3}(\pi f)^{2/3} , \tag{3.4.2}$$

where r is the distance from the source and M_c is the chirp mass of the binary system. The number of cycles of the gravitational wave is given by

$$N_{cyc} = \frac{\omega u}{2\pi} = f u , \tag{3.4.3}$$

where we have defined the gravitational wave frequency $f \equiv \omega/2\pi$. In our calculations we took a time-independent frequency, while in reality f increases with time, during the binary inspiralling. The frequency can be taken as roughly constant for the number of cycles N_{cyc} required for f to double in size. In particular, the number of cycles between f and $2f$ is given by [85]

$$\bar{N}_{cyc} = \frac{4-2^{1/3}}{128\pi}(\pi G M_c f)^{-5/3} . \tag{3.4.4}$$

Inverting these relations we can express the chirp mass as a function of the number of cycles and the frequency. Using this in eq. (3.4.2) we obtain

$$h_0^+ \sim \frac{0.0087}{f\bar{N}_{cyc} r} . \tag{3.4.5}$$

In the calculation we approximate the GW amplitude as a constant, therefore we have to limit $v \lesssim r$.

Expressing β in term of α_H, replacing h_0^+ from the above relation and using $v = r$, eq. (3.4.1) becomes

$$\frac{\Delta\gamma}{\bar{\gamma}} \sim -0.006 \times \frac{(1-c_s^2)^2}{c_s^3}\left(\frac{\alpha_H}{\alpha c_s^2}\right)^{\frac{1}{2}}\left(\frac{H_0}{M_{Pl}}\right)^{\frac{1}{6}}\left(\frac{2\pi f}{\Lambda_3}\right)^{\frac{11}{2}}(rH_0)^{\frac{5}{2}} \exp\left[\frac{0.12}{rH_0}\left(\frac{M_{Pl}}{H_0}\right)^{\frac{1}{3}}\frac{\alpha_H}{\alpha c_s^2}\frac{2\pi f}{\Lambda_3}\right] . \tag{3.4.6}$$

Note that this expression is independent of $\bar{N}_{cyc}$. Sizable effects in the GW waveform can be obtained when the argument of the exponential is $\sim \mathcal{O}(10^2)$, which translates into

$$\alpha_H \gtrsim 10^{-17} \cdot rH_0 \cdot \frac{\Lambda_3}{2\pi f}\alpha c_s^2 . \tag{3.4.7}$$

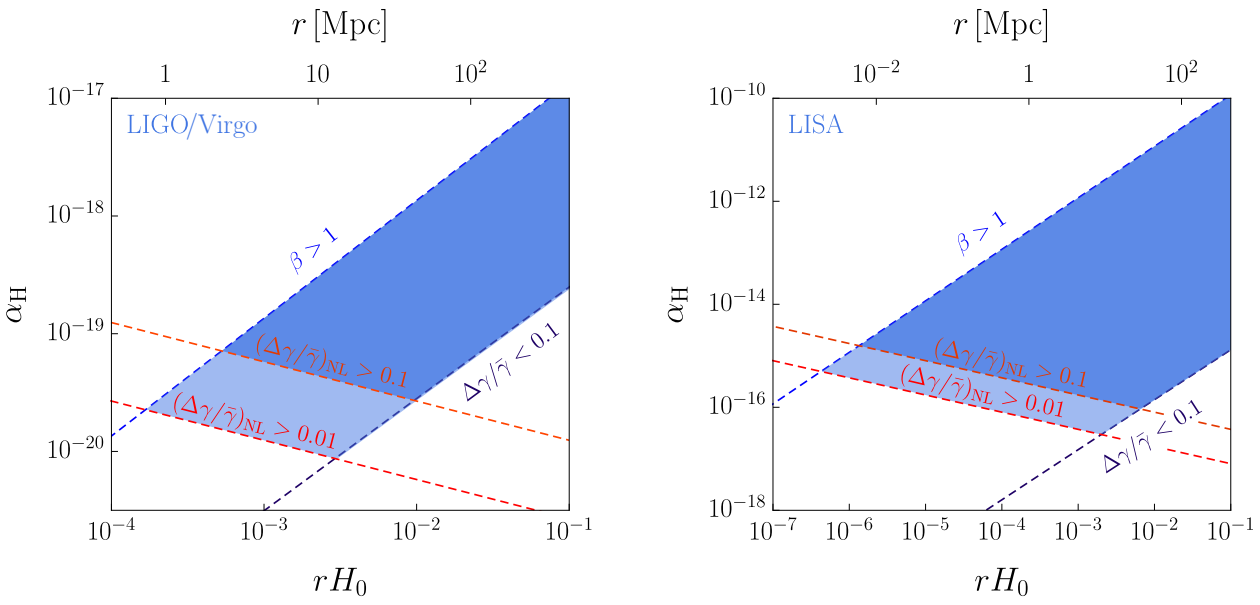

Figure 10: The blue regions indicate where our approximations apply and one has a sizable modification of the GW signal. Above the red dashed lines the effect of π non-linearities is small. The upper blue dashed lines indicate the line $\beta = 1$: our analytical approximation holds for $\beta \ll 1$ and that we extrapolate to $\beta \lesssim 1$. One has a sizable effect on the GW above the lower dashed blue lines. This mainly depends on the exponential of $\beta\bar{N}_{cyc}$ and since $\bar{N}_{cyc}$ is fixed once M_c and f are given, this constraint is to a good approximation a lower bound on β. Left panel (Figure 10a): LIGO/Virgo case: $f = 30$ Hz, $M_c = 1.188\ M_\odot$ as for GW170817. Right panel (Figure 10b): LISA case: $f = 10^{-2}$ Hz, $M_c = 30\ M_\odot$ as for GW150914.

We have also to impose the constraint of eq. (3.3.12), which using eq. (3.4.5) reads

$$\frac{\Delta\gamma}{\bar{\gamma}} \lesssim 18(\beta\bar{N}_{cyc})^{3/2} c_s^3 \alpha (rH_0)^2 \equiv \left(\frac{\Delta\gamma}{\bar{\gamma}}\right)_{NL}, \tag{3.4.8}$$

where the term $\beta\bar{N}_{cyc}$ roughly coincides with the argument of the exponential in eqs. (3.4.1) and (3.4.6). Finally, a further constraint to impose is the narrow resonance condition $\beta \ll 1$.

In Figures 10a and 10b we plot these three constraints as a function of α_H and the distance between the source and the resonant decay of the GW into π (therefore this is not the distance between the source and the detector). The first plot is done for a ground-based interferometer with LIGO/Virgo-like sensitivity; in order to maximize the number of oscillation we choose a neutron-star event similar to GW170817 [64]. The second plot is for a space-based interferometer with LISA-like sensitivity [91] and a binary black hole event similar to GW150914 [92]. The blue region corresponds to a sizable modification of the GW signal, calculable within our approximation. The neutron-star merger GW170817 is at a distance of approximately 40 Mpc. The absence of sizable effects ($\Delta\gamma > 0.1\gamma$; of course future measurements will improve this sensitivity) in the observed event puts constraints on a resonant effect that takes place at less than 40 Mpc from the source and rules out the interval:

$3 \times 10^{-20} \lesssim \alpha_H \lesssim 10^{-18}$. Future measurements by LISA of events similar to GW150914 can, on the other hand, constrain the range $10^{-16} \lesssim \alpha_H \lesssim 10^{-10}$.

It may be useful to summarize here the set of assumptions for the validity of the constraints in these Figures:

- Narrow resonance regime, i.e. $\beta \sim \alpha_H (\omega/H)^2 h_0^+ \lesssim 1$. This is displayed by the blue-dashed line in the Figures.
- The modification of the GW is sufficiently sizable to be observed, i.e. $|\Delta\gamma| > 0.1\gamma$. This is displayed by the purple-dashed line in the Figures. The modification takes place outside the Vainshtein radius, which for the values of α_H that we are considering corresponds to distances from the source smaller than those shown on the horizontal axis. Moreover, to be relevant the modification must occur before the detection.
- Nonlinearities in π are small so that their effect on the Mathieu equation is negligible, see discussion in Section 3.3.2. This is displayed by the red-dashed lines in the Figures.
- In the Figures we assume $c_s = 1/2$ and the constraints would change for different values of c_s. From eq. (3.2.44) the effect is proportional to $(1 - c_s^2)^2$ so that it is suppressed for values of c_s close to 1. Moreover, as we discussed in Section 3.2.1, for $c_s - 1 \lesssim 10^{-14}$ the π lightcone is too wide and our calculations do not apply. (Notice also that in our estimates of the various scales we are assuming that c_s is not parametrically small.)

For comparison, the bound coming from the perturbative decay of the graviton, see eq. (46) of [78], reads $\alpha_H \lesssim 10^{-10}$. Such values of α_H are outside the narrow resonance regime studied in this Chapter. One expects that the effect of large occupation number and nonlinearities of π are also important for larger values of α_H so that this perturbative bound should be revised. Moreover, notice that when the GW is closer to the source, its amplitude is larger and β will exceed unity. At a certain point one enters the Vainshtein regime and the coupling $\gamma\pi\pi$ is reduced (since we are considering very small values of the coupling, the Vainshtein radius will be correspondingly small). We will study all these aspects in Chapter 4.

3.4.2 *Higher harmonics and precursors*

Since for the operator $\tilde{m}_4^2$ one can trust the parametric growth and the change in the GW signal $\Delta\gamma$, we want to study this correction in more detail. At leading order in q the change $\Delta\gamma$ has the same frequency as the original wave. However, corrections to the leading solution (3.2.36) introduce higher harmonics in the GW signal. Higher harmonics appear in two quantitatively different ways. First, we can consider higher instability bands, see Figure 7a. However, in the narrow resonance approximation the instability coefficient in the m-th band scales as $\mu_m \sim q^m/(m!)^2 \sim \beta^m$ [83, 84]. Therefore, in the long τ limit they are exponentially suppressed compared to the fundamental band.

Second, we can stay in the first band and look at the modification of the π solution at higher orders in q. This will give an effect which is only suppressed by positive powers of q. If we include the first two corrections to eq. (3.2.36), we have[5]

$$\begin{aligned} f(\tau) &\simeq c_+ e^{(\mu+\delta\mu)\tau} F(\tau;\sigma) + c_- e^{(-\mu-\delta\mu)\tau} F(\tau;-\sigma) \\ F(\tau;\sigma) &= \sin(\tau-\sigma) + s_3 \sin(3\tau-\sigma) + c_3 \cos(3\tau-\sigma) + s_5 \sin(5\tau-\sigma) \\ s_3 &\equiv -\frac{1}{8}q + \frac{1}{64}q^2\cos(2\sigma)\,, \quad c_3 \equiv \frac{3}{64}q^2\sin(2\sigma)\,, \quad s_5 \equiv \frac{1}{192}q^2\,. \end{aligned} \tag{3.4.9}$$

Clearly, in this case the higher frequency component grows as fast as the original frequency. Therefore it is not necessary to specify the correction $\delta\mu$. The correction to $|f_{\tilde{p}}|^2$ at order q^2 is thus

$$\begin{aligned} |f_{\tilde{p}}|^2 \simeq |c_+|^2 e^{2\mu\tau} \big[&\sin^2(\tau-\sigma) + 2s_3 \sin(\tau-\sigma)\sin(3\tau-\sigma) + s_3^2 \sin^2(3\tau-\sigma) + \\ &2c_3 \sin(\tau-\sigma)\cos(3\tau-\sigma) + 2s_5 \sin(\tau-\sigma)\sin(5\tau-\sigma)\big]\,. \end{aligned} \tag{3.4.10}$$

On the other hand, when q becomes negative the solution can be obtained by performing the transformation $\tau \to \tau + \pi/2$, or equivalently $q \to -q$ together with $\sigma \to -\sigma - \pi/2$. By using the latter transformation and by recalling that by flipping the sign of q we send the decreasing mode into the growing one, we get the contribution for negative q:

$$\begin{aligned} |f_{\tilde{p}}|^2 \simeq |c'_+|^2 e^{2\mu\tau} \big[&\cos^2(\tau-\sigma) - 2s_3 \cos(\tau-\sigma)\cos(3\tau-\sigma) + s_3^2 \cos^2(3\tau-\sigma) + \\ &2c_3 \cos(\tau-\sigma)\sin(3\tau-\sigma) + 2s_5 \cos(\tau-\sigma)\cos(5\tau-\sigma)\big]\,. \end{aligned} \tag{3.4.11}$$

By direct calculation we can also show that, as in (3.2.41), $|c_+| = |c'_+| = 1$ at lowest order in q. We also note that, since all the frequencies in the expressions above are multiples of ω, the position of the saddle point is not affected and it is simply fixed by the exponential function. Hence the expression for $J(u)$ can be obtained by using the saddle-point procedure as in (3.2.43). We obtain

$$\begin{aligned} \Delta\gamma_{ij}(u,v) \simeq &-\frac{\nu}{4\Lambda^2}\frac{(1-c_s^2)^2}{c_s^5\sqrt{\beta}}\frac{\omega^{5/2}}{(8u\pi)^{3/2}}\exp\left(\frac{\beta}{4}\omega u\right)\epsilon_{ij}^+ \\ &\cdot\left\{\sin\left(\omega u+\frac{\beta}{2}\right) - \frac{\beta}{8}\cos(\omega u) + \frac{\beta^2}{768}\left[12\sin\left(\omega u-\frac{\beta}{2}\right) + 6\sin\left(\omega u+\frac{\beta}{2}\right) + \sin\left(3\omega u+\frac{\beta}{2}\right)\right]\right\}\,. \end{aligned} \tag{3.4.12}$$

(The result for the case of $\tilde{m}_4^2$, which is the focus of this Section, can be obtained by the replacement $\Lambda^2 \to \Lambda_\star^3\omega^{-1}$.) We are interested in the τ-dependent oscillatory part of (3.4.12). Compared to (3.2.43) we get a correction at the fundamental frequency linear in β (with no phase-shift). Moreover, to find the first higher harmonics we have to go to order β^2, where indeed we encounter a term with three-times the frequency ω. Note that by going to the second band instead, we would find higher harmonics of frequency 2ω.

5 In this Section we write the formulas for the case of m_3^3, so that they can be easily compared with Section 3.2.3. Notice that, since in this case π is coupled with $\dot{\gamma}$, while in the case $\tilde{m}_4^2$ it is coupled with $\ddot{\gamma}$, there is an overall shift of $\pi/2$ between the two cases.

Higher harmonics enter in the bandwidth of the detector at earlier time compared to the main signal. In some sense they are *precursors* of the main signal. To assess their potential observability, one has to consider that also the post-Newtonian expansion generates terms with a frequency which is a multiple of the original one. We leave this study to future work.

3.5 DISCUSSION AND FUTURE DIRECTIONS

We have studied the effects of a classical GW on scalar field fluctuations, in the context of dark energy models parametrized by the EFT of Dark Energy. The GW acts as a classical background and modifies the dynamics of dark energy perturbations, described by π, leading to parametric resonant production of π fluctuations. This regime is described by a Mathieau equation, where modes in the unstable bands grow exponentially. In the regime of narrow resonance, corresponding to a small amplitude of the GW, the instability can be studied analytically in detail. One can also include the back-reaction of the produced π on the original GW, which leads to a change in the signal. The resonant growth is however very sensitive to the non-linearities of the produced fields: when non-linearities of π are sizable the resonance is damped. This regime cannot be captured analytically: numerical simulations are needed to confirm this effect. This happens for the operator m_3^3, while a sizable modification of the GW signal is possible for the operator $\tilde{m}_4^2$, at least in some range of parameters, see Figures 10a and 10b.

Many questions remain open and will be the subject of further studies. For larger amplitudes of the GW, one exits the regime of narrow resonance: the GW may induce instabilities, which will be studied in Chapter 4. This will also allow to revise the robustness of the perturbative calculation of [78]. In the same Chapter we will also study how these effects are changed in the presence of Vainshtein screening. Simulations are probably required if one wants to study the regime of parametric resonance in the presence of sizable π self-interactions. Similar effects are at play in preheating after inflation and are also addressed numerically, see e.g. [87, 88]. It would also be interesting to try to envisage methods to look for the small changes in the GW signal. For instance, the generation of higher harmonics that enter the detection bandwidth before the main signal is a striking possible effect if it can be disentangled from post-Newtonian corrections. The effects that we studied look quite generic to all theories in which gravity is modified with a quite low cut-off. Therefore, it would be nice to explore other setups, starting from the DGP model. This model features the same non-linear interaction of π as the ones of the m_3^3 operator; however the extra-dimensional origin changes the dynamics of GWs so our analysis cannot be applied directly. We hope to come back to all these points in the future.

4

DARK-ENERGY INSTABILITIES INDUCED BY GRAVITATIONAL WAVES

In Chapter 2 we reviewed the decay induced by beyond Horndeski operator $\tilde{m}_4^2$ *perturbatively*, i.e. when individual gravitons decay independently of each other, and we saw that the absence of perturbative decay implies that $\Lambda_\star \gtrsim 10^3 \Lambda_3$, setting a tight bound on the parameter space of these models. More precisely, the absence of decay sets a bound on this operator: $|\tilde{m}_4^2| \lesssim 10^{-10} M_{Pl}^2$. Equivalently, this translates in the bound $|\alpha_H| \lesssim 10^{-10}$.[1] This rules out the possibility of observing the effects of these theories in the large-scale structure.

In Chapter 3 the analysis has been extended to a situation in which the coherent effects due to the large occupation number of the GW, acting as a classical background for π, is taken into account. In this case, a better description of the system is that of parametric resonance: π fluctuations are described by a Mathieu equation and are exponentially produced by parametric instability. We focused on the regime of *narrow resonance*, obtained when the GW induces a small perturbation on the π equation.[2] This regime can be used to probe only very small values of α_H. In particular, within the validity of our approximations the resonant decay takes place in the range $10^{-20} \lesssim |\alpha_H| \lesssim 10^{-17}$ for frequencies of interest for LIGO-Virgo and $10^{-16} \lesssim |\alpha_H| \lesssim 10^{-10}$ for LISA.

Another operator containing the cubic coupling $\gamma\pi\pi$ is $m_3^3(t)\delta g^{00}\delta K$. In the covariant language, it corresponds to the cubic Horndeski Lagrangian. In this case, the scale Λ that suppresses this cubic interaction is typically much higher than Λ_3, i.e. $\Lambda \sim \Lambda_2 \equiv (H_0 M_{Pl})^{1/2}$ and the perturbative decay, discussed in Chapter 2, is negligible. Moreover, we have seen in the previous Chapter that non-linearities in the dark energy field become sizable much before the effect of narrow resonance is relevant, possibly quenching the coherent instability. Therefore, the study of the perturbative and resonant decay for this operator remains inconclusive.

In this Chapter we study the effect of a classical GW on π in the regime where the amplitude of the wave is large, i.e. far from the narrow resonance, focusing on the stability of π perturbations. We initially concentrate on the operator m_3^3, introducing the action and setting up the notation in Section 4.1. (Deviations from this case are studied in Appendix D.) Inspired by the analysis of Ref. [94] reviewed in Section 4.2.1, in the rest of Section 4.2 we compute the non-linear classical solution of π generated by the GW and we study the stability of π fluctuations, outlining the differences with the analysis of [94]. We consider two different regimes: subluminal and luminal speed of π fluctuations,

1 More specifically, this constraint applies only for GLPV theories. For more general theories beyond Horndeski, such as the DHOST theories, the constraint becomes $\alpha_H + 2\beta_1 \lesssim 10^{-10}$ [78], where β_1 characterizes higher-order operators in the EFT of DE parameterization [82]. The consequences of this constraint on the Vainshtein mechanism in these theories has been studied in [90, 93].

2 The calculation in the narrow resonance regime reduces to the perturbative one when the occupation number is small enough.

respectively examined in Sections 4.2.2 and 4.2.3. Both cases display instabilities and qualitatively agree.

Without the knowledge of the UV completion of the theory, we cannot describe the evolution of the system and its endpoint. We discuss this issue in Section 4.3 with an example that displays similar instabilities and whose UV completion is known. Anyway, the theory must change qualitatively in the regions where the instability develops. In Section 4.4 we study whether the populations of binary systems and their production of GWs is enough to trigger the instability in the whole Universe. Stellar and massive black holes (BHs) are able to globally induce the instability in the regime where one has a sizable effect on structure formation ($|\alpha_B| \gtrsim 10^{-2}$). The instability is triggered by GWs as long as 10^{10} km, so that our conclusions are robust unless the theory is modified on even longer scales. In Section 4.5, we discuss the application of our study to the operator $\tilde{m}_4^2$ as well, and we derive strong bounds of order $|\alpha_H| \lesssim 10^{-20}$. Finally, we discuss our conclusions and future prospects in Section 4.6.

4.1 THE ACTION

In this Section we are going to give the action relevant to the dynamics of γ_{ij} and π. Also, we introduce an extra operator in the EFT action (2.1.9) in order to reproduce the typical interaction terms in the cubic covariant Galileon theories. Thus, We consider the following action in unitary gauge,

$$S = \int d^4x\sqrt{-g}\left[\frac{M_{Pl}^2}{2}\,{}^{(4)}R - \lambda(t) - c(t)g^{00} + \frac{m_2^4(t)}{2}(\delta g^{00})^2 - \frac{m_3^3(t)}{2}\delta g^{00}\delta K - \frac{\tilde{m}_3^3(t)}{8}(\delta g^{00})^2\delta K\right], \tag{4.1.1}$$

and focus in particular on the cubic Galileon, i.e. $\tilde{m}_3^3 = -m_3^3$ [48]. Generalizations of this case are discussed in Appendix D. We took a constant M_{Pl} with a proper choice of frame and we will discuss the general case at the end of this Chapter. As we have seen before, the operator proportional to m_2^4 affects the quadratic action for π, contributing to the overall normalization of the action and to the speed of sound. It also introduces self-interactions but in the cosmological setting these are suppressed by $\Lambda_2 \gg \Lambda_3$ and can be dropped for this discussion, because they are irrelevant for the stability. For the same reason, we can ignore higher powers of δg^{00}.

We follow the same procedure as in the previous Chapters: we work in Newtonian gauge with the solution of the constraints given by eq. (3.1.4) and we reintroduce π-field via the Stueckelberg trick. We then obtain the quadractic and cubic terms in the action for π and γ_{ij}. As usual, one canonically normalizes the fields using eq. (3.1.5) and the symbol of canonical normalizations is dropped.

Neglecting the expansion, the action for π reads $S_\pi = \int d^4x\mathscr{L}$, where the π Lagrangian is

$$\mathscr{L} = \frac{1}{2}\left[\dot{\pi}^2 - c_s^2(\partial_i\pi)^2\right] - \frac{1}{\Lambda_B^3}\Box\pi(\partial\pi)^2 + \frac{1}{\Lambda^2}\dot{\gamma}_{ij}\partial_i\pi\partial_j\pi + \frac{m_3^3}{2\sqrt{\alpha}M_{Pl}^3H}\pi\dot{\gamma}_{ij}^2\,, \tag{4.1.2}$$

where $\Box\pi \equiv \eta^{\mu\nu}\partial_\mu\partial_\nu\pi$ and $(\partial\pi)^2 \equiv \eta^{\mu\nu}\partial_\mu\pi\partial_\nu\pi$. The parameters c_s^2, Λ and Λ_B have been defined previously in eqs. (3.1.10), (3.1.7) and (3.3.2).

Let us comment on the last operator $\gamma\gamma\pi$. In fact, it is not directly obtained from the operator $m_3^3\delta g^{00}\delta K$. Instead, it comes from the Einstein-Hilbert term of the action (4.1.1) when replacing the potentials Φ and Ψ with π *via* eq. (3.1.4).[3]

For the GW, we will use the classical background solution traveling in the $\hat{z}$ direction with linear polarization $+$, used in [95],

$$\gamma_{ij} = M_{Pl} h_0^+ \sin\left[\omega(t-z)\right] \epsilon_{ij}^+ \,, \tag{4.1.3}$$

where h_0^+ is the dimensionless strain amplitude and $\epsilon_{ij}^+ = \mathrm{diag}(1,-1,0)$. For later convenience, we also define the parameter [95]

$$\beta \equiv \frac{2\omega M_{Pl} h_0^+}{c_s^2|\Lambda^2|} = \frac{2\sqrt{2}|\alpha_B|}{\alpha c_s^2}\frac{\omega}{H} h_0^+ \,. \tag{4.1.4}$$

4.2 CLASSICAL SOLUTIONS AND STABILITY OF PERTURBATIONS

In any non-linear theory one can investigate the stability of a given solution by looking at the kinetic term of small perturbations around it. This was done for the cubic Galileon (equivalent to the decoupling limit of the Dvali-Gabadadze-Porrati (DGP) model) in [94], in the absence of GWs. It was proven that solutions that are stable at spatial infinity are stable everywhere, provided the sources are non-relativistic. The analysis was later extended to higher Galileons in [96], where such strong statement does not hold and one expects that general non-linear solutions feature instabilities. Here we want to extend the analysis of [94] including GWs[4] and considering a generic speed of propagation c_s. (In order to compare with the result of [94], in the main text we stick to the non-linearity of the cubic Galileon, i.e. $\tilde{m}_3^3 = -m_3^3$. In Appendix D we generalize the analysis to the case $\tilde{m}_3^3 \neq -m_3^3$.)

For convenience we define $\bar{\eta}_{\mu\nu} \equiv \mathrm{diag}(-1, c_s^2, c_s^2, c_s^2)$ and $\bar{\Box}\pi \equiv \bar{\eta}^{\mu\nu}\partial_\mu\partial_\nu\pi = -\ddot{\pi} + c_s^2\partial_k^2\pi$. In this Section, indices are raised and lowered with the usual Minkowski metric. Moreover, we define

$$\Gamma_{\mu\nu} \equiv \frac{\dot{\gamma}_{\mu\nu}}{\Lambda^2} \,. \tag{4.2.1}$$

Using the above definitions, the action for π, eq. (4.1.2), becomes

$$\mathscr{L} = -\frac{1}{2}\bar{\eta}^{\mu\nu}\partial_\mu\pi\partial_\nu\pi - \frac{1}{\Lambda_B^3}\Box\pi(\partial\pi)^2 + \Gamma_{\mu\nu}\partial^\mu\pi\partial^\nu\pi - \frac{1}{2}\Lambda_B^3\pi\Gamma_{\mu\nu}^2 \,. \tag{4.2.2}$$

In the following we will use that $\partial^\mu\Gamma_{\mu\nu} = \eta^{\mu\nu}\Gamma_{\mu\nu} = \bar{\eta}^{\mu\nu}\Gamma_{\mu\nu} = 0$. For our GW solution (4.1.3) we have

$$\Gamma_{00} = \Gamma_{0i} = 0 \,, \qquad \Gamma_{ij} = \frac{\beta c_s^2}{2}\cos\left[\omega(t-z)\right]\epsilon_{ij}^+ \,, \tag{4.2.3}$$

3 Since we know that a tensor perturbation γ_{ij} couples with the metric in the same way as a scalar field does, one can easily obtain this interaction by considering the Lagrangian of minimally coupled scalar field and replacing the scalar field by γ_{ij}.

4 As discussed in [97], the DGP model is not a local theory of a scalar field and thus is not included in the ordinary EFT of DE action. However, the structure of the non-linear terms is analogous and the arguments used in [94] can be applied straightforwardly to the EFT of DE. On the other hand the brane-bending mode in the DGP model is not a scalar under 4d diffs [98], so that the coupling with GWs will be different from the one discussed in this Chapter.

where we have used the definition of β, eq. (4.1.4). The third term of eq. (4.2.2) suggests that for $\beta > 1$ the scalar π features a gradient instability, because $\Gamma_{\mu\nu}$ changes sign in time. This conclusion, although substantially correct, is premature, since the GW also sources a background for π and this affects through non-linearities the behavior of perturbations.

Let us split the field in a classical background part plus fluctuations, i.e. $\pi = \hat{\pi}(t, \mathbf{x}) + \delta\pi(t, \mathbf{x})$. In general $\hat{\pi}$ will be sourced by the term $\dot{\gamma}^2_{\mu\nu}$ of eq. (4.1.2), corresponding to the last term of eq. (4.2.2), and also by astrophysical matter sources. Let us first study the background solution $\hat{\pi}$. Its equation of motion reads

$$\bar{\Box}\hat{\pi} - \frac{2}{\Lambda_B^3}\left[(\partial_\mu\partial_\nu\hat{\pi})^2 - \Box\hat{\pi}^2\right] - 2\Gamma_{\mu\nu}\partial^\mu\partial^\nu\hat{\pi} - \frac{\Lambda_B^3}{2}\Gamma^2_{\mu\nu} = 0\,. \tag{4.2.4}$$

Following [94], we define the matrix

$$\mathcal{K}_{\mu\nu} \equiv -\frac{1}{\Lambda_B^3}\partial_\mu\partial_\nu\hat{\pi}\,, \tag{4.2.5}$$

and rewrite the above equation as

$$\mathcal{K}^{\mu\nu}\bar{\eta}_{\mu\nu} + 2\left(\mathcal{K}_{\mu\nu}\mathcal{K}^{\mu\nu} - \mathcal{K}^2\right) - 2\Gamma_{\mu\nu}\mathcal{K}^{\mu\nu} + \frac{1}{2}\Gamma^2_{\mu\nu} = 0\,. \tag{4.2.6}$$

Due to the Galileon symmetry and the fact the equations of motion are second order, eq. (4.2.4) reduces to an algebraic equation for the second derivatives of $\hat{\pi}$. Eq. (4.2.6) can be rewritten solely in terms of $\tilde{\mathcal{K}}_{\mu\nu} \equiv \mathcal{K}_{\mu\nu} - \frac{1}{2}\Gamma_{\mu\nu}$, and becomes

$$\tilde{\mathcal{K}}^{\mu\nu}\bar{\eta}_{\mu\nu} + 2\left(\tilde{\mathcal{K}}_{\mu\nu}\tilde{\mathcal{K}}^{\mu\nu} - \tilde{\mathcal{K}}^2\right) = 0\,. \tag{4.2.7}$$

The stability of a generic solution of eq. (4.2.6) can be assessed by studying the quadratic Lagrangian for the perturbations $\delta\pi$. These are assumed to be of a wavelength much shorter than the typical variation of $\hat{\pi}$. Expanding the action (4.2.2) at quadratic order in $\delta\pi$, after some integrations by parts we obtain

$$\mathscr{L}_{(2)} = Z^{\mu\nu}(x)\,\partial_\mu\delta\pi\partial_\nu\delta\pi\,, \qquad Z^{\mu\nu} \equiv -\frac{1}{2}\bar{\eta}^{\mu\nu} - 2\left(\tilde{\mathcal{K}}^{\mu\nu} - \eta^{\mu\nu}\tilde{\mathcal{K}}\right)\,, \tag{4.2.8}$$

where the indexes are raised and lowered with the Minkowski metric $\eta_{\mu\nu}$. In general, for time-dependent kinetic terms like (4.2.8) there is no clear definition of stability. However, in the limit that we consider here where $Z^{\mu\nu}(x)$ changes much slower than the fluctuations $\delta\pi$, the requirement of stability simply translates in the absence of ghost or gradient instabilities for the perturbations, i.e. $Z^{00} > 0$ and that $Z^{0i}Z^{0j} - Z^{ij}Z^{00}$ is a positive-definite matrix at each point [94, 99]. As explained in [99], a theory can be stable even when $Z^{00} < 0$, provided it features superluminal excitations and one can boost to a frame in which $Z^{00} > 0$.[5] However, in our problem we have a privileged frame, the cosmological one, where the Cauchy problem must be well defined. Therefore stability must be manifest in this specific frame.

5 In the absence of superluminality the sign of Z^{00} is invariant under Lorentz transformations. The positive definiteness of the matrix $Z^{0i}Z^{0j} - Z^{ij}Z^{00}$ is always invariant.

It is important to stress that the Newtonian gauge is very special for our analysis. In this Chapter we are interested in a fully non-linear analysis, but we solved for Ψ and Φ linearly, see eq. (3.1.4). This is justified in Newtonian gauge because, even when the equation of motion of π becomes non-linear, Φ and Ψ remain small and higher-order terms can be neglected. (This is analogous to what happens for non-linearities in the Large-Scale Structure: perturbation theory for the density contrast δ breaks down on short scales, but Φ and Ψ remain small and perturbative.) This does not happen in other gauges. For instance, in spatially-flat gauge one can take the solution for the shift function, see eq. (C.2.3) in Appendix C. In the regime of interest $\alpha_\psi \sim 1$ and Galileon non-linearities are relevant for $\partial^2\pi_c \sim H^2 M_{Pl}$, which implies $\partial^2\pi \sim H$. Therefore, the perturbation in the extrinsic curvature is $\delta K \sim \nabla^2\psi \sim H$, which is of the same order as the background value. Thus higher-order corrections in the constraint equations become relevant, since the Einstein-Hilbert action contains terms quadratic in the extrinsic curvature that cannot be neglected. A similar behavior occurs in comoving gauge. The analysis in these gauges is therefore much more complicated. As a partial check of our calculation, in Appendix C we verify that our Newtonian action matches the action in spatially flat gauge, but we do this only at the perturbative level, at cubic order.

It is important to stress that, although our analysis is done in a particular gauge, the matrix $\tilde{\mathcal{K}}_{\mu\nu}$ is a covariant tensor:

$$\tilde{\mathcal{K}}_{\preceq\succeq} = \mathcal{K}_{\preceq\succeq} - \frac{1}{2}\Gamma_{\mu\nu} = -\frac{\alpha_B}{\alpha H}\cdot\nabla_\mu\nabla_\nu\phi\,, \tag{4.2.9}$$

where $\phi \equiv t + \pi$ is the complete dark-energy scalar field (not in canonical normalization) and it is a scalar quantity under all diffs. (The second equality works only if we neglect non-linear terms involving π and Christoffel's symbols: one can check that these are subdominant with respect to the terms we kept.) Therefore the matrix $Z^{\mu\nu}$ is a covariant tensor[6] and the conditions for stability are gauge independent.

The matrix $Z_{\mu\nu}$ is characterized by the classical non-linear solution of eq. (4.2.6). To better see the connection between stability and background evolution, it is useful to invert the second relation in (4.2.8) and express $\tilde{\mathcal{K}}_{\mu\nu}$. We obtain

$$\tilde{\mathcal{K}}_{\mu\nu} = -\frac{1}{2}\left(Z_{\mu\nu} - \frac{1}{3}Z\eta_{\mu\nu}\right) - \frac{1}{4}\bar{\eta}_{\mu\nu} + \frac{1}{12}(1+3c_s^2)\eta_{\mu\nu}\,. \tag{4.2.10}$$

Using this expression to replace $\tilde{\mathcal{K}}_{\mu\nu}$, the equation for the background, eq. (4.2.7), becomes an equation containing only quadratic terms in $Z_{\mu\nu}$, i.e.,

$$\frac{1}{3}Z^2 - (Z_{\mu\nu})^2 = \frac{3c_s^2-1}{6}\,. \tag{4.2.11}$$

Remarkably, the terms containing $\Gamma_{\mu\nu}$ have canceled out: we obtain the same equation as the one derived in [94] without GWs, although here we have neglected the presence of matter sources, and we have considered a generic c_s^2. This is to be expected since $\dot{\gamma}_{\mu\nu}$ can be set to zero *locally* by a proper change of coordinates; thus, its value cannot affect eq. (4.2.11). On the other hand, the solution for

6 Actually, $\bar{\eta}^{\mu\nu}$ depends on π perturbations but again the terms that we are neglecting are subdominant with respect to the ones we kept.

$\hat{\pi}$ requires a global knowledge of the GWs. We can now use this equation to discuss the stability of the solution.

4.2.1 *Stability in the absence of GWs*

To warm up, we will first review the argument for the case $\Gamma_{\mu\nu} = 0$ and $c_s^2 = 1$, analogous to the DGP case discussed in [94]. A configuration that turns off at spatial infinity, i.e. for which $\mathcal{K}_{\mu\nu} = 0$ and $Z_{\mu\nu} = -\eta_{\mu\nu}/2$, is stable in this limit. One can show that such a solution cannot become unstable at any other point $\mathbf{x}$. The proof is made by further assuming that the matrix $Z_{\mu\nu}(x)$ is diagonalizable by means of a Lorentz boost, in such a way that it can be taken to the form $Z^{\mu}_{\ \nu} = \mathrm{diag}(z_0, z_1, z_2, z_3)$.

Using this form, eq. (4.2.11) reduces, for $c_s = 1$, to

$$-\frac{2}{3}\left[(z_0^2 + \ldots + z_3^2) - (z_0 z_1 + z_0 z_2 + \ldots + z_2 z_3)\right] = \frac{1}{3}\,. \tag{4.2.12}$$

In this frame, stability requires that $z_\mu < 0$, for all $\mu = \{0, 1, 2, 3\}$. Marginally stable solutions, on the other hand, lie on the hyper-planes defined by $z_\mu = 0$, for some μ. A stable solution can become unstable if and only if the solution crosses one of these critical hyper-planes at some intermediate point in the evolution. For this to happen, these critical hyper-planes should intersect the space of solutions. Without loss of generality we can consider the plane $z_0 = 0$, $z_i \neq 0$ in (4.2.12), that now reduces to

$$-\frac{1}{3}\left[(z_1 - z_2)^2 + (z_1 - z_3)^2 + (z_2 - z_3)^2\right] = \frac{1}{3}\,. \tag{4.2.13}$$

This equation does not admit any solution because the two sides have different signs: a stable solution at infinity remains stable everywhere. Notice that the right-hand side of the equation above is replaced by $(3c_s^2 - 1)/6$ for a general c_s, see eq. (4.2.11). Therefore the stability of the system, even in the absence of GWs, is not guaranteed for $c_s < 1/\sqrt{3}$.

In the next two Sections we are going to explicitly show the presence of instabilities around a GW background, respectively for $c_s < 1$ and $c_s = 1$. For $c_s > 1/\sqrt{3}$, this is somewhat surprising, since eq. (4.2.11) is qualitatively the same as in the absence of GWs. The catch is that the matrix $Z_{\mu\nu}$ will not be diagonalizable. Indeed, diagonalizability can be proven in the case of non-relativistic sources, but it does not hold for a GW background, which is clearly relativistic.

4.2.2 *The effect of GWs, $c_s < 1$*

To study the case $c_s < 1$ we start from eq. (4.2.4). For large GW amplitudes ($\beta > 1$), the $\gamma\pi\pi$ interaction leads to a wrong sign of the spatial kinetic term for $\delta\pi$. However, to confirm this assessment we need to take into account the effect of the tadpole $\gamma\gamma\pi$ and of the self-interactions of π. The tadpole will generate a background for $\hat{\pi}$ that, in turn, modifies the action for fluctuations through eq. (4.2.8).

The setup here is the same as in Chapter 3 (see Figure6). It is convenient to introduce the null coordinates,

$$u \equiv t - z\,, \qquad v \equiv t + z\,, \tag{4.2.14}$$

which implies $\partial_t = \partial_u + \partial_v$ and $\partial_z = \partial_v - \partial_u$. Moreover, the following relations will be useful below,

$$\partial_t^2 = \partial_u^2 + \partial_v^2 + 2\partial_u\partial_v\,, \qquad \partial_z^2 = \partial_u^2 + \partial_v^2 - 2\partial_u\partial_v\,, \qquad \partial_t\partial_z = \partial_v^2 - \partial_u^2\,. \tag{4.2.15}$$

In the presence of a background for the GW, of the form $\gamma_{ij}(u)$, we can solve the equation (4.2.4) for $\hat{\pi}$. In this case, since $c_s < 1$, there is no intersection between the region where the source is active and the past light-cone of π is finite (see [95]). Therefore we have translational invariance along v (at least as long as we are considering points far away from the emission of γ). For this reason we will look for solutions of the form $\hat{\pi}(u)$. Notice that the non-linear interaction arising from the cubic Galileon vanishes when π depends solely on the variable u. Indeed, eq. (4.2.15) implies

$$\partial_t^2\hat{\pi} = \partial_u^2\hat{\pi}\,, \qquad \partial_z^2\hat{\pi} = \partial_u^2\hat{\pi}\,, \qquad \partial_t\partial_z\hat{\pi} = -\partial_u^2\hat{\pi}\,, \tag{4.2.16}$$

and thus that

$$\bar{\Box}\hat{\pi} = -(1-c_s^2)\partial_u^2\hat{\pi}\,, \qquad (\partial_\mu\partial_\nu\hat{\pi})^2 - \Box\hat{\pi}^2 = 0\,. \tag{4.2.17}$$

Therefore, defining

$$\varphi \equiv \frac{\hat{\pi}}{\Lambda_B^3}\,, \tag{4.2.18}$$

where Λ_B^3 is defined in eq. (3.3.2), eq. (4.2.4) gives

$$\varphi''(u) = -\frac{\Gamma^2_{\mu\nu}}{2(1-c_s^2)} = -\frac{\beta^2 c_s^4}{4(1-c_s^2)}\cos^2(\omega u)\,, \tag{4.2.19}$$

where we used eq. (4.2.3). The solution implies that $\varphi''(u) \leqslant 0$. Note that, as one expects, the limit $c_s \to 1$ is singular: the past light-cone of π becomes sensitive to the details of the emission of the GW.

We can now use this solution to compute the kinetic matrix for the π fluctuations, eq. (4.2.8). Its non-vanishing elements are given by

$$\begin{aligned}
Z^{00} &= \frac{1}{2} + 2\varphi''(u) = \frac{1}{2}\left[1 - \frac{\beta^2 c_s^4}{1-c_s^2}\cos^2(\omega u)\right]\,,\\
Z^{11} &= -\frac{1}{2}c_s^2 + \Gamma^{11} = -\frac{c_s^2}{2}\left[1 - \beta\cos(\omega u)\right]\,,\\
Z^{22} &= -\frac{1}{2}c_s^2 + \Gamma^{22} = -\frac{c_s^2}{2}\left[1 + \beta\cos(\omega u)\right]\,,\\
Z^{33} &= -\frac{1}{2}c_s^2 + 2\varphi''(u) = -\frac{c_s^2}{2}\left[1 + \frac{\beta^2 c_s^2}{1-c_s^2}\cos^2(\omega u)\right]\,,\\
Z^{03} &= Z^{30} = 2\varphi''(u) = -\frac{\beta^2 c_s^4}{2(1-c_s^2)}\cos^2(\omega u)\,.
\end{aligned} \tag{4.2.20}$$

The background $\hat{\pi}$ does not affect the entries Z^{11} and Z^{22} (it contributes only through $\Box\hat{\pi}$ which vanishes since $\hat{\pi} = \hat{\pi}(u)$): they feature a gradient instability for $\beta > 1$. On the other hand, one can easily verify that the condition $(Z^{03})^2 - Z^{00}Z^{33} > 0$ is satisfied, i.e. the gradient instability does not appear in this direction. One has a ghost instability, $Z^{00} < 0$, for

$$\frac{\beta^2 c_s^4}{1-c_s^2} > 1 \,. \tag{4.2.21}$$

These results seem to contradict what we discussed in the previous Section, where we stated that the stability is guaranteed provided $c_s^2 > 1/3$. However in order to prove stability one has to assume that the matrix $Z^{\mu\nu}$ is diagonalizable via a boost at each point. This is possible only when $|Z^{03}| < \frac{1}{2}|Z^{00} + Z^{33}|$ [99]. In our case this condition gives

$$\frac{\beta^2 c_s^4}{1-c_s^2} < \frac{1-c_s^2}{4} \,. \tag{4.2.22}$$

Comparing this inequality with eq. (4.2.21), one sees that the $Z^{\mu\nu}$ is not diagonalizable when there is a ghost instability, so there is no contradiction with the result of Section 4.2.1. The inequality (4.2.22) can be written as

$$c_s^2 < \frac{1}{1+2\beta} \,. \tag{4.2.23}$$

In the presence of a gradient instability, $\beta > 1$, the right-hand side is smaller than $1/3$. Therefore the matrix $Z^{\mu\nu}$ can be diagonalized only if $c_s^2 < 1/3$. Again there is no contradiction with what we discussed above since for $c_s^2 < 1/3$ there is no guarantee of stability.

4.2.3 *The effect of GWs,* $c_s = 1$

Let us now turn to $c_s = 1$. This case is qualitatively different since the light-cone of π is as wide as the one of the GWs, see Figure 6, so that we should not expect the same kind of instabilities. As before, we take a GW of the form $\gamma_{ij}(u)$, but now one cannot assume that $\hat{\pi}$ only depends on u; in general it will also depend on v and it will be sensitive to the source of GWs. However, for simplicity, we stick to the equations in the absence of sources.

To find $\hat{\pi}$ we write (4.2.4) in terms of the null coordinates u and v and using eq. (4.2.15) we find

$$\Box\hat{\pi} = -4\partial_u\partial_v\hat{\pi} \,, \tag{4.2.24}$$

$$(\partial_\mu\partial_\nu\hat{\pi})^2 = (\partial_t^2\hat{\pi})^2 - 2(\partial_t\partial_z\hat{\pi})^2 + (\partial_z^2\hat{\pi})^2 = 8\left[\partial_u^2\hat{\pi}\partial_v^2\hat{\pi} + (\partial_u\partial_v\hat{\pi})^2\right] \,. \tag{4.2.25}$$

Equation (4.2.4), written in terms of $\varphi = \hat{\pi}\Lambda_B^{-3}$, becomes

$$\partial_u\partial_v\varphi + 4\left[\partial_u^2\varphi\,\partial_v^2\varphi - (\partial_u\partial_v\varphi)^2\right] = -\frac{\Gamma_{\mu\nu}^2}{8} \,. \tag{4.2.26}$$

(Notice that the coupling $\gamma\pi\pi$ does not contribute.)

It is not clear how to determine the most general solution of the above non-linear equation. However, two solutions can be easily obtained by considering $\varphi(u,v) = U(u)V(v)$. Then, one can make

the LHS of (4.2.26) independent of v by taking $V(v) = v$. In this case, the equation takes a very simple form in terms of $U(u)$,

$$U'(u)^2 - \frac{1}{4}U'(u) - \frac{\Gamma_{\mu\nu}^2}{32} = 0\,, \tag{4.2.27}$$

with solutions

$$U'_{\pm}(u) = \frac{1}{8}\left(1 \pm \sqrt{1 + 2\Gamma_{\mu\nu}^2}\right)\,, \tag{4.2.28}$$

where the solution that recovers the linear one at small couplings is $U'_{-}(u)$. (The conclusions about stability are not altered by considering the other branch.)

We can now check whether the solution (4.2.28) is stable or not. The kinetic matrix eq. (4.2.8) is given by

$$\begin{aligned}
Z^{00} &= \frac{1}{2} + 2\left[vU''(u) - 2U'(u)\right]\,,\\
Z^{11} &= -\frac{1}{2} + \Gamma^{11} + 8U'(u)\,,\\
Z^{22} &= -\frac{1}{2} + \Gamma^{22} + 8U'(u)\,,\\
Z^{33} &= -\frac{1}{2} + 2\left[vU''(u) + 2U'(u)\right]\,,\\
Z^{03} &= Z^{30} = 2vU''(u)\,.
\end{aligned} \tag{4.2.29}$$

First, we focus on possible gradient instabilities. One can easily check, using (4.2.28), that the components Z^{11} and Z^{22} are negative, so there is no gradient instability in these directions. The matrix is non-diagonal in the block t-z and stability requires $(Z^{03})^2 - Z^{00}Z^{33} > 0$. In our case

$$(Z^{03})^2 - Z^{00}Z^{33} = \left(\frac{1}{2} - 4U'(u)\right)^2 \geqslant 0\,; \tag{4.2.30}$$

the matrix $Z^{\mu\nu}$ is thus free from gradient instabilities.

Let us turn now to ghost instabilities. As already pointed out at the beginning of Section 4.2, ghosts are present whenever Z^{00} becomes negative. From eq. (4.2.29) we see that this is possible: the term linear in v can be negative and larger than the other positive contributions. To see this more explicitly, we can replace $U(u)$ in Z^{00} with the solution (4.2.28). We get

$$Z^{00} = \frac{1 + 2\Gamma_{\mu\nu}^2 - v\Gamma_{\mu\nu}\partial_u\Gamma^{\mu\nu}}{2(1 + 2\Gamma_{\mu\nu}^2)^{1/2}} \simeq \frac{1 - \Gamma_{\mu\nu}^2\omega v}{2(1 + 2\Gamma_{\mu\nu}^2)^{1/2}}\,, \tag{4.2.31}$$

where in the last equality we used that $\omega v \gg 1$ and we approximated $\partial_u\Gamma_{\mu\nu} = \omega\Gamma_{\mu\nu}\tan(\omega u) \simeq \omega\Gamma_{\mu\nu}$ (valid for a plane wave). Using $\Gamma_{\mu\nu}^2 \simeq \beta^2/2$, the condition to avoid a ghost becomes

$$\beta^2 \lesssim \frac{2}{\omega v}\,. \tag{4.2.32}$$

Since after a few oscillations $\omega v \gg 1$, we conclude that also for $c_s = 1$ the system becomes unstable. Notice that also in this case the matrix $Z^{\mu\nu}$ is not diagonalizable (the condition $|Z^{03}| < \frac{1}{2}|Z^{00} + Z^{33}|$

is not satisfied by eq. (4.2.29), but the two sides are actually equal) so that there is no contradiction with the result of Section 4.2.1.

Even if the solution we studied is not unique and does not take into account the effect on $\hat{\pi}$ of sources, we conclude that the system is generically unstable and avoids the stability argument of [94], because the GW background is relativistic and gives a non-diagonalizable $Z^{\mu\nu}$ (7). For the same reason, one expects the system to be unstable also for $c_s > 1$ (although it is not clear whether a theory of this kind allows a standard UV completion). In this case, it is not clear how to find a simple ansatz for the solution $\varphi(u, v)$, so that a dedicated study is left to future work.

4.2.4 *Vainshtein effect on the instability*

So far we assumed that GWs are the only source of $\hat{\pi}$. However, astrophysical objects also source $\hat{\pi}$ and a corresponding matrix $Z^{\mu\nu}$. As discussed above, in the presence of non-relativistic sources this matrix is healthy and it gives rise to the so-called Vainshtein effect: a large $Z^{\mu\nu}$ gives a more weakly coupled theory, in which the effect of π is suppressed. The Vainshtein effect will also suppress the instability we are studying: the astrophysical background makes the kinetic term large and healthy, while the dangerous vertex $\gamma\pi\pi$ is *not* enhanced (one does not have a term $\partial^2\hat{\pi}\dot{\gamma}\partial\pi\partial\pi$, since it would have too many derivatives). Therefore, in regions with large $Z^{\mu\nu}$ the parameter β is effectively suppressed and the instabilities can thus be stopped. However, the condition of large $Z^{\mu\nu}$ cannot be maintained over cosmological scales. Both analytical arguments [53] and simulations [101] indicate that Vainshtein screening is negligible over sufficiently large scales, say larger than 1 Mpc; see Section 4.4 for a more detailed discussion. This means that averaged over these large scales the effect of astrophysical sources is negligible[8]. Since the GWs we observe travel over cosmological distances, one expects that on average the effect of Vainshtein screening is small and that over most of their travel the gradient instability is active. We will come back to this point below, in Section 4.4.

4.3 FATE OF THE INSTABILITY

In order to understand the implications of the instability we discussed, one would like to know the fate of it. In this Section we want to argue that the dynamics of the instability and its endpoint are

7 Even in the absence of GWs, perturbations around a plane wave $\hat{\pi}(u)$, with $c_s = 1$, are unstable [100], as it is easy to check. This suggests that the instability is generic in a relativistic setting.

8 Since astrophysical sources are with good approximation non-relativistic, the entries Z^{0i} of the matrix $Z^{\mu\nu}$ are negligible (see discussion at the beginning of Section 4.2). In order to stabilize the gradient instability one should have that all the eigenvalues of the spatial part of the matrix Z^{ij} are large, much larger than the standard kinetic term, i.e. parametrically larger than unity (in absolute value). This means that also the trace should be parametrically larger than unity. To avoid the instability these conditions should be maintained over all the trajectory of the GW, i.e. over cosmological distances. This however cannot happen. If the trace were large over large regions, it would imply that the trace of the average of $Z^{\mu\nu}$ over a large region is sizable. This is in contradiction with the statement that linear perturbation theory is recovered over sufficiently large scales.

UV sensitive and cannot be studied without knowing the UV theory. First of all, notice that it is not possible to follow the development of the instability looking at what happens at the matrix $Z^{\mu\nu}$ in the presence of the growing perturbations. Since the most unstable modes are the shortest, the instability generates a configuration of $\hat{\pi}$ with very large gradients and the analysis of the previous Sections is only useful to understand the behavior of modes with wavelength much shorter than the variation of the background.

Since we do not know of any UV completion of the theories we are discussing, to gain some intuition on the possible outcome of the instability we now discuss a toy model that features gradient and ghost-like instabilities, and whose UV completion is known. Consider a $U(1)$-symmetric theory for a complex scalar h, with a quartic mexican-hat potential, in the absence of gravity[9]:

$$\mathscr{L}_{UV} = -|\partial h|^2 - V(|h|) \,, \qquad V(|h|) = \lambda\big(|h|^2 - v^2\big)^2 \,. \tag{4.3.1}$$

In the broken phase with $\langle h\rangle = v$ we have a massless degree of freedom (the Goldstone boson), and a heavy one (the 'Higgs'). It makes sense to integrate out the latter and write down a low-energy effective theory for the former.

For small λ, one can integrate out the Higgs at tree level. Let us define $h = h_0 \exp(i\phi)$. If we are interested in terms with the minimum number of derivatives acting on ϕ, one can solve the classical equation of motion for a constant h_0 in a constant X field, $X \equiv (\partial\phi)^2$, and plug the result back into the action. One gets

$$h_0^2 = -\frac{1}{2\lambda}X + v^2 = \frac{1}{4\lambda}(\mu^2 - 2X) \,, \tag{4.3.2}$$

where $\mu^2 \equiv 4\lambda v^2$ is the mass of the radial direction. Plugging this back into the action, one gets the Lagrangian

$$P(X) \simeq -\frac{1}{4\lambda}X\big(\mu^2 - X\big) \,. \tag{4.3.3}$$

Remarkably, the tree-level effective action stops at quadratic order in X, that is at fourth order in ϕ. The function $P(X)$ will receive corrections suppressed by λ at loop level. Notice that the validity of this action is not limited to small X, provided *derivatives* of X are small: operators with derivatives acting on X are suppressed by powers of ∂/μ.

Consider a background $\hat{\phi}$ with $\partial_\mu\hat{\phi} \equiv C_\mu$ and small perturbations about it, $\hat{\phi} + \delta\phi$. The matrix $Z_{\mu\nu}$, see eq. (4.2.8), is given by

$$Z^{\mu\nu} = 2\hat{P}''C^\mu C^\nu + \hat{P}'\eta^{\mu\nu} \,. \tag{4.3.4}$$

If C^μ is time-like, that is if $\hat{X} < 0$, we can choose a frame such that $C^0 = \pm\sqrt{-\hat{X}}$, $\vec{C} = 0$. In this frame we have

$$\mathscr{L}_2 = -\big(2\hat{P}''\hat{X} + \hat{P}'\big)\delta\dot{\phi}^2 + \hat{P}'(\nabla\delta\phi)^2 \,, \qquad \hat{X} < 0 \,. \tag{4.3.5}$$

For stability we thus want

$$2\hat{P}''\hat{X} + \hat{P}' < 0 \,, \qquad \hat{P}' < 0 \,. \tag{4.3.6}$$

9 This analysis is based on unpublished work by P. Creminelli and A. Nicolis. See also [102].

If instead C^μ is space-like, $\hat{X} > 0$, we can go to a frame where $C^0 = 0$, $|\vec{C}| = \sqrt{\hat{X}}$, where we get

$$\mathscr{L}_2 = -\hat{P}'\delta\dot{\phi}^2 + \hat{P}'(\nabla_\perp\delta\phi)^2 + \left(2\hat{P}''\hat{X} + \hat{P}'\right)(\nabla_\parallel\delta\phi)^2 \,, \qquad \hat{X} > 0 \,. \tag{4.3.7}$$

The parallel and normal directions are of course relative to $\vec{C}$. We thus see that in this case too the conditions for stability are those given in eq. (4.3.6).

For the case we are studying, eq. (4.3.3), one has

$$2\hat{P}''\hat{X} + \hat{P}' = \frac{1}{4\lambda}(6\hat{X} - \mu^2) \,, \qquad \hat{P}' = \frac{1}{4\lambda}(2\hat{X} - \mu^2) \,. \tag{4.3.8}$$

The system is stable for

$$\hat{X} < \frac{1}{6}\mu^2 \,. \tag{4.3.9}$$

It is interesting that for such values of $\hat{X}$, the propagation speed is always subluminal—a non-trivial check about the consistency of the effective theory. In the range

$$\frac{1}{6}\mu^2 < \hat{X} < \frac{1}{2}\mu^2 \,, \tag{4.3.10}$$

the $(\nabla_\parallel\delta\phi)^2$ in eq. (4.3.7) has the wrong sign, thus signaling a tachyon-like instability which, unlike a real tachyon instability, is dominated by the UV. That is, we have exponentially growing modes $\sim e^{k_\parallel t}$. The shorter the wavelength, the faster the growing rate. Finally, for

$$\hat{X} > \frac{1}{2}\mu^2 \tag{4.3.11}$$

all terms in eq. (4.3.7) have wrong signs. This in the low-energy effective theory looks like a ghost-like instability.

It is interesting to understand these pathologies in terms of the UV theory (4.3.1). There, the kinetic energy is positive definite. There is no room for ghost-instabilities, and the only instabilities present in certain regions of field space are real tachyons, with a decay rate of order μ. Let us therefore consider small fluctuations of the radial mode h_0 and of ϕ in the UV theory, about a background configuration with constant $\hat{X}$ and $\hat{h}_0$, related by eq. (4.3.2),

$$h_0 \to \hat{h}_0 + \delta h \,, \qquad \phi \to \hat{\phi} + \delta\phi \,. \tag{4.3.12}$$

Expanding the Lagrangian (4.3.1) at quadratic order we get

$$\mathscr{L}_{UV} \to \delta\dot{h}^2 + \delta\dot{\tilde{\phi}}^2 - \begin{pmatrix} \delta h \\ \delta\tilde{\phi} \end{pmatrix} \cdot \begin{pmatrix} -\nabla^2 + (-2\hat{X} + \mu^2) & 2\sqrt{\hat{X}}\,\nabla_\parallel \\ -2\sqrt{\hat{X}}\,\nabla_\parallel & -\nabla^2 \end{pmatrix} \cdot \begin{pmatrix} \delta h \\ \delta\tilde{\phi} \end{pmatrix} , \tag{4.3.13}$$

where we canonically normalized the angular fluctuations by defining $\delta\tilde{\phi} = \hat{h}_0\,\delta\phi$, and we specialized to the positive-$\hat{X}$ case (spacelike C^μ), given that this is the region where the pathologies discussed above show up.

First, notice that for $\hat{X} = \frac{1}{2}\mu^2$ the mass term for the radial fluctuation δh goes to zero. This means that at this particular point in field space we cannot get a local low-energy effective theory for

the $\tilde{\phi}$ by integrating δh out. Also, at the same point the radial background $\hat{h}_0$ goes to zero—see eq. (4.3.2)—and it remains zero for even larger values of $\hat{X}$. We thus see that the ghost instability we encounter in the low-energy theory for the angular mode starting from $\hat{X} = \frac{1}{2}\mu^2$, is a sign that at those values of $\hat{X}$ the low-energy theory just makes no sense—the derivative expansion breaks down at zero energy.

Then, we see from the structure of eq. (4.3.13) that the background configuration is stable if and only if the gradient/mass matrix has positive eigenvalues. For plane-waves with momentum $\vec{k}$ parallel to $\vec{C} = \vec{\nabla}\hat{\phi}$, the determinant of such matrix is

$$k_{\parallel}^2 \left[k_{\parallel}^2 + (\mu^2 - 6\hat{X})\right] . \tag{4.3.14}$$

We thus see that for $\hat{X} > \frac{1}{6}\mu^2$, the gradient/mass matrix develops a negative eigenvalue in a finite range of momenta, $0 < k_{\parallel}^2 < (6\hat{X} - \mu^2)$. This signals an instability with a rate of order μ. Indeed from the low-energy viewpoint the instability was UV-dominated, and we see that in the UV theory it is saturated at $k_{\parallel} \sim \mu$. At higher energies the UV theory makes perfect sense.

What can we learn from this example about the instability induced by GWs?

- Instabilities can arise from a perfectly sensible theory when one goes in a certain region of field space and from the EFT perspective one can only conclude that the instability exists in the regime of validity of the EFT itself: the theory may be completely healthy in the UV.

- The example we discussed has a well-defined Hamiltonian bounded from below, hence at most the instability can convert this finite amount of energy into the unstable modes. Therefore one can only conclude that an energy of order $\Lambda_{\rm UV}^4$, with $\Lambda_{\rm UV}$ the cut-off of the theory, is damped into the unstable modes; all further developments depend on the UV completion. Since in our case $\Lambda_{\rm UV}^4$ is parametrically smaller than the energy density of the GWs (which accidentally is of order Λ_2^4 for the typical amplitudes and frequencies detected by LIGO-Virgo) one cannot conclude that the GW signal will be affected.

- The appearance of the instability may signal that the EFT breaks down. This happens in the example above in the case of the ghost instability: the range of applicability of the EFT shrinks to zero. The regime of validity of the EFT is not only determined by the requirement that frequencies are sufficiently small, but it can be modified in the presence of a sizable background. Therefore it may be that the instability we studied is simply telling us that the EFT of DE breaks down. This means that we are unable to describe the propagation of GWs unless we know the UV completion of the theory.

Notice that both in the case in which the instability can be described within the EFT and in the case in which the EFT breaks down at the instability, in order to continue the time evolution of the system one needs the UV completion.

4.4 PHENOMENOLOGICAL CONSEQUENCES

Let us explore the phenomenological consequences of the instability we studied. First of all, as it is clear from the toy model we described in the previous Section, without a UV completion one cannot conclude that a sizable amount of energy goes into π. The instability may be saturated at the cut-off scale Λ_3 or even at a lower scale. This means that it is not guaranteed that the instability leads to a back-reaction on the GW signal that can be seen at the interferometers[10]. In the following, we will concentrate on the question of whether a generic point in the Universe is affected by the instability. For this we do not need to focus on the particular events observed by LIGO-Virgo (or eventually LISA and pulsar timing array, see e.g. [103]) but one has to consider the effect of all GW emissions.

Let us neglect momentarily the Vainshtein effect. The Universe is populated by binary systems and these trigger the instability in points that are close enough to the source to have $\beta > 1$. Let us divide the Universe in spheres of 10 Mpc radius and ask whether the instability is triggered in these regions. Since in first approximation the Universe is homogeneous on scales of 10 Mpc, one expects that all regions behave approximately in the same way. If within a region and in a time comparable to the age of the Universe, there is at least one binary event that gives $\beta > 1$ at a distance of 10 Mpc, one can conclude that this event will trigger the instability over the whole sphere (and thus in the whole Universe). In the following we are also going to explore regions of 1 Mpc. In this case, since the Universe is inhomogeneous on this scale, using the same criteria as before one can only conclude that sufficiently dense regions reached the instability. Indeed the events will be mostly localized in overdensities and may not be able to trigger the instability in underdense regions.

The parameters needed to characterize the instabilities discussed in Section 4.2.2 are the amplitude h_0^+ and the frequency f. Long before the merger, the amplitude h_0^+ can be written as (see for example [85])

$$h_0^+ \sim \frac{1}{\sqrt{2}} \cdot \frac{4}{r} (G M_c)^{5/3} (\pi f)^{2/3} \,, \tag{4.4.1}$$

where r is the distance from the binary, M_c is the chirp mass and f the GW frequency. (The factor of $1/\sqrt{2}$ comes from our non-standard definition of h_0^+.) This is a reasonable approximation until the orbit reaches the innermost stable circular orbit (ISCO)[11].

Figure 11 focuses on stellar mass BHs; for concreteness we chose $M_c = 28\, M_\odot$ as for GW150914 and $f = 30\,\text{Hz}$. We take the distance to be 1 Mpc. Taking a distance of 10 Mpc would require, in order to keep the same h_0^+, to consider times closer to the coalescence. However this corresponds to larger frequencies and one goes in a regime that cannot be trusted, since the frequency is higher than

10 In fact, using eq. (4.5) of [95] one can straightforwardly show that $\Delta\gamma/\bar{\gamma} \sim \Lambda_3^4/(\Lambda_2^4 h_0^+) \ll 1$, where $\bar{\gamma}$ and $\Delta\gamma$ denote the GW background and its modification respectively.

11 In a Schwarzschild geometry the ISCO is located ar $r_{\rm ISCO} = 6Gm$, where m is the total mass of the binary. Assuming equal masses and using Kepler's law to convert into frequency, we find $f_{\rm ISCO} \simeq 0.034/(\pi G M_c)$.

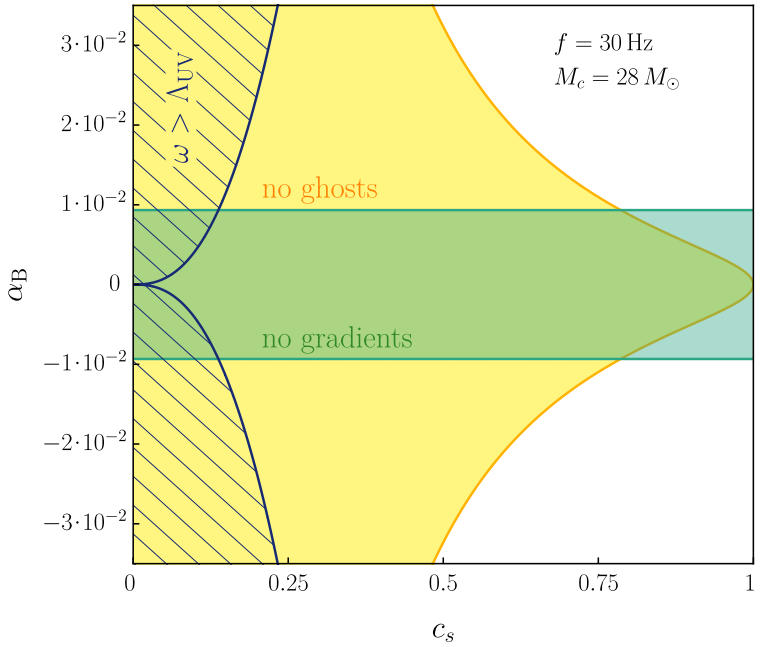

Figure 11: Stability regions on the plane (c_s, α_B). The yellow region indicates where ghost instabilities of eq. (4.2.21) are absent in which $\beta < c_s^{-2}\sqrt{1-c_s^2}$. The green region indicates where gradient instabilities are absent, i.e. $\beta < 1$. The fact that this curve is independent of c_s follows from the choice $\alpha = 1/(2c_s^2)$, see eqs. (3.1.7) and (4.1.4). In the region with the blue diagonal grid, the frequency of the GW is above the perturbative unitarity bound, $\omega > \Lambda_{\rm UV}$ (see footnote 12), and our analysis cannot be applied. In the plot we have used $M_c = 28 M_\odot$ and $f = 30\,\mathrm{Hz}$.

the unitarity cut-off.[12] In Figure 11 we plot the gradient and ghost instabilities in the plane (c_s, α_B) together with the unitarity cut-off. Models with $\alpha_B \gtrsim 10^{-2}$ are affected by one or both instabilities, but the cut-off is quite close.

On the other hand, if one considers massive BHs, frequencies are many orders of magnitude smaller than the unitarity cut-off. In Figure 12 we plot the threshold $\beta = 1$ as a function of the chirp mass of the binary for 1 Mpc and 10 Mpc distances. Independently of the chirp mass, the instability is triggered close to the ISCO for values of α_B that are of interest for future LSS experiments, i.e. $\alpha_B \gtrsim 10^{-2}$. Although there is some degree of uncertainty on the rate of massive BH mergers, one can be quite sure that in a region of 10 Mpc many mergers of halos, and therefore binary mergers of massive BHs, took place in the last Hubble time. To be more quantitative, in the range $10^7 M_\odot < M_c < 10^8 M_\odot$ one estimates between 5 and 50 events in a volume of 10 Mpc radius

12 The cut-off can be obtained as the energy scale at which perturbative unitarity is lost. In order to explicitly get such scale for m_3^3 we focus on the leading term in (4.1.2): the dominant interaction in the small-c_s limit is $\sim -\nabla^2\pi(\partial_i\pi)^2/\Lambda_B^3$. Following [104, 105] we find that for such interaction perturbative unitarity in the $\pi\pi \to \pi\pi$ scattering is lost when

$$\frac{\omega^6}{\Lambda_B^6 c_s^{11}} < \frac{3\pi}{4}\,, \tag{4.4.2}$$

where here ω is the energy of π.

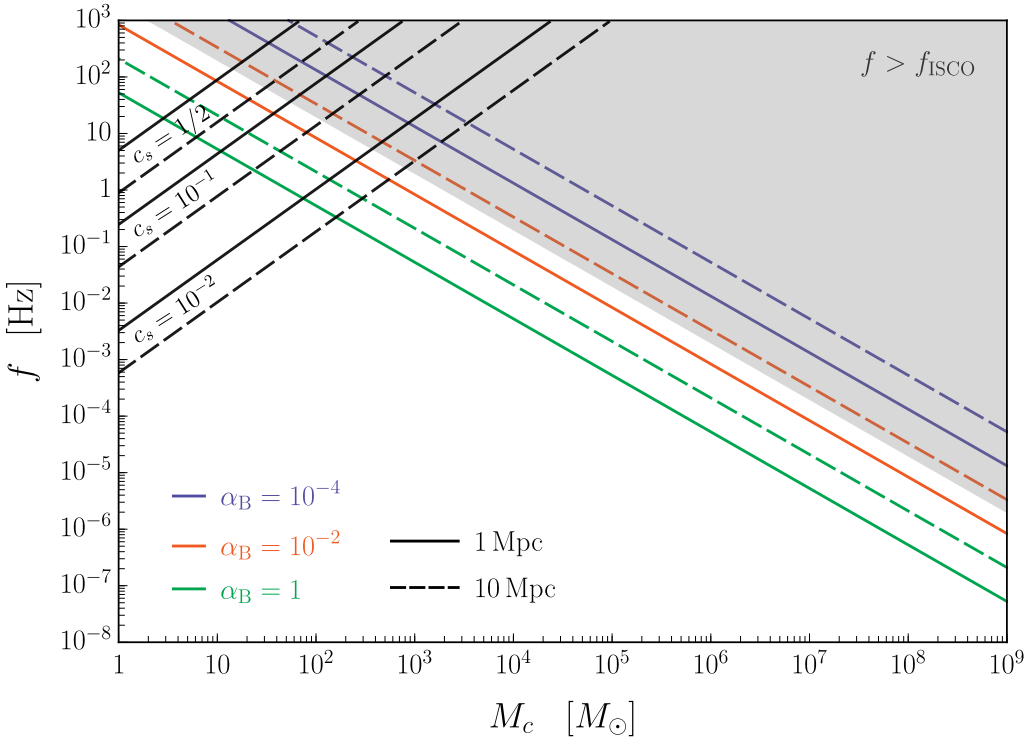

Figure 12: Gradient-instability lines, $\beta = 1$, for different value of α_B as a function of the chirp mass of the binary system, evaluated at a distance of 1 Mpc (solid lines) and 10 Mpc (dashed lines). The grey region cannot be trusted because it would correspond to extrapolating the orbit beyond the ISCO. Regions above the black lines have frequencies larger than the unitarity cut-off $\omega > \Lambda_{UV}$ (the three lines correspond to different values of c_s). At fixed $\beta = 1$, we expressed the cut-off frequency as a function of M_c using (4.4.1). All lines are evaluated with the choice $\alpha = 1/(2c_s^2)$.

between $z = 1$ and $z = 0$ [106]. Rates are larger, but considerably more uncertain, for smaller masses [107].

Let us now discuss the role of screening. As we discussed above, in regions with large field non-linearities the threshold of instability can be lifted by the Vainshtein mechanism. If the typical radius at which the screening is effective is of order 10 Mpc or smaller, then our conclusions do not qualitatively change. There may be very non-linear regions where the instability did not occur, but in most of the Universe the instability takes place. Following [53], one can estimate the scale at which the Vainshtein mechanism is relevant assuming a power-law Universe with matter power spectrum $P(k) \propto k^n$, where the relevant value near the non-linear scale for the real Universe is $n \simeq -2$. In our case one finds $\lambda_V \sim [\alpha_B/(c_s^2\alpha)]^{\frac{4}{3+n}}\lambda_{NL}$, which shows that for small α_B the Vainshtein scale λ_V is in general much shorter than 10 Mpc, which roughly corresponds to the non-linear scale for structure formation λ_{NL} (see also [101] for an estimate of the Vainshtein scale in numerical N-body simulations, confirming these estimates).

What can we conclude if a model lies in the unstable region? As we discussed, the endpoint of the instability is unknown and requires knowledge of the UV. Naively one can imagine that a

certain amount of πs with energy close to the cut-off is generated until their back-reaction stops the instability. It looks difficult to argue that the theory around this new state will resemble the original one and give similar predictions: the πs produced by the instability must qualitatively change the theory to make it stable, so that one expects that also the other predictions of the theory will be affected. One cannot make any firm prediction without understanding the fate of the instability and this requires a UV completion.

Another possibility is that the EFT breaks down at the instability, so that the instability itself cannot be trusted. Notice however that the frequencies involved may be as low as 10^{10} km. In this case one has to declare the impossibility to say anything about any process that has to do with GWs. Moreover all the successes of GR on shorter scales cannot be explained. Analyticity arguments can be used to argue that a theory with an approximate Galilean symmetry must break down at a very large scale, of order 10^7 km in the range of parameters we are discussing [108]. Although it is not straightforward to apply these arguments in a cosmological context, where Lorentz invariance is spontaneously broken, it is an independent indication that the theories at hand must break down at extremely large scales.

4.5 BEYOND HORNDESKI: $\tilde{m}_4^2$-OPERATOR

The analysis of the previous Sections focused on the stability of cubic Horndeski theories. Here we want to consider another quadratic operator of the EFT of DE that survives after GW170817 [50]. The operator

$$S_{\tilde{m}_4} = \int d^4x\sqrt{-g}\,\frac{\tilde{m}_4^2(t)}{2}\delta g^{00}\left({}^{(3)}R + \delta K^\nu_\mu \delta K^\mu_\nu - \delta K^2\right) , \tag{4.5.1}$$

where ${}^{(3)}R$ denotes the 3d Ricci scalar of the hypersurfaces at constant t, is not constrained by the requirement that GWs travel at the speed of light [50]. However, it is highly constrained by the perturbative and resonant decay $\gamma \to \pi\pi$, studied in [78, 95]. The perturbative bound is of the order

$$|\alpha_H| \lesssim 10^{-10} , \qquad \alpha_H \equiv 2\frac{\tilde{m}_4^2}{M_{Pl}^2} . \tag{4.5.2}$$

The Lagrangian of π in the presence of all the relevant non-linearities schematically reads [78] (we follow the notation of [95])

$$\mathcal{L}_\pi = -\frac{1}{2}\bar{\eta}^{\mu\nu}\partial_\mu\pi\partial_\nu\pi + \frac{1}{\Lambda_\star^3}\ddot{\gamma}_{ij}\partial_i\pi\partial_j\pi - \frac{(\partial\pi)^2}{\Lambda_\star^3}\partial^2\pi + \frac{(\partial\pi)^2}{\Lambda_c^6}[(\Box\pi)^2 - (\partial_\mu\partial_\nu\pi)^2] - \frac{\alpha_H}{2\sqrt{\alpha}HM_{Pl}}\dot{\pi}\dot{\gamma}_{ij}^2 , \tag{4.5.3}$$

where $\Lambda_\star \simeq \alpha_H^{-1/3}\alpha^{1/3}\Lambda_3$ and $\Lambda_c \simeq \alpha_H^{-1/6}\alpha^{1/3}\Lambda_3$. The second term gives an instability similar to the one discussed above and we can define, following [95],

$$\beta \equiv \frac{2\omega^2 M_{Pl}h_0^+}{c_s^2|\Lambda_\star^3|} = \frac{\sqrt{2}|\alpha_H|}{\alpha c_s^2}\left(\frac{\omega}{H}\right)^2 h_0^+ . \tag{4.5.4}$$

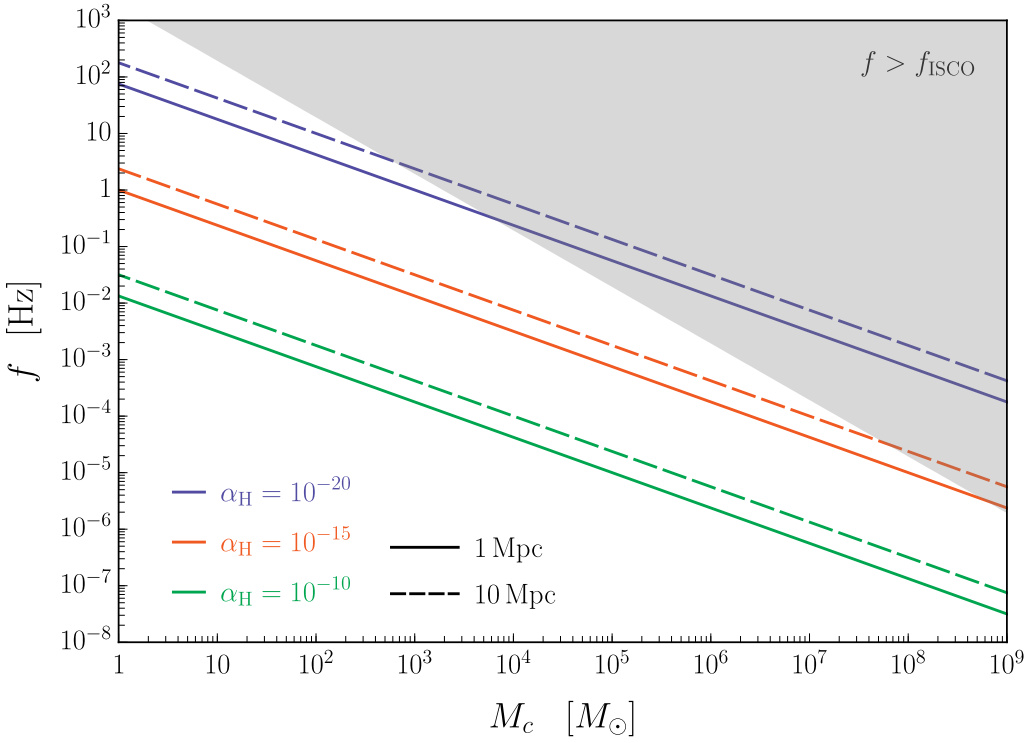

Figure 13: Gradient-instability lines $\beta = 1$ for different value of $\alpha_{\rm H}$ as a function of the chirp mass of the binary system. The grey region cannot be trusted because it would correspond to extrapolating the orbit beyond the ISCO.

It turns out that the analysis for this case is simpler, since to assess the stability of the system it is enough to look at the $\gamma\pi\pi$ interaction, while all additional non-linearities are negligible: the system is unstable for $\beta > 1$. We are going to verify this statement below. In Figure 13 we plot the instability region as a function of the chirp mass and frequency. Notice that in this case the unitarity cut-off of the theory does not appear in the Figure, since it is much higher that the frequencies of interest. The absence of instability is a constraint much tighter than the perturbative bound of eq. (4.5.2). On the other hand, the narrow-resonance regime gives even better constraints for $\alpha_{\rm H}$, of the order of $\beta \lesssim 10^{-2}$ (see Figure 5 of [95]).

Let us now verify that the other non-linear terms in the Lagrangian of eq. (4.5.3) can be neglected. (For simplicity in the following we take $\alpha \sim 1$ and $c_s \sim 1$.) First of all, let us estimate the size of the induced background $\hat{\pi}$ sourced by $\gamma\gamma\pi$. Neglecting π non-linearities and using the Lagrangian (4.5.3), one can estimate

$$\hat{\pi} \sim \frac{M_{\rm Pl}\alpha_{\rm H}\omega(h_0^+)^2}{H} \,. \tag{4.5.5}$$

In order for this estimate to be correct we must check that the cubic and quartic self-interactions of (4.5.3) are negligible. At the level of the equations of motion, the contributions of the cubic and

quartic terms are schematically given by $\mathcal{E}_{(3)} \sim (\partial^2\hat{\pi})^2\,\Lambda_\star^{-3}$ and $\mathcal{E}_{(4)} \sim (\partial^2\hat{\pi})^3\,\Lambda_c^{-6}$. These have to be compared with $\mathcal{E}_{(2)} \sim \partial^2\hat{\pi}$. Using eq. (4.5.5) we have

$$\frac{\mathcal{E}_{(3)}}{\mathcal{E}_{(2)}} \sim \alpha_H^2 \left(\frac{\omega}{H}\right)^3 (h_0^+)^2 \sim \beta^2 \frac{H}{\omega}\,, \qquad \frac{\mathcal{E}_{(4)}}{\mathcal{E}_{(2)}} \sim \alpha_H^3 \left(\frac{\omega}{H}\right)^6 (h_0^+)^4 \sim \beta^3 h_0^+\,. \tag{4.5.6}$$

For $\beta \gtrsim 1$ both these ratios are very small and (4.5.5) is valid. (The approximation may not be correct for $\beta \gg 1$, but in this case one can reduce to $\beta \gtrsim 1$ considering weaker—i.e. farther—GW sources.) The background $\hat{\pi}$ will affect the kinetic term of perturbations $Z_{\mu\nu}$: we have to compare its contribution with the one of GWs, $\partial_u \Gamma_{\mu\nu}$ (note that for $\tilde{m}_4^2$ the relevant parameter is $\ddot{\gamma}_{ij}$ rather than $\dot{\gamma}_{ij}$). For the cubic self-interaction in (4.5.3) one gets

$$\frac{\partial^2\hat{\pi}}{\ddot{\gamma}} \sim \alpha_H \frac{\omega}{H} h_0^+ \sim \beta \frac{H}{\omega} \ll 1\,. \tag{4.5.7}$$

For the quartic self-interaction in (4.5.3) one has

$$\frac{(\partial^2\hat{\pi})^2\Lambda_\star^3}{\ddot{\gamma}\Lambda_c^6} \sim \alpha_H^2 \left(\frac{\omega}{H}\right)^4 (h_0^+)^3 \sim \beta^2 h_0^+ \ll 1\,. \tag{4.5.8}$$

We conclude that one can trust the bound plotted in Figure 13.

As already mentioned, the stability properties of the cubic Galileon interactions (in the absence of GWs) do not hold for the quartic and quintic Galileon [96]. This means that these theories are in general unstable in the Vainshtein regime, even before considering GWs. However the two instabilities are quite different: one is only present in the non-linear regime of π, while the instability we discuss in this Chapter holds outside the Vainshtein regime and extend to the whole Universe.

4.6 DISCUSSION AND FUTURE DIRECTIONS

We have studied the effect of a large GW background on the stability of the Effective Field Theory of Dark Energy. We have discussed two operators where this effect is relevant: $m_3^3(t)\delta g^{00}\delta K$, associated to the dimensionless function α_B, and $\frac{1}{2}\tilde{m}_4^2(t)\delta g^{00}\left({}^{(3)}R + \delta K_\mu^\nu \delta K_\nu^\mu - \delta K^2\right)$, associated to α_H. We have first focused the analysis on the former, because this operator remains unconstrained by the perturbative decay of gravitons, since the scale suppressing the coupling $\gamma\pi\pi$ is typically too high [78]. Moreover, the resonant decay is quenched by the non-linear self-couplings of π, so that also in this regime there are no conclusive bound on this operator from the decay of GWs [95].

The stability of perturbations for this operator is studied in Section 4.2. For $c_s < 1$, perturbations of π become necessarily unstable in the presence of a GW background with

$$\beta \sim \frac{|\alpha_B|}{\alpha c_s^2}\,\frac{\omega}{H_0}\,h_0^+ > 1\ : \tag{4.6.1}$$

the kinetic matrix $Z^{\mu\nu}$ presents either ghost or gradient instabilities. These conclusions are not at variance with the well-known theorem that ensures stability for the DGP model [94] in the absence of GWs. In this case, for $c_s^2 > 1/3$ the theorem can be extended to the m_3^3 operator, but its assumptions

break down when a GW background is present. The case $c_s = 1$ is also discussed, assuming that the π background is linear in the light-cone coordinate $v = t + r$. In this case we find that ghost instabilities are generic. Our conclusions do not extend directly to the DGP model, because the coupling of the scalar bending mode to tensor modes is different. It would be interesting to verify the stability of the DGP model in the presence of a GW background.

The physical implication of these instabilities is unclear, since the most unstable modes are the closest to the cut-off. Sensible conclusions can only be drawn with the knowledge of the UV completion of the theory. We discussed this in Section 4.3 by an example unrelated to our theory: a $U(1)$-symmetric theory for a complex scalar with a mexican-hat potential. In the broken phase, at low energy this system can be described by an effective $P((\partial\phi)^2)$-theory for the angular mode ϕ. Even if the effective theory presents ghost or gradient instabilities for certain values of P' and P'', the UV completion remains perfectly healthy. From this example one can argue that it is not possible to continue the time evolution of the system without knowing the complete theory.

In Section 4.4 we explore for which values of the dimensionless function α_B the EFT becomes unstable everywhere in the Universe, losing predictability. The bounds are shown Figures 11 and 12 for different GW sources and roughly correspond to $|\alpha_B| \gtrsim 10^{-2}$. They are thus very close to the forecasted limits on this parameter reachable with future large-scale structure observations (see e.g. [109–112]). For this reason, it would be interesting to improve our analysis considering a more refined estimate of the abundance of massive BH binaries [106, 107]. Indeed, the limits obtained from these events are the most interesting, as they correspond to frequencies well below the cut-off of the theory. Of course, a logical possibility is that the EFT breaks down at extremely large scales and it cannot be used to study any GW event. In this scenario also all the classical tests of GR are outside the EFT and one cannot rely on screening mechanisms to explain the success of GR at short scales.

In Section 4.5 we discuss the instability of the operator $\tilde{m}_4^2$, triggered by a GW background with

$$\beta \sim \frac{|\alpha_H|}{\alpha c_s^2}\left(\frac{\omega}{H_0}\right)^2 h_0^+ \,. \tag{4.6.2}$$

This is easier to study because one can neglect non-linearities of π. The bounds on α_H based on $c_T = 1$ are shown in Figure 13: the effective theory becomes unstable for $|\alpha_H| \gtrsim 10^{-20}$. These are much smaller values than those constrained by the perturbative decay. If $c_T = 1$ is relaxed, the combination contrained by our analysis is $(\tilde{m}_4^2 + m_5^2 c_T^2)/M_{Pl}^2$, instead of $\tilde{m}_4^2/M_{Pl}^2$ (see eq. (4.15) of [95]).

In this Chapter we considered the effects of α_B and α_H independently but we do not expect that the combination of the two operators can provide better stability properties for π. Indeed, the lack of a general theorem for stability in the presence of GWs suggests that our conclusions hold in a more general theory, where both operators are turned on. In particular we expect α_H to also contribute to the operator $\dot{\gamma}_{ij}\partial_i\pi\partial_j\pi$: it may be possible then to tune α_H and α_B to set the operator to zero. However the dominant operator $\ddot{\gamma}_{ij}\partial_i\pi\partial_j\pi$, which has more derivatives, would then lead to instability since it cannot be removed by tuning other parameters.

EFT of DE operator	$\tilde{m}_4^2$	m_3^3
GLPV covariant Lagrangian with $c_T = 1$	$-\frac{2Xf_{,X}}{f}$	$\frac{2Xf_{,X}}{f} + \frac{\dot{\phi}XQ_{,X}}{2Hf}$
Dimensionless parameter	α_H	α_B
After conformal transformation	$\alpha_H + 2\beta_1$	$\alpha_B - \frac{\alpha_M}{2}(1-\beta_1) + \beta_1 - \frac{\dot{\beta}_1}{H}$
Perturbative decay ($\Gamma_{\gamma\to\pi\pi}/H_0 < 1$)	$\lvert\alpha_H\rvert \gtrsim 10^{-10}$	Irrelevant ($\lvert\alpha_B\rvert \gtrsim 10^{10}$)
Narrow resonance ($\beta < 1$, $\beta\omega u > 1$)	$3\times10^{-20} \lesssim \lvert\alpha_H\rvert \lesssim 10^{-17}$ $10^{-16} \lesssim \lvert\alpha_H\rvert \lesssim 10^{-10}$	Not applicable (large non-linearities)
Instability ($\beta > 1$, $\beta\omega u > 1$)	$\lvert\alpha_H\rvert \gtrsim 10^{-20}$ (see Figure 13)	$\lvert\alpha_B\rvert \gtrsim 10^{-2}$ (see Figure 12)

Table 1: Summary of the results of the constraints, discussed in this thesis and obtained in [78, 95, 113] (we assume $c_T = 1$).

We summarize these results and those of Chapter 2 and 3 in Table 1, using different notations. For simplicity, in eqs. (4.1.1) and (4.5.1) we have assumed that our starting theory has a constant effective Planck mass and no higher-derivative operators such as those appearing in DHOST theories [76, 77]. However, our results also apply after a conformal transformation with conformal factor depending on ϕ and $X \equiv g^{\mu\nu}\partial_\mu\phi\partial_\nu\phi$: $g_{\mu\nu} \to C(\phi, X)g_{\mu\nu}$. In the fourth line of the table we provide the corresponding parameters to which our analysis applies.

We conclude that for what concerns large-scale structure surveys, the surviving single-field theory that avoids the aforementioned issues is a k-essence theory [81, 114], modulo the above conformal transformation. In the covariant language, its action reads

$$\mathcal{L} = P(\phi, X) + C(\phi, X)R + \frac{6C_{,X}(\phi, X)^2}{C(\phi, X)}\phi^{;\mu}\phi_{;\mu\nu}\phi_{;\lambda}\phi^{;\nu\lambda}\,, \tag{4.6.3}$$

where the symbol ; stands for a covariant derivative. Note that there is no Vainshtein screening in these theories [90]: some other mechanism (see e.g. [115, 116] and references therein) is required to screen the fifth force on astrophysical scales. It is therefore interesting to explore further in the future work.

This finally concludes the first part of the thesis: going beyond perturbation theory in dark energy theories and its implications. The second part will be devoted to a study of going beyond perturbation theory in inflation.

Part II

INFLATION

5

BEYOND PERTURBATION THEORY IN INFLATION

In the last two Chapters we have seen that the non-perturbative effects play a very crucial role in the context of GWs and Dark Energy (DE) at late Universe, providing the constraints on the parameters of DE theories. In this part of the thesis we are going to study beyond perturbation theory in inflation, which has a very close connection to the production of Primordial Black Holes (PBHs).

5.1 INTRODUCTION AND MAIN IDEAS

Primordial fluctuations generated during inflation are approximately Gaussian [117] and deviations from Gaussianity are calculated in perturbation theory [22]. Here we point out that there are physically interesting questions whose answer lies beyond perturbation theory and we explain how to get non-perturbative results using semiclassical methods.

Let us focus for concreteness on a particular question: the calculation of the Primordial Black Hole (PBH) abundance. Roughly, the probability of forming a PBH corresponds to the probability that the primordial curvature perturbation $\zeta(\mathbf{x})$, smoothed with a typical scale that depends on the mass of the PBH we are interested in, exceeds a certain threshold of order unity, $\zeta \gtrsim 1$ (for a recent discussion see [118] and references therein). The formation of a PBH is a very unlikely event on the tail of the probability distribution. (To get a sizable amount of PBHs one considers models of inflation with a power spectrum P_ζ on short scales that is much larger than the one measured on CMB scales, but still the formation of a PBH remains a very unlikely event.) Let us see what happens in the presence of some primordial non-Gaussianity, characterized by a bispectrum $\langle\zeta\zeta\zeta\rangle$, a trispectrum $\langle\zeta\zeta\zeta\zeta\rangle$ and so on. These correlators imply that the probability distribution of ζ is, very schematically, of the form

$$\mathcal{P}[\zeta] \sim \exp\left[-\frac{\zeta^2}{2P_\zeta} + \frac{\langle\zeta\zeta\zeta\rangle}{P_\zeta^3}\zeta^3 + \frac{\langle\zeta\zeta\zeta\zeta\rangle}{P_\zeta^4}\zeta^4 + \dots\right] \sim \exp\left[-\frac{\zeta^2}{2P_\zeta}\left(1 + \frac{\langle\zeta\zeta\zeta\rangle}{P_\zeta^2}\zeta + \frac{\langle\zeta\zeta\zeta\zeta\rangle}{P_\zeta^3}\zeta^2 + \dots\right)\right] . \tag{5.1.1}$$

The corrections to the Gaussian result are thus

$$\frac{\langle\zeta\zeta\zeta\rangle}{P_\zeta^2}\zeta \sim f_{NL}\zeta \quad , \quad \frac{\langle\zeta\zeta\zeta\zeta\rangle}{P_\zeta^3}\zeta^2 \sim g_{NL}\zeta^2 . \tag{5.1.2}$$

For typical values of ζ, $\zeta \sim P_\zeta^{1/2}$, these are small corrections, compatible with the experimental bounds on non-Gaussianity [117] and amenable to a perturbative calculation. However, if we are interested in $\zeta \sim 1$, corrections are large if $|f_{NL}| \gtrsim 1$ or $|g_{NL}| \gtrsim 1$ (see Figure 14). (See for example [119, 120] and references therein.) For instance, in a single-field model of inflation with reduced speed of

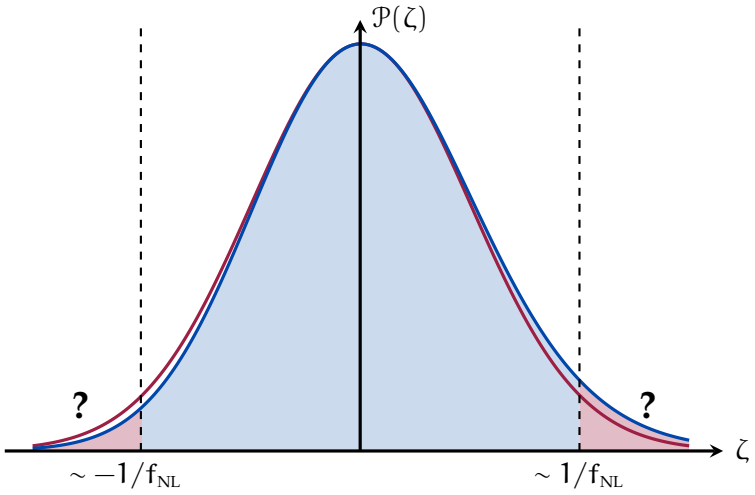

Figure 14: Gaussian distribution (red curve) compared to a non-Gaussian one (blue curve). Close to the center the two distributions are close to each other and the difference can be studied in perturbation theory. On the tails the difference is large and one has to use non-perturbative methods.

sound c_s, $f_{NL} \sim c_s^{-2} - 1$ and $g_{NL} \sim (c_s^{-2} - 1)^2$. Therefore, in these models the calculation of the PBH abundance cannot be done in perturbation theory, unless c_s is close to unity[1]. (Non-Gaussianity that cannot be represented by a finite number of n-point functions was studied in multifield models of inflation, see for example [124–126].)

The breaking of perturbation theory on the tails of the distribution can be studied in a simple toy model (see Section 5.2): a quantum mechanical oscillator in the ground state, characterized by a small anharmonicity. In general, one can treat the small anharmonicity in perturbation theory. However, if one is interested in exploring the tail of the ground-state wavefunction, very far from the origin, at a certain point the anharmonic correction to the potential will be large. This quantum-mechanical example suggests a possible approach: the tail of the wavefunction is very suppressed and one expects this regime to be amenable to a semiclassical treatment. Instead of using the WKB approximation (this is done in Appendix E), one can obtain the semiclassical wavefunction using the path integral formulation in the limit $\hbar \to 0$. This formulation can be generalized to the case of interest of cosmological inflation.

In the limit $\hbar \to 0$, inflationary perturbations go to zero. Intuitively this limit should describe rare events, i.e. events that exceed a given large "threshold": sending this threshold to infinity with

1 For a minimal slow-roll model the non-Gaussian parameters are slow-roll suppressed $f_{NL} \ll 1$ and $g_{NL} \ll 1$, so that Gaussainity is a good approximation even for $\zeta \sim 1$. Actually, even if the statistics of the inflaton perturbations can be taken as Gaussian, one needs to take into account the non-linear relation between inflaton perturbations and ζ and may need to resum the out-of-the-horizon evolution with a stochastic approach a la Starobinsky [121] (for a recent rigorous derivation see [122]), see [123] and references therein.

$\hbar$ constant is equivalent to send $\hbar \to 0$. Therefore, *the rare-event limit of inflationary perturbations is semiclassical*. Let us make this more concrete. The wavefunction of the Universe (WFU) is given by

$$\Psi[\zeta(\mathbf{x})] = \int_{\mathrm{BD}}^{\zeta_0(\mathbf{x})} \mathcal{D}\zeta e^{iS[\zeta]/\hbar} \,. \tag{5.1.3}$$

The functional integral has to be performed with Bunch-Davies boundary conditions at early times and a given configuration $\zeta_0(\mathbf{x})$ at late times. (For simplicity we stick to a single-field model of inflation and neglect tensor modes.) To specify what one means with "rare event", let us filter $\zeta_0(\mathbf{x})$ with an appropriate window function:

$$\hat{\zeta}_0(\mathbf{x}) = \int \frac{d^3k}{(2\pi)^3} W(k)\zeta_0(\mathbf{k})e^{i\mathbf{k}\cdot\mathbf{x}} \,. \tag{5.1.4}$$

The window function will select a certain range Δk, so that in real space the field $\hat{\zeta}_0$ is convoluted with an appropriate filter. A filtered field $\hat{\zeta}_0$ is relevant to describe the probability of an overdensity (or underdensity) in a certain region of the Universe, or the probability of forming a PBH of a given size. The CMB temperature in each pixel of a map is also a filtered map $\hat{\zeta}_0$ (but projected in 2 dimensions).

By translational invariance $\hat{\zeta}_0(\mathbf{x})$ has the same probability $\mathcal{P}(\hat{\zeta}_0)$ at any point. The claim is that $\mathcal{P}(\hat{\zeta}_0 = \zeta_0)$ can be calculated semiclassically in the limit $|\zeta_0| \to \infty$. Indeed in this limit we are imposing boundary conditions on the integral of eq. (5.1.3) that make the action large compared to $\hbar$. In this limit the functional integral can be calculated in saddle point approximation

$$\Psi[\zeta_0(\mathbf{x})] \sim e^{iS[\zeta_{\mathrm{cl}}]/\hbar} \,. \tag{5.1.5}$$

The action is evaluated on-shell, i.e. on the classical trajectory ζ_{cl} that satisfies the boundary condition $\zeta_{\mathrm{cl}} = \zeta_0(\mathbf{x})$ at late times and the Bunch-Davies conditions at early times. Notice that we are keeping the full non-linear action and not expanding in perturbation theory: the semiclassical expression (5.1.5) resums all non-linearities that are enhanced by the large ζ_0. Corrections to this result come from looking at perturbations around this classical action and evaluating the functional integral over them. These fluctuations are of order $P_\zeta^{1/2}$ and are not enhanced by ζ_0. They give a subleading contribution provided inflation is a weakly coupled EFT.

Before getting to a more realistic scenario of inflation, in Section 5.3 we study a simple toy model to appreciate the difference between the usual in-in perturbation theory and our semiclassical expansion. The model consists of two fields, χ and σ, with a cubic interaction $\lambda H\chi\sigma^2$ (with H the Hubble scale during inflation). We will be interested in the regime in which the modes of χ have a very large amplitude (the unlikely tail of the distribution) so that the expansion in λ is not reliable. Moreover, we are going to focus on configurations in which the modes of χ are much longer than the ones of σ. In this regime χ acts as a background for the modes of σ and its effect can be easily calculated exactly since it simply corresponds to a change in the σ mass.

The main point of this Chapter is described in Section 5.4, where the methods outlined above are applied to a particular interaction in single-field inflation: $\propto \lambda\dot{\zeta}^4$. This is a particular limit of

inflation, which is consistent and technically natural, as we will discuss. The full evaluation of the wavefunction requires the numerical solution of a PDE: this is done in Section 5.4.5, while a test of the numerical code against perturbation theory is the subject of Appendix F. One is able to understand the qualitative behavior in λ reducing the PDE to an ODE, which basically corresponds to looking at a single Fourier mode, instead of a realistic real-space profile. This ODE is numerically studied in Section 5.4.3, while an analytic understanding, based on a scaling argument is presented in Section 5.4.4. The conclusion of all these different approaches is that the tail of the distribution goes as $\exp(-\lambda^{-1/4}\zeta^{3/2})$, a result which is clearly non-perturbative in the coupling λ. The numerical approach can only be performed after an analytic continuation of time to Euclidean time, to avoid integrals with fast oscillations. The possibility of doing this analytic continuation is studied in Section 5.5.

The study of this Chapter is just a first step in the understanding of inflation beyond perturbation theory. Besides the interest in PBHs, there are many conceptual issues in being able to calculate (potentially) observable quantities in our Universe. Many directions remain open and some of them are listed in Section 5.6 together with the discussion.

5.2 ANHARMONIC OSCILLATOR

Let us consider an anharmonic oscillator with potential

$$V(x) = \hbar\omega \left[\frac{1}{2}\left(\frac{x}{d}\right)^2 + \lambda\left(\frac{x}{d}\right)^4\right] , \tag{5.2.1}$$

and $d \equiv \sqrt{\hbar/m\omega}$. As usual, perturbation theory works provided that the dimensionless parameter λ is much smaller than unity and that the particle remains close to the origin ($x/d \sim 1$). Within the validity of perturbation theory one can perform the standard computations, e.g. determine the first order corrections to the ground-state wavefunction and its energy level. The same thing happens in this example when $x/d \gg 1$ (far away from the origin), while λ is kept small (and positive). Indeed, as we shall see more in detail, the expansion parameter involves the value of the position, i.e. $\lambda(x/d)^2$ to which an analogy can be made with the case of inflation where the expansion parameter was given by (5.1.2).

We are now going to study the ground-state wavefunction $\Psi_0(x)$ using functional methods (see e.g. [127] for an introduction to path-integral methods in QM). Let us consider a particle evolving under the Hamiltonian $\hat{H}$. The real-time (Lorentzian) action $S[x(t)]$ is

$$S[x(t)] = \int_{t_i}^{t_f} dt \left[\frac{1}{2}m\left(\frac{dx}{dt}\right)^2 - V(x)\right] . \tag{5.2.2}$$

The propagator $K(x_f, t_f; x_i, t_i)$ for going from some initial position x_i at time t_i to the position x_f at time t_f can be written in both operator and path-integral languages

$$K(x_f, t_f; x_i, t_i) = \langle x_f | e^{-i\hat{H}(t_f - t_i)/\hbar} | x_i \rangle = \int_{x(t_i)=x_i}^{x(t_f)=x_f} \mathcal{D}x(t)\, e^{iS[x(t)]/\hbar} . \tag{5.2.3}$$

We can insert in the propagator a complete set of eigenstates $|n\rangle$ of $\hat{H}$ with eigenvalues E_n that we assume positive:

$$\langle x_f|e^{-i\hat{H}(t_f-t_i)/\hbar}|x_i\rangle = \sum_n e^{-iE_n(t_f-t_i)/\hbar}\,\psi_n(x_f)\psi_n^*(x_i)\,, \tag{5.2.4}$$

where $\psi_n(x) \equiv \langle x|n\rangle$ and $\psi_n^*(x)$ is its complex conjugate.

The ground state can then be extracted by performing a Wick rotation $t \to -i\tau$ and by then taking the limit of $T \equiv \tau_f - \tau_i$ large. In this way, (5.2.4) is dominated by the ground state and we obtain

$$\psi_0(x_f)\psi_0^*(x_i)\,e^{-E_0T/\hbar} = \lim_{T\to\infty}\int_{x(\tau_i)=x_i}^{x(\tau_f)=x_f}\mathcal{D}x(\tau)\,e^{-S_E[x(\tau)]/\hbar}\,, \tag{5.2.5}$$

where S_E is the Euclidean action obtained after Wick rotation and τ is the imaginary time. Notice that the point x_i can be chosen arbitrarily if our goal is to extract $\psi_0(x_f)$ (the dependence on x_i will end up in a normalization factor).

Let $y(\tau)$ be a fluctuation around the classical path x_{cl}: $x(\tau) = x_{cl}(\tau) + y(\tau)$. $x_{cl}(\tau)$ satisfies the Euclidean equation of motion (without any expansion in λ). The path integral in (5.2.5) then becomes

$$\int_{x(\tau_i)=x_i}^{x(\tau_f)=x_f}\mathcal{D}x(\tau)\,e^{-S_E[x(\tau)]/\hbar} = e^{-S_E[x_{cl}(\tau)]/\hbar}\int_{y(\tau_i)=0}^{y(\tau_f)=0}\mathcal{D}y(\tau)\,e^{-\frac{1}{\hbar}\left(\frac{1}{2}\frac{\delta^2S_E}{\delta x^2}y^2+\frac{1}{3!}\frac{\delta^3S_E}{\delta x^3}y^3+\ldots\right)}\,. \tag{5.2.6}$$

Neglecting the higher-order terms which capture the interactions of perturbations around $x_{cl}(\tau)$, we obtain the semiclassical approximation for the ground-state wavefunction $\psi_0(x_f)$,

$$\psi_0(x_f) = \mathcal{I}(x_f)e^{-S_E[x_{cl}(\tau)]/\hbar}\,, \tag{5.2.7}$$

where the path integral of the quadratic action of $y(\tau)$ gives rise to the prefactor $\mathcal{I}(x_f)$. Let us emphasize that the higher-order terms we have neglected in (5.2.6) correspond to higher-order corrections in λ in perturbation theory, which are equivalent to loop diagrams, see [127]. The on-shell action in (5.2.7) only captures all the tree-level diagrams with many external legs x. Moreover, following the standard derivation in [127] one arrives to the VanVleck-Pauli-Morette formula of the prefactor $\mathcal{I}(x_f)$,

$$\mathcal{I}(x_f) = N\sqrt{\frac{m}{2\pi i\hbar v_i v_f\int_{x_i}^{x_f}\frac{dx'}{v^3(x')}}}\,, \tag{5.2.8}$$

where we defined v_i and v_f as the initial and final velocities on the classical trajectory and N is a normalization factor. Notice that the expression (5.2.7) is correct up to corrections $\mathcal{O}(\hbar)$ and will be a good approximation in regions where $S_E \gg \hbar$.

Now let us get back to the case of the anharmonic oscillator. From the formula (5.2.7) it is convenient to write down the action (5.2.2) in Euclidean space. We now have

$$S_E[x(\tau)] = \int_{\tau_i}^{\tau_f}d\tau\left(\frac{1}{2}m\dot{x}^2 + V(x)\right)\,, \tag{5.2.9}$$

where dot denotes $d/d\tau$.

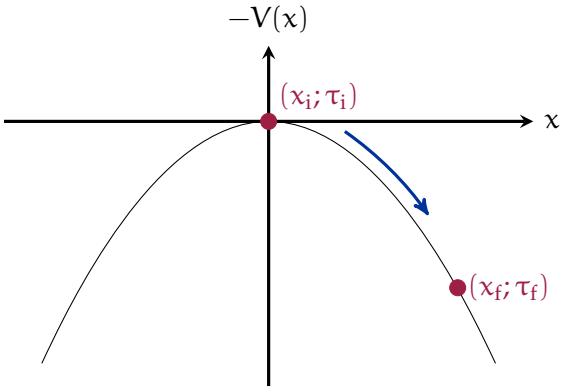

Figure 15: The inverted potential for the case of anharmonic oscillator.

Let us first anticipate the semi-classical scaling of the wavefunction $\Psi_0(x_f)$ as a function of λ and the final position x_f. From the formula (5.2.6), the leading exponent $S_E[x_{cl}(\tau)]/\hbar$ scales as[2]

$$\frac{S_E[x_{cl}(\tau)]}{\hbar} \sim \frac{1}{\lambda} F(\lambda x_f^2/d^2)\,, \tag{5.2.10}$$

where F is a function to be determined explicitly later on. Having said that, the on-shell action resums all the tree-level diagrams. The prefactor instead goes as $\lambda^0 G(\lambda x_f^2/d^2)$ with G being an arbitrary function of $\lambda x_f^2/d^2$ and it captures all the 1-loop diagrams. The terms we have neglected in (5.2.6) are associated to the higher-loop diagrams.

Let us now use the formula (5.2.7) to calculate the ground-state wavefunction. First notice that from the action (5.2.9) it is practically convenient to think of a particle moving in an inverted potential shown in Figure 15. Without loss of generality, we set $x_i = 0$[3]. Another thing one should bear in mind is that since in eq. (5.2.5) $\tau_f - \tau_i$ is taken to be very large, this means that the only real solution that exists corresponds to the zero-energy configuration (with a finite energy the particle would reach x_f from the origin in a finite time). Exploiting the conservation of energy the classical trajectory $x(\tau)$ satisfying the boundary conditions $x_{cl}(\tau_i) = x_i$ and $x_{cl}(\tau_f) = x_f$ is then determined by

$$\frac{dx}{d\tau} = \sqrt{\frac{2V(x)}{m}}\,, \tag{5.2.11}$$

which gives

$$\tau - \tau_0 = \int_\infty^x \frac{dx'}{\sqrt{2V(x')/m}} = -\frac{1}{\omega}\operatorname{arcsinh}\left(\frac{d}{\sqrt{2\lambda}\,x}\right)\,, \tag{5.2.12}$$

2 This can be easily realized by performing $x \to (\sqrt{\hbar/\lambda})x$.

3 Notice that this choice has nothing to do with the choice of the ground state of the Hamiltonian. Also, if one keeps x_i finite and non-zero, the solution that does not run to infinity is the one with zero energy (it spends an infinite amount of time around the origin).

where the integration constant τ_0 corresponds to the lower limit of x going to infinity. Inverting the expression above one gets

$$x(\tau) = -\frac{d}{\sqrt{2\lambda}\sinh(\omega\tau)}\,, \quad \tau < 0\,, \tag{5.2.13}$$

where τ_0 has been absorbed into the variable τ.

Now let us calculate the exponent of (5.2.7). The action evaluated on the classical path is

$$\begin{aligned}\frac{S_E[x_{cl}(\tau)]}{\hbar} &= \frac{1}{\hbar}\int_{\tau_i}^{\tau_f} d\tau\; m\dot{x}^2 \\ &= \frac{1}{\hbar}\int_{x_i}^{x_f} dx\;\sqrt{2mV(x)} \\ &= \frac{1}{6\lambda}\left[(1+\bar{x}^2)^{3/2}-1\right]\,,\end{aligned} \tag{5.2.14}$$

where in the first line we have used the fact that the total energy vanishes, and in the second line we have changed the integration variable from time to position. Here we define $\bar{x}^2 \equiv 2\lambda x_f^2/d^2$. Notice that to evaluate the action we did not need the explicit trajectory (5.2.13). Eq. (5.2.14) agrees with the scaling argument (5.2.10).

At this point, using the formula (5.2.8) and the classical path (5.2.13) one can easily compute the prefactor. Changing the integration variable to τ we obtain

$$v_i v_f \int_{\tau_i}^{\tau_f}\frac{d\tau}{v^2} = \frac{e^{\omega T}}{4\omega}(1+\sqrt{1+\bar{x}^2})\sqrt{1+\bar{x}^2}\,, \tag{5.2.15}$$

where $T = \tau_f - \tau_i$ which is taken to be very large. Therefore, the prefactor is

$$\mathcal{J}(x_f) = N\frac{e^{-\omega T/2}}{(1+\bar{x}^2)^{1/4}(1+\sqrt{1+\bar{x}^2})^{1/2}}\,, \tag{5.2.16}$$

where we have absorbed all the x_f-independent factors into the normalization factor N. Again, this prefactor (5.2.16) is only a function of $\lambda x_f^2/d^2$ as anticipated from the scaling argument. The expressions for the Euclidean action (5.2.14) and for the prefactor (5.2.16) can now be inserted in eq. (5.2.7) to obtain the ground-state wavefunction as

$$\Psi_0(\bar{x}) = N\frac{\exp\left\{-\frac{1}{6\lambda}\left[(1+\bar{x}^2)^{3/2}-1\right]\right\}}{(1+\bar{x}^2)^{1/4}\left(1+\sqrt{1+\bar{x}^2}\right)^{1/2}}\left(1+\mathcal{O}(\lambda)f(\bar{x})\right)\,. \tag{5.2.17}$$

This expression does not contain all λ corrections to the ground-state wavefunction, but it resums all the leading corrections $(\lambda x_f^2/d^2)^n$, the ones enhanced by x_f^2/d^2 (for $\lambda = 0$ one gets back to the harmonic ground-state $\sim \exp[-x_f^2/(2d^2)]$). Also, from (5.2.16) we can read off the energy $E_0 = \hbar\omega/2$, which is the ground-state energy of the harmonic oscillator. This is consistent with the fact that λ corrections to E_0 appear only at order $\hbar^2$ (corresponding to a two-loop effect, which we neglected).

The wavefunction eq. (5.2.17) was obtained in [128] using periodic boundary condition $x_i = x_f$: the large T limit corresponds in this case to the limit of zero temperature[4].

In the limit of large $\bar{x}$ keeping λ small one obtains

$$\Psi_0(\bar{x}) \sim \exp\left(-\lambda^{1/2}\frac{x_f^3}{d^3}\right). \tag{5.2.18}$$

This expression shows how the tails of the distribution for x_f get modified. Moreover, it makes manifest the non-perturbative nature of the semiclassical approximation, since we obtain a non-analytic expression in the coupling λ.

This result for the ground-state wavefunction can be obtained also in the more standard WKB approximation. As a consistency check for our procedure, in Appendix E we show that indeed the WKB wavefunction matches with eq. (5.2.17).

5.3 TWO FIELDS IN DS

We are now going to consider an inflationary toy model in which one is able to analytically calculate the leading effect in the semiclassical expansion, effectively resumming an infinite set of diagrams of the perturbative series. Let us consider the action for two fields σ and χ:

$$S = \int d\eta d^3x \left[\frac{1}{2\eta^2H^2}(\sigma'^2 - (\partial_i\sigma)^2) + \frac{1}{2\eta^2H^2}(\chi'^2 - (\partial_i\chi)^2) - \frac{\lambda}{\eta^4H^3}\chi\sigma^2\right]. \tag{5.3.1}$$

The two fields interact through the cubic term and $\lambda \ll 1$ is the dimensionless parameter of the standard perturbative expansion. We want to calculate the WFU in a particular regime: the modes of χ have a much longer wavelength compared to the ones of σ ($k_\chi \ll k_\sigma$), and χ is much larger than its typical fluctuation, $|\chi| \gg H$. Therefore, we do not want to assume that $\lambda\chi/H$ is small, while we are going to neglect all corrections suppressed by λ only. (Notice that we assume σ to have a typical fluctuation: $|\sigma| \sim H$.)

Loop corrections are suppressed by λ, so that the WFU can be calculated evaluating the classical action on-shell, as in eq. (5.1.5). The classical equations of motion in Fourier space read

$$\sigma'' - \frac{2}{\eta}\sigma' + k_\sigma^2\sigma + \frac{2\lambda}{\eta^2H}\chi * \sigma = 0\,, \tag{5.3.2}$$

$$\chi'' - \frac{2}{\eta}\chi' + k_\chi^2\chi + \frac{\lambda}{\eta^2H}\sigma * \sigma = 0\,, \tag{5.3.3}$$

4 An observable that is sensitive to the tail of the probability distribution is the moment $\langle x^N\rangle$ for large N. In the Gaussian case one finds that the leading contribution to the integral comes from $x \sim \sqrt{N}$. In standard perturbation theory the ground-state wavefunction gets corrections of order λx^4, so that the perturbative calculation of $\langle x^N\rangle$ is reliable for $\lambda x^4 \sim \lambda N^2 \lesssim 1$. The "resummed" wavefunction eq. (5.2.17) allows to calculate $\langle x^N\rangle$ in saddle-point approximation for large N. In this case one only gets corrections $\mathcal{O}(\lambda)$ due to subleading corrections to the wavefunction (5.2.17) and $\mathcal{O}(1/N)$ due to the saddle-point approximation.

where $*$ indicates a convolution in Fourier space. The last term on the LHS of (5.3.3) is negligible because it is of the order λ. Therefore, χ is just a free wave in de Sitter[5],

$$\chi_{cl}(\mathbf{k},\eta) = \bar{\chi}(1 - ik_\chi\eta)e^{ik_\chi\eta} \,, \tag{5.3.4}$$

with $\bar{\chi}$ its asymptotic value at late times. We need to keep, on the other hand, the last term on the LHS of (5.3.2) since $\lambda\bar{\chi}$ need not be small. Plugging χ_{cl} back into (5.3.2) we have

$$\sigma'' - \frac{2}{\eta}\sigma' + k_\sigma^2\sigma + \frac{2\lambda}{\eta^2 H}\bar{\chi}(1 - ik_\chi\eta)e^{ik_\chi\eta}\sigma = 0 \,. \tag{5.3.5}$$

The last term becomes relevant compared to the gradient term only at late times when $|\eta| \lesssim k_\sigma^{-1}$. In this regime, since $k_\chi \ll k_\sigma$, one can treat χ as a constant, equal to its asymptotic value $\bar{\chi}$. The calculation reduces to the one of a massive scalar field in dS with the mass that depends on $\bar{\chi}$:

$$S_\sigma = \int d\eta d^3x \left[\frac{1}{2\eta^2 H^2}(\sigma'^2 - (\partial_i\sigma)^2) - \frac{\alpha H^2}{2\eta^4}\sigma^2\right] , \tag{5.3.6}$$

where the dimensionless coupling α is defined by $\alpha \equiv 2\lambda\bar{\chi}/H$. Of course, one is able to solve exactly in α and there is no need of a perturbative expansion in this parameter. This corresponds to resumming the tree-level Witten diagrams shown in Figure 16a. The tree-level diagrams of Figure 16b are not enhanced by $\bar{\chi}$ (or less enhanced than the ones of Figure 16a) and are thus neglected, together with all loop diagrams, Figure 16c. The power spectrum of σ for $\alpha < 9/4$ reads at late times (prime means $(2\pi)^3\delta(\mathbf{k}+\mathbf{k}')$ was dropped)

$$\langle\sigma_{\mathbf{k}}\sigma_{-\mathbf{k}}\rangle' \simeq \frac{H^2}{2k^{3-\frac{2}{3}\alpha}} = \frac{H^2}{2k^{3-\frac{4}{3}\lambda\bar{\chi}/H}} \,. \tag{5.3.7}$$

This shows we have resummed all powers of $\lambda\bar{\chi}$.

As an aside, one may wonder whether the exact power spectrum as a function of α coincides with the result of summing the perturbative series, or there are non-perturbative effects one cannot capture in perturbation theory. It turns out that the power spectrum as a function of the complex variable α is an entire function, without singularities at any finite point. Therefore, it coincides with the perturbative series for any α. Let us verify this. Following the standard calculation for a massive field in dS (see e.g [129]), the mode function $\sigma_{cl}(\mathbf{k},\eta)$ that multiplies the operator $\hat{a}^\dagger$, with the correct behavior at early times reads

$$\sigma_{cl}(\mathbf{k},\eta) = H\frac{\sqrt{\pi}}{2}e^{-i\nu\pi/2}(-\eta)^{3/2}H_\nu^{(2)}(-k\eta) \,, \qquad \nu \equiv \sqrt{\frac{9}{4} - \alpha} \,. \tag{5.3.8}$$

This expression is even in ν so that there is no ambiguity when the square root becomes imaginary. To calculate the power spectrum one needs the complex conjugate of this. Using the properties of the Hankel function this can be written as

$$\sigma_{cl}(\mathbf{k},\eta)^* = H\frac{\sqrt{\pi}}{2}e^{i\nu\pi/2}(-\eta)^{3/2}H_\nu^{(1)}(-k\eta) \,, \tag{5.3.9}$$

5 For simplicity, we assume that there is a single Fourier mode of χ, but the results would not change considering many modes, all much longer than the ones of σ, and giving $\bar{\chi}$ as the late-time value in the region of interest.

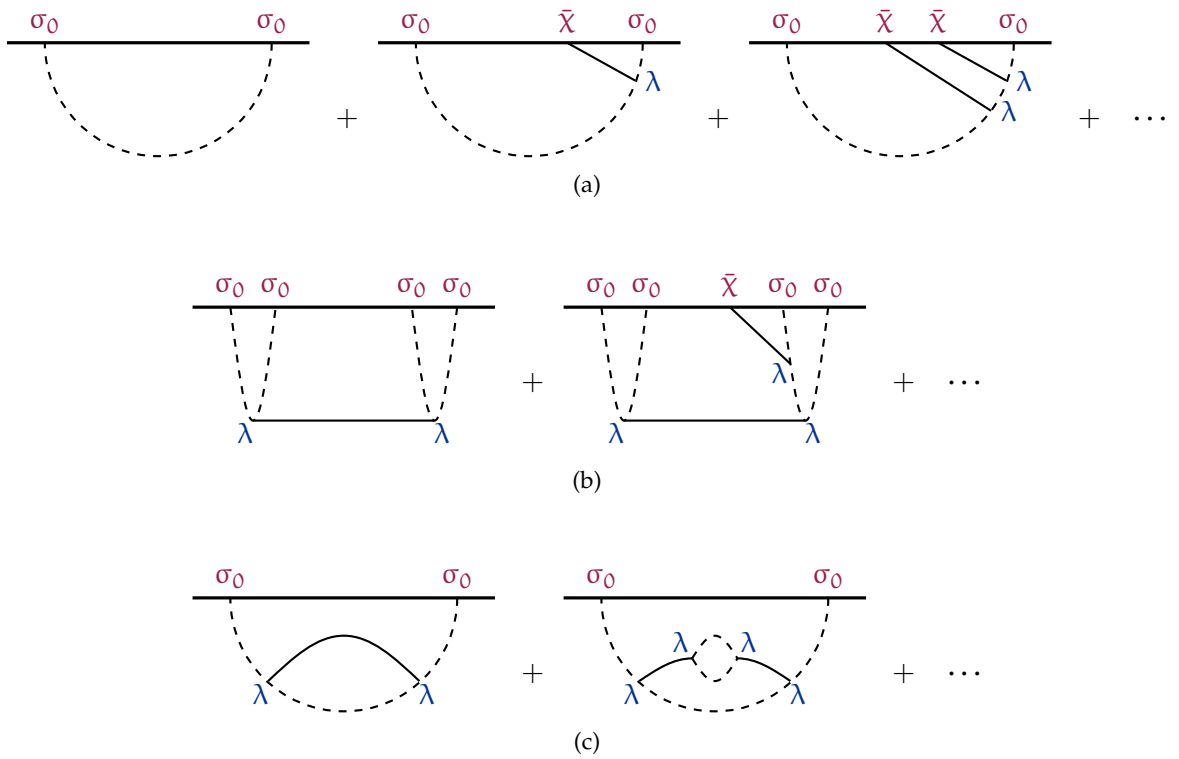

Figure 16: In the first row (Figure 16a) tree-level Witten diagrams that are enhanced by $\bar{\chi}$ and resummed. In the second (Figure 16b) tree-level diagrams with fewer powers of $\bar{\chi}$. In the third row (Figure 16c) loop-level diagrams, which are subleading in λ and not captured in the semiclassical limit.

where the equality holds for any real α. Therefore, for any real α one has

$$\langle \sigma_{\mathbf{k}} \sigma_{-\mathbf{k}} \rangle' = |\sigma_{\rm cl}(\mathbf{k}, \eta)|^2 = H^2 \frac{\pi}{4} (-\eta)^3 H_\nu^{(1)}(-k\eta) H_\nu^{(2)}(-k\eta) \,. \tag{5.3.10}$$

Using the properties of the Hankel functions, one can see that the RHS is an entire function of ν on the complex plane and moreover it is even in ν. Therefore, it is an entire function of the complex variable α. The analytic extension of the power spectrum as a function of α is entire and this implies that it coincides with its series expansion calculated around any point. (For a related discussion about analyticity of de Sitter propagators see [130].)

In general, one cannot hope to find an analytical solution as in the simple case above. One has to approach the problem numerically and in this case it is necessary to analytically continue the problem to Euclidean time τ defined as $\eta = -i\tau$. The Bunch-Davies condition is that fields decay in the limit $\eta \to -\infty + i\epsilon$ and after analytic continuation to τ, this condition becomes the requirement of decay for $\tau \to -\infty$. The advantage is that free fields exponentially decay for $\tau \to -\infty$, while in Lorentzian one has to deal with oscillating solutions. In order to perform the rotation, one has to assume (or prove) analyticity of the solution in the upper-left quadrant of the complex η plane. We are going to come back to this issue in Section 5.5. For the time being, let us notice that the solution (5.3.8) is analytic in the required quadrant and this holds for any value of α. This can also be seen as a consequence of the analyticity of the differential equation from the action (5.3.6). Another

advantage of the Euclidean rotation is that solutions are real, since both the differential equation and the boundary conditions are real. On the other hand, in the Lorentzian case, the Bunch-Davies boundary condition can only be satisfied by complex solutions.

In the following we concentrate on single-field models of inflation where there is no evolution outside the horizon. The non-perturbative results we are going to get are therefore unrelated with the stochastic approach, which resums the classical long-wavelength effects. We will study non-perturbative effects *at horizon crossing*, and these are fully quantum mechanical. In the future, it would be nice to explore the connection between the two approaches.

5.4 SINGLE-FIELD INFLATION WITH $\dot\zeta^4$ INTERACTION

Let us now apply our methods to a realistic scenario. We focus on a specific model of single-field inflation with a large quartic interaction $\dot\zeta^4$ [131]. With a single interaction it will be easier and more transparent to explore the semiclassical limit and derive analytical estimates. We leave to future work the generalization to other interactions. In the next Subsection we will review this model in the context of the Effective Field Theory of Inflation (EFTI). We will explain why it is consistent to focus on the non-linearities induced by the single operator $\dot\zeta^4$ and treat the geometry as an unperturbed de Sitter space. After that, we will concentrate on the calculations of the ζ probability distribution for large values of ζ, using both analytical and numerical methods.

5.4.1 *Single-field inflation with large 4-point function*

The model we would like to discuss is naturally described within the EFTI [49], which we review in short below[6]. In single-field inflation, the rolling of the inflaton $\phi(t)$ in a quasi-dS background leads to the spontaneous breaking of time diffeomorphisms. In unitary gauge, $\delta\phi(x) = 0$, the scalar mode is hidden inside the metric and the effective action for perturbations can be written as (see [49])

$$\begin{aligned} S = \int d^4x\sqrt{-g}\Big[&\frac{1}{2}M_{Pl}^2 R + M_{Pl}^2\dot H g^{00} - M_{Pl}^2(3H^2+\dot H) + \\ &+ \frac{1}{2}M_2(t)^4(\delta g^{00})^2 + \frac{1}{3!}M_3(t)^4(\delta g^{00})^3 + \frac{1}{4!}M_4(t)^4(\delta g^{00})^4 + \dots\Big]\,, \end{aligned} \tag{5.4.1}$$

where $g_{\mu\nu}$ is the metric, R is the Ricci scalar, $\delta g^{00} \equiv g^{00}+1$ and $M_i(t)$ are functions of time with dimensions of a mass. The operators in the first line, expanded around the inflationary background, start linear in perturbations while those in the second line start at second and higher order. The dots stand for operators starting at even higher order in perturbations or containing more derivatives.

The scalar mode π can be reintroduced by performing a broken time diffeomorphism $t \to t + \xi^0(x)$ and then promoting ξ^0 to a field, $-\pi$, that transforms non-linearly under the broken time

6 In fact, the construction of the EFTI is similar to the one of the EFT of Dark Energy, discussed briefly in Chapter 2. Notice that the energy scales of the early Universe are generally much higher than the ones of late Universe. Obviously, one might find that some formulas being used here had been mentioned before in the first part of the thesis.

diffs. $\pi(x) \to \tilde{\pi}(\tilde{x}(x)) = \pi(x) - \xi^0(x)$. In this way the resulting action is fully diff-invariant. As an example, under this Stueckelberg procedure the g^{00} component of the metric transforms (neglecting the mixing with metric perturbations) as

$$g^{00} \to -1 - 2\dot{\pi} + (\partial_\mu \pi)^2 \,. \tag{5.4.2}$$

This will be the only transformation we will need in our discussion. If one further assumes an approximate shift symmetry for π, then operators without at least one derivative acting on π will be suppressed. This assumption allows us to neglect terms coming, for instance, from the time dependence of the functions $M_i(t)$ in the action (5.4.1). Notice that the Goldstone boson π is related to the curvature perturbation ζ through the relation $\zeta = -H\pi$.

We want to explore a region of parameters where the π non-linearities are dominated by a single quartic operator. Following [131] let us start with $M_4 \neq 0$ while all the other M_i's in the action (5.4.1) are zero. We are going to come back to discuss the radiative stability of this choice momentarily. The Stueckelberg procedure eq. (5.4.2) then gives

$$\begin{aligned} S_\pi = \int d^4x\sqrt{-g}\Bigg[&- \dot{H}M_{Pl}^2\left(\dot{\pi}^2 - \frac{(\partial_i\pi)^2}{a^2}\right) + \\ &+ \frac{M_4^4}{4!}\left(16\dot{\pi}^4 - 32\dot{\pi}^3(\partial_\mu\pi)^2 + 24\dot{\pi}^2(\partial_\mu\pi)^4 - 8\dot{\pi}(\partial_\mu\pi)^6 + (\partial_\mu\pi)^8\right)\Bigg] \,. \end{aligned} \tag{5.4.3}$$

The operator M_4 contains a whole slew of non-linearities, but we want to argue that there is a regime in which only the first term, $\dot{\pi}^4$, is relevant. In perturbation theory this operator contributes to the 4-point function as

$$g_{NL} \sim \frac{\langle\zeta^4\rangle}{\langle\zeta^2\rangle^3} \sim \frac{\mathcal{L}_4}{\mathcal{L}_2}\frac{1}{P_\zeta} \sim \frac{M_4^4}{|\dot{H}|M_{Pl}^2} \,, \tag{5.4.4}$$

where, in estimating the quadratic and quartic Lagrangians $\mathcal{L}_2$ and $\mathcal{L}_4$, derivatives are taken to be of order H. In the following we will focus on the limit $g_{NL} \gg 1$. (The Planck experimental constraint on this parameter is $|g_{NL}| < 2 \cdot 10^6$ at 1σ [117].)

After going to canonical normalization, $\pi_c \equiv \sqrt{-2\dot{H}M_{Pl}^2}\,\pi$, the interactions in eq. (5.4.3) read

$$\mathcal{L}_4 \simeq \frac{1}{\Lambda_U^4}\dot{\pi}_c^4 \,, \quad \mathcal{L}_5 \simeq \frac{1}{g_{NL}^{1/2}\Lambda_U^6}\dot{\pi}_c^3(\partial_i\pi_c)^2 \,, \ldots \tag{5.4.5}$$

where we defined the scale $\Lambda_U^4 \equiv (\dot{H}M_{Pl}^2)^2/M_4^4$ and dropped factors of order unity. The quantum mechanical expansion parameter is $\lambda \equiv H^4/\Lambda_U^4$, the analogue of the quartic coupling in the anharmonic oscillator example discussed above. We always assume $\lambda \ll 1$, since this is the regime of validity of the EFT: powers of λ weight higher loops in calculating observables and in this Chapter we only look at the leading semiclassical approximation. Notice that $\lambda \simeq g_{NL}P_\zeta$, so that the regime $g_{NL} \gg 1$ is compatible with $\lambda \ll 1$. For large g_{NL} eq. (5.4.5) shows that the additional operators inside $(\delta g^{00})^4$ are suppressed by a higher scale compared to $\dot{\pi}_c^4$. This separation of scales implies, as we are going to show, that there is a regime of large values of ζ when the non-linearities associated with $\dot{\pi}^4$ are large, while the additional operators can be neglected.

Written in terms of $\zeta = -H\pi$ the Lagrangian is schematically of the form

$$S_\zeta = \int d^4x\sqrt{-g}\,\frac{|\dot H|M_{Pl}^2}{H^2}\left[(\partial_\mu\zeta)^2 + g_{NL}\frac{1}{H^2}\dot\zeta^4 + g_{NL}\frac{1}{H^3}\dot\zeta^3(\partial_\mu\zeta)^2 + \dots\right] . \tag{5.4.6}$$

Since all derivatives are of order H, classical non-linearities associated with the quartic operator are of the same order as the kinetic term for $g_{NL}\zeta^2 \sim 1$. In this regime, since $g_{NL} \gg 1$, the quintic term gives a contribution $g_{NL}\zeta^3 \ll 1$. Of course, the additional terms will become relevant if $g_{NL}\zeta^2$ becomes even larger, of order $g_{NL}^{1/3}$. In our Universe the experimental constraints impose $g_{NL}^{1/3} \lesssim 10^2$; however, since here we are mostly interested in presenting the general method and not in applying to phenomenology, in the following we are going to disregard this upper limit and explore the effect of the quartic term for arbitrarily large $g_{NL}\zeta^2$, neglecting the other operators. (Notice that if one is interested in the PBH abundance, $\zeta \sim 1$, one is actually sensitive to all the terms inside a given operator $(\delta g^{00})^n$.)

Let us now come back to the issue of whether the choice of setting to zero all operators except M_4 is stable under radiative corrections. We start with the operators M_2 and M_3, following [131], and show that these operators are automatically suppressed by an approximate symmetry in the setup we are studying. Since the quintic operator in eq. (5.4.5) is suppressed for large g_{NL}, the action (5.4.3) acquires an approximate $\mathbb{Z}_2$ symmetry $\pi \to -\pi$: odd operators are suppressed by $g_{NL}^{1/2}$. This observation guarantees that loop corrections to $(\delta g^{00})^2$ and $(\delta g^{00})^3$ are not sizable. To see this notice, using eq. (5.4.2), that the leading interactions arising from these operators are odd in π. Thus, they are generated radiatively by loops with insertions of terms odd in π hence suppressed by g_{NL}. As an example, we can estimate the scale at which the operator $\dot\pi_c(\partial_i\pi_c)^2$, contained in $(\delta g^{00})^2$, is generated. A loop with the interaction $\mathcal{L}_5$ of eq. (5.4.5) generates the cubic operator

$$\mathcal{L}_3 \sim \frac{1}{\Lambda_U^2 g_{NL}^{1/2}}\dot\pi_c(\partial_i\pi_c)^2 , \tag{5.4.7}$$

where the loop integral was cut off at the highest possible scale Λ_U. A similar estimate for the operator $\dot\pi_c^3$, contained in $(\delta g^{00})^3$, gives the same suppression scale. This corresponds to M_2^4, $M_3^4 \sim |\dot H|M_{Pl}^2 \ll M_4^4$: this model features $f_{NL} \lesssim 1$ while g_{NL} can be arbitrarily large [131]. These radiatively generated operators would contribute terms of order $(\partial_i\zeta)^2\dot\zeta/H$ and $\dot\zeta^3/H$ inside the brackets of eq. (5.4.6) and they are thus negligible for large g_{NL}.

Let us now come to the operators $(\delta g^{00})^n$ with $n \geqslant 5$. The radiative generation of the odd ones will be suppressed by the aforementioned approximate symmetry. For the even ones, however, there is no suppression, so that if the loop integral is pushed up to the unitarity cut-off Λ_U, the first operator inside each $(\delta g^{00})^n$ will read in canonical normalization

$$(\delta g^{00})^n \quad \to \quad \frac{\dot\pi_c^n}{\Lambda_U^{2n-4}} \qquad n \text{ even} . \tag{5.4.8}$$

It is easy to see that all terms in these expressions will become relevant exactly when the operator M_4 becomes of the same order as the kinetic term. Going to even larger values of ζ, the terms with larger n will dominate the lower ones. The estimate however may be pessimistic, since in general

the loop integral will be cut at a scale much lower than the unitarity cutoff Λ_U. For instance, if one considers the spontaneous breaking of a global $U(1)$ via a Higgs mechanism, the resulting EFT for the Goldstone boson is of the form $-\frac{1}{2}(\partial\pi)^2 + (\partial\pi)^4/\Lambda^4$, with all additional operators $(\partial\pi)^{2n}$ suppressed in the limit the Higgs field is weakly coupled. See, for instance, the discussion in Section 4 of [113] and references therein. In the following we are going to assume that these extra operators are sufficiently suppressed to be negligible in the regime of interest.

This discussion leads us to an important general point. The questions we are addressing are sensitive to the full non-linear structure of the EFT, including in principle the whole series of operators. One may worry that this does not make sense and goes beyond the regime of validity of the EFT itself. First of all, notice we are always in a regime of small energy: derivatives are of order H and are suppressed with respect to the cut-off of the theory. Indeed, the quantum mechanical expansion parameter λ is small. What is getting large is ζ, i.e. we are in the regime of large number of particles, or large occupation number. In general, there is nothing wrong in exploring an EFT for large values of the fields: for instance we do it in General Relativity all the times, when we study the full Einstein equations to obtain for example the Schwartzschild solution. Of course, there is no guarantee that the solution remains healthy: perturbations around the solution may become pathological signaling that the EFT is actually breaking down (see Section 4 of [113]). Thus one should always check that the non-linear solution remains healthy. Another point of concern is the knowledge of the EFT: to find a reliable solution one should have control of all the terms in the EFT with the minimum number of derivatives, but this looks challenging. In some cases the symmetries of the problem are such that the whole non-linear structure of the theory is fixed. Again GR is the prototypical example: the Ricci scalar contains an infinite series of non-linearities of the graviton, all terms with two derivatives. In the case of scalars, one can consider symmetries that enforce a complete non-linear structure. For instance the scalars that describe the embedding of a brane in an extra dimensional space have an action fixed by the (non-linear realization of) geometrical symmetries: the DBI action [132]. Another example is the one of Galileons [133]: at leading order in derivatives there are only three possible interaction terms (in 3+1 dimensions). Even in cases in which symmetries are not powerful enough, some assumptions about the UV completion may fix the full non-linear structure of the EFT. We already gave above the example of the Abelian Higgs model, while another example is the Euler-Heisenberg Lagrangian obtained integrating out the electron from QED. The necessity to know the whole non-linear action is therefore a feature more than a pathology, not that different from the necessity of knowing the full scalar potential $V(\phi)$ to describe inflation from observable scales to reheating.

Before moving to the actual calculation with the $\dot{\zeta}^4$ interaction, let us comment on another approximation: we are going to neglect metric perturbations, considering a scalar field in exact de Sitter space. This corresponds to the usual "decoupling limit": the effect of π perturbations on the metric is suppressed by the slow-roll parameter $\epsilon \equiv -\dot{H}/H^2$, which also describes the deviation of the unperturbed background from de Sitter. This is not changed by the fact that we are taking

large values of ζ; the leading interaction can be read by looking at π only and treating the metric as unperturbed.

5.4.2 $\dot\zeta^4$ *beyond perturbation theory*

We can now apply the main ideas of this Chapter to the model introduced in the previous Section, with the discussed approximations. The action for ζ using conformal time is

$$S = \int d^3x d\eta \left\{ \frac{1}{2\eta^2 P_\zeta}\left[\zeta'^2 - (\partial_i\zeta)^2\right] + \frac{\lambda\zeta'^4}{4! P_\zeta^2}\right\} , \tag{5.4.9}$$

where $P_\zeta \equiv H^2/(2\epsilon M_{Pl}^2)$ and $\lambda \equiv (H/\Lambda_U)^4 \ll 1$. The standard in-in perturbation theory for ζ corresponds to an expansion of the various correlators in powers of λ. From now on we call ζ_0 the asymptotic late-time value of ζ. Comparing the free action with the quartic interaction, one sees that the relevant expansion parameter is $\lambda\zeta_0^2/P_\zeta$. The semiclassical expansion corresponds to an expansion in $\lambda \ll 1$ keeping $\lambda\zeta_0^2/P_\zeta$ finite and not necessarily small. The wavefunction of the Universe is calculated evaluating the action on-shell

$$\Psi[\zeta_0(\mathbf{x})] \sim e^{iS[\zeta_{cl}]} . \tag{5.4.10}$$

From the expression of the action eq. (5.4.9) one can see that the on-shell action scales as

$$S[\zeta_{cl}] = \frac{1}{\lambda} F\left(\lambda\zeta_0^2/P_\zeta\right) , \tag{5.4.11}$$

where F is a function to be determined (in analogy with the case of the anharmonic oscillator in eq. (5.2.10)).

The field ζ_{cl} is a solution of the equation of motion one can derive from the action (5.4.9). For analytical and numerical purposes it is better to consider the system in Euclidean time τ defined as $\eta = -i\tau$. The equation of motion reads

$$-\zeta'' + \frac{2}{\tau}\zeta' - \partial_i^2\zeta - \frac{\lambda}{2P_\zeta}\tau^2\zeta'^2\zeta'' = 0 . \tag{5.4.12}$$

(With an abuse of notation we indicate with primes both derivatives with respect to the conformal time η and the Euclidean time τ. The appearance of η or τ in the equation should help not creating confusion.) We are going to solve the PDE above with boundary conditions at early and late times. At early times ζ must go to zero, while at late times if must give the profile $\zeta_0(\mathbf{x})$ we are interested in. The action in Euclidean time is given by

$$S_E \equiv -\int d^3x d\tau \left\{ \frac{1}{2\tau^2 P_\zeta}\left[\zeta'^2 + (\partial_i\zeta)^2\right] + \frac{\lambda\zeta'^4}{4! P_\zeta^2}\right\} , \tag{5.4.13}$$

with

$$\Psi[\zeta_0(\mathbf{x})] \sim e^{-S_E[\zeta_{cl}]} . \tag{5.4.14}$$

Notice that we started with an integral in η slightly deformed above the real axis to project in the vacuum. Now we are effectively integrating η along the positive imaginary axis. The two procedures give the same result assuming analyticity of the Lagrangian as a function of complex η, in the quadrant of interest. For the time being, we assume this property and we will come back to this point in Section 5.5.

Let us go through the calculation in the case of the free theory $\lambda = 0$, following [22]. This is useful to understand the dependence of the WFU on time: indeed we have been sloppy so far and we should have written the WFU as $\Psi[\zeta_0(\mathbf{x}), \eta_f]$, where η_f is the (late) time of interest. In Fourier space, the solution with prescribed boundary conditions at η_f that decays to zero when η acquires a small positive imaginary part in the far past is

$$\zeta_{cl}(\mathbf{k}, \eta) = \zeta_0(\mathbf{k}) \frac{(1 - ik\eta)e^{ik\eta}}{(1 - ik\eta_f)e^{ik\eta_f}} \,. \tag{5.4.15}$$

One has then to evaluate the free action on these solutions. Integrating by parts the free action gives a term proportional to the equation of motion, which is zero on-shell, and a boundary term:

$$iS = \frac{i}{2P_\zeta} \int \frac{d^3k}{(2\pi)^3} \frac{1}{\eta_f^2} \zeta_{cl}(-\mathbf{k}, \eta) \partial_\eta \zeta_{cl}(\mathbf{k}, \eta) \Big|_{\eta=\eta_f} \simeq \int \frac{d^3k}{(2\pi)^3} \frac{1}{2P_\zeta} \left(i\frac{k^2}{\eta_f} - k^3 + \dots \right) \zeta_0(-\mathbf{k}) \zeta_0(\mathbf{k}) \,, \tag{5.4.16}$$

where we dropped terms subleading for $\eta_f \to 0^-$. The time-dependence of the WFU is a pure phase that does not affect the probability of ζ_0, which is time-independent at late times (this justifies our sloppy notation).

It is useful to also do the same calculation in Euclidean time τ since this is what we are going to use for the interacting theory. One has

$$\zeta_{cl}(\mathbf{k}, \tau) = \zeta_0(\mathbf{k}) \frac{(1 - k\tau)e^{k\tau}}{(1 - k\tau_f)e^{k\tau_f}} \,, \tag{5.4.17}$$

$$S_E = -\frac{1}{2P_\zeta} \int \frac{d^3k}{(2\pi)^3} \frac{1}{\tau_f^2} \zeta_{cl}(-\mathbf{k}, \tau) \partial_\tau \zeta_{cl}(\mathbf{k}, \tau) \Big|_{\tau=\tau_f} \simeq \int \frac{d^3k}{(2\pi)^3} \frac{1}{2P_\zeta} \left(\frac{k^2}{\tau_f} + k^3 + \dots \right) \zeta_0(-\mathbf{k}) \zeta_0(\mathbf{k}) \,. \tag{5.4.18}$$

This is the same as the Lorentzian result after the analytic continuation of τ_f. Notice that in the Euclidean calculation both the divergent part and the finite part are real. Notice also that since $\tau_f \to 0^-$, $S_E < 0$ and indeed there is an overall minus sign in front of eq. (5.4.13). However, after analytic continuation $1/\tau_f$ becomes purely imaginary and the remaining piece is positive as it should. In the interacting case, one has to deal with this divergence to make the problem numerically tractable. The crucial simplification is that the divergence, which in Lorentzian describes the phase of the wavefunction is a late-time effect and at late times the interaction is negligible, since it contains more derivatives than the free action. Therefore, as we will see, one can extract a finite result comparing the interacting case with the free one.

The semiclassical approach effectively resums a subset of diagrams of the standard in-in perturbation theory. In dS space, $\Psi[\zeta_0(\mathbf{x})]$ is defined by the path integral of eq. (5.1.3) where one imposes

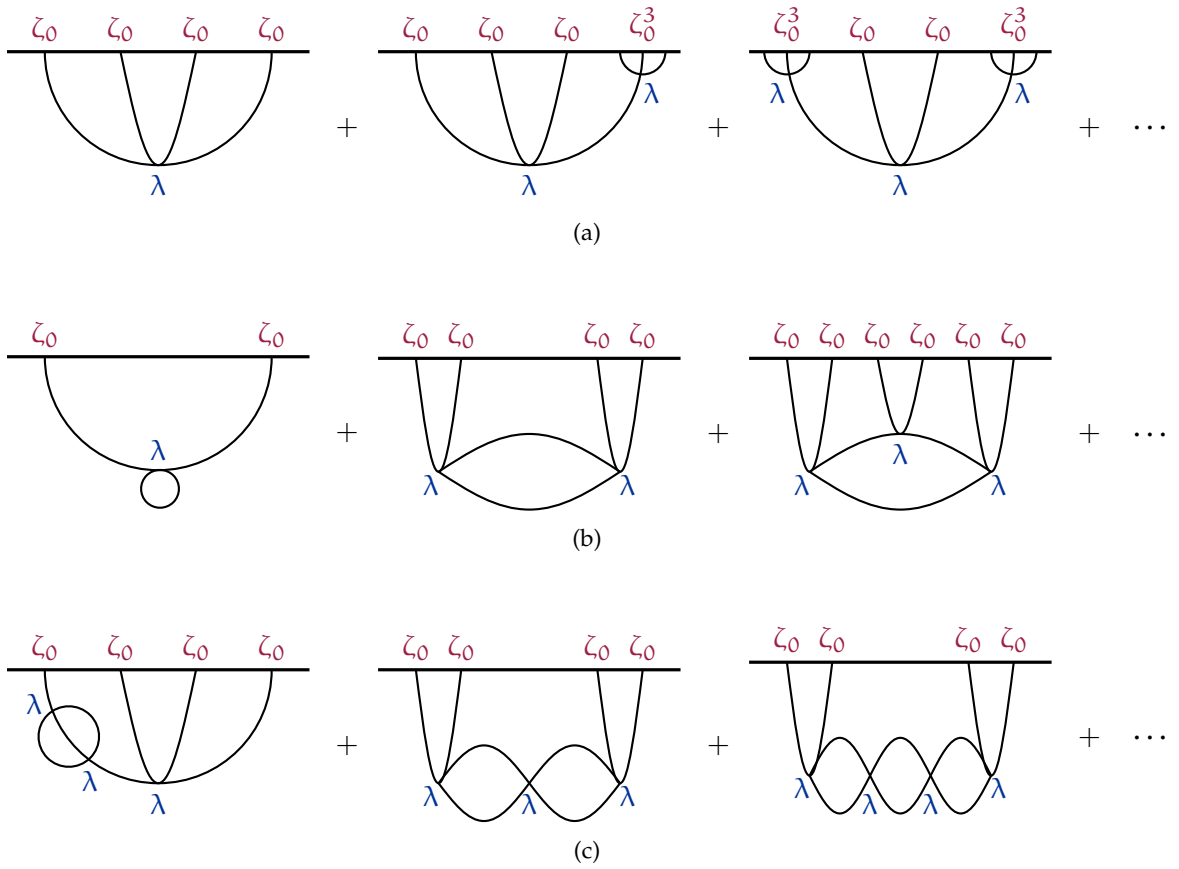

Figure 17: In the first row (Figure 17a) tree-level Witten diagrams; these are captured by the semi-classical method. In the second row (Figure 17b) one-loop diagrams; these would be captured by the (one-loop) prefactor in the semi-classical method. In the third row (Figure 17c) higher-loop diagrams; these are only captured at subleading order in the semi-classical calculation.

Dirichlet boundary conditions for ζ at late times. This path integral can be conveniently computed in perturbation theory as a sum of Witten diagrams (see for example [134]). The tree-level Witten diagrams of Figure 17a have the same scaling as the lowest-order term in the semiclassical expansion, which corresponds to the on-shell action (5.4.11). This is immediate to realize since for any additional vertex we add we increase the number of boundary legs by two. Thus, a tree-level diagram with V vertices scales as $\sim \frac{1}{\lambda}(\lambda\zeta_0^2)^{V+1}$. The subleading order in λ in the semiclassical expansion is instead obtained through a one-loop calculation around a non-trivial background for ζ (this corresponds to the calculation of the prefactor in eq. (5.2.8) in our quantum mechanical example). The scaling of this factor is $\lambda^0 G(\lambda\zeta_0^2)$, which corresponds to the scaling of the one-loop Witten diagrams of Figure 17b, while the diagrams of Figure 17c are computed by two- or higher- loop calculations around the semiclassical solution for ζ.

Before moving to the actual calculation of the action, it is useful to comment on the choice of the asymptotic value $\zeta_0(\mathbf{x})$. To answer a concrete question, like the probability of producing a PBH,

one would be interested in evaluating the WFU for all functions that are above a certain threshold[7]. More specifically, as we discussed in the introduction, one would consider a filtered field $\hat{\zeta}_0(\mathbf{x})$ and require that this field exceeds a certain numerical threshold at a point of interest. In the limit of a very high threshold all configurations $\zeta_0(\mathbf{x})$ that are above threshold have a "large ζ_0" and as such the WFU can be calculated semiclassically. Of course, to get to the final answer one should eventually sum over all $\zeta_0(\mathbf{x})$ that are above threshold. This final integral can also be done in saddle-point approximation: since the probability of all interesting configurations is small, the integral will be dominated by the least unlikely. In this study we do not want to commit to a very specific question, which would require the details of the window function and the threshold. We are going simply to choose a given $\zeta_0(\mathbf{x})$ and take it large enough for our approach to be applicable. Since the question we are addressing is not completely specified, we will be mostly interested in the behavior of the probability as a function of the parameter $\lambda\zeta_0^2/P_\zeta$, especially once this becomes large. We leave the actual implementation of these techniques to the calculation of the PBH abundance to future work.

5.4.3 *ODE approximation*

The qualitative behavior of the action as a function of the boundary values of ζ can be understood focusing on a single Fourier mode and thus reducing the problem to an ordinary differential equation (ODE). In perturbation theory the interaction ζ'^4 induces coupling mainly among modes with comparable wavelength: this is the reason why one gets non-Gaussianities of "equilateral" kind [135]. For the same reason one expects that if the boundary condition at late times $\zeta_0(\mathbf{x})$ has Fourier transform concentrated on a typical value k ([8]) then only modes with similar wavelength will be relevant in the full solution $\zeta_{cl}(\mathbf{x},\tau)$. Therefore, one can concentrate on a single Fourier mode and eq. (5.4.12) reduces to the following ODE

$$-\zeta'' + \frac{2}{\tau}\zeta' + H^2\zeta - \frac{\lambda}{2P_\zeta}\tau^2\zeta'^2\zeta'' = 0\,, \tag{5.4.19}$$

where we have set $k/H = 1$, using scale-invariance. The boundary conditions we need to impose are

$$\zeta(\tau \to -\infty) = 0\,, \quad \zeta(\tau_f) = \zeta_0\,, \tag{5.4.20}$$

7 The threshold is of course an approximate concept: one should know the precise boundary in the functional space $\zeta_0(\mathbf{x})$ that separates the configurations giving rise to a PBH from the ones that do not.

8 For instance PBH with a certain mass will typically form at a given time and the modes of interest will be the ones with wavelength comparable with the Hubble radius at that moment.

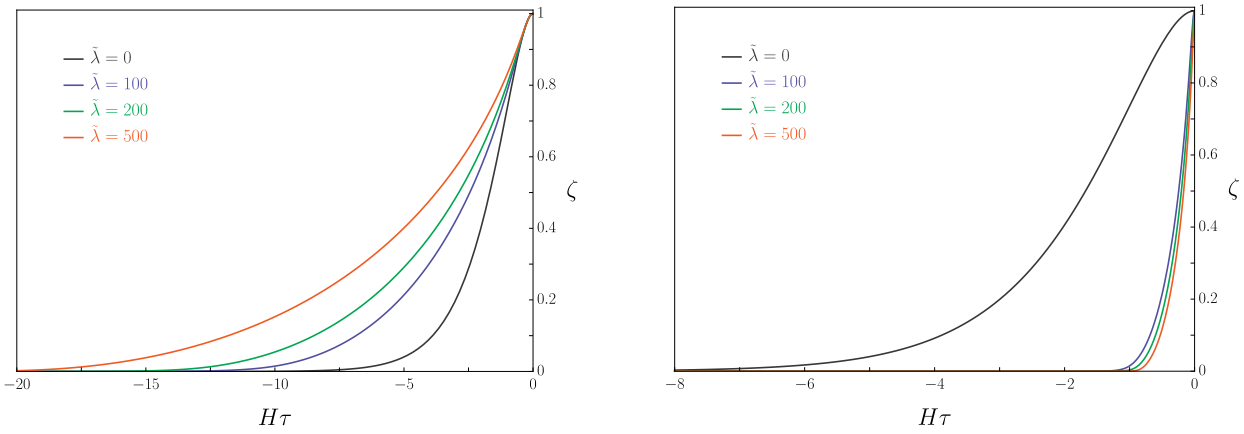

Figure 18: Left panel (Figure 18a): the numerical solutions for $\tilde\lambda = \{0, 100, 200, 500\}$ and $\zeta_0 = 1$. Right panel (Figure 18b): the same solutions after $\tau \to \sqrt{\tilde\lambda}\tau$ (the solution for $\tilde\lambda = 0$ is copied for comparison).

where τ_f is the final conformal time.[9] This approximation, as we are going to argue, is useful in order to obtain an analytic understanding of the scaling of S as a function of λ and ζ_0. In Section 5.4.5 we will instead solve the full PDE and we will compare with the results of the ODE approximation.

In order to solve eq. (5.4.19) numerically and compare different solutions, it is convenient to rescale $\zeta \to \zeta_0\zeta$ so that one has $\zeta(\tau_f) = 1$. Moreover, one can define

$$\tilde\lambda \equiv \lambda\zeta_0^2/P_\zeta \,, \tag{5.4.22}$$

this is the parameter that quantifies the classical non-linearities, the analogue of $\bar x$ in the quantum mechanical example of Section 5.2. In this way the EoM (5.4.19) keeps the same form with λ replaced by $\tilde\lambda$ and P_ζ set to 1, while the action rescales as $S \to (\zeta_0^2/P_\zeta)S$. Our analysis will be exact in $\tilde\lambda$, but perturbative in $\lambda \ll 1$: this separation requires $\zeta_0^2/P_\zeta \gg 1$, corresponding to $\tilde\lambda \gg \lambda$. (For instance at first order in λ we are keeping the first graph of Figure 17a, but we are dropping the first diagram of Figure 17b. The first is larger than the second by a factor ζ_0^2/P_ζ.)

The numerical solutions are shown in Figure 18a (we set $\zeta(\tau_f) = 1$ and $H\tau_f = -0.001$). Notice that the non-linear interaction acts as a sort of non-linear friction so that the solution varies more slowly as $\tilde\lambda$ increases. (Thus one has to correspondingly adjust the value of $H\tau_i$ to earlier and earlier values.)

We notice that the solutions approach a universal behavior for large $\tilde\lambda$ that can be obtained by rescaling $\tau \to \sqrt{\tilde\lambda}\tau$. The rescaled solutions are illustrated in Figure 18b. We will come back to this point in the next Section.

9 Since the field goes to zero at early times, the free theory becomes a good approximation. Numerically we implement the boundary condition at an early time τ_i as

$$\zeta'(\tau_i) = \frac{H\tau_i}{H\tau_i - 1}\zeta(\tau_i) \,, \tag{5.4.21}$$

which is the relation between the field and the derivative in the free theory.

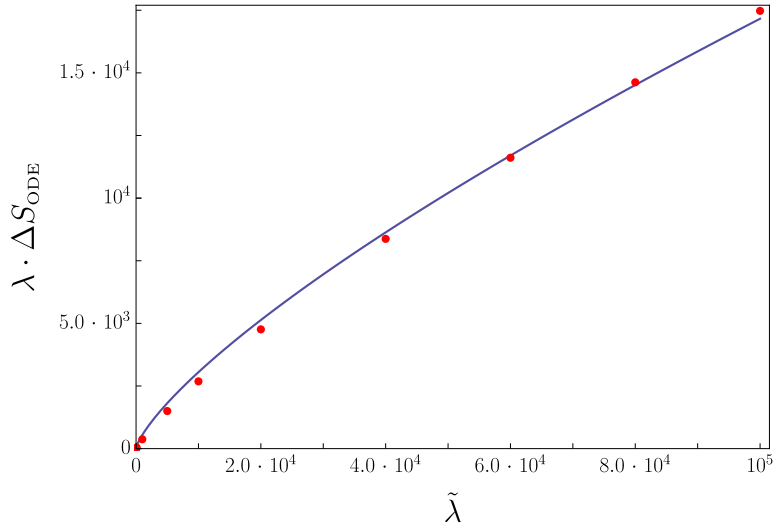

Figure 19: The on-shell action as a function of the expansion parameter $\tilde{\lambda} = \lambda\zeta_0^2/P_\zeta$. The blue curve is the best fit curve proportional to $\tilde{\lambda}^{3/4}$. The red points indicate the numerical values of $\lambda \cdot \Delta S_{\rm ODE}$.

Now let us evaluate the on-shell action. First we note that, as in the case of a free field in dS discussed above, the action (in particular the free gradient energy) gives a singularity for $\tau \to 0$. This can be completely removed since its contribution to the wavefunction is purely imaginary:

$$\Delta S_{\rm ODE} = -\frac{\zeta_0^2}{P_\zeta}\int_{\tau_i}^{\tau_f} d\tau \left\{\frac{1}{2\tau^2}\left[\zeta'^2 + H^2(\zeta^2-1)\right] + \frac{\tilde{\lambda}}{4!}\zeta'^4\right\} = \frac{1}{\lambda}F(\tilde{\lambda})\,. \tag{5.4.23}$$

We have subtracted 1, the asymptotic value of ζ, inside the innermost parentheses. This additional term gives a term proportional to $1/\tau_f$ after integration and this becomes purely imaginary after rotation to η. Therefore, the extra term does not contribute to the probability of ζ. The advantage is that, after this subtraction, the action is finite and can be treated numerically.

The behavior of the on-shell action evaluated on the numerical solutions is given in Figure 19. It shows that the on-shell action $\Delta S_{\rm ODE} \sim \frac{1}{\lambda}\tilde{\lambda}^{3/4}$ for large $\tilde{\lambda}$. The real part of the WFU therefore behaves as

$$\Psi[\zeta_0] \sim \exp\left[-\frac{1}{\lambda}\tilde{\lambda}^{3/4}\right]\,, \tag{5.4.24}$$

with some unspecified order one coefficient in front of the exponent. The WFU is multiplied by a time-dependent phase, the same as in the free theory eq. (5.4.16), which does enter in the calculation of the correlation functions of ζ.

5.4.4 *Analytic understanding of the ODE result*

In this Section we show that the behavior of the ODE for large $\tilde{\lambda}$ that we found numerically can also be understood analytically. First we notice that there are three regimes for the ODE solution, summarized in Figure 20. At very early times $\tau \to -\infty$, the field must approach the BD vacuum,

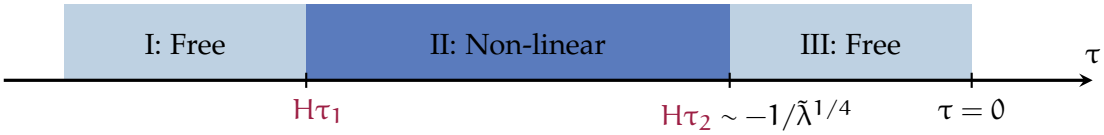

Figure 20: Three regimes of the solution.

so its amplitude is exponentially small. Therefore, in this regime the interaction term becomes negligible and we approach a free solution. We define τ_1 as the earliest time at which the interaction term is comparable with the free time kinetic term. For $\tau < \tau_1$ the solution is approximatively free (region I of the Figure), while for $\tau > \tau_1$ we enter the non-linear regime (region II).

At very late times, $\tau \to 0^-$, the interaction term becomes subdominant once again since it contains more derivatives than the kinetic term. Thus the solution becomes free (region III) for times $\tau > \tau_2$. In region III the solution is approximately given by

$$\zeta_{III} \simeq (1 - H\tau)e^{H\tau}, \tag{5.4.25}$$

since our boundary condition, after rescaling, is $\zeta(\tau_f) = 1$. From this we can estimate τ_2 as the time when ζ'' and the non-linear term in eq. (5.4.19) are of the same order

$$\tilde{\lambda}\tau_2^2\zeta'_{III}(\tau_2)^2 \sim 1\,. \tag{5.4.26}$$

Since this happens after horizon crossing, we can expand this equation at lowest order in τ_2. We obtain

$$-H\tau_2 \sim \frac{1}{\tilde{\lambda}^{1/4}}\,, \tag{5.4.27}$$

which for large $\tilde{\lambda}$ is consistent with the expansion we performed. In this approximation we can take $\zeta_{III} \sim 1$ at τ_2.

Now we can focus on region II. In this regime one expects the non-linear term to dominate over the kinetic term and Hubble friction, and to be compensated in the equation of motion by the spacial kinetic term. To see this let us consider eq. (5.4.19) and rescale $\tau = \sqrt{\tilde{\lambda}}\tilde{\tau}$. We obtain

$$\frac{1}{\tilde{\lambda}}\left(-\ddot{\zeta} + \frac{2}{\tilde{\tau}}\dot{\zeta}\right) + H^2\zeta - \frac{1}{2}\tilde{\tau}^2\dot{\zeta}^2\ddot{\zeta} = 0\,, \tag{5.4.28}$$

where $\dot{\zeta} \equiv d\zeta/d\tilde{\tau}$. We see that, when $\tilde{\lambda}$ is large, the first and the second terms can be neglected compared to the rest (one can check this in the numerical solutions). Therefore, in this regime one has

$$H^2\zeta_{II} - \frac{\tilde{\lambda}}{2}\tau^2\zeta'^2_{II}\zeta''_{II} = 0\,. \tag{5.4.29}$$

This explains why in the previous Section we found a universal solution as a function of $\tau/\sqrt{\tilde{\lambda}}$. This equation does not have an analytic solution. However, let us now assume that $\zeta \sim 1$ for small τ (as

we argued from the behavior in region III). Then, from (5.4.29) ζ_{II}, ζ'_{II} and ζ''_{II} can be approximated, neglecting factors of order one, as

$$\zeta_{II} \sim 1 - \frac{H^{2/3}|\tau|^{2/3}}{\tilde{\lambda}^{1/3}} , \quad \zeta'_{II} \sim \frac{H^{2/3}}{(\tilde{\lambda}|\tau|)^{1/3}} , \quad \zeta''_{II} \sim \frac{H^{2/3}}{\tilde{\lambda}^{1/3}|\tau|^{4/3}} . \tag{5.4.30}$$

As we increase $\tilde{\lambda}$, the time dependence of the solution becomes milder. In comparison, the free solution decays exponentially when moving to earlier times. This analytic behavior is in agreement with the numerical results of Figure 18a. Physically this is expected: for the model at hand the non-linearities have the effect of increasing the time kinetic term, hence reducing the forcing term. In Euclidean time this induces a slower decay at early times, and in the limit $\tilde{\lambda} \to \infty$ one recovers $\zeta \sim 1$ at any τ.

The solution in region I is again free, proportional to eq. (5.4.25), but with a different normalization. Time τ_1 is approximately given by

$$\tilde{\lambda}\tau_1^2 \zeta'_{II}(\tau_1)^2 \sim 1 . \tag{5.4.31}$$

We do not know how to estimate τ_1, since we do not have an analytic expression of ζ_{II}. However, since for large enough $\tilde{\lambda}$, ζ_{II} is a function of $\tau/\sqrt{\tilde{\lambda}}$, one can argue that $|\tau_1|$ grows at least as fast as $\sqrt{\tilde{\lambda}}$, and this is sufficient to estimate the action. (Numerically one finds actually $|\tau_1| \sim \sqrt{\tilde{\lambda}}$.)

With these observations at hand we are now ready to estimate the on-shell action. We note that in the limit $\tilde{\lambda} \to \infty$ the regularized action (5.4.23) approaches zero (since we have $\zeta \sim 1$ and $\zeta' \sim 0$). On the other hand, for small $\tilde{\lambda}$ we need to recover the free result $\Delta S_{ODE}^{free} = \zeta_0^2/(2P_\zeta)$. Therefore, one expects ΔS_{ODE} to be a decreasing function of $\tilde{\lambda}$.

Let us assume momentarily that the contribution to the action of region I is negligible. Using the approximate solutions for regions II and III, eq. (5.4.25) and (5.4.30), we obtain

$$\begin{aligned}
\Delta S_{ODE} &= -\frac{\zeta_0^2}{P_\zeta}\int_{-\infty}^{0} d\tau \left\{ \frac{1}{2\tau^2}\left[\zeta'^2 + H^2(\zeta^2-1)\right] + \frac{\tilde{\lambda}}{4!}\zeta'^4 \right\} \\
&\sim -\frac{\zeta_0^2}{P_\zeta}\left\{ \int_{\tau_1}^{\tau_2} d\tau \left[\frac{1}{2\tau^2}\left(\zeta'^2_{II} + H^2(\zeta^2_{II}-1)\right) + \frac{\tilde{\lambda}}{4!}\zeta'^4_{II}\right] + \int_{\tau_2}^{0} d\tau \left[\frac{1}{2\tau^2}\left(\zeta'^2_{III} + H^2(\zeta^2_{III}-1)\right) + \frac{\tilde{\lambda}}{4!}\zeta'^4_{III}\right] \right\} \\
&\sim \frac{\zeta_0^2}{P_\zeta}\frac{1}{\tilde{\lambda}^{1/4}} = \frac{1}{\lambda}(\lambda\zeta_0^2/P_\zeta)^{3/4} .
\end{aligned} \tag{5.4.32}$$

Both integrals are dominated by the region around τ_2. One can check that each single term in the action, ζ'^2, (ζ^2-1) and $\tilde{\lambda}\zeta'^4$ contributes, both in region II and III, to a term of order $\tilde{\lambda}^{-1/4}$. This result confirms the numerical behavior found in the previous Section.

To conclude, let us check that the contribution of region I is actually negligible. In this region we can use free modes (whose normalization, however, we do not know) to integrate the action. The integral of the free action can be written as

$$-\frac{\zeta_0^2}{P_\zeta}\int_{-\infty}^{\tau_1} d\tau \left\{ \frac{1}{2\tau^2}\left[\zeta'^2_I + H^2\zeta_I^2\right]\right\} \sim -\frac{\zeta_0^2}{P_\zeta}\frac{H\zeta'^2_I(\tau_1)}{\tau_1^2} . \tag{5.4.33}$$

Using eq. (5.4.31) and that $|\tau_1|$ increases at least as fast as $\sqrt{\tilde{\lambda}}$, one sees that this term goes as $\tilde{\lambda}^{-3}$, and it is thus subleading compared with eq. (5.4.32). One gets the same estimate for the contribution of the term $\tilde{\lambda}\zeta'^4$. The integral of the ζ-independent term in the action, $-H^2/(2\tau^2)$, gives a contribution of order $1/\tau_1 \sim \tilde{\lambda}^{-1/2}$, which is also subleading.

5.4.5 *PDE analysis*

In the last two Sections we have seen how the tail of the WFU can be estimated (as a function of the parameter $\tilde{\lambda}$) assuming that all the modes have comparable wavelength: the PDE was reduced to an ODE. The ODE is easy to treat numerically (Section 5.4.3) and one can also provide an analytic understanding of the numerical result (Section 5.4.4). However, in this way one can only capture the qualitative dependence on $\tilde{\lambda}$ and not the constants of order unity: if one wants to use our semi-classical method to answer some specific questions, e.g. compute the PBH abundance, the full PDE analysis is required. We are now going to study the PDE and check that the ODE treatment correctly captured the qualitative behavior in $\tilde{\lambda}$ and that this result holds quite generally as we change the space dependence of the boundary condition $\zeta_0(\mathbf{x})$ ([10]). In particular we are going to make two choices for $\zeta_0(\mathbf{x})$: a sinusoidal wave and a spherically symmetric Gaussian profile.

Let us first start with the sinusoidal case. For simplicity, we impose the conditions

$$\zeta(\tau_f, x) = \zeta_0 \sin(kx) \,, \tag{5.4.34}$$

with $kx \in [0, 2\pi]$. Notice that the action we are considering is even in ζ so that it is consistent to impose that ζ vanishes at 0 and 2π for any τ. Also in the PDE case we implement the initial condition (5.4.21) and take $k = H$ using scale-invariance. Like the ODE Section, we redefine $\zeta \to \zeta_0\zeta$ so that the condition (5.4.34) becomes $\zeta(\tau_f, x) = \sin(kx)$.

The problem does not depend on y and z, thus the PDE (5.4.12) simplifies to a $1+1$-dimensional problem:

$$-\zeta'' + \frac{2}{\tau}\zeta' - \frac{\partial^2\zeta}{\partial x^2} - \frac{\tilde{\lambda}}{2}\tau^2\zeta'^2\zeta'' = 0 \,, \tag{5.4.35}$$

where $\tilde{\lambda}$ was previously defined in Section 5.4.3. The numerical solutions for $\tilde{\lambda} = 0$ and $\tilde{\lambda} = 200$ are given by Figures 21a and 21b. (We took $H\tau_f = -0.001$ and $H\tau_i = -80$. As in the ODE case the value of $|\tau_i|$ must be taken larger and larger as $\tilde{\lambda}$ increases. We used `Mathematica` for all numerical analysis.) The plots show that the solution remains smooth going to large $\tilde{\lambda}$, without generating large higher harmonics: this justifies the use of the ODE as an approximation to the full problem.

10 In the model we are studying there is a neat separation: the Euclidean action has an overall dependence on the amplitude of $\zeta_0(\mathbf{x})$, i.e. $\propto \zeta_0^{3/2}$, and a subleading dependence on the precise shape of $\zeta_0(\mathbf{x})$. It is not obvious a priori that the same will hold for any possible interaction.

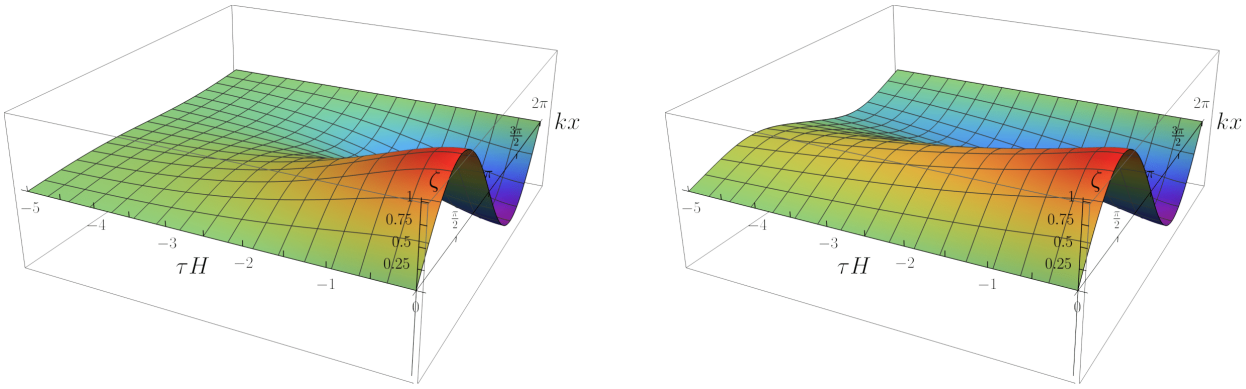

(a) (b)

Figure 21: Numerical solutions with sinusoidal boundary condition at late times with $\tilde{\lambda} = 0$ (left panel, Figure 21a) and $\tilde{\lambda} = 200$ (right panel, Figure 21b).

Let us now compute the Euclidean action evaluated on the numerical solutions. Following the same procedure of the ODE Section, the finite part of the action $\Delta S_{\rm PDE}$ is given by

$$\Delta S_{\rm PDE} = -\frac{\zeta_0^2}{P_\zeta}\int_{\tau_i}^{\tau_f} d\tau \int_{x_i}^{x_f} dx \left\{ \frac{1}{2\tau^2}\left[\zeta'^2 + (\partial_x\zeta)^2 - k^2\cos^2(kx)\right] + \frac{\tilde{\lambda}}{4!}\zeta'^4 \right\} = \frac{1}{\lambda}F(\tilde{\lambda})\,. \tag{5.4.36}$$

The $k^2\cos^2(kx)$ term is added to remove the divergence of the free action at late times (at $\tau = \tau_f$ one has $(\partial_x\zeta)^2 = k^2\cos^2(kx)$). We now evaluate the integral in (5.4.36) numerically on the solutions $\zeta(\tau, x)$ for different values of $\tilde{\lambda}$, starting from $\tilde{\lambda} = 0$ up to $\tilde{\lambda} = 10^5$. We then plot in Figure 22 the function $F(\tilde{\lambda}) = \lambda \cdot \Delta S_{\rm PDE}$ against the parameter $\tilde{\lambda}$. For large $\tilde{\lambda}$ the function $F(\tilde{\lambda})$ approaches $\tilde{\lambda}^{3/4}$ in agreement with the ODE result (5.4.24).

The advantage of considering a single Fourier mode is that it is easy to check the numerical result with perturbation theory in the limit of small $\tilde{\lambda}$: we leave this check to Appendix F.

Let us now come to the study of the PDE with a Gaussian, spherically symmetric profile of ζ at late times. This is similar to what one should do for a proper calculation of PBH formation, where the assumption of spherical symmetry should be reasonably accurate. Notice that one should eventually sum over all the radial profiles exceeding a certain threshold. Here we simply choose a certain profile, leaving a proper investigation about PBH formation to future work.

We simply impose the conditions

$$\zeta(\tau_f, r) = \zeta_0 \exp(-k^2 r^2)\,, \tag{5.4.37}$$

and $\partial_r\zeta(\eta, r_i) = 0 = \zeta(\eta, r_f)$ where $r \in [r_i, r_f]$. As usual the condition (5.4.21) at early times has been imposed. Following the same rescaling procedure as before, we have $\zeta \to \zeta_0\zeta$, so that the condition above becomes $\zeta(\tau_f, r) = \exp(-k^2r^2)$.

Now let us proceed with the PDE. Given spherical symmetry eq. (5.4.12) takes the form,

$$-\zeta'' + \frac{2}{\tau}\zeta' - \frac{1}{r^2}\frac{\partial}{\partial r}\left(r^2\frac{\partial\zeta}{\partial r}\right) - \frac{\tilde{\lambda}}{2}\tau^2\zeta'^2\zeta'' = 0\,. \tag{5.4.38}$$

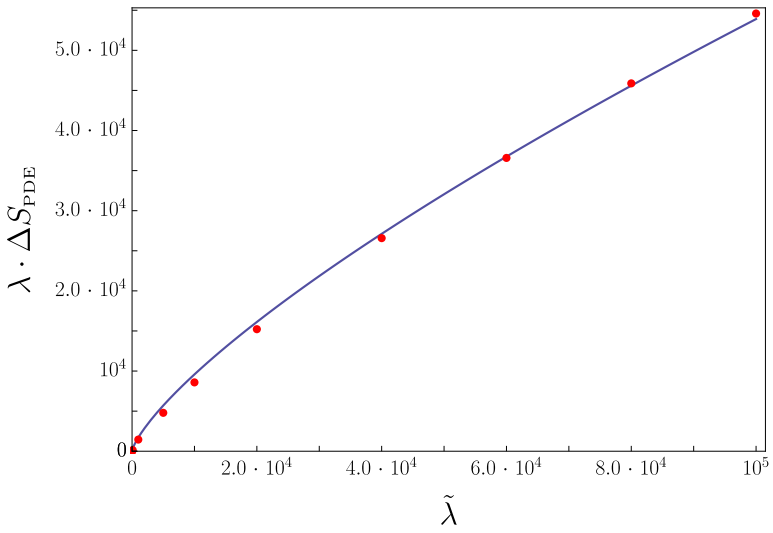

Figure 22: The function $F(\tilde{\lambda}) = \lambda \cdot \Delta S_{\rm PDE}$ for the sinusoidal case. The blue curve shows the best fit of $\lambda \cdot \Delta S_{\rm PDE}$ (red points), proportional to $\tilde{\lambda}^{3/4}$.

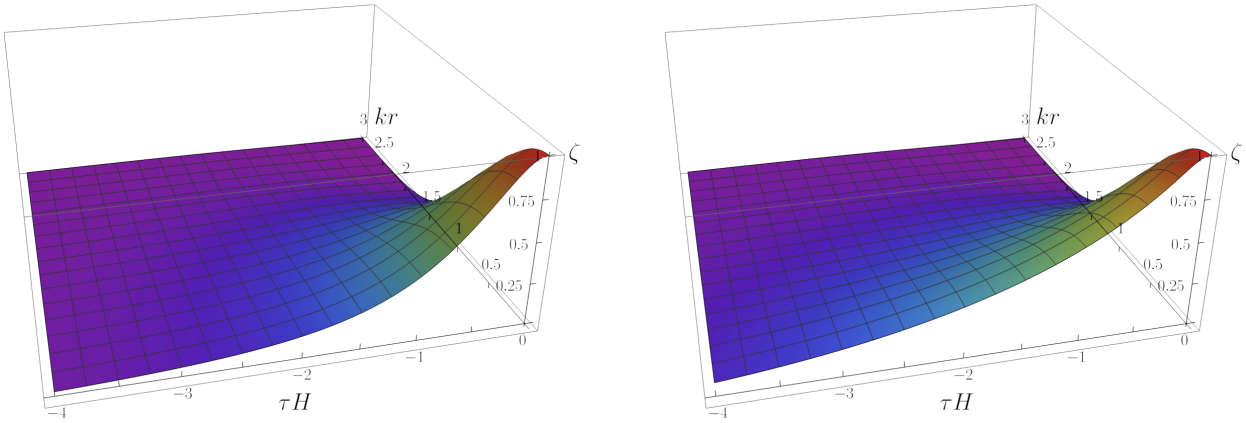

(a) (b)

Figure 23: Numerical solutions with Gaussian boundary condition at late times for $\tilde{\lambda} = 0$ (left panel, figure 23a) and $\tilde{\lambda} = 200$ (right panel, figure 23b).

The numerical solutions are shown in Figures 23a and 23b for $\tilde{\lambda} = 0$ and $\tilde{\lambda} = 200$, respectively. (We chose $H\tau_i = -80$, $H\tau_f = -0.001$. The value of r_f has to be sufficiently large to capture the decay of the Gaussian far from the center.)

Like in the previous case, the finite part of the action $\Delta S_{\rm PDE}$ reads

$$\Delta S_{\rm PDE} = -\frac{\zeta_0^2}{P_\zeta}\int_{\tau_i}^{\tau_f} d\tau \int_{r_i}^{r_f} dr\, r^2 \left\{ \frac{1}{2\tau^2}\left[\zeta'^2 + (\partial_r\zeta)^2 - 4k^4 r^2 e^{-2k^2r^2}\right] + \frac{\tilde{\lambda}}{4!}\zeta'^4 \right\} = \frac{1}{\lambda} F(\tilde{\lambda})\,. \tag{5.4.39}$$

As before, we subtracted the late-time value of $(\partial_r\zeta)^2$, i.e. $4k^4r^2e^{-2k^2r^2}$, from the full action to get rid of the divergent piece at late times. We now perform the integral in (5.4.39) numerically on the solutions for $\tilde{\lambda} = 0$ up to $\tilde{\lambda} = 10^5$. We then again plot in Figure 24 the numerical value of

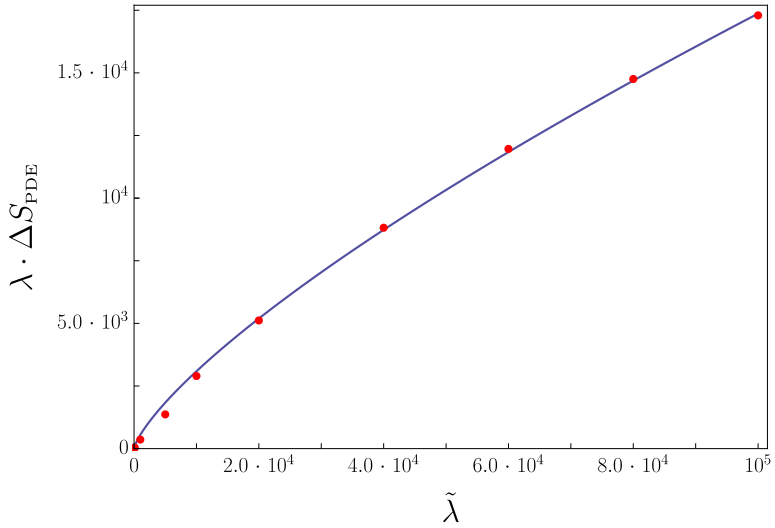

Figure 24: The function $F(\tilde{\lambda}) = \lambda \cdot \Delta S_{\rm PDE}$ for the Gaussian case. The blue curve shows the best fit of $\lambda \cdot \Delta S_{\rm PDE}$ (red points), proportional to $\tilde{\lambda}^{3/4}$.

$F(\tilde{\lambda}) = \lambda \cdot \Delta S_{\rm PDE}$ as a function of $\tilde{\lambda}$. As expected, the asymptotic behavior of $F(\tilde{\lambda})$ fits very well with $\tilde{\lambda}^{3/4}$, in agreement with the ODE result (5.4.24).

5.5 ANALYTIC CONTINUATION TO EUCLIDEAN TIME

The analysis of the previous Sections relies on the analytic continuation of the action in η. This continuation corresponds to a rotation of the contour of integration as in Figure 25. After this rotation one has a negative-definite metric

$$ds^2 = -\frac{1}{H^2\tau^2}(d\tau^2 + d\mathbf{x}^2)\,, \tag{5.5.1}$$

which we dub $-\text{EAdS}_4$ (for a related discussion see [136, 137]). (We will only comment at the end about the possibility of further continuing this to Euclidean AdS, EAdS_4, with an analytic continuation of the Hubble radius $H \to -i/L$, where L is the EAdS_4 radius.)

In this Section we would like to justify this analytic continuation by proving that the classical trajectory, and thus the Lagrangian, are analytic in the upper-left quadrant of the complex-η plane. The proof holds at any order of tree-level perturbation theory, i.e. for the diagrams we are resumming in the semiclassical expansion. As in the previous Sections we consider the geometry as unperturbed. This implies that the integral that gives the action and then the WFU can indeed be rotated from dS_4 to its Euclidean version, $-\text{EAdS}_4$, without encountering singularities. Towards the end of the Section we give a plausible non-perturbative argument for analyticity.

As already emphasized, the Lagrangian has a pole at $\eta = 0$ so that there is a contribution of Γ_ε in Figure 25. This pole is due to the quadratic part of $\mathcal{L}$ and gives a divergent contribution to the integral $\propto 1/\tau_f = -i/\eta_f$, see the discussion below eq. (5.4.18). This is only a phase in the WFU

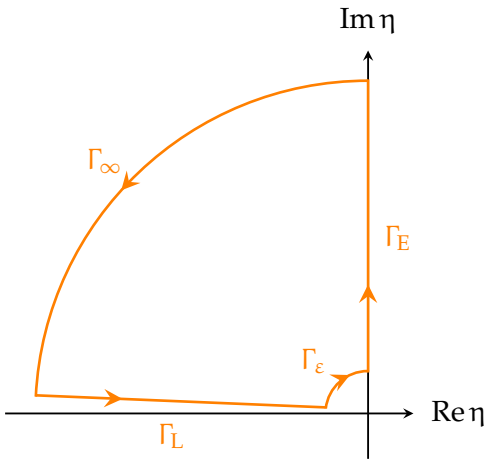

Figure 25: Complex contour for the evaluation of the action. The Lorentzian action (dS_4) is obtained integrating along Γ_L (notice the $i\epsilon$ prescription) while the Euclidean action ($-EAdS_4$) along $-\Gamma_E$. The large semicircle Γ_∞ goes to zero for large radii because of the Bunch-Davies vacuum condition. The small circle Γ_ε contains a singularity as $\eta_f \to 0$.

and it does not affect the statistical properties of ζ. From now we assume that this divergent part is removed (see the discussion below eq. (5.4.23)) and the integral can be extended to the origin. Provided that ζ is analytic for $\mathrm{Re}\,\eta < \eta_f < 0$, $\mathrm{Im}\,\eta > 0$, the Lagrangian is also analytic in the same domain (we assume it is an analytic function of derivatives of ζ). Hence, our goal is to show that, at any order in perturbation theory in some coupling λ, the classical solution with fixed boundary conditions at $\eta = \eta_f$ for ζ remains analytic.

We start by writing the formal classical solution for ζ in dS_4, with Bunch-Davies vacuum conditions for $\eta \to -\infty$ and Dirichlet boundary conditions at late times: $\zeta(\eta_f, \mathbf{k}) = \zeta_0(\mathbf{k})$. Given a generic interaction term in the action S_{int}, $\zeta(\eta, \mathbf{k})$ reads

$$\zeta(\eta, \mathbf{k}) = K(\eta, \mathbf{k})\zeta_0(\mathbf{k}) + \int_{-\infty(1-i\epsilon)}^{\eta_f} G(\eta, \eta'; \mathbf{k}) \frac{\delta S_{int}}{\delta \zeta(\eta', \mathbf{k})}\, d\eta' \,, \tag{5.5.2}$$

where $K(\eta, \mathbf{k})$ is the *bulk-to-boundary* propagator and $G(\eta, \eta'; \mathbf{k})$ is the *bulk-to-bulk* propagator (see for instance [134]). For a massless scalar in dS_4 they read

$$K(\eta, \mathbf{k}) = \frac{(1 - ik\eta)}{(1 - ik\eta_f)} e^{ik(\eta - \eta_f)} \,, \tag{5.5.3}$$

and

$$G(\eta, \eta'; \mathbf{k}) = \frac{-iH^2}{2k^3} \left[\theta(|\eta'| - |\eta|)\phi_+(\eta')\phi_-(\eta) + \theta(|\eta| - |\eta'|)\phi_+(\eta)\phi_-(\eta') - \frac{\phi_-(\eta_f)}{\phi_+(\eta_f)} \phi_+(\eta')\phi_+(\eta) \right] \,, \tag{5.5.4}$$

where θ is the step function and $\phi_-(\eta)$, $\phi_+(\eta)$ are the wave-modes solving the free equation of motion

$$\phi_-(\eta) \equiv (1 + ik\eta)e^{-ik\eta} \,, \quad \phi_+(\eta) \equiv (1 - ik\eta)e^{ik\eta} \,. \tag{5.5.5}$$

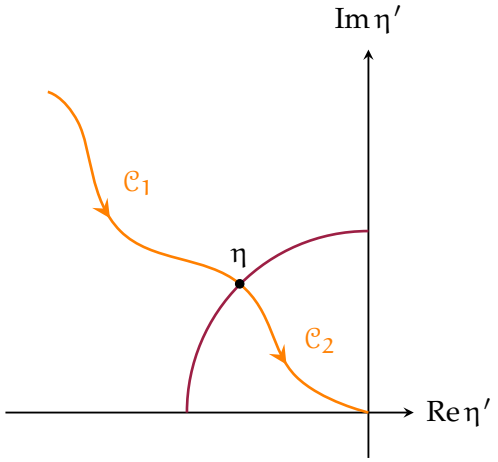

Figure 26: In orange, the complex contour for the integral in eq. (5.5.2). The red line indicates the points where $G(\eta, \eta'; \mathbf{k})$ is discontinuous.

Expression (5.5.2) is a formal solution that can be used iteratively to obtain corrections to ζ as a power series in the coupling λ. Indeed, by evaluating the source $S(\eta', \mathbf{k}) \equiv \delta S_{\rm int}/\delta\zeta(\eta', \mathbf{k})$ at order n in λ, we can obtain the solution for ζ at order $n+1$ by evaluating the right-hand side of eq. (5.5.2). Such perturbative iteration corresponds to an expansion in tree-level Witten diagrams (with an increasing number of legs connected to the boundary).

We can proceed by induction. We will start by assuming that the source term $S(\eta', \mathbf{k})$ is analytic at order n in the perturbative expansion in λ. Then, we will argue that the solution for ζ at order $n+1$ is also analytic. Since the zeroth-order solution for ζ, given by $\zeta^{(0)}(\eta, \mathbf{k}) = K(\eta, \mathbf{k})\zeta_0(\mathbf{k})$, is manifestly analytic this will prove that ζ remains analytic at any order.

In order to show analyticity, we need to properly extend eq. (5.5.2) to complex-η values. Assuming analyticity for the source $S(\eta', \mathbf{k})$, the only difficulty resides in the propagator $G(\eta, \eta'; \mathbf{k})$, which displays a discontinuity in the complex-η' plane when $|\eta| = |\eta'|$ with $\arg\eta \neq \arg\eta'$. Note however that $G(\mathbf{k}; \eta, \eta')$ is analytic in η and η' in the two regions $|\eta| > |\eta'|$ and $|\eta| < |\eta'|$.

Because of these properties, we can extend eq. (5.5.2) to complex η by choosing a proper contour of integration in η' for the integral on the right-hand side. As shown in Figure 26, we pick a path $\mathcal{C}_1$ going from infinity (in the upper-left quadrant) to η, and then a second path $\mathcal{C}_2$ from η to 0. The explicit expression for ζ for complex η, in terms of the wave-modes, is then

$$\zeta(\eta, \mathbf{k}) = K(\eta, \mathbf{k})\zeta_0(\mathbf{k}) - \frac{iH^2}{2k^3}\left[\phi_-(\eta)\int_{\mathcal{C}_1}\phi_+(\eta')S(\eta', \mathbf{k})d\eta' + \phi_+(\eta)\int_{\mathcal{C}_2}\phi_-(\eta')S(\eta', \mathbf{k})d\eta' - \phi_+(\eta)\int_{\mathcal{C}_1\cup\mathcal{C}_2}\phi_+(\eta')S(\eta', \mathbf{k})d\eta'\right]. \tag{5.5.6}$$

Because of the decaying properties of the Green functions in eqs. (5.5.3) and (5.5.4), the integrals are convergent and the solution is overall exponentially decaying at infinity, as expected. Due to Cauchy's theorem, the paths $\mathcal{C}_1$ and $\mathcal{C}_2$ can be chosen arbitrarily (as long as they do not cross the

$|\eta'| = |\eta|$ and they remain in the upper-left quadrant) and therefore the integral over η' will depend on η but not on its complex conjugate η^*, as a consequence of the fundamental theorem of calculus. This means that the result is holomorphic ($\partial_{\eta^*}\zeta = 0$). Finally, in order to prove analyticity, we only need to show that $\partial_\eta\zeta$ exists everywhere. This is the case, as we can see by direct inspection

$$\begin{aligned}\partial_\eta\zeta(\eta,\mathbf{k}) = \partial_\eta K(\eta,\mathbf{k})\zeta_0(\mathbf{k}) - \frac{iH^2}{2k^3}\Big[&\partial_\eta\phi_-(\eta)\int_{\mathcal{C}_1}\phi_+(\eta')S(\eta',\mathbf{k})d\eta' \\ &+ \partial_\eta\phi_+(\eta)\int_{\mathcal{C}_2}\phi_-(\eta')S(\eta',\mathbf{k})d\eta' - \partial_\eta\phi_+(\eta)\int_{\mathcal{C}_1\cup\mathcal{C}_2}\phi_+(\eta')S(\eta',\mathbf{k})d\eta'\Big] .\end{aligned} \tag{5.5.7}$$

This shows that indeed ζ is analytic, as claimed.

Additionally, it is easy to realize that this choice of the contour is the correct one since ζ then satisfies its classical equation of motion, even for η complex. Therefore, when η is purely imaginary (with positive imaginary part), ζ reduces to the correct $-\text{EAdS}_4$ classical solution. This can be checked by noticing that, in this case, one can take the two paths $\mathcal{C}_1$ and $\mathcal{C}_2$ to belong to the imaginary η' axis. Hence, in eq. (5.5.6) we can simply replace $\eta \to iz$, $\eta' \to iw$, with $z, w \in \mathbb{R}_+$. The bulk-to-boundary propagator and the two wave-modes of eqs. (5.5.3) and (5.5.5) map to their $-\text{EAdS}_4$ counterparts ($K_{dS}(iz,\mathbf{k}) = K_{-\text{EAdS}}(z,\mathbf{k})$, $\phi_+(iz) = \phi_+^{-\text{EAdS}}(z)$ and $\phi_-(iz) = \phi_-^{-\text{EAdS}}(z)$), whereas the bulk-to-bulk propagator picks up a phase ($G_{dS}(iz,iw;\mathbf{k}) = iG_{-\text{EAdS}}(z,w;\mathbf{k})$), as we see from its expression eq. (5.5.4). This factor of i then combines with the measure of integration in eq. (5.5.6) so to obtain the correct formal solution for ζ in $-\text{EAdS}_4$.[11] (Notice also that, by further rotating $H \to -i/L$, our expressions in $-\text{EAdS}_4$ maps to the expressions to EAdS_4. See [134] for a dictionary between dS_4 and EAdS_4. We will comment more about this point below.)

This concludes the proof of why we can analytically rotate to $-\text{EAdS}$. At this point we want to give an argument about analyticity when we treat interactions non-perturbatively in the couplings. In particular, we focus on the case where the EoM can be approximated by an ODE. Formally speaking, our discussion only applies to QM but, as we saw for the model $\lambda\dot{\zeta}^4$, an ODE can be a good approximation for the behavior of ζ. It looks quite challenging to have a rigorous proof in the case of the PDE. Further, we assume that a solution to the boundary-value problem for our ODE exists. Given this solution, we can think of our problem as an initial-value problem by computing the value of $\dot{\zeta}$ at early times and using it as an initial condition. By doing so, we are now allowed to apply standard results in the theory of ODEs.

This ODE can be written as a first-order system of equations that we study in the full complex plane, schematically of the form $\dot{x}(\tau) = f(x,\tau;\lambda)$[12], where τ is a complex-time variable and λ is a generic coupling of the theory. Let us assume in the following that $f(x,\tau;\lambda)$ is an analytic function

11 When going to Euclidean one should also consider the rotation of the background solution, which is time dependent. This will induce some extra phases in the coefficient of some of the π interactions.

12 In QM, the EoM $\ddot{x} = -V'(x)$ can be converted to a first order form by defining $y \equiv \dot{x}$. The equation then takes the form of a 2-dimensional system $\dot{x} = y$, $\dot{y} = -V'(x)$. For simplicity we schematically write the system as a single equation since our conclusions would not change.

on all its three variables.[13] If this is the case, then it follows that around any point τ_0, $x(\tau)$ can be written as an analytic series in $\tau - \tau_0$, with radius of convergence determined by $|f|$ (see e.g. [138]). This fact implies that the solution will be analytic at every point where $|f|$ is bounded. From this observation we conclude that $x(\tau)$ is also analytic, except in the cases where this solution probes regions of the potential infinitely far away, where $|f|$ is expected to diverge. (Given that f is analytic by assumption, it must be unbounded in some direction, otherwise it would be a constant.) By gluing together these local solutions we expect that the overall solution is also analytic, with no obstacle for analytic continuation. In the case of the anharmonic oscillator the non-linear solution eq. (5.2.13) is indeed analytic in the quadrant of interest, since the function $1/\sinh$ has poles only for imaginary τ, i.e. for real time t and these are avoided in the Lorentzian calculation by the $i\epsilon$ prescription. Notice also that the solution decays for large radius in the quadrant of interest.

Let us finally comment on the rotation to $EAdS_4$. This continuation involves, on top of the rotation of η, also a rotation of Hubble $H \to -i/L$. It seems difficult that this rotation can be done at full non-perturbative level. Indeed many couplings of the theory depend on H so that analyticity in this parameter is similar to analyticity in the couplings λ of the theory. A standard result in ODEs shows that $x(\tau)$ is an entire function of λ for any fixed τ, provided that the initial conditions for x and $\dot{x}$ are λ-independent. However we have here a boundary value problem and this may create non-analyticity. This happens for instance in the case of the anharmonic oscillator discussed above. Let us choose the origin of τ in eq. (5.2.13) in such a way that the solution sits at x_f at $\tau = 0$ (we remind the definition $\bar{x}^2 \equiv 2\lambda x_f^2/d^2$):

$$x(\tau) = -\frac{d}{\sqrt{2\lambda}} \frac{1}{\sinh(\omega\tau - \operatorname{arcsinh}(1/\bar{x}))} = \frac{x_f}{\cosh(\omega\tau)} \frac{1}{1 - \sqrt{1+\bar{x}^2}\tanh(\omega\tau)} \,. \tag{5.5.8}$$

(Notice that for $\bar{x} \ll 1$ the solution reduces to $x_f e^{\omega\tau}$.) We see that one can rotate the solution from positive to negative λ only if $|\lambda|$ is small enough. When $2\lambda x_f^2/d^2 < -1$ the square root becomes imaginary and indeed it is easy to realize one cannot find a solution in this regime. The point of transition corresponds to $\bar{x} = -1$, which is the point where the action eq. (5.2.14) reaches a branch point. This shows that in general one cannot expect analyticity in λ. Actually the full series in λ has zero radius of convergence, following Dyson's argument [139], while the series we are resumming, $(\lambda x_f^2/d^2)^n$, has a finite radius.

The rotation to $EAdS_4$ surely works at tree-level [140]: this can be seen using the perturbative argument we gave in the first part of this Section upon continuation of H. However it is probably not correct at the non-perturbative level as already suggested in [140].[14]

13 In the case of the ODE of Section 5.4.3, the function f has a singularity around a time η_0 where $1 + \tilde{\lambda}\eta_0^2\zeta'^2(\eta_0) = 0$. We do not think however this is an obstacle to rotation: one can readily check that around η_0, $\zeta(\eta)$ admits a series expansions without singularities.

14 We thank V. Gorbenko and L. Di Pietro for discussions about this point.

5.6 DISCUSSION AND FUTURE DIRECTIONS

The standard perturbation-theory approach to inflationary non-Gaussianity fails when one is interested in very unlikely events, on the tail of the probability distribution, like for instance in the case of PBHs. We showed that in this case one has to resort to semiclassical methods, approximating the wavefunction of the Universe with a non-linear saddle point, i.e. a non-linear solution of the (Euclidean) classical equations of motion. In this Chapter we explained the general logic of the approach and we applied it to a specific interaction of single-field inflation, $\propto \lambda\dot{\zeta}^4$. One is able to make predictions for arbitrarily large values of ζ and in particular, with a combination of analytic and numerical analyses, one is able to show that the tail of the probability distribution behaves as $\exp(-\lambda^{-1/4}\zeta^{3/2})$. The non-analytic dependence on λ makes clear that this result cannot be reproduced by perturbation theory.

This Chapter represents a first step in understanding inflation beyond perturbation theory and many directions remain open. Let us list some of them.

- On the more phenomenological side, it will be interesting to explore the effects on PBH production. One should first of all understand the impact of the various inflaton operators on the tail of the ζ distribution. In general the tail will fall slower or faster than in the Gaussian case, but one can also envisage a scenario in which the combination of various operators produces a "bump" in the distribution for large values of ζ, boosting the PBH abundance. Besides affecting the rate, one expects that going beyond perturbation theory will also change the clustering properties of PBH and therefore their merger rate [141].

- In a minimal scenario of slow-roll inflation, non-Gaussianities are slow-roll suppressed $f_{\rm NL} \sim \mathcal{O}(\epsilon, \eta)$ and the non-perturbative effects we studied are only relevant for $\zeta \gtrsim \mathcal{O}(\epsilon^{-1}, \eta^{-1})$. This is not relevant for PBHs. However, it would still be interesting to explore the unlikely tail of the wavefunction of the Universe in this minimal scenario. It is important conceptually, since we should learn how to make predictions about the initial conditions of our Universe and it also may have some impact in the study of eternal inflation [142–144]. It is not obvious what is the best strategy to approach the problem, since in this case one has to take into account the modification of the geometry. It looks challenging to derive the full non-linear action of ζ solving for the constraint variables, like one does in the standard perturbation theory approach, so one may have to resort to a direct solution of Einstein equation with prescribed boundary conditions. The same logic applies to tensor modes: the exploration of the tail of the distribution is clearly not interesting phenomenologically, but it is appealing theoretically since it is fixed by the non-linearities of General Relativity and it is intrinsic of de Sitter space. Exact solutions of gravitational waves in de Sitter [145] may be a good starting point for this problem.

- For the operator we studied in Section 5.4, $\dot{\zeta}^4$, the Euclidean non-linear solution exists for arbitrarily large values of the ζ. This does not happen for all possible operators (for instance

with the interaction $-(\partial_i\zeta)^4$). It is not clear what happens after the solution stops existing. One possibility is that one finds complex saddle solutions that dominate the path integral. In general, starting from the Lorentzian path integral it is a challenging problem to understand which saddles contribute. The scenario at hand, in which one can neglect perturbations of the geometry, may be a good place to understand how to make a more precise sense of the wavefunction of the Universe (for a recent discussion see [146]).

- Scattering amplitudes and correlation functions in the limit of large number of external legs have been studied using semiclassical methods. (See [147] for recent studies in flat space and [125, 126] in the case of inflation.) Naively, one expects that correlation functions with many legs $\langle\zeta^N\rangle$ are related to the behavior of the probability distribution on the tail. It would be nice to make this connection explicit and relate our approach with the existing literature on the subject.

- In this Chapter we studied solutions of the scalar equations of motion in dS with prescribed boundary conditions, without resorting to perturbation theory. The same kind of approach should be possible also in AdS in the context of AdS/CFT. This would correspond to study the dual CFT in the presence of a *finite* external source, without treating the source perturbatively.

Work is needed in all directions.

6

CONCLUSIONS

Over the past several decades perturbation theory (PT) has been a central framework for one to understand physics of our Universe. Yet, there are many regimes in cosmology, as we pointed out in Chapter 1, where the analysis within PT does not suffice to explain the relevant physics we are interested in. In this thesis we have studied various examples which can be divided into two parts: dark energy (DE) theories and inflation.

We first started reviewing the construction of the EFT of DE, which amounts to write down the most general action for scalar and tensor perturbations around the flat FLRW background compatible with the 3d diffeomorphism. After that, we studied the implications of the bound on c_T at LIGO/Virgo on the DE theories, which turned out to rule out a large class of beyond Horndeski theories. Interestingly, thanks to the fact that the Lorentz invariance is spontaneously broken by the cosmological background, we then studied in Section 2.3 the decay of GWs into DEs. At first approximation the decay was treated perturbatively, i.e. the decay of a single graviton into two DE fluctuations. The analysis (assuming $c_T = 1$) thus showed that the decay rate due to the quartic beyond Horndeski operator parametrized by α_H is very large compared to the typical cosmological scales at LIGO/Virgo frequencies. Obviously, this result is incompatible with the observations, leaving a very strong constraint on the parameter α_H. It is crucial to note that all the aforementioned constraints apply provided that the EFT of DE is a good description at LIGO/Virgo scales.

Having seen that, the analysis done in Chapter 2 was heavily based on PT - a single graviton decays into two DE fluctuations. However, in reality GWs emitted from the mergers are a collection of gravitons, and therefore one should take into account this coherent effect which can lead to sizable enhancements of the decay rate of GWs. (The idea is very reminiscent of the case of preheating in the early Universe.) This in fact served as the first non-perturbative regime studied in this thesis. With this idea, we then performed the analysis of the decay of GWs taking into account a large occupation number of γ in Chapter 3. More specifically, we treated the GWs as a background field for DE. It turned out that the classical equation of motion governing the evolution of π can be recast in the form of a Mathieu equation. Moreover, in the narrow-resonant regime where the amplitude of GWs is small the solution for π can be obtained analytically. The field π as we saw grows exponentially in time and results in an exponential growth of its energy density. Subsequently, the modification of GW background was computed analytically due to the back-reaction of the π solution.

Apart from the back-reaction on the GW signal, we also analyzed the importance of the non-linearities of π. It showed that in the case of quartic beyond Horndeski theories the self-couplings of π, in some certain regimes, are not big enough to halt the resonant effect, and thus the bound on the parameter α_H can be put stronger than the one obtained in the perturbative analysis. On the other hand, the cubic self-couplings of π quickly become important soon after the resonance occurs, which makes our analysis inconclusive - the resonant effect is not applicable to put a bound on α_B.

A possible way out is to perform the numerical simulations including the π non-linearities and see when exactly the resonance stops being efficient. Nevertheless, we expect that the non-linearities will significantly modify the instability bands of π and will possibly make the instability rate to become lower, leading to very mild constraints on α_B.

The analysis of the regime of large amplitude of GWs was studied in detail in Chapter 4. This is the second example of beyond PT presented in this thesis. The main point of this Chapter was to study the instabilities of π in the presence of the GW background whose amplitude is large. We found that unlike the case of non-relativistic matter and no gravity, the fluctuations π unavoidably develop both ghost and gradient instabilities. Hence, in order for the π to remain healthy the parameter α_B is required to be less than 10^{-2}. Unlike the case of narrow resonance, we do not expect to have a large modification on the GW signal, even though the instabilities occur catastrophically. Furthermore, it is also possible that the EFT for π and γ breaks down once the instabilities happen, and thus one needs to know the UV completion. We then studied in Section 4.3 a toy model of a $U(1)$ complex scalar field with the Mexican hat potential. The analysis showed that the angular mode ϕ of the IR theory features the instabilities in some particular regimes in field space, whereas all the modes in the UV are perfectly healthy. Although this example seems to suggest that the UV physics is expected to cure all the pathologies appearing in the IR, the fact that no concrete UV completion of the EFT of DE has been found gives us no clue of what will happen once the instabilities occur.

We then moved to the second part of the thesis: beyond PT in inflation. Despite the fact that physics of DE differs from the one of inflation in many ways, e.g. the Hubble scales, the common theme of this thesis of going beyond PT remains unchanged.

In Chapter 5 we studied the statistics of the tail of the distribution of inflaton fluctuations ζ. It is evident that around the peak of the distribution the statistics is well-described by a small deviation from Gaussianity - PT works extremely well in this regime. However, we pointed out that the relevant expansion parameter, as going to the tail, involves not only the usual coupling in PT, but also the value of the field itself. This implies that when ζ is of order $1/f_{NL}$ (for cubic interactions) PT breaks down and one needs to find a new treatment in order to capture physics on the tail. We then proposed that the way one should perform the calculations of the wavefunction of the Universe in the large field limit is to make use of the semiclassical approximation. This is due to the fact that the events on the tail are very unlikely which is equivalent to sending $\hbar \to 0$. For simplicity, we first considered the case of anharmonic oscillator in QM, which showed explicitly the calculation of the ground-state wavefunction in the semiclassical limit. In the last Section we then analyzed the simple toy model within the EFT of Inflation, namely the interaction ζ'^4. (The construction of the EFT of inflation is similar to the EFT of DE, except the cut-off and the Hubble scales.) The results of both ODE and PDE analyses exhibited the non-perturbative behavior of the wavefunction of the Universe: $\exp(-\lambda^{-1/4}\zeta^{3/2})$. Many questions discussed in Section 5.6 remain open; we leave these to the future work.

All the examples presented in this thesis are a recent progress in understanding the physics beyond PT in cosmology. Some of them have had the direct implications on the late Universe such

as putting a bound on the parameters of DE theories. Some of them, however, may have an impact on the early Universe such as PBH formation. Many future directions remain open as we have already pointed out at the end of each Chapter. For instance, concerning DE side it is worth exploring the instabilities of π in the presence of GWs in the higher dimensional theories of gravity, e.g. Dvali-Gabadadze-Porrati (DGP) model [148]. On the inflation side, it is phenomenologically interesting to investigate further towards the direction of PBH formation for which one scans over all the late-times configurations whose amplitude exceeds the threshold of the formation. Many work in all directions is needed.

Part III

APPENDIX

A

PARAMETRIC RESONANCE AS BOSE ENHANCEMENT

In this Appendix we want to reinterpret the exponential growth due to parametric resonance as the Bose enhancement of the perturbative decay $\gamma \to \pi\pi$. To see this, we study the Boltzmann equation for the number density of dark energy fluctuations. We denote by $n^{\pi}_{\mathbf{k}}$ and $n^{\gamma}_{\mathbf{k}}$ the occupation numbers, respectively, of π and γ. Moreover, the number density for the particle species π is defined as

$$n_{\pi} \equiv \int \frac{d^3\mathbf{k}}{(2\pi)^3} n^{\pi}_{\mathbf{k}} \,, \tag{A.0.1}$$

and an analogous definition holds for γ.

Let us consider a collection of gravitons with frequency ω, each of them decaying into two π-particles. For concreteness, we will focus on the case $c_s^2 \ll 1$, for which the two momenta of π, $\mathbf{k}$ and $-\mathbf{k}$, have opposite directions and equal magnitudes $k = \omega/(2c_s)$. Following [149] and denoting by $\Gamma_{\gamma\to\pi\pi}$ the tree-level decay rate (see e.g. (3.1.11)), the rate of change of n_{π} in a given volume V is

$$\frac{dn_{\pi}}{du} \simeq 2\frac{\Gamma_{\gamma\to\pi\pi}}{V}[(n^{\pi}_{\mathbf{k}}+1)(n^{\pi}_{-\mathbf{k}}+1)n^{\gamma}_{\omega} - n^{\pi}_{\mathbf{k}} n^{\pi}_{-\mathbf{k}}(n^{\gamma}_{\omega}+1)] \,, \tag{A.0.2}$$

where the factor of 2 accounts for two identical particles in the final state. As explained earlier in Sec. 3.2.1, for small c_s we can use u as time. On the right-hand side, we have neglected integration over the angle φ which would appear when considering only one of the GW polarizations. For $n^{\pi}_{\mathbf{k}} = n^{\pi}_{-\mathbf{k}} = n^{\pi}_{k}$ and $n^{\gamma}_{\omega} \gg \{n^{\pi}_{\mathbf{k}}, 1\}$ we find

$$\frac{dn_{\pi}}{du} \simeq 2\Gamma_{\gamma\to\pi\pi} n_{\gamma}\,(1+2n^{\pi}_{k}) \,, \tag{A.0.3}$$

where we have introduced the number density of gravitons, here given by $n_{\gamma} = n^{\gamma}_{\omega}/V$.

The produced π-particles end up populating the spherical shell $k = k_0 \pm \Delta k/2$ of radius $k_0 \simeq \omega/(2c_s)$ and thickness Δk, so that their occupation number is related to their number density by

$$n^{\pi}_{k} \simeq \frac{n_{\pi}}{4\pi k_0^2 \Delta k/(2\pi)^3} \,. \tag{A.0.4}$$

The thickness is given by comparing the time-independent part of the equation of motion for π, eq. (3.2.3), with the amplitude of its periodic part. Using $\Omega = c_s \ll 1$ valid for small c_s, we obtain

$$\Delta k = \beta k_0 \ll k_0 \,. \tag{A.0.5}$$

Plugging the expressions of k_0 and Δk into (A.0.4) and using $n_{\gamma} \simeq \omega(M_{\rm Pl}h_0^+)^2$, the occupation number can be written as

$$n^{\pi}_{k} = 4\beta c_s^7 \pi^2 \left(\frac{\Lambda}{\omega}\right)^4 \frac{n_{\pi}}{n_{\gamma}} \,, \tag{A.0.6}$$

where we have focused on the case of the operator m_3^3 (which can be straightforwardly extended to the case of the operator $\tilde{m}_4^2$ by the replacement $\Lambda^2 \to \Lambda_\star^3 \omega^{-1}$, see discussion in Sec. 3.1.2) and used the definition of β, eq. (3.1.15), to rewrite $(M_{\rm Pl} h_0^+)^2$. The Bose condensation effect becomes important for $n_k^\pi \gg 1$ or, using the above equation, for

$$n_\pi \gg \frac{n_\gamma}{4\beta c_s^7 \pi^2} \left(\frac{\omega}{\Lambda}\right)^4 . \tag{A.0.7}$$

In this case, we can solve eq. (A.0.3) with the decay rate given by eq. (3.1.11). This gives

$$n_\pi \propto \exp\left(\frac{\pi\beta}{30}\omega u\right) , \tag{A.0.8}$$

which displays an instability similar to that encountered above in eq. (3.2.27), but with a different exponent. Notice that the approach of Appendix A is approximate and does not reproduce the correct numerical factors in the timescale of the instability. Of course, a more precise calculation would give the same answer.

It is useful to check that our formula for the modification of the GW, eq. (3.2.44), smoothly interpolates with the perturbative decay result, eq. (3.1.11), when the occupation number becomes small. In the regime in which Bose enhancement is negligible $n_\pi/n_\gamma \sim \Gamma u$, see Figure 6. Using this in eq. (A.0.6) we get $n_k^\pi \sim \beta\omega u$. Not surprisingly this is the parameter that enters the exponential growth of the instability. Our saddle-point treatment is valid for $\beta\omega u \gg 1$, but we expect that, when $\beta\omega u \sim 1$, it gives a result of the same order as the perturbative decay of gravitons. Indeed if we plug this equality in eq. (3.2.44) one gets (for $c_s \ll 1$)

$$\Delta\gamma \simeq \frac{\nu}{\Lambda^2}\frac{1}{c_s^5}\beta\omega^4 \simeq M_{\rm Pl} h_0^+ \Gamma\nu . \tag{A.0.9}$$

This is indeed the perturbative result: the original GW, $M_{\rm Pl} h_0^+$, changes with a rate Γ for a time of order ν.

B

DETAILS ON THE CONSERVATION OF ENERGY

In this Appendix we check the conservation of energy discussed in Section 3.2.5 for both m_3^3- and $\tilde{m}_4^2$- operators.

B.1 m_3^3-OPERATOR

In this Section we check the energy conservation for m_3^3-operator. First of all, let us verify that GWs do not contribute to the flux of energy across $\partial\mathcal{V}_0$ (see Figure 8). This is clearly true for $\bar{\gamma}_{ij}$ but it holds at order $\Delta\gamma$ too. Indeed we have, using $\dot{\bar{\gamma}}_{ij} = -\partial_z\bar{\gamma}_{ij}$ and $\partial_k\bar{\gamma}_{ij} = \delta_{kz}\partial_z\bar{\gamma}_{ij}$,

$$\begin{aligned}\left(T^{00} - T^{z0}\right)\big|_{u=|z_0|} \supset\ & \frac{1}{4}\left[(\dot{\bar{\gamma}}_{ij})^2 + (\partial_k\bar{\gamma}_{ij})^2\right] + \frac{1}{2}\dot{\bar{\gamma}}_{ij}\partial_z\bar{\gamma}_{ij} \\ & + \frac{1}{2}\dot{\bar{\gamma}}_{ij}\Delta\dot{\gamma}_{ij} + \frac{1}{2}\partial_k\bar{\gamma}_{ij}\partial_k\Delta\gamma_{ij} + \frac{1}{2}\dot{\bar{\gamma}}_{ij}\partial_z\Delta\gamma_{ij} + \frac{1}{2}\Delta\dot{\gamma}_{ij}\partial_z\bar{\gamma}_{ij} \\ & = 0 + \frac{1}{2}\dot{\bar{\gamma}}_{ij}(\Delta\dot{\gamma}_{ij} - \partial_z\Delta\gamma_{ij}) + \frac{1}{2}\dot{\bar{\gamma}}_{ij}(\partial_z\Delta\gamma_{ij} - \Delta\dot{\gamma}_{ij}) = 0\,.\end{aligned} \tag{B.1.1}$$

Let us now calculate the LHS of eq. (3.2.60), *i.e.* the variation of the total energy in the region. This is only due to $\Delta\gamma_{ij}$, since π and $\bar{\gamma}_{ij}$ depend on u only. One has

$$\begin{aligned}T^{00} \supset\ & \frac{1}{2}\dot{\bar{\gamma}}_{ij}\Delta\dot{\gamma}_{ij} + \frac{1}{2}\partial_k\bar{\gamma}_{ij}\partial_k\Delta\gamma_{ij} = \frac{1}{2}\dot{\bar{\gamma}}_{ij}\left(\Delta\dot{\gamma}_{ij} - \partial_z\Delta\gamma_{ij}\right) = \frac{1}{2}\dot{\bar{\gamma}}_{ij}2\partial_u\Delta\gamma_{ij} \\ & = -\dot{\bar{\gamma}}_{ij}\left(\frac{\nu}{4\Lambda^2}\partial_u J_{ij}(u)\right) = -\dot{\bar{\gamma}}_{ij}\epsilon^+_{ij}\left(\frac{\nu}{4\Lambda^2}\partial_u\left\langle(\partial_x\pi)^2 - (\partial_y\pi)^2\right\rangle\right) \equiv \nu\mathcal{F}(u)\,.\end{aligned} \tag{B.1.2}$$

The integral over $\partial\mathcal{V}_2 \cup \partial\mathcal{V}_1$ reduces to

$$\begin{aligned}&\int_{\partial\mathcal{V}_2} T^{00}\,dz - \int_{\partial\mathcal{V}_1} T^{00}\,dz = \int_{T-|z_0|}^{T} \nu\mathcal{F}(u)\big|_{t=T}\,dz - \int_{-|z_0|}^{0} \nu\mathcal{F}(u)\big|_{t=0}\,dz = \\ &\int_{T-|z_0|}^{T}(T+z)\mathcal{F}(T-z)\,dz - \int_{-|z_0|}^{0} z\mathcal{F}(-z)\,dz = \int_{-|z_0|}^{0}(2T+\tilde{z})\mathcal{F}(-\tilde{z})\,d\tilde{z} - \int_{-|z_0|}^{0} z\mathcal{F}(-z)\,dz \\ &= 2T\int_{-|z_0|}^{0}\mathcal{F}(-z)\,dz\,.\end{aligned} \tag{B.1.3}$$

The RHS of eq. (3.2.60) gets contribution only from π:

$$\int_{\partial\mathcal{V}_0}\left(T^{00} - T^{z0}\right)dt = \int_0^T \left(T^{00}_\pi - T^{z0}_\pi\right)\big|_{u=|z_0|}dt = T\left(T^{00}_\pi - T^{z0}_\pi\right)\big|_{u=|z_0|}\,. \tag{B.1.4}$$

The equation for energy conservation, eq. (3.2.60), becomes

$$0 = T\left(T^{00}_\pi - T^{z0}_\pi\right)\big|_{u=|z_0|} + 2T\int_{-|z_0|}^{0}\mathcal{F}(-z)\,dz \tag{B.1.5}$$

$$= T\left[\left(T^{00}_\pi - T^{z0}_\pi\right)\big|_{u=|z_0|} - \frac{1}{2\Lambda^2}\int_0^{|z_0|}\dot{\bar{\gamma}}_{ij}(u)\epsilon^+_{ij}\partial_u\left\langle(\partial_x\pi)^2 - (\partial_y\pi)^2\right\rangle\,du\right]\,. \tag{B.1.6}$$

Note that the linear v dependence of $\Delta\gamma$ is essential: if it was not the case then the two terms in (B.1.6) would have a different T dependence, with no chance of adding up to zero. To explicitly check energy conservation one should integrate (B.1.6). A faster way to check this is to take a derivative with respect to $|z_0|$ (or equivalently u). The resulting equation can be shown to be satisfied by the solution for π, (3.2.13). After simplifying T and taking the derivative with respect to z_0, (B.1.6) becomes

$$\partial_u \left[\langle T^{00}_\pi(u)\rangle - \langle T^{z0}_\pi(u)\rangle\right] - \frac{1}{2\Lambda^2}\dot{\gamma}_{ij}(u)\epsilon^+_{ij}\partial_u\left\langle(\partial_x\pi)^2-(\partial_y\pi)^2\right\rangle = 0\,. \tag{B.1.7}$$

The expression of $\langle T^{00}_\pi\rangle$ is given by eq. (3.2.17) while

$$\langle T^{z0}_\pi(u)\rangle = -c_s^2\left\langle\dot{\pi}\partial_z\pi\right\rangle = -\int\frac{d^3\tilde{\mathbf{p}}}{(2\pi)^3}\frac{1}{4c_s^2p_u}\left[-2c_s^2|\partial_u f_{\tilde{\mathbf{p}}}|^2 - 2p_s^2|f_{\tilde{\mathbf{p}}}|^2 + \text{const}\right]\,. \tag{B.1.8}$$

Therefore we can write

$$\partial_u\left[\langle T^{00}_\pi(u)\rangle - \langle T^{z0}_\pi(u)\rangle\right] = \int\frac{d^3\tilde{\mathbf{p}}}{(2\pi)^3}\frac{1}{4c_s^2p_u}\left[\partial_u f^\star_{\tilde{\mathbf{p}}}\left((1-c_s^2)\partial_u^2 f_{\tilde{\mathbf{p}}} + f_{\tilde{\mathbf{p}}}\left((1-c_s^2)c_s^{-2}p_s^2 + c_s^2(p_x^2+p_y^2)\right)\right) + \text{h.c.}\right]. \tag{B.1.9}$$

The remaining term contains

$$\partial_u\left\langle(\partial_x\pi)^2-(\partial_y\pi)^2\right\rangle = \partial_u\int\frac{d^3\tilde{\mathbf{p}}}{(2\pi)^3}\frac{1}{4c_s^2p_u}2(p_x^2-p_y^2)|f_{\tilde{\mathbf{p}}}|^2 = \int\frac{d^3\tilde{\mathbf{p}}}{(2\pi)^3}\frac{1}{4c_s^2p_u}2(p_x^2-p_y^2)f^{\star\prime}_{\tilde{\mathbf{p}}}f_{\tilde{\mathbf{p}}} + \text{h.c.} \tag{B.1.10}$$

At this point by adding up these contributions we can collect the terms with $\partial_u f^\star_{\tilde{\mathbf{p}}}$. They are

$$\partial_u f^\star_{\tilde{\mathbf{p}}}\left[(1-c_s^2)\partial_u^2 f_{\tilde{\mathbf{p}}} + f_{\tilde{\mathbf{p}}}\left((1-c_s^2)c_s^{-2}p_s^2 + c_s^2(p_x^2+p_y^2) - \frac{1}{\Lambda^2}\dot{\gamma}^b_{ij}(u)\epsilon^+_{ij}(p_x^2-p_y^2)\right)\right] + \text{h.c.} \tag{B.1.11}$$

This equation is solved by $f_{\tilde{\mathbf{p}}}$: this is easily seen by comparing with equation (3.2.13).

B.2 $\tilde{m}^2_4$-OPERATOR

In this Section we are going to use the same logic as the one in the previous Section to verify the conservation of energy for $\tilde{m}^2_4$-operator. According to the Lagrangian (3.1.16), the components of the energy-momentum tensor are given by

$$T^0_0 = -\left[\frac{1}{4}\dot{\gamma}^2_{ij} + \frac{1}{4}(\partial_k\gamma_{ij})^2 + \frac{1}{2}\dot{\pi}^2 + \frac{1}{2}c_s^2(\partial_i\pi)^2 - \frac{2}{\Lambda^3_\star}\dot{\gamma}_{ij}\partial_i\dot{\pi}\partial_j\pi\right]\,, \tag{B.2.1}$$

$$T^0_i = -\frac{1}{2}\dot{\gamma}_{kl}\partial_i\gamma_{kl} - \dot{\pi}\partial_i\pi + \frac{2}{\Lambda^3_\star}\partial_i\gamma_{kl}\partial_k\dot{\pi}\partial_l\pi - \frac{1}{\Lambda^3_\star}\partial_i\dot{\gamma}_{kl}\partial_k\pi\partial_l\pi\,, \tag{B.2.2}$$

$$T^i_0 = \frac{1}{2}\dot{\gamma}_{kl}\partial_i\gamma_{kl} + c_s^2\dot{\pi}\partial_i\pi - \frac{2}{\Lambda^3_\star}\ddot{\gamma}_{ij}\dot{\pi}\partial_j\pi\,, \tag{B.2.3}$$

$$\begin{aligned}T^i_j = {}& \frac{1}{2}\partial_i\gamma_{kl}\partial_j\gamma_{kl} + c_s^2\partial_i\pi\partial_j\pi - \frac{2}{\Lambda^3_\star}\ddot{\gamma}_{ik}\partial_j\pi\partial_k\pi \\ & + \frac{1}{2}\delta^i_j\left[\frac{1}{2}\dot{\gamma}^2_{kl} - \frac{1}{2}(\partial_m\gamma_{kl})^2 + \dot{\pi}^2 - c_s^2(\partial_l\pi)^2 + \frac{2}{\Lambda^3_\star}\ddot{\gamma}_{kl}\partial_k\pi\partial_l\pi\right]\,.\end{aligned} \tag{B.2.4}$$

Notice that there is an extra term in T^0_0 due to the interaction $\gamma\pi\pi$, unlike the case of m_3^3-operator. Since this new piece is second order in π, it can be approximated as $-\frac{2}{\Lambda_\star^3}\dot{\bar{\gamma}}_{ij}\partial_i\dot{\pi}\partial_j\pi$.

Let us first consider the RHS of (3.2.60), taking into account that $\dot{\bar{\gamma}}_{ij} = -\partial_z\bar{\gamma}_{ij}$ and $\partial_k\bar{\gamma}_{ij} = \delta_{kz}\partial_z\bar{\gamma}_{ij}$,

$$\begin{aligned}\int_{\partial\mathcal{V}_0}\left(T^{00}-T^{z0}\right)\big|_{u=|z_0|} &= T\left(\frac{1}{2}\dot{\pi}^2+\frac{c_s^2}{2}(\partial_k\pi)^2+c_s^2\dot{\pi}\partial_z\pi-\frac{2}{\Lambda_\star^3}\dot{\bar{\gamma}}_{ij}\partial_i\dot{\pi}\partial_j\pi\right)_{u=|z_0|}\\ &\equiv T\left(T^{00}_\pi-T^{z0}_\pi-\frac{2}{\Lambda_\star^3}\dot{\bar{\gamma}}_{ij}\partial_i\dot{\pi}\partial_j\pi\right)_{u=|z_0|}\,,\end{aligned}\tag{B.2.5}$$

where all terms involving only GWs added up to zero because of eq. (B.1.1). The LHS of (3.2.60) gets contributions only from $\Delta\gamma_{ij}$, as for the m_3^3-operator case. We have

$$T^{00}\supset\dot{\bar{\gamma}}_{ij}\left(\frac{\nu}{4\Lambda_\star^3}\partial_u^2 J_{ij}(u)\right)=\dot{\bar{\gamma}}_{ij}\epsilon^+_{ij}\left(\frac{\nu}{4\Lambda_\star^3}\partial_u^2\left\langle(\partial_x\pi)^2-(\partial_y\pi)^2\right\rangle\right)\equiv\nu\tilde{\mathcal{F}}(u)\,.\tag{B.2.6}$$

Integrating T^{00} over $\partial\mathcal{V}_2\cup\partial\mathcal{V}_1$ gives

$$\int_{\partial\mathcal{V}_2}T^{00}\,dz-\int_{\partial\mathcal{V}_1}T^{00}\,dz=2T\int_{-|z_0|}^0\tilde{\mathcal{F}}(-z)\,dz\,,\tag{B.2.7}$$

similarly to eq. (B.1.3). Using (B.2.5) and (B.2.7), eq. (3.2.60) becomes

$$\begin{aligned}0&=T\left(T^{00}-T^{z0}\right)\big|_{u=|z_0|}+2T\int_{-|z_0|}^0\tilde{\mathcal{F}}(-z)\,dz\\ &=T\left[\left(T^{00}_\pi-T^{z0}_\pi-\frac{2}{\Lambda_\star^3}\dot{\bar{\gamma}}_{ij}\partial_i\dot{\pi}\partial_j\pi\right)_{u=|z_0|}+\frac{1}{2\Lambda_\star^3}\int_0^{|z_0|}\dot{\bar{\gamma}}_{ij}(u)\epsilon^+_{ij}\partial_u^2\left\langle(\partial_x\pi)^2-(\partial_y\pi)^2\right\rangle\,du\right]\,.\end{aligned}\tag{B.2.8}$$

Like in the previous Section, one can verify this equation by taking a derivative with respect to $|z_0|$ (or equivalently u):

$$\partial_u\left[\langle T^{00}_\pi(u)\rangle-\langle T^{z0}_\pi(u)\rangle\right]-\frac{1}{\Lambda_\star^3}\ddot{\bar{\gamma}}_{ij}(u)\epsilon^+_{ij}\partial_u\left\langle(\partial_x\pi)^2-(\partial_y\pi)^2\right\rangle=0\,.\tag{B.2.9}$$

As we have shown before, the first term of LHS can be expressed as

$$\partial_u\left[\langle T^{00}_\pi(u)\rangle-\langle T^{z0}_\pi(u)\rangle\right]=\int\frac{d^3\tilde{\mathbf{p}}}{(2\pi)^3}\frac{1}{4c_s^2p_u}\left[\partial_u f^\star_{\tilde{\mathbf{p}}}\left((1-c_s^2)\partial_u^2 f_{\tilde{\mathbf{p}}}+f_{\tilde{\mathbf{p}}}\left((1-c_s^2)c_s^{-2}p_s^2+c_s^2(p_x^2+p_y^2)\right)\right)+\text{h.c.}\right]\,.\tag{B.2.10}$$

Similarly, the second term can be rewritten as

$$-\frac{1}{\Lambda_\star^3}\ddot{\bar{\gamma}}_{ij}(u)\epsilon^+_{ij}\partial_u\left\langle(\partial_x\pi)^2-(\partial_y\pi)^2\right\rangle=-\frac{1}{\Lambda_\star^3}\ddot{\bar{\gamma}}_{ij}(u)\epsilon^+_{ij}\int\frac{d^3\tilde{\mathbf{p}}}{(2\pi)^3}\frac{1}{4c_s^2p_u}2(p_x^2-p_y^2)f^{\star\prime}_{\tilde{\mathbf{p}}}f_{\tilde{\mathbf{p}}}+\text{h.c.}\tag{B.2.11}$$

Adding up (B.2.10) and (B.2.11) together one therefore obtains

$$\partial_u f^\star_{\tilde{\mathbf{p}}}\left[(1-c_s^2)\partial_u^2 f_{\tilde{\mathbf{p}}}+f_{\tilde{\mathbf{p}}}\left((1-c_s^2)c_s^{-2}p_s^2+c_s^2(p_x^2+p_y^2)-\frac{1}{\Lambda_\star^3}\ddot{\gamma}^b_{ij}(u)\epsilon^+_{ij}(p_x^2-p_y^2)\right)\right]+\text{h.c.}\tag{B.2.12}$$

This coincides with the equation of motion for $f_{\tilde{\mathbf{p}}}$, which can be obtained by expanding eq. (3.1.20) in Fourier modes.

C

INTERACTIONS IN SPATIALLY-FLAT GAUGE

In this Appendix we are going to derive the interactions $\gamma\pi\pi$ and $\gamma\gamma\pi$ in spatially-flat gauge.

C.1 THE INTERACTION $\gamma\pi\pi$

In this Section we are interested in redoing the computation of Section 3.1.1 in the spatial-flat gauge. Here the metric is written in the general decomposition (see e.g. [150])

$$ds^2 = -(1+\delta N)^2 d\tilde{t}^2 + a(\tilde{t})^2 (e^{\tilde{\gamma}})_{ij} (d\tilde{x}^i + \tilde{N}^i d\tilde{t})(d\tilde{x}^j + \tilde{N}^j d\tilde{t}) \tag{C.1.1}$$

with $\tilde{\gamma}_{ij}$ being transverse, $\tilde{\partial}_i \tilde{\gamma}_{ij} = 0$, and traceless $\delta_{ij}\tilde{\gamma}_{ij} = 0$. The shift vectors $\tilde{N}_i$ can be decomposed as $\tilde{N}_i = \tilde{\partial}_i \tilde{\psi} + \hat{\tilde{N}}_i$ where $\tilde{\partial}_i \hat{\tilde{N}}_i = 0$ ($\tilde{\partial}_\mu \equiv \partial/\partial \tilde{x}^\mu$). Note that in this gauge $\tilde{\pi}(\tilde{x})$ denotes the Goldstone field. Since both δN and $\tilde{N}_i$ are Lagrange multipliers in this spatially-flat gauge, by solving the constraint equations (see e.g. [22, 78]) they can be expressed up to first order as

$$\delta N = \frac{m_3^3}{m_3^3 - 2M_{Pl}^2 H}\dot{\tilde{\pi}} + \frac{2M_{Pl}^2 \dot{H}}{m_3^3 - 2M_{Pl}^2 H}\tilde{\pi} \equiv \alpha_N \dot{\tilde{\pi}} + \tilde{\alpha}_N \tilde{\pi} \tag{C.1.2}$$

and

$$\tilde{\psi} = -\frac{m_3^3 + 4H\tilde{m}_4^2}{m_3^3 - 2HM_{Pl}^2}\tilde{\pi} - \frac{3m_3^6 H - 4HM_{Pl}^2(\dot{H}M_{Pl}^2 - 2m_2^4)}{(m_3^3 - 2M_{Pl}^2 H)^2}\frac{a^2}{\tilde{\nabla}^2}\dot{\tilde{\pi}} \equiv \alpha_\psi \tilde{\pi} + \tilde{\alpha}_\psi \frac{a^2}{\tilde{\nabla}^2}\dot{\tilde{\pi}}\,, \tag{C.1.3}$$

where $\tilde{\nabla}^2 \equiv \tilde{\partial}_i \tilde{\partial}_i$. Notice that we have kept the non-local term in (C.1.3) since this will contribute to the vertex that we are going to consider. According to [78], $\tilde{\pi}$ is canonically normalized as

$$\tilde{\pi} = \frac{2HM_{Pl}^2 - m_3^3}{\sqrt{2}HM_{Pl}[3m_3^6 + 4M_{Pl}^2(c + 2m_2^4)]^{1/2}}\pi_c\,, \tag{C.1.4}$$

while the canonical normalization of $\tilde{\gamma}_{ij}$ remains the same as in the Newtonian gauge. Here we keep a distinction between the canonical field π_c and the non-canonical field $\tilde{\pi}$ unlike in the main text.

We are going to investigate the non-linear $\gamma\pi\pi$ vertex which contains three or more derivatives (we will drop all the rest). In principle, this vertex gets contributions from the action (3.0.2) through the Einstein-Hilbert and the S_{m_3} terms. Let us first consider the contribution from S_{m_3} term. As usual, the extrinsic curvature is defined by

$$\tilde{K}_{ij} = \frac{1}{2N}(\dot{\tilde{h}}_{ij} - \tilde{D}_i \tilde{N}_j - \tilde{D}_i \tilde{N}_j)\,, \tag{C.1.5}$$

where $\tilde{D}_i$ denotes the 3d covariant derivative with respect to the induced metric $\tilde{h}_{ij}$. It is straightforward to show that a variation of $\tilde{K}$ ($\tilde{K} = \tilde{h}^{ij}\tilde{K}_{ij}$) subjected to the metric (C.1.1) contains $a^{-2}\tilde{\gamma}_{ij}\tilde{\partial}_i\tilde{\partial}_i\tilde{\psi}$.

After performing the Stuekelberg trick of eq. (3.1.1) and (3.1.2), the contribution from S_{m_3} which has three derivatives reads

$$S_{m_3} \supset \frac{2m_3^3 M_{Pl}^4 H^2}{(m_3^3 - 2M_{Pl}^2 H)^2} \int d^4\tilde{x}\, a\, \dot{\tilde{\gamma}}_{ij} \tilde{\partial}_i \tilde{\pi} \tilde{\partial}_j \tilde{\pi}\,, \tag{C.1.6}$$

where we have taken the term $-2(1-\alpha_N)\dot{\tilde{\pi}}$ from $\delta\tilde{g}^{00}$ and used (C.1.2)-(C.1.3).

Using the canonical normalizations both for $\tilde{\pi}$ (C.1.4) and $\tilde{\gamma}_{ij}$ one obtains the same interaction that we have obtained in the Newtonian gauge (3.1.6). Thus we expect that the contribution arising from S_{EH} cancels out. To show this, notice that the contribution from the Einstein-Hilbert term comes from $N(\tilde{K}_{ij}\tilde{K}^{ij} - \tilde{K}^2)$. More specifically, we have

$$S_{EH} \supset \frac{M_{Pl}^2}{2} \int d^4\tilde{x}\, a \left(4H\delta N \tilde{\gamma}_{ij} \tilde{\partial}_i \tilde{\partial}_j \tilde{\psi} + \delta N \dot{\tilde{\gamma}}_{ij} \tilde{\partial}_i \tilde{\partial}_j \tilde{\psi} + \frac{1}{2a^2} \tilde{\nabla}^2 \tilde{\gamma}_{ij} \tilde{\partial}_i \tilde{\psi} \tilde{\partial}_j \tilde{\psi} \right)\,, \tag{C.1.7}$$

where we have performed a few integration by parts. Using (C.1.2) and (C.1.3) in S_{EH} one obtains

$$\begin{aligned} S_{EH} \supset \frac{M_{Pl}^2}{2} \int d^4\tilde{x}\, a \Big\{ & \alpha_\psi(\alpha_N + \alpha_\psi)\dot{\tilde{\pi}} \dot{\tilde{\gamma}}_{ij} \tilde{\partial}_i \tilde{\partial}_j \tilde{\pi} - a^2 \tilde{\alpha}_\psi (\alpha_N + \alpha_\psi) \tilde{\pi} \ddot{\tilde{\gamma}}_{ij} \tilde{\partial}_i \tilde{\partial}_j \frac{1}{\tilde{\nabla}^2} \dot{\tilde{\pi}} \\ & + [H\alpha_\psi(2\alpha_N + \alpha_\psi) - \alpha_\psi(\tilde{\alpha}_N + \dot{\alpha}_\psi) + \alpha_N \tilde{\alpha}_\psi c_s^2] \dot{\tilde{\gamma}}_{ij} \tilde{\partial}_i \tilde{\pi} \tilde{\partial}_j \tilde{\pi} \Big\}\,, \end{aligned} \tag{C.1.8}$$

where we have used the linear equations of motion for $\tilde{\gamma}_{ij}$, $\ddot{\tilde{\gamma}}_{ij} + 3H\dot{\tilde{\gamma}}_{ij} - \frac{1}{a^2}\tilde{\nabla}^2\tilde{\gamma}_{ij} = 0$, and for $\tilde{\pi}$, $\ddot{\tilde{\pi}} + 3H\dot{\tilde{\pi}} - \frac{c_s^2}{a^2}\tilde{\nabla}^2\tilde{\pi} = 0$.

Notice that the first two terms on RHS vanish due to the fact that $\alpha_N + \alpha_\psi = 0$. Let us consider the prefactor of the last term. Using the expression of c_s^2 (3.1.10) and the definitions of all those α-parameters (C.1.2)-(C.1.3), the prefactor can be rewritten as

$$H\alpha_\psi(2\alpha_N + \alpha_\psi) - \alpha_\psi(\tilde{\alpha}_N + \dot{\alpha}_\psi) + \alpha_N \tilde{\alpha}_\psi c_s^2 = H\alpha_\psi(\alpha_N + \alpha_\psi) + \frac{H\tilde{\alpha}_N^2}{M_{Pl}^2 \dot{H}^2}(M_{Pl}^2 \dot{H}\alpha_\psi - c\alpha_\psi)\,. \tag{C.1.9}$$

In our case the coupling with matter has been neglected ($\rho_m = P_m = 0$), therefore the parameter c is equal to $-M_{Pl}^2\dot{H}$ (see e.g. [48, 49]). The prefactor is then given by

$$H\alpha_\psi(2\alpha_N + \alpha_\psi) - \alpha_\psi(\tilde{\alpha}_N + \dot{\alpha}_\psi) + \alpha_N \tilde{\alpha}_\psi c_s^2 = (\alpha_\psi + \alpha_N)(H\alpha_\psi + \frac{H\tilde{\alpha}_N^2}{\dot{H}}) \tag{C.1.10}$$

which is again zero since $\alpha_N + \alpha_\psi = 0$ in this case. Therefore S_{EH} gives no contribution to our $\gamma\pi\pi$ vertex and S_{m_3}, on the other hand, gives the same result that we have obtained in the Newtonian gauge (3.1.6).

C.2 THE INTERACTION $\gamma\gamma\pi$

In this Section we are going to check that the cubic term $\gamma\gamma\pi$ in the Lagrangian (4.1.2), computed in Newtonian gauge, can be obtained also in spatially-flat gauge up to field redefinitions. The same

check for the $\gamma\pi\pi$ interaction was already done in [95]. For simplicity we limit our check to the case in which the contribution of matter is negligible ($\rho_m = P_m = 0$); in this case one has $c = -M_{Pl}^2\dot{H}$ in the action (3.0.2) (see e.g. [48, 49]).

Here the metric is decomposed as

$$ds^2 = -(1+\delta N)^2 d\tilde{t}^2 + a(\tilde{t})^2 \left(e^{\gamma}\right)_{ij} (d\tilde{x}^i + \tilde{N}^i d\tilde{t})(d\tilde{x}^j + \tilde{N}^j d\tilde{t}) \,, \tag{C.2.1}$$

where $\tilde{\gamma}_{ij}$ is transverse and traceless ($\delta_{ij}\tilde{\gamma}_{ij} = 0$, $\tilde{\partial}_i\tilde{\gamma}_{ij} = 0$) and the shift vector $\tilde{N}_i$ is decomposed as $\tilde{N}_i = \tilde{\partial}_i\psi + \hat{\tilde{N}}_i$ with $\tilde{\partial}_i\hat{\tilde{N}}_i = 0$ ($\tilde{\partial}_\mu = \partial/\partial\tilde{x}^\mu$). We are going to denote the Goldstone field as $\tilde{\pi}(\tilde{x})$.

The action in spatially-flat gauge does not contain time derivatives of δN and $\tilde{N}_i$, which are therefore Lagrange multipliers. Hence, at the perturbative level they are fixed by the constraint equations as (see e.g. [22, 95])

$$\delta N = \frac{m_3^3}{m_3^3 - 2M_{Pl}^2 H}\dot{\tilde{\pi}} + \frac{2M_{Pl}^2\dot{H}}{m_3^3 - 2M_{Pl}^2 H}\tilde{\pi} \equiv \alpha_N\dot{\tilde{\pi}} + \tilde{\alpha}_N\tilde{\pi} \tag{C.2.2}$$

and

$$\tilde{\psi} = -\frac{m_3^3}{m_3^3 - 2M_{Pl}^2 H}\tilde{\pi} - \frac{3m_3^3 H - 4HM_{Pl}^2(\dot{H}M_{Pl}^2 - 2m_2^4)}{(m_3^3 - 2M_{Pl}^2 H)^2}\frac{a^2}{\tilde{\nabla}^2}\dot{\tilde{\pi}} \equiv \alpha_\psi\tilde{\pi} + \tilde{\alpha}_\psi\frac{a^2}{\tilde{\nabla}^2}\dot{\tilde{\pi}} \,, \tag{C.2.3}$$

where $\tilde{\nabla}^2 = \tilde{\partial}_i\tilde{\partial}_i$. Following [95], the field $\tilde{\pi}$ is canonically normalized as

$$\tilde{\pi} = \frac{2HM_{Pl}^2 - m_3^3}{\sqrt{2}HM_{Pl}[3m_3^6 + 4M_{Pl}^2(c + 2m_2^4)]^{1/2}}\pi_c \,, \tag{C.2.4}$$

while the canonical normalization for $\tilde{\gamma}_{ij}$ is the same as in Newtonian gauge.

It is straightforward to realize that the vertex $\gamma\gamma\pi$ is not generated by the term $m_3^3\delta\tilde{g}^{00}\delta\tilde{K}$ in the action (it is not possible to get γ^2 out of either δg^{00} or δK). On the other hand, the sought out vertex is generated by the Einstein-Hilbert term. In order to simplify the derivation we are going to exploit the fact that, as in Newtonian gauge, tensor perturbations $\tilde{\gamma}_{ij}$ couple to the metric as a minimally-coupled scalar does (this statement can be verified explicitly by expanding the Einstein-Hilbert term up to cubic order). Therefore the quadratic Lagrangian for $\tilde{\gamma}_{ij}$ is

$$\begin{aligned}\mathcal{L} &= -\frac{M_{Pl}^2}{8}\tilde{g}^{\mu\nu}\tilde{\partial}_\mu\tilde{\gamma}_{ij}\tilde{\partial}_\nu\tilde{\gamma}_{ij}\sqrt{-\tilde{g}} \\ &= -a^3\frac{M_{Pl}^2}{8}\left[-\dot{\tilde{\gamma}}_{ij}^2 + \frac{1}{a^2}(\tilde{\partial}_k\tilde{\gamma}_{ij})^2 + \delta N\left(\dot{\tilde{\gamma}}_{ij}^2 + \frac{1}{a^2}(\tilde{\partial}_k\tilde{\gamma}_{ij})^2\right) + \frac{2}{a^2}\tilde{\partial}_k\tilde{\psi}\tilde{\partial}_k\tilde{\gamma}_{ij}\dot{\tilde{\gamma}}_{ij}\right] \,.\end{aligned} \tag{C.2.5}$$

The first two terms in the last equation are the standard kinetic term for the graviton, and the remaining terms contribute to our cubic vertex.

Let us focus on these relevant terms. By replacing δN and $\tilde{\psi}$ by the constraints (C.2.2) and (C.2.3) we obtain, after several integrations by part and after dropping terms with less than two derivatives,

$$\begin{aligned}\mathcal{L}_{\gamma\gamma\pi} = &-a^3\frac{M_{Pl}^2}{8}\left[(\alpha_N + \alpha_\psi)\left(\dot{\tilde{\gamma}}_{ij}^2 + \frac{1}{a^2}(\tilde{\partial}_k\tilde{\gamma}_{ij})^2\right)\dot{\tilde{\pi}} + (\alpha_\psi H + \dot{\alpha}_\psi + \tilde{\alpha}_N + c_s^2\tilde{\alpha}_\psi)\frac{1}{a^2}(\tilde{\partial_k}\tilde{\gamma}_{ij})^2\tilde{\pi}\right. \\ &\left. - (3H\alpha_\psi - \dot{\alpha}_\psi - \tilde{\alpha}_N - c_s^2\tilde{\alpha}_\psi)\dot{\tilde{\gamma}}_{ij}^2\,\tilde{\pi}\right] \,,\end{aligned} \tag{C.2.6}$$

where we have used the linear equations of motion for $\tilde{\gamma}_{ij}$, $\ddot{\tilde{\gamma}}_{ij} + 3H\dot{\tilde{\gamma}}_{ij} - \frac{1}{a^2}\tilde{\nabla}^2\tilde{\gamma}_{ij} = 0$ and for $\tilde{\pi}$, $\ddot{\tilde{\pi}} + 3H\dot{\tilde{\pi}} - \frac{c_s^2}{a^2}\tilde{\nabla}^2\tilde{\pi} = 0$. The first term in the above equation vanishes since $\alpha_N + \alpha_\psi = 0$, as one can see from the definitions of α_N and α_ψ in eqs. (C.2.2) and (C.2.3). Then, using the expression for c_s^2 in eq. (3.1.10), also the second term of (C.2.6) vanishes (notice that our expression for c_s^2 assumes $\dot{m}_3 = 0$, but the cancellation works also in the more general case [58]). Therefore one is left only with the term in the last line, which simplifies to

$$\mathscr{L}_{\gamma\gamma\pi} = \frac{a^3}{2}\frac{m_3^3 M_{Pl}^2 H}{2M_{Pl}^2 H - m_3^3}\dot{\tilde{\gamma}}_{ij}^2\,\tilde{\pi}\,. \tag{C.2.7}$$

After using (C.2.4) and (3.1.5) to go to canonical normalization for $\tilde{\pi}$ and $\tilde{\gamma}_{ij}$, equation (C.2.7) matches exactly with the vertex in Newtonian gauge (4.1.2).

D

DEVIATION FROM CUBIC GALILEON

The discussion of Section 4.2 assumes that the relevant cubic non-linearities are of the form $\tilde{m}_3^3 = -m_3^3$ (as is the case for cubic Galileon interactions). However, one could wonder whether a different choice of operators can make the theory stable around GW backgrounds. To address this possibility, in this Appendix we are going to study the stability properties of theories that deviate from the cubic Galileon for the case $c_s < 1$. For concreteness we focus on the case $\tilde{m}_3^3 = -m_3^3(1+\eta)$, with $\eta \neq 0$ parametrizing such deviations.

The leading non-linear interactions of π arising from this coupling are again cubic. The Lagrangian takes then the form

$$\mathscr{L} = -\frac{1}{2}\bar{\eta}_{\mu\nu}\partial^\mu\pi\partial^\nu\pi - \frac{1}{\Lambda_B^3}\Box\pi(\partial\pi)^2 + \frac{\eta}{\Lambda_B^3}\ddot{\pi}(\partial_i\pi)^2 + \Gamma_{\mu\nu}\partial^\mu\pi\partial^\nu\pi - \frac{\Lambda_B^3}{2}\pi\Gamma_{\mu\nu}\Gamma^{\mu\nu} \,. \tag{D.0.1}$$

Notice that the terms proportional to η do not change the couplings with $\Gamma_{\mu\nu}$ and $\Gamma_{\mu\nu}\Gamma^{\mu\nu}$: the operator $(\delta g^{00})^2\delta K$ yields interactions between γ_{ij} and π that only start at quartic order. Straightforwardly, the equation of motion reads

$$\bar{\Box}\pi - \frac{2}{\Lambda_B^3}\left[(\partial_\mu\partial_\nu\pi)^2 - \Box\pi^2\right] + \frac{2\eta}{\Lambda_B^3}\left[(\partial_i\dot{\pi})^2 - \ddot{\pi}\nabla^2\pi\right] - 2\,\Gamma_{\mu\nu}\partial^\mu\partial^\nu\pi - \frac{\Lambda_B^3}{2}\Gamma_{\mu\nu}\Gamma^{\mu\nu} = 0 \,. \tag{D.0.2}$$

Following the discussion of Section 4.2.2, we have that for $c_s < 1$ the solution is a function of u only: $\varphi = \varphi(u)$. In this case one can check that there are no contributions proportional to η, hence the above equation reduces to (4.2.19).

At this stage we can compute the kinetic matrix $Z^{\mu\nu}$ for perturbations $\delta\pi$. By expanding (D.0.1) at quadratic order we obtain

$$Z^{\mu\nu} = -\frac{1}{2}\bar{\eta}^{\mu\nu} + \Gamma^{\mu\nu} + \frac{2}{\Lambda_B^3}\left[\partial^\mu\partial^\nu\hat{\pi} - \eta^{\mu\nu}\Box\hat{\pi}\right] + \eta\mathcal{R}^{\mu\nu} \,, \tag{D.0.3}$$

where the matrix $\mathcal{R}^{\mu\nu}$ is defined as

$$\mathcal{R}^{\mu\nu} \equiv \frac{1}{\Lambda_B^3}\left[\begin{array}{c|c} \nabla^2\hat{\pi} & -\partial_j\dot{\hat{\pi}} \\ \hline -\partial_i\dot{\hat{\pi}} & \ddot{\hat{\pi}}\,\delta_{ij} \end{array}\right] \,. \tag{D.0.4}$$

This expression for $Z^{\mu\nu}$ should be compared with the case $\eta = 0$ of eq. (4.2.8).

Using the u-dependent solution (4.2.19) for $\varphi(u)$ and the change of variables of eq. (4.2.15), one finds the non-vanishing components of $Z^{\mu\nu}$, that are given by

$$\begin{aligned} Z^{00} &= \frac{1}{2} + (2+\eta)\varphi''(u)\,, \\ Z^{11} &= -\frac{1}{2}c_s^2 + \Gamma^{11} + \eta\varphi''(u)\,, \\ Z^{22} &= -\frac{1}{2}c_s^2 + \Gamma^{22} + \eta\varphi''(u)\,, \\ Z^{33} &= -\frac{1}{2}c_s^2 + (2+\eta)\varphi''(u)\,, \\ Z^{03} &= Z^{30} = (2+\eta)\varphi''(u)\,. \end{aligned} \tag{D.0.5}$$

Now we can see that with this choice of solution the contributions arising from η-term are the same in all the entries: $\eta\varphi''$. To avoid gradient instabilities along x, one requires $\eta > 0$ and sufficiently large. However with this choice one clearly encounters ghosts. Hence, for any value of η the system remains unstable.

E

COMPARISON WITH THE WKB APPROXIMATION

The result we obtained for $\Psi_0(x)$ in eq. (5.2.17) matches with the standard WKB approximation in both the large distance ($\bar{x} \gg 1$) and small coupling ($\lambda \ll 1$) limit, as we are going to show. From the calculation of the WKB wavefunction we can also appreciate how the prefactor of Ψ_0 induces a subleading x-dependence with respect to the exponential factor.

In the WKB approximation, the wavefunction is given by

$$\Psi_{\text{WKB}}(x) = \frac{N}{\sqrt{p(x)}} \exp\left(\pm i \int_{x_0}^{x} \frac{p(x')}{\hbar}\, dx'\right) , \tag{E.0.1}$$

where N is again a normalization, x_0 is an arbitrary point, $p(x) = \sqrt{2m(E - V(x))}$ is the momentum of the classical trajectory with energy E and the sign at the exponent is fixed by requiring appropriate boundary conditions at infinity. For the WKB approximation to be valid one requires that $\hbar|p'(x)| \ll p^2(x)$. Note that in the case of the anharmonic oscillator with potential (5.2.1), this condition is satisfied even for the ground state in the classically-forbidden region $V(x) \gg E$. For small λ, this point is parametrically smaller than the point where the quartic term starts to dominate the potential ($\bar{x} \sim 1$). This means that the WKB should match eq. (5.2.17) even for small $\bar{x}$.

Let us start from the prefactor. For fixed $\bar{x}$ and small λ we obtain

$$\frac{N}{\sqrt{p(x)}} \simeq \frac{N'}{\sqrt{\bar{x}}\,(1+\bar{x}^2)^{1/4}} . \tag{E.0.2}$$

Notice that this expression matches with the prefactor obtained in the semiclassical expansion for $\bar{x} \gg 1$, but for general values differs. Therefore, in order to have a match with the full wavefunction, we expect some correction to come from the exponent.

The exponent can be rewritten as the following integral

$$\begin{aligned} \int_{x_0}^{x} \frac{p(x')}{\hbar}\, dx' &= i\frac{\sqrt{2m}}{\hbar} \int_{x_0}^{x} \sqrt{V(x') - E}\, dx' \\ &= \frac{i}{2\lambda} \int_{\bar{x}_0}^{\bar{x}} \sqrt{y^2(1+y^2) - \epsilon}\, dy , \end{aligned} \tag{E.0.3}$$

where in the second line we defined $y^2 \equiv 2\lambda x^2/d^2$ and $\epsilon \equiv 4\lambda E/(\hbar\omega)$. To perform the integration above, one can either expand the integrand for small $\alpha \equiv \epsilon/(y^2(1+y^2))$ first and perform the integral after, or evaluate the integral first and expand it for small α after. The latter method is more complicated than the former since the integral will involve Elliptic functions of the first and second kind, so one needs proper care in taking the small α limit. In any case the two ways of performing

that calculation must coincide. Let us now proceed with the first method. Expanding the integrand for small α and performing the integral afterwards yields

$$\int_{x_0}^{x} \frac{p(x')}{\hbar}\,dx' = \frac{i}{6\lambda}\left\{\left[\left(1+\bar{x}^2\right)^{3/2}-1\right]+\frac{6\lambda E}{\hbar\omega}\log\left(\frac{1+\sqrt{1+\bar{x}^2}}{\bar{x}}\right)+\text{const}\right\}+\mathcal{O}(\alpha^2)\,, \tag{E.0.4}$$

where the constant terms only depend on $\bar{x}_0$ and can be absorbed into a redefinition of the normalization. Notice that the term $-i/(6\lambda)$ is needed in order to match our result with the wavefunction of the harmonic oscillator when λ is taken to be zero. We notice that at order $\sim 1/\lambda$ the exponent matches with the one found from the Euclidean action eq. (5.2.14). Moreover, we have corrections at order $\sim \lambda^0$. The logarithmic term can be important for small $\bar{x}$ and in fact affects the prefactor of eq. (E.0.2).

By putting both the prefactor (E.0.2) and the exponent (E.0.3) together (and choosing the appropriate sign) we obtain

$$\Psi_{\text{WKB}}(x) \simeq \frac{N}{\sqrt{\bar{x}}(1+\bar{x}^2)^{1/4}}\left[\frac{1+\sqrt{1+\bar{x}^2}}{\bar{x}}\right]^{-E/(\hbar\omega)} \exp\left\{-\frac{1}{6\lambda}\left[\left(1+\bar{x}^2\right)^{3/2}-1\right]\right\}\,. \tag{E.0.5}$$

Clearly, by choosing the ground-state energy at leading order $E = \hbar\omega/2$ we recover the result from semiclassics eq. (5.2.17), as expected.

F

PERTURBATIVE CHECK OF THE PDE

As a check, one expects that the numerical result found in Section 5.4.5 is reduced to the one obtained using perturbation theory when the coupling $\tilde{\lambda}$ is small. More precisely, the check we are going to do will be a comparison between the 4-point coefficient of the WFU derived from perturbation theory and its numerical value evaluated on the classical solutions with the sinusoidal profile. It is more complicated to do a similar check for the Gaussian profile, since one would have to integrate over Fourier space in the perturbative calculation.

Let us start with the perturbative calculation. For simplicity, we only focus on the first order correction in $\tilde{\lambda}$ which corresponds to the first graph in Figure 17a. To compute such a diagram one just needs to know the bulk-to-boundary propagator (5.5.3). Then the 4-point coefficient $\psi^{(4)}$ of the WFU is given by

$$\psi^{(4)}(k_1,k_2,k_3,k_4) = \frac{i\lambda}{P_\zeta^2}\int_{-\infty(1-i\epsilon)}^{\eta_f} d\eta\; K'(\eta,\mathbf{k}_1)K'(\eta,\mathbf{k}_2)K'(\eta,\mathbf{k}_3)K'(\eta,\mathbf{k}_4)\,, \tag{F.0.1}$$

where as usual the $i\epsilon$ prescription has been imposed for the integral to converge. The integral above can be performed analytically so we get

$$\psi^{(4)}(k_1,k_2,k_3,k_4) = \frac{24\lambda k_1^2k_2^2k_3^2k_4^2}{P_\zeta^2(k_1+k_2+k_3+k_4)^5}\,. \tag{F.0.2}$$

Note that there is no divergence one has to worry about at late times. We now want to compare this perturbative result and the numerical one done in Section 5.4.5.

Before that, it is instructive to put the coefficient $\psi^{(4)}$ back in the on-shell action:

$$iS_{int} = \frac{1}{4!}\int\left(\prod_{i=1}^4\frac{d^3k_i}{(2\pi)^3}\right)(2\pi)^3\delta(\sum_{i=1}^4\mathbf{k}_i)\;\psi^{(4)}(k_1,k_2,k_3,k_4)\;\zeta_0(\mathbf{k}_1)\zeta_0(\mathbf{k}_2)\zeta_0(\mathbf{k}_3)\zeta_0(\mathbf{k}_4)\,. \tag{F.0.3}$$

This on-shell action, as we have said before, does not capture the loop diagrams shown in Figures 17b and 17c. Apparently, the formula (F.0.3) depends on the late-times boundary condition $\zeta_0(\mathbf{k})$. One can generally apply this formula to a generic boundary condition at late times, but here we are going to choose a single Fourier mode which is exactly what we considered in Section 5.4.5.

Let us now focus on the single Fourier mode namely, $\zeta(\eta_f,x) = \zeta_0\sin(kx)$. Trivially, the mode $\sin(kx)$ will be converted into the Dirac delta function in k-space,

$$\zeta_0(\mathbf{k}) = -\zeta_0\frac{i}{2}(2\pi)^3\delta(k_z)\delta(k_y)\Big[\delta(k_x-k)-\delta(k_x+k)\Big]\,. \tag{F.0.4}$$

This form of $\zeta_0(\mathbf{k})$ greatly simplifies the interacting action (F.0.3) into

$$iS'_{int} = \frac{3\lambda k^3\zeta_0^4}{8192P_\zeta^2} = \frac{\zeta_0^2}{P_\zeta}\frac{3\tilde{\lambda}k^3}{8192}\,, \tag{F.0.5}$$

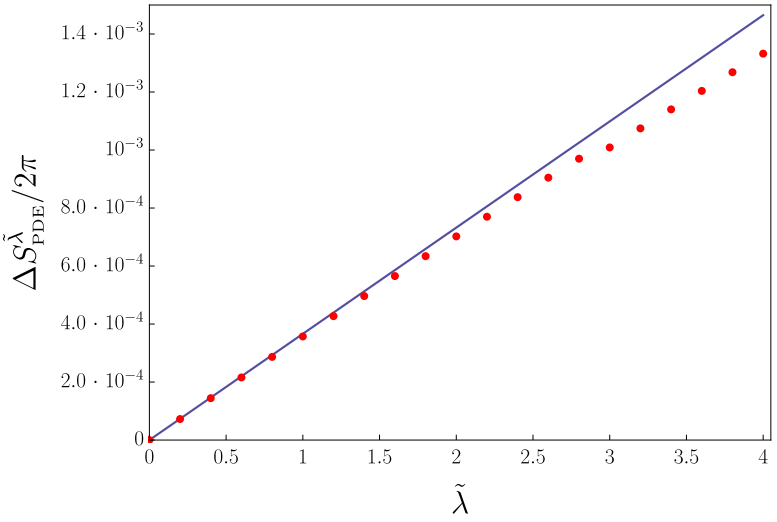

Figure 27: The blue curve shows the perturbative result (F.o.5) as a function of $\tilde{\lambda}$. The red points indicate the numerical values of (F.o.6). As expected, for small $\tilde{\lambda}$ the two approaches coincide, whereas the departure happens around $\tilde{\lambda} \sim \mathcal{O}(1)$.

where iS' denotes the action divided by the factor $(2\pi)^3\delta(k_x - k)\delta(k_y)\delta(k_z)$, and we have written in terms of $\tilde{\lambda}$ for the second equality. Again, this is the first order correction in $\tilde{\lambda}$ obtained using perturbation theory.

Let us turn to the numerical calculation. Let $\Delta S^{\tilde{\lambda}}_{\rm PDE}$ be the corrections of order $\tilde{\lambda}$ or higher. Then, one way to extract $\Delta S^{\tilde{\lambda}}_{\rm PDE}$ from (5.4.36) is to subtract the finite part of the free on-shell action, denoted by $\Delta S^{0}_{\rm PDE}$:

$$\Delta S^{\tilde{\lambda}}_{\rm PDE} = -(\Delta S_{\rm PDE} - \Delta S^{0}_{\rm PDE}) \,. \tag{F.o.6}$$

The minus sign in front is to make $\Delta S^{\tilde{\lambda}}_{\rm PDE}$ positive definite. Note that in general this $\Delta S^{\tilde{\lambda}}_{\rm PDE}$ contains all orders in $\tilde{\lambda}$, but we will show below that for small $\tilde{\lambda}$ it is dominated by the first order corrections (it fits almost perfectly with (F.o.5)). We then numerically evaluate the $\Delta S^{\tilde{\lambda}}_{\rm PDE}$, divided by the spatial volume 2π, on the classical solution for small $\tilde{\lambda}$ ($\lambda, \zeta_0 \ll 1$). Omitting the common factor ζ_0^2/P_ζ, we find that $\Delta S^{\tilde{\lambda}}_{\rm PDE}/2\pi$ matches with the analytic calculation (F.o.5) for small values of $\tilde{\lambda}$, setting $k = 1$.

Finally, it is also worth checking that for small $\tilde{\lambda}$ (F.o.6) is dominated by the first order corrections in $\tilde{\lambda}$, as expected in perturbation theory. This result is confirmed in Figure 27, where the blue line represents the perturbative result (F.o.5) and the red points denote the numerical value of $\Delta S^{\tilde{\lambda}}_{\rm PDE}/2\pi$ for $\tilde{\lambda} \in \{0.2, 0.4, \ldots, 4\}$. Notice that as $\tilde{\lambda}$ increases, one expects that (F.o.6) no longer coincides with (F.o.5) and, indeed, from Figure 17a this departure happens when $\tilde{\lambda}$ is of order unity.

BIBLIOGRAPHY

[1] S. Perlmutter et al. "Measurements of Ω and Λ from 42 high redshift supernovae." In: *Astrophys. J.* 517 (1999), pp. 565–586. DOI: 10.1086/307221. arXiv: astro-ph/9812133.

[2] Adam G. Riess et al. "Observational evidence from supernovae for an accelerating universe and a cosmological constant." In: *Astron. J.* 116 (1998), pp. 1009–1038. DOI: 10.1086/300499. arXiv: astro-ph/9805201.

[3] Brian P. Schmidt et al. "The High Z supernova search: Measuring cosmic deceleration and global curvature of the universe using type Ia supernovae." In: *Astrophys. J.* 507 (1998), pp. 46–63. DOI: 10.1086/306308. arXiv: astro-ph/9805200.

[4] G. Hinshaw et al. "NINE-YEAR WILKINSON MICROWAVE ANISOTROPY PROBE (WMAP) OBSERVATIONS: COSMOLOGICAL PARAMETER RESULTS." In: *The Astrophysical Journal Supplement Series* 208.2 (2013), p. 19. ISSN: 1538-4365. DOI: 10.1088/0067-0049/208/2/19. URL: http://dx.doi.org/10.1088/0067-0049/208/2/19.

[5] P. de Bernardis et al. "A Flat universe from high resolution maps of the cosmic microwave background radiation." In: *Nature* 404 (2000), pp. 955–959. DOI: 10.1038/35010035. arXiv: astro-ph/0004404.

[6] Z. Hou et al. "CONSTRAINTS ON COSMOLOGY FROM THE COSMIC MICROWAVE BACKGROUND POWER SPECTRUM OF THE 2500 deg2SPT-SZ SURVEY." In: *The Astrophysical Journal* 782.2 (2014), p. 74. ISSN: 1538-4357. DOI: 10.1088/0004-637x/782/2/74. URL: http://dx.doi.org/10.1088/0004-637X/782/2/74.

[7] N. Aghanim et al. "Planck 2018 results. VI. Cosmological parameters." In: *Astron. Astrophys.* 641 (2020), A6. DOI: 10.1051/0004-6361/201833910. arXiv: 1807.06209 [astro-ph.CO].

[8] Uros Seljak et al. "Cosmological parameter analysis including SDSS Ly-alpha forest and galaxy bias: Constraints on the primordial spectrum of fluctuations, neutrino mass, and dark energy." In: *Phys. Rev. D* 71 (2005), p. 103515. DOI: 10.1103/PhysRevD.71.103515. arXiv: astro-ph/0407372.

[9] Max Tegmark et al. "Cosmological parameters from SDSS and WMAP." In: *Phys. Rev. D* 69 (2004), p. 103501. DOI: 10.1103/PhysRevD.69.103501. arXiv: astro-ph/0310723.

[10] Lado Samushia et al. "The clustering of galaxies in the SDSS-III DR9 Baryon Oscillation Spectroscopic Survey: testing deviations from and general relativity using anisotropic clustering of galaxies." In: *Monthly Notices of the Royal Astronomical Society* 429.2 (2012), 1514–1528. ISSN: 1365-2966. DOI: 10.1093/mnras/sts443. URL: http://dx.doi.org/10.1093/mnras/sts443.

[11] Philip Bull et al. "Beyond ΛCDM: Problems, solutions, and the road ahead." In: *Phys. Dark Univ.* 12 (2016), pp. 56–99. DOI: 10.1016/j.dark.2016.02.001. arXiv: 1512.05356 [astro-ph.CO].

[12] A. Conley et al. "SUPERNOVA CONSTRAINTS AND SYSTEMATIC UNCERTAINTIES FROM THE FIRST THREE YEARS OF THE SUPERNOVA LEGACY SURVEY." In: *The Astrophysical Journal Supplement Series* 192.1 (2010), p. 1. ISSN: 1538-4365. DOI: 10.1088/0067-0049/192/1/1. URL: http://dx.doi.org/10.1088/0067-0049/192/1/1.

[13] Daniel Baumann. *Lecture notes on Cosmology*.

[14] Y. Akrami et al. "Planck 2018 results. VII. Isotropy and Statistics of the CMB." In: *Astron. Astrophys.* 641 (2020), A7. DOI: 10.1051/0004-6361/201935201. arXiv: 1906.02552 [astro-ph.CO].

[15] J. R. Bond and G. Efstathiou. "Cosmic background radiation anisotropies in universes dominated by nonbaryonic dark matter." In: *Astrophysical Journal* 285 (Oct. 1984), pp. L45–L48. DOI: 10.1086/184362.

[16] Wayne Hu and Naoshi Sugiyama. "Anisotropies in the cosmic microwave background: An Analytic approach." In: *Astrophys. J.* 444 (1995), pp. 489–506. DOI: 10.1086/175624. arXiv: astro-ph/9407093.

[17] F. Bernardeau, S. Colombi, E. Gaztanaga, and R. Scoccimarro. "Large scale structure of the universe and cosmological perturbation theory." In: *Phys. Rept.* 367 (2002), pp. 1–248. DOI: 10.1016/S0370-1573(02)00135-7. arXiv: astro-ph/0112551 [astro-ph].

[18] John Joseph M. Carrasco, Mark P. Hertzberg, and Leonardo Senatore. "The Effective Field Theory of Cosmological Large Scale Structures." In: *JHEP* 09 (2012), p. 082. DOI: 10.1007/JHEP09(2012)082. arXiv: 1206.2926 [astro-ph.CO].

[19] Guido D'Amico, Yaniv Donath, Leonardo Senatore, and Pierre Zhang. "Limits on Clustering and Smooth Quintessence from the EFTofLSS." In: (Dec. 2020). arXiv: 2012.07554 [astro-ph.CO].

[20] Diogo P. L. Bragança, Matthew Lewandowski, David Sekera, Leonardo Senatore, and Raphael Sgier. "Baryonic effects in the Effective Field Theory of Large-Scale Structure and an analytic recipe for lensing in CMB-S4." In: (Oct. 2020). arXiv: 2010.02929 [astro-ph.CO].

[21] N. Aghanim et al. "Planck 2018 results. I. Overview and the cosmological legacy of Planck." In: *Astron. Astrophys.* 641 (2020), A1. DOI: 10.1051/0004-6361/201833880. arXiv: 1807.06205 [astro-ph.CO].

[22] Juan Martin Maldacena. "Non-Gaussian features of primordial fluctuations in single field inflationary models." In: *JHEP* 0305 (2003), p. 013. DOI: 10.1088/1126-6708/2003/05/013. arXiv: astro-ph/0210603 [astro-ph].

[23] Alexandre Le Tiec. "The Overlap of Numerical Relativity, Perturbation Theory and Post-Newtonian Theory in the Binary Black Hole Problem." In: *Int. J. Mod. Phys. D* 23.10 (2014), p. 1430022. DOI: 10.1142/S0218271814300225. arXiv: 1408.5505 [gr-qc].

[24] Luc Blanchet. "Gravitational Radiation from Post-Newtonian Sources and Inspiralling Compact Binaries." In: *Living Rev. Rel.* 17 (2014), p. 2. DOI: 10.12942/lrr-2014-2. arXiv: 1310.1528 [gr-qc].

[25] Gerhard Schaefer. "Post-Newtonian methods: Analytic results on the binary problem." In: *Fundam. Theor. Phys.* 162 (2011). Ed. by Luc Blanchet, Alessandro Spallicci, and Bernard Whiting, pp. 167–210. arXiv: 0910.2857 [gr-qc].

[26] J. Blümlein, A. Maier, P. Marquard, and G. Schäfer. "Fourth post-Newtonian Hamiltonian dynamics of two-body systems from an effective field theory approach." In: *Nucl. Phys. B* 955 (2020), p. 115041. DOI: 10.1016/j.nuclphysb.2020.115041. arXiv: 2003.01692 [gr-qc].

[27] Luc Blanchet, Thibault Damour, Gilles Esposito-Farese, and Bala R. Iyer. "Dimensional regularization of the third post-Newtonian gravitational wave generation from two point masses." In: *Phys. Rev. D* 71 (2005), p. 124004. DOI: 10.1103/PhysRevD.71.124004. arXiv: gr-qc/0503044.

[28] Luc Blanchet, Guillaume Faye, Bala R. Iyer, and Siddhartha Sinha. "The Third post-Newtonian gravitational wave polarisations and associated spherical harmonic modes for inspiralling compact binaries in quasi-circular orbits." In: *Class. Quant. Grav.* 25 (2008). [Erratum: Class.Quant.Grav. 29, 239501 (2012)], p. 165003. DOI: 10.1088/0264-9381/25/16/165003. arXiv: 0802.1249 [gr-qc].

[29] Michael Boyle, Duncan A. Brown, Lawrence E. Kidder, Abdul H. Mroue, Harald P. Pfeiffer, Mark A. Scheel, Gregory B. Cook, and Saul A. Teukolsky. "High-accuracy comparison of numerical relativity simulations with post-Newtonian expansions." In: *Phys. Rev. D* 76 (2007), p. 124038. DOI: 10.1103/PhysRevD.76.124038. arXiv: 0710.0158 [gr-qc].

[30] Misao Sasaki and Hideyuki Tagoshi. "Analytic black hole perturbation approach to gravitational radiation." In: *Living Rev. Rel.* 6 (2003), p. 6. DOI: 10.12942/lrr-2003-6. arXiv: gr-qc/0306120.

[31] William H. Press and Paul Schechter. "Formation of galaxies and clusters of galaxies by selfsimilar gravitational condensation." In: *Astrophys. J.* 187 (1974), pp. 425–438. DOI: 10.1086/152650.

[32] J. R. Bond, S. Cole, G. Efstathiou, and Nick Kaiser. "Excursion set mass functions for hierarchical Gaussian fluctuations." In: *Astrophys. J.* 379 (1991), p. 440. DOI: 10.1086/170520.

[33] Andrew R. Wetzel. "On the Orbits of Infalling Satellite Halos." In: *Mon. Not. Roy. Astron. Soc.* 412 (2011), p. 49. DOI: 10.1111/j.1365-2966.2010.17877.x. arXiv: 1001.4792 [astro-ph.CO].

[34] Anatoly Klypin, Gustavo Yepes, Stefan Gottlober, Francisco Prada, and Steffen Hess. "MultiDark simulations: the story of dark matter halo concentrations and density profiles." In: *Mon. Not. Roy. Astron. Soc.* 457.4 (2016), pp. 4340–4359. DOI: 10.1093/mnras/stw248. arXiv: 1411.4001 [astro-ph.CO].

[35] Philip Bett, Vincent Eke, Carlos S. Frenk, Adrian Jenkins, John Helly, and Julio Navarro. "The spin and shape of dark matter haloes in the Millennium simulation of a lambda-CDM universe." In: *Mon. Not. Roy. Astron. Soc.* 376 (2007), pp. 215–232. DOI: 10.1111/j.1365-2966.2007.11432.x. arXiv: astro-ph/0608607.

[36] J. R. Gott. "Creation of Open Universes from de Sitter Space." In: *Nature* 295 (1982), pp. 304–307. DOI: 10.1038/295304a0.

[37] Sidney R. Coleman. "The Fate of the False Vacuum. 1. Semiclassical Theory." In: *Phys. Rev. D* 15 (1977). [Erratum: Phys.Rev.D 16, 1248 (1977)], pp. 2929–2936. DOI: 10.1103/PhysRevD.16.1248.

[38] Hassan Firouzjahi, Sadra Jazayeri, Asieh Karami, and Tahereh Rostami. "Bubble nucleation and inflationary perturbations." In: *JCAP* 12 (2017), p. 029. DOI: 10.1088/1475-7516/2017/12/029. arXiv: 1707.07550 [gr-qc].

[39] Stephan J. Huber and Thomas Konstandin. "Gravitational Wave Production by Collisions: More Bubbles." In: *JCAP* 09 (2008), p. 022. DOI: 10.1088/1475-7516/2008/09/022. arXiv: 0806.1828 [hep-ph].

[40] Lev Kofman, Andrei D. Linde, and Alexei A. Starobinsky. "Towards the theory of reheating after inflation." In: *Phys. Rev. D* 56 (1997), pp. 3258–3295. DOI: 10.1103/PhysRevD.56.3258. arXiv: hep-ph/9704452.

[41] Matthew D. Duez and Yosef Zlochower. "Numerical Relativity of Compact Binaries in the 21st Century." In: *Rept. Prog. Phys.* 82.1 (2019), p. 016902. DOI: 10.1088/1361-6633/aadb16. arXiv: 1808.06011 [gr-qc].

[42] Yosef Zlochower, Marcelo Ponce, and Carlos O. Lousto. "Accuracy Issues for Numerical Waveforms." In: *Phys. Rev. D* 86 (2012), p. 104056. DOI: 10.1103/PhysRevD.86.104056. arXiv: 1208.5494 [gr-qc].

[43] Tony Chu, Heather Fong, Prayush Kumar, Harald P. Pfeiffer, Michael Boyle, Daniel A. Hemberger, Lawrence E. Kidder, Mark A. Scheel, and Bela Szilagyi. "On the accuracy and precision of numerical waveforms: Effect of waveform extraction methodology." In: *Class. Quant. Grav.* 33.16 (2016), p. 165001. DOI: 10.1088/0264-9381/33/16/165001. arXiv: 1512.06800 [gr-qc].

[44] Prayush Kumar, Kevin Barkett, Swetha Bhagwat, Nousha Afshari, Duncan A. Brown, Geoffrey Lovelace, Mark A. Scheel, and Béla Szilágyi. "Accuracy and precision of gravitational-wave models of inspiraling neutron star-black hole binaries with spin: Comparison with matter-free numerical relativity in the low-frequency regime." In: *Phys. Rev. D* 92.10 (2015), p. 102001. DOI: 10.1103/PhysRevD.92.102001. arXiv: 1507.00103 [gr-qc].

[45] Mark Hannam, Patricia Schmidt, Alejandro Bohé, Leïla Haegel, Sascha Husa, Frank Ohme, Geraint Pratten, and Michael Pürrer. "Simple Model of Complete Precessing Black-Hole-Binary Gravitational Waveforms." In: *Phys. Rev. Lett.* 113.15 (2014), p. 151101. DOI: 10.1103/PhysRevLett.113.151101. arXiv: 1308.3271 [gr-qc].

[46] Antoine Klein, Yannick Boetzel, Achamveedu Gopakumar, Philippe Jetzer, and Lorenzo de Vittori. "Fourier domain gravitational waveforms for precessing eccentric binaries." In: *Phys. Rev. D* 98.10 (2018), p. 104043. DOI: 10.1103/PhysRevD.98.104043. arXiv: 1801.08542 [gr-qc].

[47] Stephen Fairhurst, Rhys Green, Charlie Hoy, Mark Hannam, and Alistair Muir. "Two-harmonic approximation for gravitational waveforms from precessing binaries." In: *Phys. Rev. D* 102.2 (2020), p. 024055. DOI: 10.1103/PhysRevD.102.024055. arXiv: 1908.05707 [gr-qc].

[48] Giulia Gubitosi, Federico Piazza, and Filippo Vernizzi. "The Effective Field Theory of Dark Energy." In: *JCAP* 1302 (2013), p. 032. DOI: 10.1088/1475-7516/2013/02/032. arXiv: 1210.0201 [hep-th].

[49] Clifford Cheung, Paolo Creminelli, A. Liam Fitzpatrick, Jared Kaplan, and Leonardo Senatore. "The Effective Field Theory of Inflation." In: *JHEP* 0803 (2008), p. 014. DOI: 10.1088/1126-6708/2008/03/014. arXiv: 0709.0293 [hep-th].

[50] Paolo Creminelli and Filippo Vernizzi. "Dark Energy after GW170817 and GRB170817A." In: *Phys. Rev. Lett.* 119.25 (2017), p. 251302. DOI: 10.1103/PhysRevLett.119.251302. arXiv: 1710.05877 [astro-ph.CO].

[51] Richard P. Woodard. "Ostrogradsky's theorem on Hamiltonian instability." In: *Scholarpedia* 10.8 (2015), p. 32243. DOI: 10.4249/scholarpedia.32243. arXiv: 1506.02210 [hep-th].

[52] Jerome Gleyzes, David Langlois, Federico Piazza, and Filippo Vernizzi. "Essential Building Blocks of Dark Energy." In: *JCAP* 1308 (2013), p. 025. DOI: 10.1088/1475-7516/2013/08/025. arXiv: 1304.4840 [hep-th].

[53] Giulia Cusin, Matthew Lewandowski, and Filippo Vernizzi. "Nonlinear Effective Theory of Dark Energy." In: *JCAP* 1804.04 (2018), p. 061. DOI: 10.1088/1475-7516/2018/04/061. arXiv: 1712.02782 [astro-ph.CO].

[54] Dario Bettoni and Stefano Liberati. "Disformal invariance of second order scalar-tensor theories: Framing the Horndeski action." In: *Phys.Rev.* D88.8 (2013), p. 084020. DOI: 10.1103/PhysRevD.88.084020. arXiv: 1306.6724 [gr-qc].

[55] Gregory Walter Horndeski. "Second-order scalar-tensor field equations in a four-dimensional space." In: *Int.J.Theor.Phys.* 10 (1974), pp. 363–384. DOI: 10.1007/BF01807638.

[56] C. Deffayet, Xian Gao, D.A. Steer, and G. Zahariade. "From k-essence to generalised Galileons." In: *Phys.Rev.* D84 (2011), p. 064039. DOI: 10.1103/PhysRevD.84.064039. arXiv: 1103.3260 [hep-th].

[57] Jérôme Gleyzes, David Langlois, Federico Piazza, and Filippo Vernizzi. "Healthy theories beyond Horndeski." In: *Phys. Rev. Lett.* 114.21 (2015), p. 211101. DOI: 10.1103/PhysRevLett.114.211101. arXiv: 1404.6495 [hep-th].

[58] Jérôme Gleyzes, David Langlois, Federico Piazza, and Filippo Vernizzi. "Exploring gravitational theories beyond Horndeski." In: *JCAP* 1502 (2015), p. 018. DOI: 10.1088/1475-7516/2015/02/018. arXiv: 1408.1952 [astro-ph.CO].

[59] David Pirtskhalava, Luca Santoni, Enrico Trincherini, and Filippo Vernizzi. "Weakly Broken Galileon Symmetry." In: *JCAP* 1509.09 (2015), p. 007. DOI: 10.1088/1475-7516/2015/09/007. arXiv: 1505.00007 [hep-th].

[60] Emilio Bellini and Ignacy Sawicki. "Maximal freedom at minimum cost: linear large-scale structure in general modifications of gravity." In: *JCAP* 1407 (2014), p. 050. DOI: 10.1088/1475-7516/2014/07/050. arXiv: 1404.3713 [astro-ph.CO].

[61] Jérôme Gleyzes, David Langlois, and Filippo Vernizzi. "A unifying description of dark energy." In: *Int. J. Mod. Phys.* D23.13 (2015), p. 1443010. DOI: 10.1142/S021827181443010X. arXiv: 1411.3712 [hep-th].

[62] Cedric Deffayet, Oriol Pujolas, Ignacy Sawicki, and Alexander Vikman. "Imperfect Dark Energy from Kinetic Gravity Braiding." In: *JCAP* 1010 (2010), p. 026. DOI: 10.1088/1475-7516/2010/10/026. arXiv: 1008.0048 [hep-th].

[63] Enis Belgacem et al. "Testing modified gravity at cosmological distances with LISA standard sirens." In: *JCAP* 07 (2019), p. 024. DOI: 10.1088/1475-7516/2019/07/024. arXiv: 1906.01593 [astro-ph.CO].

[64] Benjamin P. Abbott et al. "GW170817: Observation of Gravitational Waves from a Binary Neutron Star Inspiral." In: *Phys. Rev. Lett.* 119.16 (2017), p. 161101. DOI: 10.1103/PhysRevLett.119.161101. arXiv: 1710.05832 [gr-qc].

[65] A. Goldstein et al. "An Ordinary Short Gamma-Ray Burst with Extraordinary Implications: Fermi-GBM Detection of GRB 170817A." In: *Astrophys. J.* 848.2 (2017), p. L14. DOI: 10.3847/2041-8213/aa8f41. arXiv: 1710.05446 [astro-ph.HE].

[66] Jose Mara Ezquiaga and Miguel Zumalacrregui. "Dark Energy After GW170817: Dead Ends and the Road Ahead." In: *Phys. Rev. Lett.* 119.25 (2017), p. 251304. DOI: 10.1103/PhysRevLett.119.251304. arXiv: 1710.05901 [astro-ph.CO].

[67] T. Baker, E. Bellini, P. G. Ferreira, M. Lagos, J. Noller, and I. Sawicki. "Strong constraints on cosmological gravity from GW170817 and GRB 170817A." In: *Phys. Rev. Lett.* 119.25 (2017), p. 251301. DOI: 10.1103/PhysRevLett.119.251301. arXiv: 1710.06394 [astro-ph.CO].

[68] Jeremy Sakstein and Bhuvnesh Jain. "Implications of the Neutron Star Merger GW170817 for Cosmological Scalar-Tensor Theories." In: *Phys. Rev. Lett.* 119.25 (2017), p. 251303. DOI: 10.1103/PhysRevLett.119.251303. arXiv: 1710.05893 [astro-ph.CO].

[69] B. P. Abbott et al. "Gravitational Waves and Gamma-Rays from a Binary Neutron Star Merger: GW170817 and GRB 170817A." In: *Astrophys. J.* 848.2 (2017), p. L13. DOI: 10.3847/2041-8213/aa920c. arXiv: 1710.05834 [astro-ph.HE].

[70] Lucas Lombriser and Andy Taylor. "Breaking a Dark Degeneracy with Gravitational Waves." In: *JCAP* 1603.03 (2016), p. 031. DOI: 10.1088/1475-7516/2016/03/031. arXiv: 1509.08458 [astro-ph.CO].

[71] Dario Bettoni, Jose María Ezquiaga, Kurt Hinterbichler, and Miguel Zumalacárregui. "Speed of Gravitational Waves and the Fate of Scalar-Tensor Gravity." In: *Phys. Rev.* D95.8 (2017), p. 084029. DOI: 10.1103/PhysRevD.95.084029. arXiv: 1608.01982 [gr-qc].

[72] Guy D. Moore and Ann E. Nelson. "Lower bound on the propagation speed of gravity from gravitational Cherenkov radiation." In: *JHEP* 0109 (2001), p. 023. DOI: 10.1088/1126-6708/2001/09/023. arXiv: hep-ph/0106220 [hep-ph].

[73] Claudia de Rham and Scott Melville. "Gravitational Rainbows: LIGO and Dark Energy at its Cutoff." In: *Phys. Rev. Lett.* 121.22 (2018), p. 221101. DOI: 10.1103/PhysRevLett.121.221101. arXiv: 1806.09417 [hep-th].

[74] Edmund J. Copeland, Michael Kopp, Antonio Padilla, Paul M. Saffin, and Constantinos Skordis. "Dark energy after GW170817 revisited." In: *Phys. Rev. Lett.* 122.6 (2019), p. 061301. DOI: 10.1103/PhysRevLett.122.061301. arXiv: 1810.08239 [gr-qc].

[75] Lorenzo Bordin, Edmund J. Copeland, and Antonio Padilla. "Dark energy loopholes some time after GW170817." In: *JCAP* 11 (2020), p. 063. DOI: 10.1088/1475-7516/2020/11/063. arXiv: 2006.06652 [astro-ph.CO].

[76] David Langlois and Karim Noui. "Degenerate higher derivative theories beyond Horndeski: evading the Ostrogradski instability." In: *JCAP* 1602.02 (2016), p. 034. DOI: 10.1088/1475-7516/2016/02/034. arXiv: 1510.06930 [gr-qc].

[77] Marco Crisostomi, Kazuya Koyama, and Gianmassimo Tasinato. "Extended Scalar-Tensor Theories of Gravity." In: *JCAP* 1604.04 (2016), p. 044. DOI: 10.1088/1475-7516/2016/04/044. arXiv: 1602.03119 [hep-th].

[78] Paolo Creminelli, Matthew Lewandowski, Giovanni Tambalo, and Filippo Vernizzi. "Gravitational Wave Decay into Dark Energy." In: *JCAP* 1812.12 (2018), p. 025. DOI: 10.1088/1475-7516/2018/12/025. arXiv: 1809.03484 [astro-ph.CO].

[79] Paolo Creminelli, Guido D'Amico, Jorge Norena, and Filippo Vernizzi. "The Effective Theory of Quintessence: the $w < -1$ Side Unveiled." In: *JCAP* 0902 (2009), p. 018. DOI: 10.1088/1475-7516/2009/02/018. arXiv: 0811.0827 [astro-ph].

[80] R. R. Caldwell, Rahul Dave, and Paul J. Steinhardt. "Cosmological imprint of an energy component with general equation of state." In: *Phys. Rev. Lett.* 80 (1998), pp. 1582–1585. DOI: 10.1103/PhysRevLett.80.1582. arXiv: astro-ph/9708069 [astro-ph].

[81] C. Armendariz-Picon, Viatcheslav F. Mukhanov, and Paul J. Steinhardt. "A Dynamical solution to the problem of a small cosmological constant and late time cosmic acceleration." In: *Phys.Rev.Lett.* 85 (2000), pp. 4438–4441. DOI: 10.1103/PhysRevLett.85.4438. arXiv: astro-ph/0004134 [astro-ph].

[82] David Langlois, Michele Mancarella, Karim Noui, and Filippo Vernizzi. "Effective Description of Higher-Order Scalar-Tensor Theories." In: *JCAP* 1705.05 (2017), p. 033. DOI: 10.1088/1475-7516/2017/05/033. arXiv: 1703.03797 [hep-th].

[83] N. W. McLachlan. *Theory and application of Mathieu functions*. Clarendon Press, 1951.

[84] Frank WJ Olver, Daniel W Lozier, Ronald F Boisvert, and Charles W Clark. *NIST handbook of mathematical functions hardback and CD-ROM*. Cambridge university press, 2010.

[85] Michele Maggiore. *Gravitational Waves. Vol. 1: Theory and Experiments*. Oxford Master Series in Physics. Oxford University Press, 2007. ISBN: 9780198570745, 9780198520740. URL: http://www.oup.com/uk/catalogue/?ci=9780198570745.

[86] Robert M. Wald. *General Relativity*. Chicago, USA: Chicago Univ. Pr., 1984. DOI: 10.7208/chicago/9780226870373.001.0001.

[87] Tomislav Prokopec and Thomas G. Roos. "Lattice study of classical inflaton decay." In: *Phys. Rev.* D55 (1997), pp. 3768–3775. DOI: 10.1103/PhysRevD.55.3768. arXiv: hep-ph/9610400 [hep-ph].

[88] Peter Adshead, John T. Giblin, and Zachary J. Weiner. "Non-Abelian gauge preheating." In: *Phys. Rev.* D96.12 (2017), p. 123512. DOI: 10.1103/PhysRevD.96.123512. arXiv: 1708.02944 [hep-ph].

[89] Luca Santoni, Enrico Trincherini, and Leonardo G. Trombetta. "Behind Horndeski: Structurally Robust Higher Derivative EFTs." In: *JHEP* 08 (2018), p. 118. DOI: 10.1007/JHEP08(2018)118. arXiv: 1806.10073 [hep-th].

[90] Marco Crisostomi, Matthew Lewandowski, and Filippo Vernizzi. "Vainshtein regime in Scalar-Tensor gravity: constraints on DHOST theories." In: (2019). arXiv: 1903.11591 [gr-qc].

[91] Pau Amaro-Seoane et al. "Laser Interferometer Space Antenna." In: (2017). arXiv: 1702.00786 [astro-ph.IM].

[92] B. P. Abbott et al. "Observation of Gravitational Waves from a Binary Black Hole Merger." In: *Phys. Rev. Lett.* 116.6 (2016), p. 061102. DOI: 10.1103/PhysRevLett.116.061102. arXiv: 1602.03837 [gr-qc].

[93] Shin'ichi Hirano, Tsutomu Kobayashi, and Daisuke Yamauchi. "Screening mechanism in degenerate higher-order scalar-tensor theories evading gravitational wave constraints." In: *Phys. Rev.* D99.10 (2019), p. 104073. DOI: 10.1103/PhysRevD.99.104073. arXiv: 1903.08399 [gr-qc].

[94] Alberto Nicolis and Riccardo Rattazzi. "Classical and quantum consistency of the DGP model." In: *JHEP* 06 (2004), p. 059. DOI: 10.1088/1126-6708/2004/06/059. arXiv: hep-th/0404159 [hep-th].

[95] Paolo Creminelli, Giovanni Tambalo, Filippo Vernizzi, and Vicharit Yingcharoenrat. "Resonant Decay of Gravitational Waves into Dark Energy." In: (2019). arXiv: 1906.07015 [gr-qc].

[96] Solomon Endlich and Junpu Wang. "Classical Stability of the Galileon." In: *JHEP* 11 (2011), p. 065. DOI: 10.1007/JHEP11(2011)065. arXiv: 1106.1659 [hep-th].

[97] Benjamin Bose, Kazuya Koyama, Matthew Lewandowski, Filippo Vernizzi, and Hans A. Winther. "Towards Precision Constraints on Gravity with the Effective Field Theory of Large-Scale Structure." In: *JCAP* 1804.04 (2018), p. 063. DOI: 10.1088/1475-7516/2018/04/063. arXiv: 1802.01566 [astro-ph.CO].

[98] Markus A. Luty, Massimo Porrati, and Riccardo Rattazzi. "Strong interactions and stability in the DGP model." In: *JHEP* 09 (2003), p. 029. DOI: 10.1088/1126-6708/2003/09/029. arXiv: hep-th/0303116 [hep-th].

[99] Sergei Dubovsky, Thomas Gregoire, Alberto Nicolis, and Riccardo Rattazzi. "Null energy condition and superluminal propagation." In: *JHEP* 2006.03 (2006), p. 025. DOI: 10.1088/1126-6708/2006/03/025. arXiv: 0512.260 [hep-th].

[100] Clare Burrage, Claudia de Rham, Lavinia Heisenberg, and Andrew J. Tolley. "Chronology Protection in Galileon Models and Massive Gravity." In: *JCAP* 1207 (2012), p. 004. DOI: 10.1088/1475-7516/2012/07/004. arXiv: 1111.5549 [hep-th].

[101] Fabian Schmidt. "Self-Consistent Cosmological Simulations of DGP Braneworld Gravity." In: *Phys. Rev.* D80 (2009), p. 043001. DOI: 10.1103/PhysRevD.80.043001. arXiv: 0905.0858 [astro-ph.CO].

[102] Eugeny Babichev, Sabir Ramazanov, and Alexander Vikman. "Recovering P(X) from a canonical complex field." In: *JCAP* 2018.11 (2018), pp. 023–023. DOI: 10.1088/1475-7516/2018/11/023. arXiv: 1807.10281. URL: https://doi.org/10.1088%2F1475-7516%2F2018%2F11%2F023.

[103] G. Hobbs et al. "The international pulsar timing array project: using pulsars as a gravitational wave detector." In: *Class. Quant. Grav.* 27 (2010), p. 084013. DOI: 10.1088/0264-9381/27/8/084013. arXiv: 0911.5206 [astro-ph.SR].

[104] Daniel Baumann and Daniel Green. "Equilateral Non-Gaussianity and New Physics on the Horizon." In: *JCAP* 1109 (2011), p. 014. DOI: 10.1088/1475-7516/2011/09/014. arXiv: 1102.5343 [hep-th].

[105] David Pirtskhalava, Luca Santoni, Enrico Trincherini, and Filippo Vernizzi. "Large Non-Gaussianity in Slow-Roll Inflation." In: (2015). arXiv: 1506.06750 [hep-th].

[106] Matteo Bonetti, Alberto Sesana, Enrico Barausse, and Francesco Haardt. "Post-Newtonian evolution of massive black hole triplets in galactic nuclei III. A robust lower limit to the nHz stochastic background of gravitational waves." In: *Mon. Not. Roy. Astron. Soc.* 477.2 (2018), pp. 2599–2612. DOI: 10.1093/mnras/sty874. arXiv: 1709.06095 [astro-ph.GA].

[107] Matteo Bonetti, Alberto Sesana, Francesco Haardt, Enrico Barausse, and Monica Colpi. "Post-Newtonian evolution of massive black hole triplets in galactic nuclei IV. Implications for LISA." In: *Mon. Not. Roy. Astron. Soc.* 486.3 (2019), pp. 4044–4060. DOI: 10.1093/mnras/stz903. arXiv: 1812.01011 [astro-ph.GA].

[108] Brando Bellazzini, Matthew Lewandowski, and Javi Serra. "Amplitudes' Positivity, Weak Gravity Conjecture, and Modified Gravity." In: (2019). arXiv: 1902.03250 [hep-th].

[109] Jérôme Gleyzes, David Langlois, Michele Mancarella, and Filippo Vernizzi. "Effective Theory of Dark Energy at Redshift Survey Scales." In: *JCAP* 1602.02 (2016), p. 056. DOI: 10.1088/1475-7516/2016/02/056. arXiv: 1509.02191 [astro-ph.CO].

[110] David Alonso, Emilio Bellini, Pedro G. Ferreira, and Miguel Zumalacrregui. "Observational future of cosmological scalar-tensor theories." In: *Phys. Rev.* D95.6 (2017), p. 063502. DOI: 10.1103/PhysRevD.95.063502. arXiv: 1610.09290 [astro-ph.CO].

[111] Johannes Noller and Andrina Nicola. "Cosmological parameter constraints for Horndeski scalar-tensor gravity." In: *Phys. Rev.* D99.10 (2019), p. 103502. DOI: 10.1103/PhysRevD.99.103502. arXiv: 1811.12928 [astro-ph.CO].

[112] Noemi Frusciante and Louis Perenon. "Effective Field Theory of Dark Energy: a Review." In: (2019). arXiv: 1907.03150 [astro-ph.CO].

[113] Paolo Creminelli, Giovanni Tambalo, Filippo Vernizzi, and Vicharit Yingcharoenrat. "Dark-Energy Instabilities induced by Gravitational Waves." In: *JCAP* 05 (2020), p. 002. DOI: 10.1088/1475-7516/2020/05/002. arXiv: 1910.14035 [gr-qc].

[114] C. Armendariz-Picon, Viatcheslav F. Mukhanov, and Paul J. Steinhardt. "Essentials of k essence." In: *Phys.Rev.* D63 (2001), p. 103510. DOI: 10.1103/PhysRevD.63.103510. arXiv: astro-ph/0006373 [astro-ph].

[115] Austin Joyce, Bhuvnesh Jain, Justin Khoury, and Mark Trodden. "Beyond the Cosmological Standard Model." In: *Phys.Rept.* 568 (2015), pp. 1–98. DOI: 10.1016/j.physrep.2014.12.002. arXiv: 1407.0059 [astro-ph.CO].

[116] Philippe Brax and Patrick Valageas. "K-mouflage Cosmology: Formation of Large-Scale Structures." In: *Phys. Rev.* D90.2 (2014), p. 023508. DOI: 10.1103/PhysRevD.90.023508. arXiv: 1403.5424 [astro-ph.CO].

[117] Y. Akrami et al. "Planck 2018 results. IX. Constraints on primordial non-Gaussianity." In: *Astron. Astrophys.* 641 (2020), A9. DOI: 10.1051/0004-6361/201935891. arXiv: 1905.05697 [astro-ph.CO].

[118] Ilia Musco, Valerio De Luca, Gabriele Franciolini, and Antonio Riotto. "The Threshold for Primordial Black Hole Formation: a Simple Analytic Prescription." In: (Nov. 2020). arXiv: 2011.03014 [astro-ph.CO].

[119] G. Franciolini, A. Kehagias, S. Matarrese, and A. Riotto. "Primordial Black Holes from Inflation and non-Gaussianity." In: *JCAP* 03 (2018), p. 016. DOI: 10.1088/1475-7516/2018/03/016. arXiv: 1801.09415 [astro-ph.CO].

[120] Vicente Atal and Cristiano Germani. "The role of non-gaussianities in Primordial Black Hole formation." In: *Phys. Dark Univ.* 24 (2019), p. 100275. DOI: 10.1016/j.dark.2019.100275. arXiv: 1811.07857 [astro-ph.CO].

[121] Alexei A. Starobinsky. "STOCHASTIC DE SITTER (INFLATIONARY) STAGE IN THE EARLY UNIVERSE." In: *Lect. Notes Phys.* 246 (1986), pp. 107–126. DOI: 10.1007/3-540-16452-9_6.

[122] Victor Gorbenko and Leonardo Senatore. "$\lambda\phi^4$ in dS." In: (Oct. 2019). arXiv: 1911.00022 [hep-th].

[123] Chris Pattison, Vincent Vennin, Hooshyar Assadullahi, and David Wands. "Quantum diffusion during inflation and primordial black holes." In: *Journal of Cosmology and Astroparticle Physics* 2017.10 (2017), pp. 046–046. DOI: 10.1088/1475-7516/2017/10/046. URL: https://doi.org/10.1088%2F1475-7516%2F2017%2F10%2F046.

[124] Xingang Chen, Gonzalo A. Palma, Walter Riquelme, Bruno Scheihing Hitschfeld, and Spyros Sypsas. "Landscape tomography through primordial non-Gaussianity." In: *Phys. Rev. D* 98.8 (2018), p. 083528. DOI: 10.1103/PhysRevD.98.083528. arXiv: 1804.07315 [hep-th].

[125] George Panagopoulos and Eva Silverstein. "Primordial Black Holes from non-Gaussian tails." In: (June 2019). arXiv: 1906.02827 [hep-th].

[126] George Panagopoulos and Eva Silverstein. "Multipoint correlators in multifield cosmology." In: (Mar. 2020). arXiv: 2003.05883 [hep-th].

[127] Riccardo Rattazzi. *The Path Integral approach to Quantum Mechanics Lecture Notes for Quantum Mechanics IV*.

[128] M.A. Escobar-Ruiz, E. Shuryak, and A.V. Turbiner. "Fluctuations in quantum mechanics and field theories from a new version of semiclassical theory. II." In: *Phys. Rev. D* 96.4 (2017), p. 045005. DOI: 10.1103/PhysRevD.96.045005. arXiv: 1705.06159 [hep-th].

[129] Nima Arkani-Hamed and Juan Maldacena. "Cosmological Collider Physics." In: (Mar. 2015). arXiv: 1503.08043 [hep-th].

[130] Harry Goodhew, Sadra Jazayeri, and Enrico Pajer. "The Cosmological Optical Theorem." In: (Sept. 2020). arXiv: 2009.02898 [hep-th].

[131] Leonardo Senatore and Matias Zaldarriaga. "A Naturally Large Four-Point Function in Single Field Inflation." In: *JCAP* 01 (2011), p. 003. DOI: 10.1088/1475-7516/2011/01/003. arXiv: 1004.1201 [hep-th].

[132] Mohsen Alishahiha, Eva Silverstein, and David Tong. "DBI in the sky." In: *Phys. Rev. D* 70 (2004), p. 123505. DOI: 10.1103/PhysRevD.70.123505. arXiv: hep-th/0404084.

[133] Alberto Nicolis, Riccardo Rattazzi, and Enrico Trincherini. "The Galileon as a local modification of gravity." In: *Phys. Rev.* D79 (2009), p. 064036. DOI: 10.1103/PhysRevD.79.064036. arXiv: 0811.2197 [hep-th].

[134] Dionysios Anninos, Tarek Anous, Daniel Z. Freedman, and George Konstantinidis. "Late-time Structure of the Bunch-Davies De Sitter Wavefunction." In: *JCAP* 11 (2015), p. 048. DOI: 10.1088/1475-7516/2015/11/048. arXiv: 1406.5490 [hep-th].

[135] Daniel Babich, Paolo Creminelli, and Matias Zaldarriaga. "The Shape of non-Gaussianities." In: *JCAP* 08 (2004), p. 009. DOI: 10.1088/1475-7516/2004/08/009. arXiv: astro-ph/0405356.

[136] Thomas Hertog and James Hartle. "Holographic No-Boundary Measure." In: *JHEP* 05 (2012), p. 095. DOI: 10.1007/JHEP05(2012)095. arXiv: 1111.6090 [hep-th].

[137] Juan Maldacena, Gustavo J. Turiaci, and Zhenbin Yang. "Two dimensional Nearly de Sitter gravity." In: *JHEP* 01 (2021), p. 139. DOI: 10.1007/JHEP01(2021)139. arXiv: 1904.01911 [hep-th].

[138] Gerald Teschl. *Ordinary differential equations and dynamical systems*. Vol. 140. American Mathematical Soc., 2012.

[139] Freeman J Dyson. "Divergence of perturbation theory in quantum electrodynamics." In: *Physical Review* 85.4 (1952), p. 631.

[140] Daniel Harlow and Douglas Stanford. "Operator Dictionaries and Wave Functions in AdS/CFT and dS/CFT." In: (Apr. 2011). arXiv: 1104.2621 [hep-th].

[141] Yacine Ali-Haïmoud. "Correlation Function of High-Threshold Regions and Application to the Initial Small-Scale Clustering of Primordial Black Holes." In: *Phys. Rev. Lett.* 121.8 (2018), p. 081304. DOI: 10.1103/PhysRevLett.121.081304. arXiv: 1805.05912 [astro-ph.CO].

[142] Paolo Creminelli, Sergei Dubovsky, Alberto Nicolis, Leonardo Senatore, and Matias Zaldarriaga. "The Phase Transition to Slow-roll Eternal Inflation." In: *JHEP* 09 (2008), p. 036. DOI: 10.1088/1126-6708/2008/09/036. arXiv: 0802.1067 [hep-th].

[143] Sergei Dubovsky, Leonardo Senatore, and Giovanni Villadoro. "The Volume of the Universe after Inflation and de Sitter Entropy." In: *JHEP* 04 (2009), p. 118. DOI: 10.1088/1126-6708/2009/04/118. arXiv: 0812.2246 [hep-th].

[144] Sergei Dubovsky, Leonardo Senatore, and Giovanni Villadoro. "Universality of the Volume Bound in Slow-Roll Eternal Inflation." In: *JHEP* 05 (2012), p. 035. DOI: 10.1007/JHEP05(2012)035. arXiv: 1111.1725 [hep-th].

[145] Jiri Bicak and Jiri Podolsky. "Gravitational waves in vacuum space-times with cosmological constant. 1. Classification and geometrical properties of nontwisting type N solutions." In: *J. Math. Phys.* 40 (1999), pp. 4495–4505. DOI: 10.1063/1.532981. arXiv: gr-qc/9907048.

[146] Job Feldbrugge, Jean-Luc Lehners, and Neil Turok. "Lorentzian Quantum Cosmology." In: *Phys. Rev. D* 95.10 (2017), p. 103508. DOI: 10.1103/PhysRevD.95.103508. arXiv: 1703.02076 [hep-th].

[147] Gil Badel, Gabriel Cuomo, Alexander Monin, and Riccardo Rattazzi. "Feynman diagrams and the large charge expansion in $3 - \varepsilon$ dimensions." In: *Phys. Lett. B* 802 (2020), p. 135202. DOI: 10.1016/j.physletb.2020.135202. arXiv: 1911.08505 [hep-th].

[148] G. R. Dvali, Gregory Gabadadze, and Massimo Porrati. "4-D gravity on a brane in 5-D Minkowski space." In: *Phys. Lett. B* 485 (2000), pp. 208–214. DOI: 10.1016/S0370-2693(00)00669-9. arXiv: hep-th/0005016.

[149] V. Mukhanov. *Physical Foundations of Cosmology*. Oxford: Cambridge University Press, 2005. ISBN: 0521563984, 9780521563987. URL: http://www-spires.fnal.gov/spires/find/books/www?cl=QB981.M89::2005.

[150] Karim A. Malik and David Wands. "Cosmological perturbations." In: *Phys. Rept.* 475 (2009), pp. 1–51. DOI: 10.1016/j.physrep.2009.03.001. arXiv: 0809.4944 [astro-ph].